

**ENGINEERING CYTOCHROME P450
BM-3 FOR SELECTIVE
HYDROXYLATION OF ALKANES**

Thesis by

Peter Meinhold

In Partial Fulfillment of the Requirements for the
degree of

Doctor of Philosophy

CALIFORNIA INSTITUTE OF TECHNOLOGY

Pasadena, California

2005

(Defended May, 31, 2005)

© 2005

Peter Meinhold

All Rights Reserved

ACKNOWLEDGEMENTS

The first time I left Caltech, I had just finished a six month internship in Frances Arnold's laboratory. The second time, I had completed my diploma thesis research in her lab. On both occasions I had enjoyed working at Caltech, and the decision to start graduate school here was not a difficult one. Now, I have almost completed my tenure at Caltech and I will leave with the fondest memories. My time at Caltech has given me more than I ever expected. Working in a world-class institute was not only helpful for gaining the scientific knowledge necessary to compete on the job market. In addition, I was able to learn how to manage myself, and was able to interact with some of the smartest and most amazing people I have ever met. Caltech has given me the opportunity to grow scientifically and personally and I will forever be indebted to this place and its people.

I would like to thank my advisor Frances Arnold for giving me the opportunity to earn my Ph.D. at Caltech. I would also like to thank her for her constant enthusiasm for my project, for her guidance and for her support throughout the years. Her encouragement helped me get things done in a timely manner without feeling pressured. I hope to have acquired at least some of her managing, multitasking, and writing skills, which continue to amaze me. Frances has been the best advisor I could have wished for and I hope to continue this successful collaboration into the future.

I would like to thank Doug Rees, Jay Labinger and Dianne Newman for serving on my candidacy and thesis committee. Jay critically read my manuscripts and his advice from

a chemist's perspective has been invaluable. I thank Nathan Dalleska for his assistance with the gas chromatography. Carl Hansen and Megan Anderson tried hard to crystallize one of our enzymes and Yerga Meharennia actually succeeded in solving the crystal structure of one of the early enzymes.

The Arnold lab has always been a good work environment, despite the flux of people expected at an academic institution. The diversity of backgrounds and expertise of these people is key to the successful multidisciplinary research performed in this lab and helped me produce lots of results in a relatively short period of time. I wish to acknowledge all current and former Arnold lab members for their help, advice and friendship over the years.

I am most grateful to Matt Peters who joined the lab as a postdoc three years ago. Most of what is written in this thesis originated from discussions between the two of us. Matt has been an excellent mentor and friend and I hope to continue our successful partnership in the future. I thank Volker Sieber for introducing me to (the art of) molecular biology during my first visit at Caltech. I thank John Joern for mentoring me during my undergraduate thesis research. Toni Glieder, Edgardo Farinas and Pat Cirino comprised the P450 subgroup when I joined the lab as a graduate student. I thank them for teaching me the basics of P450 research. Toni has become a good collaborator upon his return to Austria, and is always a great source of advice. Geethani Bandera keeps the lab running. Alisha Hernandez, a hard working summer student, had to endure weeks of picking colonies. Adam Hartwick helped me with characterizing one of the enzymes.

Sports are one of the most important elements of my life. Cycling, running and swimming helped me keep my life in balance during stressful weeks at work. Cycling in Los Angeles isn't always a pleasant experience and I am grateful to all those people who kept me company during rides, especially Tobias Kippenberg, Carl Hansen, and Ben Deverman. I would also like to acknowledge my friends back in Germany, who still remember me despite my rare appearances.

I find myself extremely lucky to have parents that gave me the opportunity to do whatever I wanted to. I thank them for their support over the years. I would like to thank my grandma for her encouragement. She is probably the only family member who actually understands my work. My girlfriend Claire has been amazingly patient and helpful during times in which I did not have a lot of time to spend with her. Thank you for keeping up with me.

Finally, I would like to acknowledge the National Science Foundation for helping to fund my research.

ABSTRACT

Cytochromes P450 are of potential synthetic value because they hydroxylate a large array of substrates, often with high regio- and enantioselectivity. In contrast to most P450s, the BM-3 variant from *Bacillus megaterium* is soluble, easily expressed in *E. coli*, and does not require additional electron transfer proteins. A highly efficient enzyme for its preferred reaction, hydroxylation of medium-chain (C₁₂ to C₁₈) fatty acids, BM-3 is a good candidate for engineering for applications requiring activity on other substrates.

Using iterations of random mutagenesis, recombination, and high throughput screening, we engineered P450 BM-3 mutants to hydroxylate linear alkanes as short as propane. Activity towards linear alkanes was further increased by changing two key active site residues. The resulting mutants hydroxylate linear alkanes with high regioselectivity and, notably, enantioselectivity.

We further engineered these enzymes with guidance from the crystal structure of substrate-bound P450 BM-3. Eleven active-site residues were chosen for saturation mutagenesis, and the resulting mutants were screened for improved activity towards alkanes, as measured by total product formation. Substitutions at these positions generally did not affect correct folding of the enzyme, and a large fraction of folded proteins retained similar levels of activity as their predecessor. Moreover, several of the 11 selected amino acid substitutions yielded mutants that were both more active and produced various combinations of product regioisomers.

Recombination of these beneficial active-site mutations generated BM-3 variants that catalyze: (a) regio- and enantioselective hydroxylation of linear alkanes; (b) terminal hydroxylation of linear alkanes; (c) regio- and enantioselective hydroxylation of heterocyclic compounds; and (d) ethane hydroxylation.

The selective conversion of ethane to ethanol, not previously reported for any P450, is catalyzed by the most active mutant from this library. In nature, this reaction is solely observed for methane monooxygenases (MMOs) and related enzymes in alkane-assimilating bacteria.

Additionally, we have found that the reductase domain can be engineered to increase the efficiency of these reactions. Our progress in converting BM-3 from a fatty-acid hydroxylase into an enzyme able to selectively hydroxylate smaller alkanes, including ethane, is an important step towards our ultimate goal, achieving selective BM-3 catalyzed conversion of methane to methanol.

THESIS SUMMARY

Methane is a potent greenhouse gas that is emitted from natural and human-influenced sources. Reducing methane emissions by increasing its recovery in the form of chemicals, such as methanol, would have significant economic and environmental benefits. Methane is currently converted to methanol via the syngas reaction, an energy-intensive steam reformation process that is economically feasible only on a large scale. The most common source of methane is excavation of subterranean raw natural gas or petroleum. In many instances, transportation limitations prevent methane recovery, and methane is therefore typically burned on-site or vented directly to the atmosphere.

Oxidation of *n*-alkanes to *n*-alcohols is extremely difficult, due to the high alkane C-H bond strength, and the fact that the catalyst must control the oxidation to stop at the alcohol and not continue further to the thermodynamically favoured oxidation products, e.g., aldehydes, ketones, carboxylic acids or carbon dioxide. Despite decades of research, this transformation continues to pose a great challenge to classic chemistry. The solutions nature has found for this reaction are monooxygenases. These enzymes catalyze the selective insertion of one oxygen atom into a C-H bond of a non-activated carbon atom, while reducing the second oxygen atom to H₂O with electrons from NADH or NADPH. These enzymes perform this reaction at room temperature, and utilize dioxygen as a cheap and non-toxic oxidant. The methane monooxygenases (MMO), for example, enable methanotrophic bacteria to use methane as a source of carbon and energy. Microorganisms that grow on C₂ to C₄ gaseous alkanes are dependent on non-heme (di-iron) monooxygenases to catalyze the first oxidation step. These enzymes have long been

a source of inspiration for designers of synthetic catalysts. That they are not yet used in large-scale industrial oxidation processes reflects their large size and complexity: despite much effort, these multi-component enzymes have never been functionally expressed in a heterologous organism. Thus it has been extremely difficult to use modern metabolic and protein engineering tools to generate optimized industrial strains of MMO-utilizing microorganisms for biological production of chemicals or fuels from methane or ethane. We therefore chose to follow a completely different strategy by trying to convert a cytochrome P450 into a methane hydroxylating catalyst.

Cytochromes P450 are a large superfamily of heme-containing monooxygenases that catalyze the oxidation of a vast array of substrates, including n-alkanes. Chapter 1 of this thesis provides an introduction to cytochromes P450 and a detailed review of progress made in the engineering of these enzymes. In particular, the diversity of P450-catalyzed reactions is illustrated, and site-directed mutagenesis studies that provide much of our present knowledge about how these systems work are presented. P450s are now a relatively well understood class of proteins, making them a good target for engineering approaches. Rational design and directed evolution have been applied to engineer these proteins. The engineering of a select group of P450s to accept novel substrates, to change their regio- and enantioselectivity of substrate hydroxylation, and to alter protein-protein interactions and electron transfer processes are described.

Although the hydroxylation of non-activated C-H bonds is the most common P450 catalyzed reaction, none of the thousand-plus members of this family are known to oxidize the gaseous alkanes ethane or methane. Engineering a P450 capable of selectively

hydroxylating these substrates is the focus of this thesis. For several reasons, cytochrome P450 BM-3, a bacterial P450 from *Bacillus megaterium* was chosen as the starting point for this effort: the enzyme is robust and soluble; it presents one of the rare cases in which heme and FAD- and FMN-containing NADPH dependent reductase domain are fused to form a single polypeptide; and it catalyzes the hydroxylation of a range (C12 to C18) of fatty acids with a k_{cat} of $17,100 \text{ min}^{-1}$, which is the highest catalytic activity reported amongst P450 monooxygenases.

Three postdoctoral scholars in our laboratory (Ulrich Schwaneberg, Edgardo T. Farinas, and Anton Glieder) initiated the work on P450 BM-3 in our laboratory. Their first step in converting this P450 into a methane monooxygenase was to engineer variants active towards linear alkanes lacking the carboxylate moiety. Directed evolution – iterations of random mutagenesis, recombination, and screening – was applied to generate P450 variants with improved alkane hydroxylation activity. A colorimetric screening system employing *p*-nitrophenoxy octane as a surrogate substrate was chosen. In addition, NADPH oxidation in presence of the linear alkane substrate was monitored. This approach had important limitations: the surrogate substrate does not resemble the linear alkane structure very well, and electron transfer from NADPH to the heme is not necessarily coupled to product formation. Nevertheless, variants exhibiting high activity towards octane were identified. Limited activity towards propane, a substrate not hydroxylated at all by the wild-type enzyme, was also observed. At this point, I took over the P450 alkane hydroxylase project.

Chapter 2 describes the further steps in elevating the activity towards linear alkanes. Directed evolution was used to identify mutants with increased activity towards these substrates. Initially, the selection of mutants was based on monitoring NADPH depletion in the presence of an alkane substrate. To overcome the problem of identifying mutants in which cofactor oxidation is not coupled to product formation, a new screening system (developed by Matthew W. Peters) that employs methyl ether derivatives of linear alkanes. Upon hydroxylation of the methoxy group, formaldehyde is released, which is readily detectable in high-throughput format using a commercially available dye.

Initially, random mutagenesis was applied to the heme domain. Improvements in activity, however, were hard to achieve, and mutations were repeatedly identified in the active site. This led us to investigate further the active site. At first, two active-site residues were chosen based on the crystal structure and prior research for saturation mutagenesis and site-directed mutagenesis. The resulting mutants oxidize *n*-alkanes, including propane, to the corresponding alcohols at high rates (up to 660 min⁻¹) and product turnovers (thousands per active site). It was further observed that the regioselectivity of these mutants was significantly altered by introducing mutations in the active site, with the 2-alkanol being the major product isomer. Matthew W. Peters made the remarkable observations that linear alkanes were hydroxylated enantioselectively; this was the first report of enantioselective hydroxylation of linear alkanes.

The success of applying mutagenesis directly to the active site encouraged us to investigate further the role of specific active site residues. Chapter 3 describes the generation of saturation mutagenesis libraries of 11 key active site residues. These were

chosen for their proximity to the bound fatty acid substrates co-crystallized with BM-3 heme domain in published crystal structures. Unexpectedly, a large fraction of mutants remained folded and active towards at least one of two screening substrates, hexyl methyl ether and dimethyl ether. The most active mutants were then recombined to generate a library of approximately 9,000 P450 BM-3 variants, each of which contains a characteristic active site. 17 mutants with significantly increased alkane hydroxylation activity were further analysed. Each of these mutants produced a distinct mixture of product regioisomers. Remarkably, and this is detailed in Chapter 4, one of the mutants was able to catalyze the terminal hydroxylation of octane. This had never before been observed in a P450 BM-3 variant.

The regio- and enantioselective hydroxylation of non-activated carbon atoms is a highly useful reaction in organic chemistry. The synthesis of chiral alcohols that can be used as synthons or pharmaceutical intermediates has received much attention in recent years, but still remains a challenge in synthetic chemistry. Cytochromes P450 catalyze the selective hydroxylation of a wide variety of substrates, often with high regio- and enantioselectivity. The fact that P450s are involved in the degradation of most drug compounds currently on the market makes them well-suited candidates for this application. To access these activities, it is necessary to identify a highly active and robust P450 with the desired substrate specificity. These demands, however, were not targeted during the natural evolution of enzymes, therefore making it necessary to improve upon existing ones. In Chapter 5, the application of active site variants of P450 BM-3 for the regio- and enantioselective hydroxylation of compounds differing

remarkably from linear alkanes is described. P450 mutants with modified active sites were tested for their ability to hydroxylate the achiral carboxylic acid derivative 2-cyclopentanebenzoxazole. This work was done in collaboration with Anna de Raadt (TU Graz, Austria) who had previously used this derivative to make carboxylic acid compounds amenable to enzymatic hydroxylation reactions. Mutants previously identified for the efficient and selective conversion of linear alkanes also proved to be useful hydroxylation catalysts for this compound. We anticipate that a vast variety of substrates can be hydroxylated regioselectively by at least one of the variants.

The main goal of this research, selective hydroxylation of methane or ethane, was partially achieved: The active site variant with the highest activity towards propane was subsequently examined for its ability to hydroxylate ethane. In Chapter 6, the first cytochrome P450 that selectively converts ethane to ethanol is described. This is also the first report of a porphyrin-based catalyst for this reaction. The limited productivity of the enzyme (50 turnovers per active site) was further improved by evolving the reductase domain. The resulting enzyme catalyzes at least 250 turnovers of ethane to ethanol, with no overoxidation, at room temperature and pressure, using oxygen from the air. This is a key step towards P450-catalyzed methane oxidation that would open new opportunities the bioconversion methane to fuels and chemicals.

Chapter 7 provides a discussion of the protein engineering strategy chosen for this research and proposes future experiments aimed at overcoming some of the problems and limitations associated with it. Finally, Chapter 8 details experimental procedures used throughout the studies described in this thesis.

TABLE OF CONTENTS

	PAGE
ACKNOWLEDGEMENTS	iii
ABSTRACT	vi
THESIS SUMMARY	viii
TABLE OF CONTENTS	xiv
LIST OF TABLES	xix
LIST OF FIGURES	xxi
NOMENCLATURE	xxiii
CHAPTER	
1. Enzymatic Alkane Oxidation by Heme- and Non-Heme Oxygenases	1
A. Introduction	2
B. Organisms that Grow Aerobically on Alkanes	4
B.1. Methanotrophs	5
B.2. Gaseous Alkane Utilizers	6
B.3. Microorganisms that Grow on Liquid Alkanes	8
C. Alkane Oxidizing Enzymes	10
C.1. Methane Monooxygenases	11
C.2. Alkane Hydroxylase	12
C.3. Cytochrome P450	13
C.3.1. The Catalytic Cycle	15
C.3.2. Common P450 Catalyzed Reactions	17
C.3.3. Less Common P450 Catalyzed Reactions	19
D. Engineering Cytochromes P450	19
D.1. Substrate Selectivity and Regioselectivity of Mammalian P450s	19

D.2. Substrate Selectivity and Regioselectivity of Bacterial P450s	21
D.2.1. P450cam.....	22
D.2.2. P450 BM-3	24
D.2.2.1. Substrate Specificity and Regioselectivity of P450 BM-3....	26
D.2.2.2. Electron Transfer in P450 BM-3.....	30
D.2.2.3. Peroxide Drive Catalysis.....	33
E. References	35
 2. Regio- and Enantioselective Alkane Hydroxylation with Engineered Cytochromes	
P450 BM-3	48
A. Abstract	49
B. Introduction	50
C. Results and Discussion.....	52
C.1. Previous Work.....	52
C.2. Alkane Hydroxylation Reactions	54
C.3. Directed Evolution	56
C.4. Site-Directed Mutagenesis	61
C.5. Recombination	64
C.6. Coupling of NADPH Reducing Equivalents to Product Formation	66
C.7. Whole-Cell Biotransformations	69
D. Conclusions.....	71
E. References	72
 3. Active Site Engineering of Cytochrome P450 BM-3	77
A. Abstract	78
B. Introduction	79
C. Results	81
C.1. Screening for Alkane Hydroxylation Activity	81
C.2. Construction of Active Site Saturation Mutagenesis Libraries of 9-10A	84

C.3. Active Site Saturation Mutagenesis Library Folding Data	86
C.4. Active Site Saturation Mutagenesis Library Screening Data.....	87
C.5. Improved Mutants Selected from Saturation Mutagenesis Libraries.....	90
C.6. Recombination of Active Site Mutations	96
C.7. Characterization of Active Site Mutants	97
D. Discussion	98
E. References	105
 4. Engineered Cytochrome P450 BM-3 Variants with Terminal Hydroxylation	
Activity	109
A. Abstract	110
B. Introduction	111
C. Results and Discussion.....	113
C.1. Properties of Improved Mutants and Correlation With Screening Data	113
C.2. Regioselectivity of Mutant 77-9H on n-Alkanes and Fatty Acids	117
C.3. Total Turnover Numbers, Rates, and Coupling Efficiency.....	121
D. Conclusions.....	124
E. References	125
 5. Regio- and Enantioselective Hydroxylation of an Achiral Cyclopentanecarboxylic Acid Derivative with Engineered Cytochromes P450 BM-3	129
A. Abstract	130
B. Introduction	131
C. Results and Discussion.....	134
C.1. Whole-Cell Biotransformation.....	134
C.2. Characterization of Purified Enzymes.....	135
D. References.....	141
 6. Direct Conversion of Ethane to Ethanol by Engineered Cytochrome P450 BM-3	143
A. Abstract	144

B. Introduction	145
C. Results and Discussion.....	148
D. References.....	162
7. Discussion of the Engineering Strategy.....	165
A. Random vs. Targeted Mutagenesis	166
B. Single vs. Multiple, Simultaneous Substitutions.....	166
C. Alternative Strategies	168
D. Selection Systems for Identifying P450 Alkane Hydroxylases	169
E. References	171
8. Materials and Experimental Procedures	172
A. Reagents	173
B. Expression of P450 BM-3	174
C. Purification of P450 BM-3	174
C.1. Single-Step Purification of P450 BM-3	174
C.2. Four-Step Purification of P450 BM-3	175
D. Library Generation of P450 BM-3 Mutants and Site Directed Mutagenesis.....	177
D.1. Recombination of P450 BM-3 Variants.....	177
D.2. Random Mutagenesis of P450 BM-3	177
D.3. Site-Directed/Saturation Mutagenesis.....	178
D.4. Recombination of P450 BM-3 Variants.....	178
D.5. Random Mutagenesis of Variant 1-12G	179
D.6. Construction of Saturation Mutagenesis Libraries.....	179
D.7. Construction of Recombination Libraries.....	181
D.8. Construction of the Reductase Library	183
D.9. Construction of F87A Variants of Wild-Type BM-3 and Variant 9-10A....	184
E. High-Throughput Screening of P450 BM-3 Mutant Libraries.....	184
E.1. Preparation of Cell Lysates for High-Throughput Screening.....	184

E.2. High-Throughput Protein Folding Assay	185
E.3. High-Throughput NADPH Consumption Assay	186
E.4. High-Throughput Product-Formation Assays	187
F. Determination of NADPH Consumption Rates	188
G. Alkane Hydroxylation Reactions	188
G.1. Linear Alkanes (C5 to C10)	188
G.2. Chiral Analysis of Alkane Reactions	191
G.3. Propane Hydroxylation Reactions	192
G.4. Ethane Reactions	194
H Fatty Acid Hydroxylation Reactions	195
I. Hydroxylation Reaction of 2-Cyclopentanebenzoxazole	196
J. Gas Chromatography	198
J.1. Linear Alkanes Oxidation Products(C5 to C10)	198
J.2. Chiral Analysis of Alkane Reactions	199
J.3. Gaseous Alkanes (C1 to C4) Oxidation Products	199
J.4. Fatty Acid Hydroxylation Products	200
J.5. Hydroxylation Reactions of 2-Cyclopentanebenzoxazole	201
K. Overoxidation of Ethanol by BM-3 Variant 53-5H	201
L. Absorption Spectra of BM-3 Variants 1-12G, 53-5H and 35-E11	202
M. Whole-Cell Reactions	203
N. References	204

APPENDICES

A. Stability of Cytochrome P450 BM-3 Alkane Hydroxylase Mutants	206
B. Sequences of Wild-type and Mutant Cytochromes P450 BM-3 and pCWori Vector	213
C. Activity Profiles of Saturation Mutagenesis Libraries	230
D. Materials and Methods Used by Collaborators at the TU Graz	235

LIST OF TABLES

TABLE	PAGE
1.1. Alkane hydroxylating enzymes.....	11
1.2. Common cytochrome P450-catalyzed reactions.....	18
1.3. Substrates of Engineered P450s BM-3	27
2.1. Product distributions and % ee of selected products	59
2.2. Catalytic properties of P450 BM-3 variants	60
3.1. Activities of single active site mutants towards the screening substrates DME HME.....	92
3.2. Regioselectivities, rate of product formation and total turnover numbers of octane hydroxylation reactions catalyzed by variants of BM-3 containing single active site mutations.....	93
4.1. Mutations in active site variants and activity towards the screening substrates DME and HME	114
4.2. Product distribution, rates and total turnover numbers of octane hydroxylation reactions catalyzed by variants of BM-3 containing active site mutations.....	115
4.3. Product distributions of 77-9H-catalyzed alkane hydroxylation reactions.....	117
4.4. Product distributions of 77-9H-catalyzed fatty acid hydroxylation reactions	118
4.5. Product distributions of wt F87A- and 9-10A F87A-catalyzed alkane hydroxylation reactions.....	119
4.6. Product distributions of wt F87A- and 9-10A F87A-catalyzed fatty acid hydroxylation	120
4.7. Total turnover, product formation rates, NADPH oxidation rates, and coupling efficiency of 77-9H-catalyzed alkane hydroxylations	122

5.1. Biohydroxylation of 2 with whole cell P450 BM-3 systems	134
5.2. Biohydroxylation of 2 with purified enzymes	136
5.3. Rates and total turnover numbers of P450 BM-3 catalyzed hydroxylation reactions	137
5.4. Biohydroxylation of 2 with purified enzymes with multiple active site substitutions	139
6.1. Propane hydroxylation activities of wild-type and mutant cytochromes P450 BM-3	152
6.2. Alkane hydroxylation activities of wild-type and mutant cytochromes P450 BM-3	153
6.3. Rates of NADPH oxidation by ethane hydroxylation catalysts 53-5H and 35-E11	154
A.1. Thermostability parameters for wild-type P450 BM-3 and variants selected for improved alkane hydroxylation activity	209
B.1. P450 BM-3 variants generated by random mutagenesis and recombination prior to my involvement in the project	224
B.2. P450 BM-3 variants described in Chapter 2	225
B.3. Variants of P450 BM-3 containing single active site mutations as described in Chapter 3	226
B.4. Variants of P450 BM-3 containing multiple active site mutations as described in Chapters 3, 4, and 5	227
B.5. Amino acid substitutions in reductase mutants described in Chapter 5	228

LIST OF FIGURES

FIGURE	PAGE
1.1. Metabolism of methane by methanotrophs.....	6
1.2. Metabolism of gaseous alkanes	8
1.3. Metabolism of liquid alkanes.....	10
1.4. The cytochrome P450 catalytic cycle	16
1.5. Crystal Structure of P450 BM-3	25
2.1. Dimethyl ether hydroxylation assay	57
2.2. Hydroxylation product distribution of BM-3 mutants	58
2.3. Positions of A328 and A82 in the active site of wild-type P450 BM-3	62
2.4. GC/FID analysis of the (-)-menthyl carbonate diastereomers of the 2-octanol Produced by mutant BM-3 catalyzed alkane oxidation	65
2.5. GC/FID analysis of the octane hydroxylation product using 9-10A-A328V as a) purified protein and b) a whole-cell catalyst	70
3.1. Alkylmethyl ether assays	82
3.2. Standard curves for formaldehyde and hexanal using Purpald.....	83
3.3. The active site of cytochrome P450 BM-3 showing the 11 active site residues in contact with the last eight carbon atoms of the bound fatty acid substrates.....	85
3.4. Fraction of folded proteins in the 11 saturation mutagenesis libraries	86
3.5. DME activity profile for the V78 saturation mutagenesis library	88
3.6. Fraction of folded mutants that remain active towards DME and HME in the saturation mutagenesis libraries at each of the 11 positions	89
3.7. Active site positions 78, 82 and 260, at which mutations with increased activity towards DME relative to HME were identified.....	94
3.8. Active site residues with increased activity towards HME relative to DME	95

4.1. The amount of 1-octanol formed during an octane hydroxylation reaction correlates well with the screening data	116
4.2. Regioselectivity of 77-9H-catalyzed alkane hydroxylation.....	117
4.3. The coupling efficiency ((product formation rate) / (NADPH oxidation rate)) correlates with the product formation rate	123
5.1. The conversion of carboxylic acid 1 to product 4 employing the docking/protecting group concept.....	132
5.2. Structure of carbovir	133
6.1. Reduction of substrate size and increase in C-H bond dissociation energy achieved by directed evolution	148
6.2. UV/VIS Spectra of P450 BM-3 mutant 1-12G in its unbound, low-spin configuration, and in its high-spin configuration in ethane-saturated buffer.....	150
6.3. Final ethanol concentrations in 53-5H and 35-E11 catalyzed reactions.....	155
6.4. Gas chromatograms of ethanol reaction mixtures using variant 53-5H as the catalyst.	156
6.5. ¹³ C NMR spectrum of singly ¹³ C-labeled ethanol incubated with 53-5H and an NADPH regeneration system in 0.1M potassium phosphate buffer, pH 8.0, with 10% deuterium oxide added.....	157
6.6. Absorption spectrum of 53-5H	160
B.1. Nucleotide sequence of full-length, wild-type cytochrome P450 BM-3	216
B.2. Amino acid sequence of full-length, wild-type cytochrome P450 BM-3	218
B.3. Nucleotide sequence of the pCWori vector containing wild-type cytochrome P450 BM-3 (pBM3_WT18-6)	219
B.4. Plasmid map of pCWori vector containing wild-type P450 BM-3 (pBM3_WT18-6)	223
C.1. Activity profiles of saturation mutagenesis libraries.....	231

ABBREVIATIONS

NADH	Nicotinamide adenine dinucleotide, reduced form.
NAD⁺	Nicotinamide adenine dinucleotide, oxidized form.
NADPH	Nicotinamide adenine dinucleotide phosphate, reduced form.
NADP⁺	Nicotinamide adenine dinucleotide phosphate, oxidized form.
FAD.	Flavin adenine dinucleotide.
FMN	Flavin mononucleotide.
MMO	Methane Monooxygenase.
DME	Dimethyl ether
HME	Hexyl methyl ether

C h a p t e r 1

Enzymatic Alkane Oxidation by Heme- and Non-Heme Oxygenases

A. Introduction

Petroleum and natural gas compounds are the cheapest and most abundant hydrocarbons available. Due to the lack of catalysts for the selective activation of the notoriously inert C-H bonds, these hydrocarbon sources cannot be converted directly into more valuable products. Instead, they are either used as fuels to produce energy, or are converted to more reactive alkenes by energy-intensive high temperature, endothermic processes, such as dehydrogenation or cracking. These processes also produce unwanted and often environmentally hazardous side products [1-3]. The ability to perform direct and selective activation of alkanes to high value products such as alcohols, ketones, amines or acids would allow more efficient utilization of the hydrocarbon feedstocks.

Natural gas reserves, including methane hydrates, are thought to be twice as large as known oil reserves [4]. In addition to these reservoirs, methane is constantly produced by methanogenic organisms capable of reducing carbon dioxide to methane. A large portion of gaseous methane cannot be used as fuel due to the economic and practical limitations of current methods of safe transport and storage on a large scale. Some of these problems could be solved by the efficient conversion of these methane resources into liquid methanol. Existing methods to do this on a large scale are energy-intensive, multi-step processes that are uneconomical for use of methanol as a fuel. Efficient methods for direct conversion of methane to methanol are intensively sought after because these would be energetically much more efficient [3,5].

Alkanes are among the least reactive of organic compounds, and are inert even to common acids or bases, or common oxidizing or reducing agents [6]. This lack of chemical reactivity arises from the high bond energy of C-C and C-H bonds. Alkanes do, however, react with oxygen at high temperature, yielding carbon dioxide and water. This reaction is thermodynamically favored over selective oxidation stopping at one of the first stages of the reaction (e.g., at the alcohol), because the oxidation products have more reactive C-H bonds than the alkane itself [7]. The regioselectivity of the oxidation reaction is typically governed by the relative bond dissociation energies; i.e., tertiary and secondary carbon atoms are favored over primary carbon atoms. Therefore, the terminal (i.e., methyl carbon) hydroxylation of linear alkanes is disfavored and regioselective oxidation (i.e., oxidation of a specific C-H bond) of alkanes is difficult because the C-H bonds of the methylene groups are very similar in energy. Functionalization of alkane C-H bonds to yield the respective alcohols or acids is highly desirable and would have far reaching economic implications. Such methods are, however, are not generally available.

The functionalization of alkanes has received much attention in recent years. Major advances toward transformation of alkane C-H bonds have been achieved using transition metal catalysts [8], but these reactions are generally only possible in organic solvents and are water and/or air sensitive. Nature has provided examples of efficient alkane functionalization achievable under environmentally benign conditions. The advantages of such biological processes lie in the ability of enzymes to catalyze selective alkane oxidation reactions under mild temperatures and pressures, using dioxygen or peroxide as the oxidant, and producing no side-products other than water. A biotechnological process in

which enzymes are used as catalysts to activate alkanes would lead to reductions in energy and toxic waste products while simultaneously increasing the safety of the process.

Several enzymes abundant throughout nature have been reported that are able to catalyze these difficult reactions. Monooxygenases are a class of enzymes capable of inserting an oxygen atom into a wide variety of substrates. Three distinct types of monooxygenases are utilized by a variety of organisms to active alkanes: diiron monooxygenase enzymes, such as soluble methane monooxygenase (sMMO) and alkane hydroxylase (AlkB); copper containing monooxygenases, such as the particulate methane monooxygenase; and cytochromes P450. Several recent review articles focus on the biochemistry and mechanism of these enzymes [9-12]. In this chapter, we will briefly review the organisms that utilize these enzymes for alkane assimilation and the enzymes themselves. Particular emphasis will be placed on cytochromes P450, especially bacterial ones and prior work focused on engineering cytochromes P450.

B. Organisms that Grow Aerobically on Alkanes

Several microorganisms have been found to aerobically utilize alkanes of various chain lengths. In the first step, they oxidize *n*-alkanes to the corresponding primary or secondary alcohols by terminal (i.e., methyl carbon), subterminal (i.e., methylene carbon) or biterminal (i.e., methyl carbons at both ends) oxidation. Methane-oxidizing bacteria, methanotrophs, are capable of utilizing methane as a growth-supporting alkane [13]. The other gaseous alkanes (C₂-C₄) also support growth of alkane-oxidizing bacteria [14], as do

medium (C5-C12) to long chain (C10-C20) alkanes [10]. The groups of alkane utilizing organisms are briefly reviewed below. Most previous studies in this area have focused on the isolation and characterization of the organisms themselves. Considerably less is known about the enzymes involved in the first alkane oxidation step.

B.1. Methanotrophs

Methanotrophic bacteria are unique in their ability to utilize methane as their sole carbon and energy source. Methanotrophs have been classified in six different genera: *Methylococcus*, *Methylomicrobium*, *Methylobacter*, *Methylomonas*, *Methylocystis*, and *Methylosinus* [13]. Their defining characteristic is the use of enzymes known as methane monooxygenases to catalyze the oxidation of methane to methanol. All methanotrophs can produce a membrane-bound particulate form of MMO (pMMO) while only some methanotrophs can additionally produce a soluble form of MMO (sMMO) under conditions of copper limitation [15]. Methanol is further oxidized to formaldehyde, formate and finally CO₂ (Figure 1.1), generating two equivalents of NADPH, one of which is utilized by MMO, the other of which is fed into the respiratory chain to support generation of ATP. A fraction of the formaldehyde is not further oxidized but instead used to synthesize cell material [16].



Figure 1.1. Metabolism of methane by methanotrophs. Methane is oxidized by a methane monooxygenase, forming methanol (1). The second oxidation step involves oxidation of methanol to formaldehyde, which is catalyzed by a pyrroloquinoline (PQQ) dependent methanol dehydrogenase (2). Formaldehyde is further oxidized to formate by formaldehyde dehydrogenase (3), and formate is finally oxidized to carbon dioxide by formate dehydrogenase (4).

B.2. Gaseous Alkane Utilizers

Microorganisms that assimilate gaseous hydrocarbons other than methane (ethane, propane, butane) as a source of carbon and energy have been known for a long time. Initial interest arose due to the possibility of producing biomass from natural gas components other than methane. In the 1970s and 1980s, substantial research focused on isolating bacterial strains capable of growing on gaseous alkanes. Since then, several such microorganisms have been isolated, and are reviewed in [14]. These are mainly species belonging to the Gram positive bacteria *Corynebacterium*, *Nocardia*, *Mycobacterium*, *Rhodococcus*, *Arthrobacter*, *Brevibacterium* [17-21], but Gram negative bacteria such as certain *Pseudomonas* species have also been isolated [18]. Fungi that utilize gaseous alkane have been reported as well. Species of *Acremonium*, *Allescheria*, *Candida*,

Fusarium, *Graphium*, *Penicillium* and *Phialophora* have been shown to utilize C2 to C4 *n*-alkanes [22-25].

Fundamental knowledge of the monooxygenases involved in the first alkane oxidation step of C2 to C4 gaseous alkanes remains scant. Propane monooxygenases from *Rhodococcus* species have been described and evidence exists that these enzymes are not a cytochrome P450 monooxygenase [20,26-28]. Propane oxidation in a *Gordonia* strain is catalyzed by an NADH-dependent multi-component enzyme system belonging to the family of non-heme diiron monooxygenases [29]. Also, in at least three cases, the sequences of butane monooxygenases have been found to align most closely with non-heme diiron monooxygenases [30-32].

A variety of degradative pathways for gaseous alkanes hydroxylated by a monooxygenase at the terminal and subterminal carbon have been proposed. Ethane, propane and butane are each metabolized differently, also depending on whether the alkane is oxidized terminally or subterminally (Figure 1.2). Pathways originating from terminal alcohols are well understood. In general, the primary alcohol is oxidized to an aldehyde, which is then subsequently converted to acetyl- or propionyl-CoA. Subterminal oxidation of propane and butane has also been observed. The pathways for metabolizing these molecules are not well understood. In the case of 2-propanol, for example, several pathways have been proposed for the further metabolism [14].

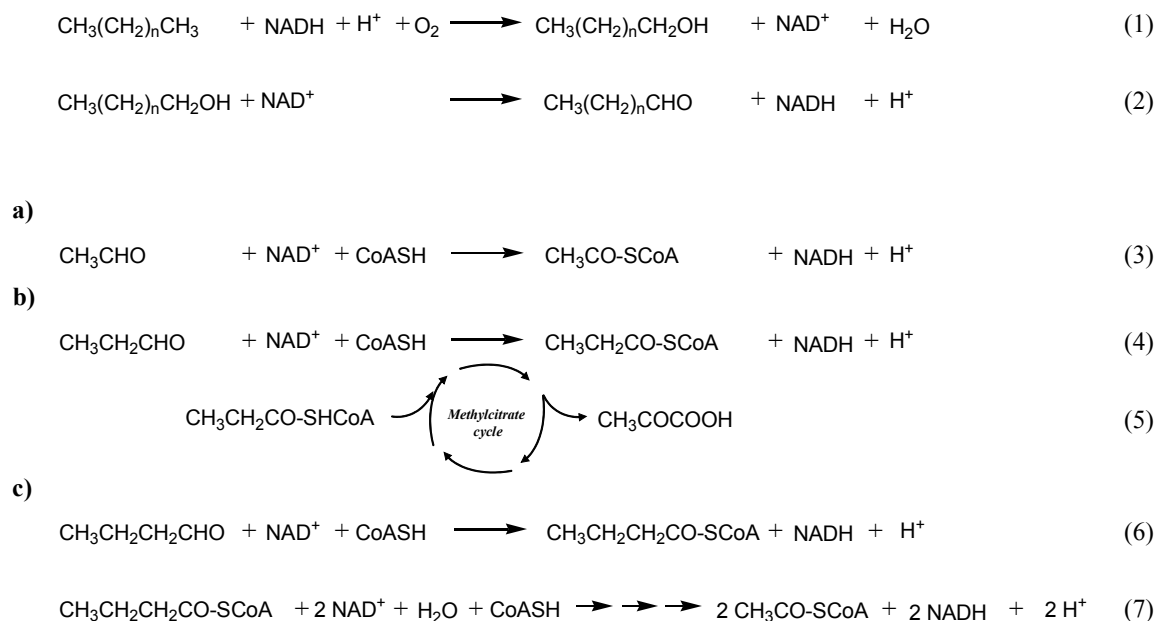


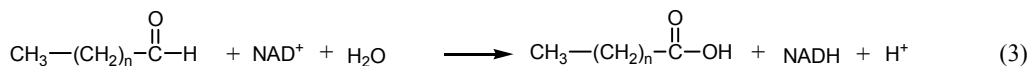
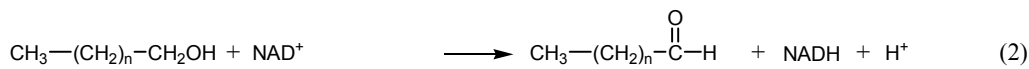
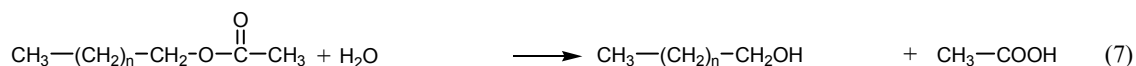
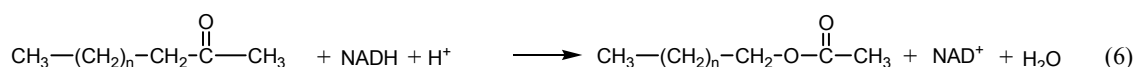
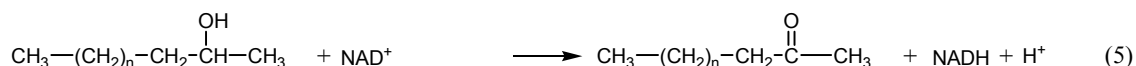
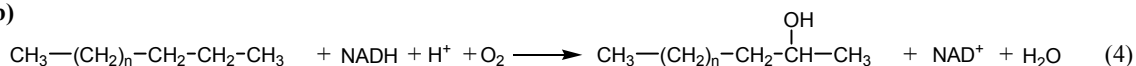
Figure 1.2. Metabolism of gaseous alkanes. The alkane (C2 to C4) is hydroxylated by a monooxygenase to form a terminal alcohol (1) which is subsequently oxidized by an alcohol dehydrogenase to the aldehyde (2). Depending on the carbon length, further metabolism proceeds differently. **a)** Acetaldehyde is directly converted to acetyl-CoA (3) and then oxidized further via the Krebs-cycle. **b)** Propionaldehyde is converted to propionyl-CoA (4). Several pathways have been proposed for propionyl-CoA [33]. One of them involves conversion to pyruvate via the methylcitrate cycle (5) [34]. **c)** Butyraldehyde is converted to butyryl-CoA (6) and subsequently oxidized via the β -oxidation pathway to yield two molecules of acetyl-CoA (7).

B.3. Microorganisms that Grow on Liquid Alkanes

Organisms that utilize liquid alkanes (C5 to C12) and their corresponding enzyme systems have been studied in more detail. *Pseudomonas putida* is capable of growing on n-alkanes and was found to contain an alkane hydroxylase system [35,36]. The substrate range includes straight-chain, branched, and cyclic alkanes and fatty acids [37]. The hydroxylase part of this system is a non-heme diiron monooxygenase. Homologous proteins have been

identified in species of alkane utilizing bacteria of the genera *Acinetobacter*, *Alcanivorax*, *Burkholderia*, *Mycobacterium*, *Pseudomonas* and *Rhodococcus*. While the *Pseudomonas putida* alkane hydroxylase system primarily acts on C5 to C12 alkanes, most of these homologous enzymes hydroxylate alkanes of more than 10 carbon atoms [38].

Several alkane assimilating yeasts have been reported, such as *Candida maltosa*, *C. tropicalis*, *C. apicola*, *Yarrowia lipolytica* and *Debaryomyces hansenii*, that utilize a cytochrome P450 for the oxidation of *n*-alkanes [39-41]. These yeasts utilize cytochromes P450 of the CYP52 family for alkane degradation by ω -hydroxylation. Reports of bacteria that utilize P450s for the degradation of *n*-alkanes are not as frequent. An octane assimilating *Corynebacterium* was reported by Cardini et al. that utilizes a P450 system for the first oxidation step [42]. And a new bacterial class of P450s was cloned from *Acinetobacter calcoaceticus* grown on *n*-hexadecane [43]. The further metabolism of alkanes is described in Figure 1.3 (see captions for details) [16].

a)**b)**

Scheme 1.3. Metabolism of liquid alkanes. **a)** The alkane is hydroxylated by a monooxygenase to form a terminal alcohol (1) which is subsequently oxidized to the aldehyde (2) and the carboxylic acid (3) by an alcohol dehydrogenase and an aldehyde dehydrogenase, respectively. The carboxylic acid is then metabolised via the β -oxidation pathway. **b)** The alkane is hydroxylated by a monooxygenase to form subterminal oxidation products (4). These are further oxidized to a ketone by a alcohol dehydrogenase (5) and subsequently converted into an acetyester by a second monooxygenase (6). The acetyester is hydrolyzed by an acetylerase to form acetate, which is further converted to acetyl-CoA and oxidized via the Krebs cycle, and a primary alcohol, which is oxidized as in (1).

C. Alkane Oxidizing Enzymes

The enzymes utilized by the organisms described above have generally not been purified, cloned or characterized. Previous research has focused on four distinct enzymes, listed in Table 1.1. Enzyme systems identified in other alkane assimilating microorganisms appear to be homologs of these.

Table 1.1. Alkane hydroxylating enzymes [44].

Enzyme (EC number)	Microorganism	Substrates	Active Site
pMMO (1.14.13.25)	All methanotrophs	C1-C5 linear alkanes	Copper cluster
sMMO (1.14.13.25)	<i>M. capsulatus</i> , <i>M. trichosporium</i> , <i>Methylosinus sporium</i> , <i>Methylocystis spp.</i> , <i>Methylomonoas methanica</i>	C1-C7 linear and branched alkanes	Diiron cluster
Alkane Hydroxylase (1.14.15.3)	<i>Acinetobacter spp.</i> , <i>Alcanivorax spp.</i> , <i>Burkholderia spp.</i> , <i>Mycobacterium spp.</i> , <i>Pseudomonas spp.</i> , <i>Rhodococcus spp.</i>	C5-C24 alkanes	Diiron cluster
Cytochrome P450 (1.14.14.1)	<i>Bacillus megaterium</i> , <i>Candida spp.</i> , <i>Acinetobacter spp.</i>	C6-C12	Heme

C.1. Methane Monooxygenases

Methane monooxygenases (MMO) are the only enzymes known capable of efficiently catalyzing oxidative cleavage of the extremely stable C-H bond of methane. All methanotrophs can produce a membrane-bound, particulate form of MMO (pMMO) while only a subset of methanotrophs can produce a soluble form of MMO (sMMO) which is produced under conditions of copper limitation [15].

Soluble methane monooxygenase has been purified and is well characterized. It consists of three protein components: a hydroxylase (245 kDa) containing a binuclear iron cluster that is the active site of MMO, an NADH-dependent reductase (40kDa), containing FAD and a [2Fe-2S] cluster, and a regulatory subunit (16 kDa). It exhibits broader substrate specificity

than pMMO, and can accept substrates such as alkenes, aromatic and heterocyclic compounds [45]. In contrast to sMMO, pMMO is produced under conditions of copper sufficiency in methanotrophs. It has a narrower substrate range than sMMO, but can still catalyze the co-oxidation of alternative substrates, including propane and butane [10,11]. pMMO consists of three polypeptides with molecular masses of 47, 27 and 25 kDa and is arranged as an $\alpha_3\beta_3\gamma_3$ trimer. The crystal structure of pMMO was solved recently [46] and revealed two metal centers, modelled as mononuclear and a dinuclear copper centers. The active site in which methane is oxidized was, however, not identified.

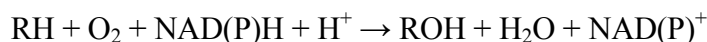
C.2. Alkane Hydroxylase

Biochemical and genetic studies have thus far focused on a very limited number of alkane hydroxylases, such as the *Pseudomonas putida* GPo1 alkane hydroxylase [47], which facilitates growth on C4 to C12 *n*-alkanes by oxidizing them to terminal alcohols, thereby allowing the host to grow on these compounds. Only recently has it become apparent that this enzyme is the prototype of a very diverse collection of related non-heme iron integral membrane oxygenases, reviewed in [10]. The *P. putida* GPo1 alkane hydroxylase system consists of three components: alkane hydroxylase (AlkB), rubredoxin (AlkG), and rubredoxin reductase (AlkT). AlkB is a non-heme iron integral membrane protein that carries out the hydroxylation reaction [37,48,49]. Rubredoxin transfers electrons from the NADH-dependent flavoprotein rubredoxin reductase to AlkB. The molecular genetics of this enzyme system has been reviewed recently [50]. Genes that

related to the alkane hydroxylase gene (*alkB*) of GPo1 have been detected in several species of Gram-positive and negative bacteria [51,52].

C.3. Cytochrome P450

Cytochromes P450 are a large superfamily of heme proteins found in all domains of life that, as a whole, perform a diverse array of redox chemistries on an extremely wide variety of substrates. Most P450s are NADPH-dependent monooxygenases, introducing an oxygen atom from dioxygen into non activated carbon atoms to yield often optically pure products according to reaction:



Less common reactions catalyzed by these versatile enzymes include, but are not limited to, alkene epoxidation, amine and thioether oxidations, dealkylation of amines, ethers, and thioethers, oxidative and reductive dehalogenations, and dehydrogenations. P450s are used for the catabolic degradation of alkanes and aromatics in bacteria, drugs and xenobiotics in animals, and herbicides (both natural and synthetic) in plants. Additionally, key steps in the biosynthesis of physiologically important compounds, such as steroids, fatty and bile acids, eicosanoids, and fat-soluble vitamins, are catalyzed by P450s. The ability of the P450 platform to accommodate different substrates and chemistries has been repeatedly demonstrated by nature, providing much inspiration both to biochemists trying to

understand how these systems work, and to protein engineers trying to introduce new activities into this malleable platform.

Cytochrome P450s (CYPs) were first discovered in the 1960s. Since then more than 3,000 different P450 genes have been described (updated regularly at <http://drnelson.utmem.edu/CytochromeP450.html>) and much has been learned about the catalytic cycle of dioxygen activation and substrate oxidation, although structure-function relationships are far from being well understood. Despite their catalytic variety, P450s all share the same reaction center: a protoporphyrin-IX-coordinated iron (i.e., heme) with a distal cysteinate as its fifth ligand. The sixth coordination site on the iron is used to bind molecular oxygen upon the reduction of the iron to its ferrous state upon substrate binding [53]. Carbon monoxide bound to this iron center (reduced *in vitro* with dithionite) has an absorption maximum at 450 nm, giving P450s (pigment 450) their name. The superfamily of P450 proteins (and their respective genes) is divided into families, subfamilies and individual members according to the similarity in their primary structure. A new nomenclature has been introduced where CYP is used to characterize the respective P450 as a heme protein. The first Arabic number defines the gene family, the following letter the subfamily and the second number the individual enzyme, e.g., CYP1A1 for cytochrome P4501A1 (previously P450c). Members of the same gene family are defined as usually having $\leq 40\%$ sequence identity to a P450 protein from any other family. Mammalian sequences within the same subfamily are always $> 55\%$ identical. The numbers of individual P450s in a species differs widely.

The mechanism of dioxygen activation at the heme is the same in most P450s, the chemical promiscuity of this family being determined mostly by the shape and polarity of the substrate-binding pocket used to position the substrate above the heme. In this chapter, the diversity of P450-catalyzed reactions is illustrated and site-directed mutagenesis studies that have provided much of our present knowledge about how these systems work are detailed. In light of these facts, the engineering of a few P450s to accept novel substrates, to change their regio- and stereoselectivity of substrate hydroxylation, and to alter their protein-protein interactions and electron transfer processes are described. Recent review articles provide detailed discussions on protein engineering of P450s [54], and their general application [55] and utilization as biocatalysts [56,57].

C.3.1. The Catalytic Cycle

The catalytic cycle of cytochromes P450 generally starts with binding of substrate (Figure 1.4), inducing a change in spin state of the ferric heme iron from low to high spin and leaving the heme iron in a pentacoordinated state with higher reduction potential. This makes possible the introduction of the first electron from NAD(P)H via an electron transport chain, reducing the heme iron to ferrous iron. Next, oxygen binds, yielding an unstable ferrous-dioxy species, which is capable of accepting the second electron to produce a ferric peroxy anion. In the next steps, the ferric peroxy anion is protonated to ferric hydroperoxy complex, which undergoes subsequent heterolytic cleavage with the

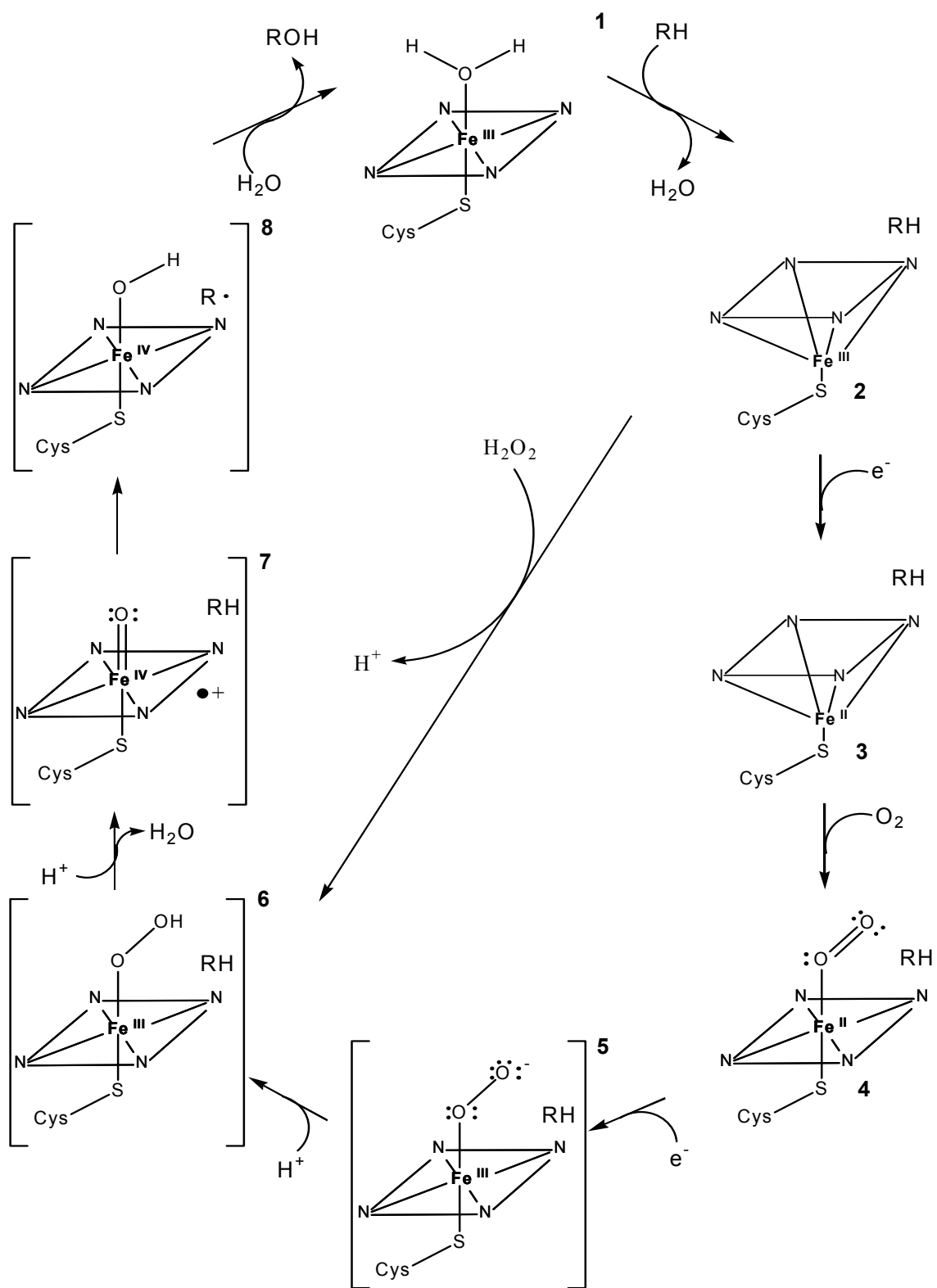


Figure 1.4. The cytochrome P450 catalytic cycle. See main text for details.

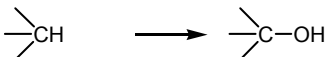
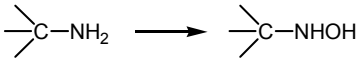
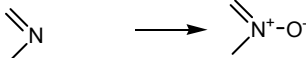
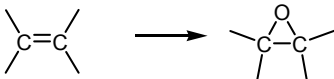
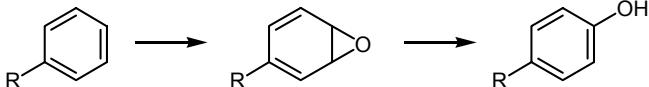
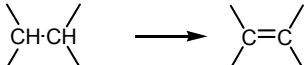
formation of a putative ferryl species, formally equivalent to a Fe(V)=O species (Compound I). Crystallographic measurements of P450 intermediates are consistent with the formation of an oxyferryl intermediate [58]. This species (or a similar reactive, electrophilic iron-oxo intermediate) then attacks the substrate, yielding the hydroxylated product which dissociates to let the cycle start again. Interestingly, in many, but not all P450s, a so-called "shunt" reaction can proceed, where the substrate can be hydroxylated directly by peroxides such as hydrogen peroxide, cumene hydroperoxide and *tert*-butyl hydroperoxide without the necessity of stepwise activation of molecular oxygen and interaction with an electron donating systems [59]. Most reactions catalyzed by P450s appear to be consistent with this catalytic cycle and are briefly presented below.

C.3.2. Common P450 Catalyzed Reactions

The iron-oxo species described above is responsible for most P450 catalyzed reactions (Table 1.2). This electron deficient intermediate is sufficiently reactive to insert its oxygen into inert C-H bonds, yielding an alcohol from an alkane in the most common case. The similar hydroxylation of a carbon atom α to a heteroatom leads to O-, N-, or S-dealkylations. The active oxygen can also be used for the two-electron oxidation of S, N, P, and I atoms in organic compounds to form sulfoxides, N-oxides and hydroxides, phosphine oxides and iodoso-compounds. Another common P450 reaction on which a lot of research and engineering effort has focused is oxidation of C=C double bonds to epoxides from olefins, and arene oxides from aromatic compounds. The identity of the

oxidizing species (iron-oxo or iron-peroxo) for this reaction is still being debated. P450s can also act as dehydrogenases. In this case, the Fe(IV)-OH species is thought to abstract a hydrogen atom β to the substrate radical, instead of transferring the OH to the substrate radical. Substrate specificity and regioselectivity in all of these reactions are determined by the surrounding protein scaffold. The substrates can range in size from short linear alkanes up to large polycyclic aromatic compounds.

Table 1.2. Common cytochrome P450-catalyzed reactions [60].

C-H bond hydroxylation	
N-dealkylation	$\text{R}-\overset{\text{H}}{\text{N}}-\text{CH}_3 \longrightarrow [\text{R}-\overset{\text{H}}{\text{N}}-\text{CH}_2\text{OH}] \longrightarrow \text{R}-\text{NH}_2 + \text{H}_2\text{C}=\text{O}$
S-dealkylation	$\text{R}-\text{S}-\text{CH}_3 \longrightarrow [\text{R}-\text{S}-\text{CH}_2\text{OH}] \longrightarrow \text{R}-\text{SH} + \text{H}_2\text{C}=\text{O}$
O-dealkylation	$\text{R}-\text{O}-\text{CH}_3 \longrightarrow [\text{R}-\text{O}-\text{CH}_2\text{OH}] \longrightarrow \text{R}-\text{OH} + \text{H}_2\text{C}=\text{O}$
N-hydroxylation	
N-oxidation	
S-oxidation	$\text{R}-\text{S}-\text{CH}_3 \longrightarrow \text{R}-\overset{\text{O}^-}{\text{S}^+}-\text{CH}_3$
Alkene epoxidation	
Arene epoxidation	
Dehydrogenation	

C.3.3. Less common P450 Catalyzed Reactions

In addition to the common P450 catalyzed reactions briefly discussed above, members of the P450 superfamily are capable of a wide variety of other chemical transformations. important in the metabolism of drugs and xenobiotics. It should be noted, however, that the biological significance of these reactions is not necessarily proven. No protein engineering efforts have yet been undertaken to modify P450s involved in these reactions and thus, while they are interesting targets for future work, they are not discussed in this chapter. The list of uncommon reactions is rather long: activities such as reduction, desaturation, oxidative ester cleavage, ring expansions, ring formations, aldehyde scissions, dehydration, ipso attack, one-electron oxidations, coupling reactions, rearrangements of fatty acids and prostaglandin hydroperoxides, isomerization and phospholipase D activity have been observed. An extensive review discussing these various reactions and their proposed mechanisms was published recently [61].

D. Engineering Cytochromes P450

D.1. Substrate Selectivity and Regioselectivity of Mammalian P450s

Many of the mammalian cytochromes P450, especially those involved in metabolizing drugs and xenobiotics, exhibit broad substrate specificity, while the biosynthetically active P450s, such as the adrenal steroid hydroxylases, are rather specific. Conversion of even a small fraction of mammalian P450 systems into useful synthetic catalysts, however, is

limited by several factors: the multi-component nature of most of these enzymes (they include an NADPH reductase component with or without a separate electron transfer component and a separate hydroxylase domain), the fact that most are membrane-bound, their limited stabilities, and their generally slow rates. Many isoforms of mammalian P450s differ only in very few amino acids in the hydroxylase domain, while sharing the electron transfer systems. Crystal structures of these membrane-bound P450s are not generally available. To date, only the structures of mutants of CYP2C5 [62-64], CYP2C8 [65], CYP2C9 [66,67], CYP2B4 [68,69], and CYP3A4 [70,71] have been solved.

Biosynthetically active P450s have been investigated using site-directed mutagenesis. These studies have helped unravel the structural basis of stereo- and regioselectivity of substrate hydroxylation in some mammalian isoforms [72-75], and have provided insight into the identity of substrate recognition sites in less related P450s [73,74,76-78].

Drug-metabolizing microsomal P450s have also been investigated using site-directed mutagenesis, capitalizing on the similarity of these enzymes among different species. The results have been reviewed recently [79]. Most of the residues studied in these experiments are located in one of the so-called SRSs (substrate recognition sites), identified by Gotoh [80] on the basis of sequence comparison between the CYP2 family members and the structurally characterized bacterial P450_{cam} (CYP101). In some cases, chimeragenesis was applied to define regions of related P450s that are responsible for substrate specificity. The results, which have been summarized in a recent review by Domanski and Halpert [79], have added considerably to our understanding of the role of specific residues in substrate binding and substrate specificity in these mammalian P450s.

The rational engineering of the substrate access channel of a protein for new substrates requires dynamic and structure-function information about the protein, information that is often missing. An approach for obtaining proteins (especially poorly characterized ones) with new activities is to select them from libraries generated by random mutagenesis of key residues. For example, Nakamura et al. [81] applied random mutagenesis to the substrate recognition sequences (SRS) of the indole-hydroxylating CYP2A6 and identified mutants that form primarily indigo from indole.

It has become apparent that active site redesign of mammalian P450s to alter the hydroxylation regioselectivity of their natural substrates, or to accept new substrates is feasible. Based on the increasing number of crystal structures and refined homology models, it is possible to study the affects of particular amino acids on substrate binding, or to engineer P450s with new activities, by identifying potentially important residues and performing mutagenesis experiments.

D.2. Substrate Selectivity and Regioselectivity of Bacterial P450s

Bacterial P450 systems generally exhibit higher catalytic rates than eukaryotic P450s and are easier to handle in the laboratory due to their solubility and high expressibility in heterologous hosts. These properties also make bacterial P450s ideal targets for protein engineering. Most work has focused on the two proteins P450_{cam} (CYP101) and P450 BM-3 (CYP102), and both have been engineered to accept a wide variety of substrates. P450_{cam}, from *Pseudomonas putida*, requires the two additional electron transfer proteins

putidaredoxin, a ferredoxin of the [2Fe-2S] type, and putidaredoxin reductase, a FAD-containing enzyme, for catalysis. P450 BM-3 from *Bacillus megaterium*, is a single polypeptide chain, comprised of a heme domain and a FAD and FMN containing NADPH-dependent reductase domain [82]. At hydroxylation rates on fatty acid substrates in the range of thousands min^{-1} , P450 BM-3 has the highest known catalytic rate of any P450. These two proteins were the first two members of the P450 superfamily of which crystal structures became available [83,84], providing research groups with some insight into their mechanisms and ideas for their rational engineering. Additional crystal structures of these enzymes bound to different substrates [85-89] and containing mutations [90-96] have become available and have contributed to this insight. Most engineering work with these systems has focussed on altering the specificity and regioselectivity of hydroxylation reactions catalyzed by these proteins.

D.2.1. P450_{cam}

The first attempts at engineering a P450 were performed with P450_{cam} which hydroxylates camphor at its 5-exo position. Based on the three-dimensional structure of substrate-bound P450_{cam} [97], active site substitutions T101M, T185F, and V247M were introduced to alter the stereochemistry and efficiency of ethylbenzene hydroxylation. The reaction of the wild-type enzyme with this substrate produces one regioisomer, 1-phenylethanol, with only 5% coupling of NADPH-consumption to product formation (i.e., 95% of reducing equivalents are nonproductively used to form hydrogen peroxide or water from dioxygen),

and a ratio of 73:27 for *R*- and *S*-alcohols, respectively. The triple mutant hydroxylates ethylbenzene to give an *R*:*S* ratio of 87:13 and a coupling of reducing equivalents to product of 13% [98]. Various mutants of Y96 (Y96A, Y96G, Y96F), which hydrogen bonds to camphor, contain active sites with improved ability to oxidize aromatic compounds such as diphenylmethane, diphenylamine, 1,1-diphenylethylene, phenylcyclohexane, naphthalene and pyrene [99-103]. Moreover, the ability of P450_{cam} to perform styrene oxidation using mutant Y87F was improved 25-fold, with a concomitant increase in coupling efficiency from 7% to 32% [104]. An additional mutation, V24L, further increased coupling efficiency to 60%, with substrate oxidation rates of approximately 100 min⁻¹ [102]. Mutations at F87 and Y96 also greatly enhanced the monooxygenase activity of P450_{cam} toward polycyclic aromatic hydrocarbons phenanthrene, fluoranthene, pyrene and benzo[α]pyrene [105], as well as for polychlorinated benzenes [106]. When the volume of the substrate binding pocket above the heme was decreased with mutant F87W, a 10-fold increase in activity with most of the polychlorinated substrates was observed. The coupling rate was increased to >90% by the addition of F98W, although the NADH-dependent reaction decreased in those mutants [107]. In an effort to engineer P450_{cam} for the selective oxidation of (+)-*R*-pinene, a structural relative to (+)-camphor, active-site mutants containing combinations of the Y96F, F87A, F87L, F87W, and V247L mutations were chosen based on the crystal structure. The most active was the Y96F/V247L mutant, with a (+)-*R*-pinene oxidation rate of 270 min⁻¹ [93]. French and coworkers improved P450_{cam} catalyzed 2-ethylhexanoic acid production from ethylhexanol. The F87W and Y96W mutations improved regioselectivity, giving almost exclusively the desired product. The T185F

mutation improved coupling of NADH to product formation, and the L244A mutation altered the stereoselectivity of 2-ethylhexanoic acid production [108]. A definitive demonstration of the flexibility of the P450 platform was provided by Bell *et al.* with the engineering of P450_{cam} to hydroxylate short-chain alkanes. In this study, the volume of the active site above the heme was decreased by introducing bulky, hydrophobic residues, with the mutant F87W/Y96F/T101L/V247L showing butane oxidation rates of 750 min⁻¹, and 95% coupling to NADH oxidation [109]. The rate of propane hydroxylation in this study was 110 min⁻¹ with 32% NADH coupling, but in a subsequent study using the mutant F87W/Y96F/T101L/V247L/L244M, this rate was increased to 170 min⁻¹ with 66% NADH coupling [93].

D.2.2. P450 BM-3

Cytochrome P450 BM-3 from *Bacillus megaterium* is a fast, water soluble, single-component fatty acid hydroxylase readily expressed in laboratory strains of *Escherichia coli*, making it an ideal candidate for protein engineering. In this P450, large structural changes are induced by substrate-binding. A hydrophobic channel between the surface of the protein and the proximal side of the heme is evident in crystal structures of P450 BM-3 (Figure 1.5). In substrate free BM-3 [84], this channel is open while structures of BM-3 complexed to palmitoleic acid [86] or N-palmitoylglycine [87] reveal a significant change upon substrate binding, involving closure of the active site channel. The conformational changes correspond to a molecular switch, in which substrate binding converts the enzyme from an inactive form to a catalytically active one [87]. The hydrophobic residues in this

channel presumably contact the substrate during catalysis and comprise the majority of residues studied by site-directed mutagenesis.

The propensity of wild-type P450 BM-3 to hydroxylate primarily fatty acids with chain lengths between C12 and C18 is reflected in the geometry of the active site. The fatty acid substrates are hydroxylated at the ω -1, ω -2 and ω -3 positions, but the regioselectivity is rather low. The exact regioselectivity of the reaction is dependent on the substrate chain length [110].

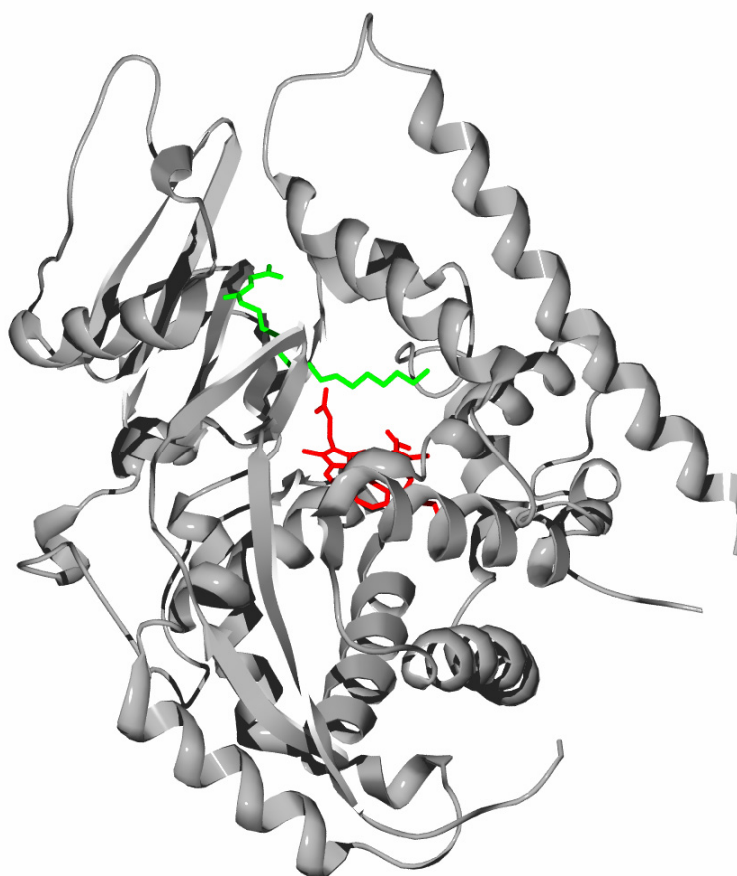


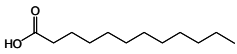
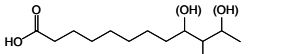
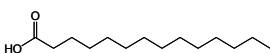
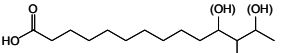
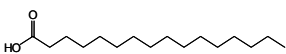
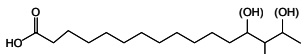
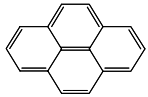
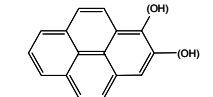
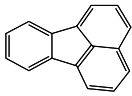
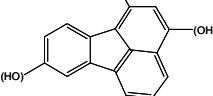
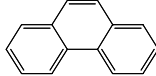
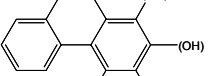
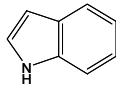
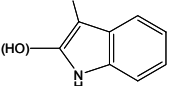
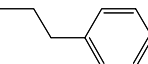
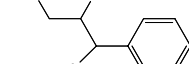
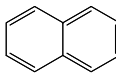
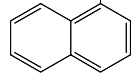
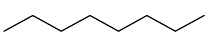
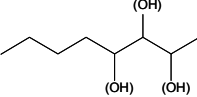
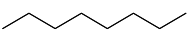
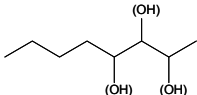

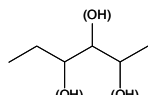
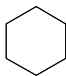
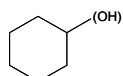
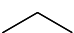
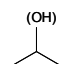
Figure 1.5. Crystal structure of P450 BM-3 (PDB access number 1JPZ [87]). The heme is shown in red, while the palmitoylglycine substrate is shown in green. The substrate is bound within a long, narrow channel that leads to the heme.

D.2.2.1. Substrate Specificity and Regioselectivity of P450 BM-3

To extend the use of this fast and efficient enzyme for biotechnology applications, various groups have focused on engineering P450 BM-3 to accept and hydroxylate a variety of substrates (Table 1.3).

In particular, active site residues that putatively contact the substrate during catalysis have been modified. The active site residue F87, one of the first residues extensively studied by site directed mutagenesis, has been shown to affect both the substrate specificity and regioselectivity of fatty acid hydroxylation. Engineering activity towards non-natural substrates, such as alkanes and arene compounds, usually involves these residues. For example, a study to define the role of F87 in the substrate access channel of P450 BM-3 was performed by Graham-Lorence et al. [119] Replacement of F87 with valine converted the enzyme into a regio- and stereoselective arachidonic acid epoxygenase. Mutants of this residue were used as the starting point for both the creation of new site-directed mutants with specificities towards other substrates, as well as the initiation of directed evolution experiments to evolve this P450 for biotechnological application (see below). The mutant F87V/L188Q/A74G was designed by saturation mutagenesis of multiple sites that were chosen based on crystallographic data. This approach, termed “rational evolution,” was used with the assistance of a *p*-nitrophenol based screen described below. The mutant was shown to oxidize indole [114] and can also hydroxylate alkanes, cycloalkanes, arenes and heteroarenes [116]. This mutant was later shown to have hydroxylation activity on polycyclic, aromatic hydrocarbons such as naphthalene, fluorene, acenaphthene, acenaphthylene and 9-methylanthracene [120].

Table 1.3. Substrates of engineered P450s BM-3

BM-3 variant	Substrate	Product	Rate [min ⁻¹]	Coupling [%]	Ref.
wt			5100	100	[111]
			2400	100	[112]
			4600	100	[82]
R47L/ Y51F/ A264G			91	5.4	[113]
			110	12.5	[113]
			19.5	6.4	[113]
F87V/ L188Q/ A74G			160	n.d.	[114]
			330	45	[115]
			n.d.	n.d.	[116]
			n.d.	n.d.	[116]
139-3			480		[117]
			n.d.		[118]
			n.d.		[118]
			12		[117]

However, coupling efficiencies for this mutant were very low – on the order of 5-15% [120]. Charmichael et al. [113] were also successful in obtaining activity towards polycyclic aromatic hydrocarbons using site-directed mutants of P450 BM-3. Their mutant R47L/Y51F/A264G displayed the highest product formation rates when phenanthrene and fluoranthrene were used as substrates, while mutant R47L/Y51F/F87A/A264G was most active towards pyrene. This study also observed very low NADPH coupling efficiencies.

Inspired by the diversity of activities supported by the P450 scaffold in nature, our laboratory has focused on engineering BM-3 to generate practical, P450-based oxidation catalysts. In particular, we are interested in creating useful biocatalysts using directed evolution as the engineering strategy for the controlled oxidation of alkanes. P450 BM-3 is particularly suited for directed evolution experiments since it is highly expressible in *E. coli*, soluble (i.e., not membrane bound), stable, fast (rates up to 3000 min⁻¹), and self-sufficient (i.e., the reductase, electron transfer, and hydroxylase components are included in a single protein). In these experiments, a library of randomly mutated P450 BM-3 proteins is generated and screened for new or improved activities. Mutants with improved activities are isolated and then used to generate new libraries. This iterative cycle continues until the desired mutant or mutants is obtained [121,122]. Ideally, the screen used to identify these new mutants should contain a colorimetric aspect dependent either directly or indirectly upon formation of the desired products. Alternatively, new mutants may be identified by increased NADPH consumption rates with a given substrate, which can be measured spectrophotometrically in a high-throughput manner using readily available plate readers. Using NADPH consumption rates as a screen is particularly useful for substrates which

cannot be examined colorimetrically, although care must be taken to ensure that NADPH oxidation is coupled to product formation. The mutations accumulated over several rounds of directed evolution often appear in unpredictable places in the protein (i.e., not in the active site), illustrating the limitations to rational approaches to protein engineering.

Schwaneberg et al. developed a product-based screen for detecting mutants with increased fatty acid hydroxylation activity using the “surrogate” substrates 8-*p*-nitrophenoxyoctanoic acid and 10-*p*-nitrophenoxydecanoic acid. These substrates release the yellow compound *p*-nitrophenolate upon hydroxylation at their terminal carbon [123]. Saturation mutagenesis of several amino acids which had previously been shown to be important in defining the substrate and regioselectivity of the enzyme led to an increase in activity towards the surrogate substrates as well the corresponding fatty acids [124].

Using a modified version of the assay described above (8-*p*-nitrophenyl octane instead of the carboxylate), Farinas et al. were able to generate mutants that oxidized *n*-octane up to five times faster than the wild-type enzyme [125]. By additionally employing a cofactor dependent screen using short alkanes as substrates, the authors generated a mutant that readily oxidized not only octane at a higher initial rate than any known alkane hydroxylase, but also propane [118]. This enzyme was also more active towards its natural substrates. Interestingly, none of the eleven amino acid substitutions were homologous to the mutations Bell et al. introduced into P450_{cam} [109] to achieve butane and propane oxidation. While the enzyme exhibited high rates of substrate hydroxylation, it was not regioselective and produced a variety of subterminal alcohols.

The engineered BM-3 mutants described above were acquired either by altering individual amino acids in the protein, or by accumulating point mutations in directed evolution experiments. An alternative method for obtaining P450s with new or altered properties is chimeragenesis, in which large portions of homologous P450s are swapped to form functional chimeras. Recombination of homologous proteins generates variants in which every amino acid substitution has already proven to be successful in one of the parents. Recently, Voigt et al. [126] developed and Meyer et al. validated [127] a structure-based algorithm SCHEMA that identifies fragments of proteins that can be recombined to minimize disruptive interactions that would prevent protein folding. Otey et al. [128] applied SCHEMA to design chimeras of P450 BM-3 and its homolog CYP102A2, sharing 63% amino acid sequence identity. Fourteen of the seventeen constructed hybrid proteins were able to fold correctly, as determined by CO difference spectra. Half of the chimeras had altered substrate specificities, while three mutants acquired activities towards a new substrate not hydroxylated by either parent.

D.2.2.2. Electron Transfer in P450 BM-3

P450 catalyzed monooxygenation reactions require two distinct electron transfer (ET) processes per substrate turnover. The first electron is used to reduce the ferric heme iron. After binding of molecular oxygen to the reduced, ferrous heme iron, the second electron is transferred to activate the O=O bond. ET between the heme and an external partner protein or domain is essential for the catalytic cycle, making its study a subject of extensive

research. Most cytochromes P450 depend on interactions with partner proteins to receive electrons for oxygen activation and substrate conversion. Class I proteins obtain electrons via a redoxin and an FAD-containing NAD(P)H-dependent reductase. Class II proteins require only the FAD/FMN-containing NADPH-P450 reductase. Other classes, e.g., those using FMN as electron donor or a [4Fe-4S] protein have been identified in bacteria by genome analysis [129]. Only a few P450s do not require additional proteins for catalysis, e.g., class III P450s such as CYP5A1 and CYP74, which employ either endoperoxide or hydroperoxide substrates; CYP55A1 (P450_{nor}, a class IV P450), which receives electrons directly from reduced pyridine nucleotides; and P450 BM-3 with its heme-containing hydroxylase domain and diflavin reductase domains fused into a single polypeptide chain.

The catalytic mechanism of diflavin reductases, in particular of P450 BM-3, has been studied in detail. Based on the observations that a) the degree of reductase reduction during catalysis does not exceed two electrons [130] b) a double semiquinone is formed [130] and c) the FMN cofactor serves as the heme reducing electron donor [130,131], the following mechanism of electron transfer from NADPH over FAD, FMN to the heme domain has been proposed [132]: NADPH binds to the cofactor binding pocket of the diflavin reductase. Next, hydride transfer from NADPH to FAD occurs, leading to a two-electron reduced hydroquinone form of FAD. Electrons from FAD are transferred to FMN separately, to form the catalytically active semiquinone form of FMN that, in the final step, transfers electrons to the heme domain. Reduction of the reductase by three electrons

inactivates the enzyme, and a four electron reduced state could not be obtained under aerobic conditions [130,133].

Electron transfer in P450 BM-3 is tightly regulated in multiple ways to ensure that electron transfer is coupled to substrate oxidation without wasting energy from NADPH and producing reactive oxygen species. First, the redox potentials of the flavins (FAD and FMN) during catalysis [134] are significantly altered compared to those calculated from equilibrium potentiometric titrations [135]. It has been proposed that conformational changes as well as NADPH binding and NADPH oxidation influence the redox properties of the cofactors [132,136]. Secondly, preincubation of P450 BM-3 with NADPH without substrate leads to a catalytically inactive, three electron reduced state of the reductase domain [130,133]. Thirdly, substrate binding perturbs the spin-state equilibrium of the heme iron in favor of the high-spin form and also increases the heme iron reduction potential by approximately 130 mV [135]. These events trigger electron transfer to the substrate bound heme and start the catalytic cycle. Later work pin-pointed the spin-shift, rather than the change in redox potential as the primary effector in activating electron transfer [95]. Substrate binding therefore acts as an enzyme activating switch.

This beautifully regulated mechanism needs to be considered when engineering P450 BM-3 for the hydroxylation of non-natural substrates. Substrates other than the favored fatty acids that do not correctly fit into the active site thus adversely affect the fine-tuned electron transfer apparatus required for catalysis. These electron-transfer difficulties are manifest as uncoupling of NADPH oxidation from substrate turnover, which can occur at various points of the electron transfer chain: If electron transfer from FAD to FMN is

disturbed, electrons could be transferred to NADP^+ . Dioxygen can potentially accept electrons from either FAD or FMN to produce superoxide or peroxide, depending on whether one- or two-electron reduction occurs (NADPH oxidase activity) [137]. In the active site, unproductive dissociation of reduced oxygen species can lead to the formation of superoxide, peroxide or water from the heme prior to reaction with substrate [53]. All this must be kept in mind when engineering a P450 for practical use, and monitoring of the coupling efficiency is a crucial aspect of any engineering approach.

D.2.2.3. Peroxide Driven Catalysis

Dependence on the expensive cofactor NADPH limits the common use of most P450s as oxidation catalysts. An inefficient peroxide shunt pathway, in which oxygen pre-reduced by two electrons to a peroxide is used for catalysis in place of dioxygen and NADPH, exists in most P450s and allows them to function without the additional cofactor and electron transport proteins. Directed evolution was used to improve peroxide driven catalysis of P450_{cam} and 102. Cirino et al. characterized hydrogen peroxide driven catalysis with the heme domain of P450 BM-3 and its mutant F87A and found that mutation F87A significantly enhances peroxxygenase activity towards medium-chain fatty acids while shifting regioselectivity away from the terminal position [138]. However, catalytic rates using hydrogen peroxide were still orders of magnitude slower than using NADPH as a cofactor. Using directed evolution, a mutant P450 BM-3 heme domain was obtained that supports the H_2O_2 -driven hydroxylation of fatty acids and epoxidation of styrene at catalytic rates and total turnover numbers improved by an order of magnitude relative to the

F87A mutant. A significant decrease in thermostability of the enzyme, however, was observed [139]. None of the nine amino acid changes in this mutant (relative to wild-type P450 BM-3) were located in the substrate binding pocket. In the first report on the thermostabilization of a P450, Salazar et al. were able to restore this loss in thermostability while maintaining its peroxxygenase activity using directed evolution [140].

E. References

1. Ishii, Y., Sakaguchi, S. & Iwahama, T. (2001). **Innovation of hydrocarbon oxidation with molecular oxygen and related reactions.** *Adv. Synth. Catal.* **343**, 393-427.
2. Olah, G. A. & Molnar, A. (1995). **Hydrocarbon chemistry**, John Wiley & Sons, Inc., New York.
3. Arakawa, H. et al. (2001). **Catalysis research of relevance to carbon management: progress, challenges, and opportunities.** *Chem. Rev.* **101**, 953-996.
4. Madigan, M. T. (2002). **Brock biology of microorganisms**. 10th edit., Pearson Education, Inc., Upper Saddle River, NJ.
5. Gesser, H. D., Hunter, N. R. & Prakash, C. B. (1985). **The direct conversion of methane to methanol by controlled oxidation.** *Chem. Rev.* **85**, 235-244.
6. Louden, M. G. (1995). **Organic chemistry**. 3rd edit., the Benjamin/Cummings Publishing Company, Redwood City.
7. Labinger, J. A. (2004). **Selective alkane oxidation: hot and cold approaches to a hot problem.** *J. Mol. Catal. A: Chem.* **220**, 27-35.
8. Labinger, J. A. & Bercaw, J. E. (2002). **Understanding and exploiting C-H bond activation.** *Nature* **417**, 507-514.
9. Baik, M. H., Newcomb, M., Friesner, R. A. & Lippard, S. J. (2003). **Mechanistic studies on the hydroxylation of methane by methane monooxygenase.** *Chem. Rev.* **103**, 2385-2419.
10. van Beilen, J. B., Li, Z., Duetz, W. A., Smits, T. H. M. & Witholt, B. (2003). **Diversity of alkane hydroxylase systems in the environment.** *Oil Gas Sci. Technol.* **58**, 427-440.
11. Lieberman, R. L. & Rosenzweig, A. C. (2004). **Biological methane oxidation: regulation, biochemistry, and active site structure of particulate methane monooxygenase.** *Critical Reviews in Biochemistry and Molecular Biology* **39**.
12. Meunier, B., de Visser, S. P. & Shaik, S. (2004). **Mechanism of oxidation reactions catalyzed by cytochrome P450 enzymes.** *Chem. Rev.* **104**, 3947-3980.
13. Hanson, R. S. & Hanson, T. E. (1996). **Methanotrophic bacteria.** *Microbiol. Rev.* **60**, 439-471.

14. Kulikova, A. K. (1995). **Microorganisms assimilating gaseous hydrocarbons (C₂ - C₄).** *Appl. Biochem. Microbiol.* **31**, 136-146.
15. Lipscomb, J. D. (1994). **Biochemistry of the soluble methane monooxygenase.** *Annu. Rev. Microbiol.* **48**, 371-399.
16. White, D. (2000). **The physiology and biochemistry of prokaryotes.** 2nd edit., Oxford University Press, Inc., New York.
17. McLee, A. G., Wayman, M. & Kormendy, A. C. (1972). **Isolation and characterization of butane-utilizing microorganisms.** *Can. J. Microbiol.* **18**, 1191-&.
18. Patel, R. N., Hou, C. T., Laskin, A. I., Felix, A. & Derelanko, P. (1983). **Oxidation of alkanes by organisms grown on C₂-C₄ alkanes.** *J. Appl. Biochem.* **5**, 107-120.
19. Ashraf, W., Mihdhir, A. & Murrell, J. C. (1994). **Bacterial oxidation of propane.** *FEMS Microbiology Letters* **122**, 1-6.
20. Kulikova, A. K. & Bezborodov, A. M. (2000). **Oxidation of organic compounds by propane monooxygenase of *Rhodococcus erythropolis* 3/89.** *Appl. Biochem. Microbiol.* **36**, 227-230.
21. Hamamura, N., Storfa, R. T., Semprini, L. & Arp, D. J. (1999). **Diversity in butane monooxygenases among butane-grown bacteria.** *Appl. Environ. Microbiol.* **65**, 4586-4593.
22. Dworkin, M. & Foster, J. W. (1958). **Experiments with some microorganisms which utilize ethane and hydrogen.** *J. Bacteriol.* **75**, 592-603.
23. Davies, I. S., Wellman, A. M. & Zajic, J. E. (1973). **Hyphomycetes utilizing natural gas.** *Can. J. Microbiol.* **19**, 81-&.
24. Davies, J. S., Wellman, A. M. & Zajic, J. E. (1976). **Oxidation of ethane by an *Acremonium* species.** *Appl. Environ. Microbiol.* **32**, 14-20.
25. Kormendy, A. C. & Wayman, M. (1974). **Characteristic cytoplasmic structures in microorganisms utilizing n-butane and 1-butanol.** *Can. J. Microbiol.* **20**, 225-&.
26. Woods, N. R. & Murrell, J. C. (1989). **The metabolism of propane in *Rhodococcus rhodochrous* Pnkb1.** *J. Gen. Microbiol.* **135**, 2335-2344.

27. Woods, N. R. & Murrell, J. C. (1990). **Epoxidation of gaseous alkenes by a *Rhodococcus sp.*** *Biotechnol. Lett.* **12**, 409-414.
28. Kulikova, A. K. & Bezborodov, A. M. (2001). **Assimilation of propane and characterization of propane monooxygenase from *Rhodococcus erythropolis* 3/89.** *Appl. Biochem. Microbiol.* **37**, 164-167.
29. Kotani, T., Yamamoto, T., Yurimoto, H., Sakai, Y. & Kato, N. (2003). **Propane monooxygenase and NAD⁺-dependent secondary alcohol dehydrogenase in propane metabolism by *Gordonia sp.* strain TY-5.** *J. Bacteriol.* **185**, 7120-7128.
30. Hamamura, N., Yeager, C. M. & Arp, D. J. (2001). **Two distinct monooxygenases for alkane oxidation in *Nocardioides sp.* strain CF8.** *Appl. Environ. Microbiol.* **67**, 4992-4998.
31. Sluis, M. K., Sayavedra-Soto, L. A. & Arp, D. J. (2002). **Molecular analysis of the soluble butane monooxygenase from '*Pseudomonas butanovora*'.** *Microbiology* **148**, 3617-3629.
32. Padda, R. S., Pandey, K. K., Kaul, S., Nair, V. D., Jain, R. K., Basu, S. K. & Chakrabarti, T. (2001). **A novel gene encoding a 54 kDa polypeptide is essential for butane utilization by *Pseudomonas sp.* IMT37.** *Microbiology-Sgm* **147**, 2479-2491.
33. Textor, S., Wendisch, V. F., De Graaf, A. A., Muller, U., Linder, M. I., Linder, D. & Buckel, W. (1997). **Propionate oxidation in *Escherichia coli*: evidence for operation of a methylcitrate cycle.** *Arch. Microbiol.* **168**, 428-436.
34. London, R. E., Allen, D. L., Gabel, S. A. & DeRose, E. F. (1999). **Carbon-13 nuclear magnetic resonance study of metabolism of propionate by *Escherichia coli*.** *J. Bacteriol.* **181**, 3562-3570.
35. Babbitt, J. N., Gholson, R. K. & Coon, M. J. (1963). **Hydrocarbon oxidation by a bacterial enzyme system: products of octane oxidation.** *Biochim. Biophys. Acta* **69**, 40-47.
36. van Beilen, J. B., Wubbolts, M. & Witholt, B. (1994). **Genetics of alkane oxidation by *Pseudomonas oleovorans*.** *Biodegradation* **5**, 161-174.
37. McKenna, E. J. & Coon, M. J. (1970). **Enzymatic omega oxidation. 4. purification and properties of omega-hydroxylase of *Pseudomonas oleovorans*.** *J. Biol. Chem.* **245**, 3882-&.

38. Smits, T. H. M., Balada, S. B., Witholt, B. & van Beilen, J. B. (2002). **Functional analysis of alkane hydroxylases from Gram-negative and Gram-positive bacteria.** *J. Bacteriol.* **184**, 1733-1742.
39. Lida, T., Sumita, T., Ohta, A. & Takagi, M. (2000). **The cytochrome P450alk multigene family of an n-alkane assimilating yeast, *Yarrowia lipolytica*: cloning and characterization of genes coding for new CYP52 family members.** *Yeast* **16**, 1077-1087.
40. Yadav, J. S. & Loper, J. C. (1999). **Multiple P450alk (cytochrome P450 alkane hydroxylase) genes from the halotolerant yeast *Debaryomyces hansenii*.** *Gene* **226**, 139-146.
41. Ohkuma, M., Zimmer, T., Iida, T., Schunck, W.-H., Ohta, A. & Takagi, M. (1998). **Isozyme function of n-alkane-inducible cytochromes P450 in *Candida maltosa* revealed by sequential gene disruption.** *J. Biol. Chem.* **273**, 3948-3953.
42. Cardini, G. & Jurtshuk, P. (1970). **Enzymatic hydroxylation of normal-octane by *Corynebacterium sp* strain 7E1C.** *J. Biol. Chem.* **245**, 2789-&.
43. Maier, T., Forster, H. H., Asperger, O. & Hahn, U. (2001). **Molecular characterization of the 56-kDa CYP153 from *Acinetobacter sp.* EB104.** *Biochem. Biophys. Res. Commun.* **286**, 652-658.
44. Ayala, M. & Torres, E. (2004). **Enzymatic activation of alkanes: constraints and prospective.** *Applied Catalysis A: General* **272**, 1-13.
45. Murrell, J. C., Gilbert, B. & McDonald, I. R. (2000). **Molecular biology and regulation of methane monooxygenase.** *Arch. Microbiol.* **173**, 325-332.
46. Lieberman, R. L. & Rosenzweig, A. C. (2005). **Crystal structure of a membrane-bound metalloenzyme that catalyses the biological oxidation of methane.** *Nature* **434**, 177-182.
47. Peterson, J. A., Basu, D. & Coon, M. J. (1966). **Enzymatic omega-oxidation. I. Electron carriers in fatty acid and hydrocarbon hydroxylation.** *J. Biol. Chem.* **241**, 5162-&.
48. van Beilen, J. B., Penninga, D. & Witholt, B. (1992). **Topology of the membrane-bound alkane hydroxylase of *Pseudomonas oleovorans*.** *J. Biol. Chem.* **267**, 9194-9201.
49. Kok, M., Oldenhuis, R., Vanderlinden, M. P. G., Raatjes, P., Kingma, J., Vanlelyveld, P. H. & Witholt, B. (1989). **The *Pseudomonas oleovorans* alkane hydroxylase gene - sequence and expression.** *J. Biol. Chem.* **264**, 5435-5441.

50. van Beilen, J. B., Panke, S., Lucchini, S., Franchini, A. G., Rothlisberger, M. & Witholt, B. (2001). **Analysis of *Pseudomonas putida* alkane-degradation gene clusters and flanking insertion sequences: evolution and regulation of the *alk* genes.** *Microbiology* **147**, 1621-1630.
51. Vomberg, A. & Kliner, U. (2000). **Distribution of *alkB* genes within n-alkane-degrading bacteria.** *J. Appl. Microbiol.* **89**, 339-348.
52. van Beilen, J. B., Smits, T. H. M., Whyte, L. G., Schorcht, S., Rothlisberger, M., Plaggemeier, T., Engesser, K. H. & Witholt, B. (2002). **Alkane hydroxylase homologues in Gram-positive strains.** *Environ. Microbiol.* **4**, 676-682.
53. de Montellano, P. R. (1995). **Cytochrome P450: structure, mechanism, and biochemistry.** 2nd edit., Plenum Press, New York.
54. Miles, C. S., Ost, T. W. B., Noble, M. A., Munro, A. W. & Chapman, S. K. (2000). **Protein engineering of cytochromes P-450.** *Biochim. Biophys. Acta* **1543**, 383-407.
55. Guengerich, F. P. (2002). **Cytochrome P450 enzymes in the generation of commercial products.** *Nat. Rev. Drug Discov.* **1**, 359-366.
56. Urlacher, V. & Schmid, R. D. (2002). **Biotransformations using prokaryotic P450 monooxygenases.** *Curr. Opin. Biotech.* **13**, 557-564.
57. Cirino, P. C. & Arnold, F. H. (2002). **Protein engineering of oxygenases for biocatalysis.** *Curr. Opin. Chem. Biol.* **6**, 130-135.
58. Schlichting, I. et al. (2000). **The catalytic pathway of cytochrome P450cam at atomic resolution.** *Science* **287**, 1615-1622.
59. Joo, H., Lin, Z. L. & Arnold, F. H. (1999). **Laboratory evolution of peroxide-mediated cytochrome P450 hydroxylation.** *Nature* **399**, 670-673.
60. Sono, M., Roach, M. P., Coulter, E. D. & Dawson, J. H. (1996). **Heme-containing oxygenases.** *Chem. Rev.* **96**, 2841-2887.
61. Guengerich, F. P. (2001). **Common and uncommon cytochrome P450 reactions related to metabolism and chemical toxicity.** *Chem. Res. Toxicol.* **14**, 611-650.
62. Williams, P. A., Cosme, J., Sridhar, V., Johnson, E. F. & McRee, D. E. (2000). **Microsomal cytochrome P450C5: comparison to microbial P450s and unique features.** *J. Inorg. Biochem.* **81**, 183-190.

63. Wester, M. R., Johnson, E. F., Marques-Soares, C., Dansette, P. M., Mansuy, D. & Stout, C. D. (2003). **Structure of a substrate complex of mammalian cytochrome P450 2C5 at 2.3 Å resolution: evidence for multiple substrate binding modes.** *Biochemistry* **42**, 6370-6379.
64. Wester, M. R., Johnson, E. F., Marques-Soares, C., Dijols, S., Dansette, P. M., Mansuy, D. & Stout, C. D. (2003). **Structure of mammalian cytochrome P4502C5 complexed with diclofenac at 2.1 angstrom resolution: evidence for an induced fit model of substrate binding.** *Biochemistry* **42**, 9335-9345.
65. Schoch, G. A., Yano, J. K., Wester, M. R., Griffin, K. J., Stout, C. D. & Johnson, E. F. (2004). **Structure of human microsomal cytochrome P450 2C8: evidence for a peripheral fatty acid binding site.** *J. Biol. Chem.* **279**, 9497-9503.
66. Williams, P. A., Cosme, J., Ward, A., Angova, H. C., Vinkovic, D. M. & Jhoti, H. (2003). **Crystal structure of human cytochrome P4502C9 with bound warfarin.** *Nature* **424**, 464-468.
67. Wester, M. R., Yano, J. K., Schoch, G. A., Yang, C., Griffin, K. J., Stout, C. D. & Johnson, E. F. (2004). **The structure of human cytochrome P450 2C9 complexed with flurbiprofen at 2.0-Å resolution.** *J. Biol. Chem.* **279**, 35630-35637.
68. Scott, E. E., He, Y. A., Wester, M. R., White, M. A., Chin, C. C., Halpert, J. R., Johnson, E. F. & Stout, C. D. (2003). **An open conformation of mammalian cytochrome P450 2B4 at 1.6-Å resolution.** *Proc. Natl. Acad. Sci.* **100**, 13196-13201.
69. Scott, E. E., White, M. A., He, Y. A., Johnson, E. F., Stout, C. D. & Halpert, J. R. (2004). **Structure of mammalian cytochrome P450 2B4 complexed with 4-(4-chlorophenyl)imidazole at 1.9-Å resolution: insight into the range of P450 conformations and the coordination of redox partner binding.** *J. Biol. Chem.* **279**, 27294-27301.
70. Yano, J. K., Wester, M. R., Schoch, G. A., Griffin, K. J., Stout, C. D. & Johnson, E. F. (2004). **The structure of human microsomal cytochrome P450 3A4 determined by x-ray crystallography to 2.05-Å resolution.** *J. Biol. Chem.* **279**, 38091-38094.
71. Williams, P. A., Cosme, J., Vinkovic, D. M., Ward, A., Angove, H. C., Day, P. J., Vonnrhein, C., Tickle, I. J. & Jhoti, H. (2004). **Crystal structures of human cytochrome P450 3A4 bound to metyrapone and progesterone.** *Science* **305**, 683-686.

72. Lindberg, R. L. P. & Negishi, M. (1989). **Alteration of mouse cytochrome P450c₁₁ substrate specificity by mutation of a single amino-acid residue.** *Nature* **339**, 632-634.
73. Bottner, B., Schrauber, H. & Bernhardt, R. (1996). **Engineering a mineralocorticoid- to a glucocorticoid- synthesizing cytochrome P450.** *J. Biol. Chem.* **271**, 8028-8033.
74. Bottner, B. & Bernhardt, R. (1996). **Changed ratios of glucocorticoids/mineralocorticoids caused by point mutations in the putative I-helix regions of CYP11B1 and CYP11B2.** *Endocr Res* **22**, 455-461.
75. Bottner, B., Denner, K. & Bernhardt, R. (1998). **Conferring aldosterone synthesis to human CYP11B1 by replacing key amino acid residues with CYP11B2-specific ones.** *Eur. J. Biochem.* **252**, 458-466.
76. Belkina, N. V., Lisurek, M., Ivanov, A. S. & Bernhardt, R. (2001). **Modelling of three-dimensional structures of cytochromes P45011B1 and 11B2.** *J. Inorg. Biochem.* **87**, 197-207.
77. Bechtel, S., Belkina, N. & Bernhardt, R. (2002). **The effect of amino-acid substitutions I112P, D147E and K152N in CYP11B2 on the catalytic activities of the enzyme.** *Eur. J. Biochem.* **269**, 1118-1127.
78. Pascoe, L., Curnow, K., Slutsker, L., Rosler, A. & White, P. (1992). **Mutations in the human CYP11B2 (aldosterone synthase) gene causing corticosterone methyloxidase II deficiency.** *Proc. Natl. Acad. Sci.* **89**, 4996-5000.
79. Domanski, T. L. & Halpert, J. R. (2001). **Analysis of mammalian cytochrome P450 structure and function by site-directed mutagenesis.** *Curr. Drug Metab.* **2**, 117-137.
80. Gotoh, O. (1992). **Substrate recognition sites in cytochrome P450 family 2 (Cyp2) proteins inferred from comparative analyses of amino-acid and coding nucleotide sequences.** *J. Biol. Chem.* **267**, 83-90.
81. Nakamura, K., Martin, M. V. & Guengerich, F. P. (2001). **Random mutagenesis of human cytochrome P450 2A6 and screening with indole oxidation products.** *Arch. Biochem. Biophys.* **395**, 25-31.
82. Narhi, L. O., Fulco, A.J. (1986). **Characterization of a catalytically self-sufficient 119,000- dalton cytochrome P450 monooxygenase induced by barbiturates in *Bacillus megaterium*.** *J. Biol. Chem.* **261**, 7160-7169.

83. Poulos, T. L., Finzel, B. C., Gunsalus, I. C., Wagner, G. C. & Kraut, J. (1985). **The 2.6-Å crystal structure of *Pseudomonas putida* cytochrome P-450.** *J. Biol. Chem.* **260**, 6122-6130.
84. Ravichandran, K. G., Bodupalli, S. S., Hasemann, C. A., Peterson, J. A. & Deisenhofer, J. (1993). **Crystal structure of hemoprotein domain of P450BM-3, a prototype for microsomal P450's.** *Science* **261**, 731-736.
85. Raag, R. & Poulos, T. L. (1991). **Crystal structures of cytochrome P-450cam complexed with camphane, thiocamphor, and adamantane: factors controlling P-450 substrate hydroxylation.** *Biochemistry* **30**, 2674-2684.
86. Li, H. & Poulos, T. L. (1997). **The structure of the cytochrome P450BM-3 haem domain complexed with the fatty acid substrate, palmitoleic acid.** *Nat. Struct. Biol.* **4**, 140-146.
87. Haines, D. C., Tomchick, D. R., Machius, M. & Peterson, J. A. (2001). **Pivotal role of water in the mechanism of P450BM-3.** *Biochemistry* **40**, 13456-13465.
88. Schlichting, I., Jung, C. & Schulze, H. (1997). **Crystal structure of cytochrome P-450cam complexed with the (1S)-camphor enantiomer.** *FEBS Lett.* **415**, 253-257.
89. Lee, D. S., Park, S. Y., Yamane, K., Obayashi, E., Hori, H. & Shiro, Y. (2001). **Structural characterization of n-butyl-isocyanide complexes of P450nor and P450cam.** *Biochemistry* **40**, 2669-2677.
90. Raag, R., Martinis, S. A., Sligar, S. G. & Poulos, T. L. (1991). **Crystal structure of the cytochrome-P-450cam active site mutant Thr252Ala.** *Biochemistry* **30**, 11420-11429.
91. Vidakovic, M., Sligar, S. G., Li, H. Y. & Poulos, T. L. (1998). **Understanding the role of the essential Asp251 in cytochrome P450cam using site-directed mutagenesis, crystallography, and kinetic solvent isotope effect.** *Biochemistry* **37**, 9211-9219.
92. Chen, X. H., Christopher, A., Jones, J. P., Bell, S. G., Guo, Q., Xu, F., Rao, Z. H. & Wong, L. L. (2002). **Crystal structure of the F87W/Y96F/V247L mutant of cytochrome P-450cam with 1,3,5-trichlorobenzene bound and further protein engineering for the oxidation of pentachlorobenzene and hexachlorobenzene.** *J. Biol. Chem.* **277**, 37519-37526.
93. Bell, S. G., Chen, X. H., Sowden, R. J., Xu, F., Williams, J. N., Wong, L. L. & Rao, Z. (2003). **Molecular recognition in (+)-α-pinene oxidation by cytochrome P450cam.** *J. Am. Chem. Soc.* **125**, 705-714.

94. Ost, T. W. B. et al. (2001). **Structural and spectroscopic analysis of the F393H mutant of flavocytochrome p450 BM3.** *Biochemistry* **40**, 13430-13438.
95. Ost, T. W. B., Clark, J., Mowat, C. G., Miles, C. S., Walkinshaw, M. D., Reid, G. A., Chapman, S. K. & Daff, S. (2003). **Oxygen activation and electron transfer in flavocytochrome P450BM3.** *J. Am. Chem. Soc.* **125**, 15010-15020.
96. Joyce, M. G., Girvan, H. M., Munro, A. W. & Leys, D. (2004). **A single mutation in cytochrome P450 BM3 induces the conformational rearrangement seen upon substrate binding in the wild-type enzyme.** *J. Biol. Chem.* **279**, 23287-23293.
97. Poulos, T. L., Finzel, B. C. & Howard, A. J. (1987). **High-resolution crystal structure of cytochrome-P450cam.** *J. Mol. Biol.* **195**, 687-700.
98. Loida, P. J. & Sligar, S. G. (1993). **Engineering cytochrome P-450cam to increase the stereospecificity and coupling of aliphatic hydroxylation.** *Protein Eng.* **6**, 207-212.
99. Bell, S. G., Rouch, D. A. & Wong, L. L. (1997). **Selective aliphatic and aromatic carbon-hydrogen bond activation catalysed by mutants of cytochrome P450cam.** *Journal of Molecular Catalysis B-Enzymatic* **3**, 293-302.
100. Fowler, S. M. et al. (1994). **Cytochrome P-450(Cam) monooxygenase can be redesigned to catalyze the regioselective aromatic hydroxylation of diphenylmethane.** *J. Chem. Soc.-Chem. Commun.*, 2761-2762.
101. England, P. A., Rouch, D. A., Westlake, A. C. G., Bell, S. G., Nickerson, D. P., Webberley, M., Flitsch, S. L. & Wong, L. L. (1996). **Aliphatic vs aromatic C-H bond activation of phenylcyclohexane catalysed by cytochrome P450cam.** *Chem. Commun.*, 357-358.
102. Bell, S. G., Harford-Cross, C. F. & Wong, L. L. (2001). **Engineering the CYP101 system for in vivo oxidation of unnatural substrates.** *Protein Engineering* **14**, 797-802.
103. England, P. A., Harford-Cross, C. F., Stevenson, J. A., Rouch, D. A. & Wong, L. L. (1998). **The oxidation of naphthalene and pyrene by cytochrome P450(cam).** *FEBS Lett.* **424**, 271-274.
104. Nickerson, D. P., HarfordCross, C. F., Fulcher, S. R. & Wong, L. L. (1997). **The catalytic activity of cytochrome P450(cam) towards styrene oxidation is increased by site-specific mutagenesis.** *FEBS Lett.* **405**, 153-156.

105. Harford-Cross, C. F., Carmichael, A. B., Allan, F. K., England, P. A., Rouch, D. A. & Wong, L. L. (2000). **Protein engineering of cytochrome P450(cam) (CYP101) for the oxidation of polycyclic aromatic hydrocarbons.** *Protein Eng.* **13**, 121-128.
106. Jones, J. P., O'Hare, E. J. & Wong, L. L. (2000). **The oxidation of polychlorinated benzenes by genetically engineered cytochrome P450(cam): potential applications in bioremediation.** *Chem. Commun.*, 247-248.
107. Jones, J. P., O'Hare, E. J. & Wong, L. L. (2001). **Oxidation of polychlorinated benzenes by genetically engineered CYP101 (cytochrome P450(cam)).** *Eur. J. Biochem.* **268**, 1460-1467.
108. French, K. J., Rock, D. A., Manchester, J. I., Goldstein, B. M. & Jones, J. P. (2002). **Active site mutations of cytochrome P450cam alter the binding, coupling, and oxidation of the foreign substrates (R)- and (S)- 2-ethylhexanol.** *Arch. Biochem. Biophys.* **398**, 188-197.
109. Bell, S. G., Stevenson, J. A., Boyd, H. D., Campbell, S., Riddle, A. D., Orton, E. L. & Wong, L. L. (2002). **Butane and propane oxidation by engineered cytochrome P450(cam).** *Chem. Commun.*, 490-491.
110. Boddupalli, S. S., Pramanik, B. C., Slaughter, C. A., Estabrook, R. W. & Peterson, J. A. (1992). **Fatty-acid monooxygenation by P450BM-3 - product identification and proposed mechanisms for the sequential hydroxylation reactions.** *Arch. Biochem. Biophys.* **292**, 20-28.
111. Noble, A. & et al. (1999). **Roles of key active-site residues in flavocytochrome P450 BM3.** *Biochem. J.* **339**, 371-379.
112. Yeom, H. Y. & Sligar, S. G. (1997). **Oxygen activation by cytochrome P450 BM-3: effects of mutating an active site acidic residue.** *Arch. Biochem. Biophys.* **337**, 209-216.
113. Carmichael, A. B. & Wong, L. L. (2001). **Protein engineering of *Bacillus megaterium* CYP102 - The oxidation of polycyclic aromatic hydrocarbons.** *Eur. J. Biochem.* **268**, 3117-3125.
114. Li, Q. S., Schwaneberg, U., Fischer, P. & Schmid, R. D. (2000). **Directed evolution of the fatty-acid hydroxylase P-450 BM3 into an indole-hydroxylating catalyst.** *Chem. Eur. J.* **6**, 1531-1536.
115. Li, Q. S., Ogawa, J., Schmid, R. D. & Shimizu, S. (2001). **Residues size at position 87 of cytochrome P450 BM-3 determines its stereoselectivity in propylbenzene and 3-chlorostyrene oxidation.** *FEBS Lett.* **508**.

116. Appel, D., Lutz-Wahl, S., Fischer, P., Schwaneberg, U. & Schmid, R. D. (2001). **A P450 BM-3 mutant hydroxylates alkanes, cycloalkanes, arenes and heteroarenes.** *J. Biotechnol.* **88**, 167-171.
117. Peters, M. W., Meinhold, P. & Arnold, F. H. (2003). **Regio- and enantioselective alkane hydroxylation with engineered cytochromes P450 BM-3.** *J. Am. Chem. Soc.* **125**, 13442 -13450.
118. Glieder, A., Farinas, E. T. & Arnold, F. H. (2002). **Laboratory evolution of a soluble, self-sufficient, highly active alkane hydroxylase.** *Nat. Biotechnol.* **20**, 1135-1139.
119. Graham-Lorence, S., Truan, G. L., Peterson, J. A., Falck, J. R., Wei, S., Helvig, C. & Capdevila, J. H. (1997). **An active site substitution, F87V, converts cytochrome P450 BM-3 into a regio- and stereoselective (14S, 15R)-arachidonic acid epoxygenase.** *J. Biol. Chem.* **272**, 1127-1135.
120. Li, Q. S., Ogawa, J., Schmid, R. D. & Shimizu, S. (2001). **Engineering cytochrome P450 BM-3 for oxidation of polycyclic aromatic hydrocarbons.** *Appl. Environ. Microbiol.* **67**, 5735-5739.
121. Farinas, E. T., Bulter, T. & Arnold, F. H. (2001). **Directed enzyme evolution.** *Curr. Opin. Biotech.* **12**, 545-551.
122. Cirino, P. & Arnold, F. H. (2002). **Exploring the diversity of heme enzymes through directed evolution.** In *Directed Molecular Evolution of Proteins* (Brakmann, S. & Johnson, K., eds.), pp. 215-243. Wiley-VCH, Germany.
123. Schwaneberg, U., Schmidt-Dannert, C., Schmitt, J. & Schmid, R. D. (1999). **A continuous spectrophotometric assay for P450 BM-3, a fatty acid hydroxylating enzyme, and its mutant F87A.** *Anal. Biochem.* **269**, 359-366.
124. Li, Q. S., Schwaneberg, U., Fischer, M., Schmitt, J., Pleiss, J., Lutz-Wahl, S. & Schmid, R. D. (2001). **Rational evolution of a medium chain-specific cytochrome P-450 BM-3 variant.** *Biochim. Biophys. Acta* **1545**.
125. Farinas, E. T., Schwaneberg, U., Glieder, A. & Arnold, F. H. (2001). **Directed evolution of a cytochrome P450 monooxygenase for alkane oxidation.** *Adv. Synth. Catal.* **343**, 601-606.
126. Voigt, C. A., Martinez, C., Wang, Z. G., Mayo, S. L. & Arnold, F. H. (2002). **Protein building blocks preserved by recombination.** *Nat. Struct. Biol.* **9**, 553-558.

127. Meyer, M. M., Silberg, J. J., Voigt, C. A., Endelmann, J. B., Mayo, S. L., Wang, Z.-G. & Arnold, F. H. (2003). **Library analysis of SCHEMA-guided protein recombination.** *Protein Sci.* **12**, 1686-1693.
128. Otey, C., R., Silberg, J. J., Voigt, C. A., Endelmann, J. B., Bandara, G. & Arnold, F. H. (2004). **Functional evolution and structural conservation in chimeric cytochromes p450: calibrating a structure-guided approach.** *Chem. Biol.* **11**, 309-318.
129. De Mot, R. & Parret, A. H. A. (2002). **A novel class of self-sufficient cytochrome P450 monooxygenases in prokaryotes.** *Trends Microbiol.* **10**, 502-508.
130. Murataliev, M. B., Klein, M., Fulco, A. & Feyereisen, R. (1997). **Functional interactions in cytochrome P450BM3: flavin semiquinone intermediates, role of NADP(H), and mechanism of electron transfer by the flavoprotein domain.** *Biochemistry* **36**, 8401-8412.
131. Sevrioukova, I., Shaffer, C., Ballou, D. P. & Peterson, J. A. (1996). **Equilibrium and transient state spectrophotometric studies of the mechanism of reduction of the flavoprotein domain of P450BM-3.** *Biochemistry* **35**, 7058-7068.
132. Murataliev, M. B., Feyereisen, R. & Walker, A. (2004). **Electron transfer by diflavin reductases.** *Biochim. Biophys. Acta* **1698**, 1-26.
133. Li, H. Y., Darwish, K. & Poulos, T. L. (1991). **Characterization of recombinant *Bacillus megaterium* cytochrome P450 BM-3 and its 2 functional domains.** *J. Biol. Chem.* **266**, 11909-11914.
134. Murataliev, M. B. & Feyereisen, R. (2000). **Functional interactions in cytochrome P450(BM3). Evidence that NADP(H) binding controls redox potentials of the flavin cofactors.** *Biochemistry* **39**, 12699-12707.
135. Daff, S. N., Chapman, S. K., Turner, K. L., Holt, R. A., Govindaraj, S., Poulos, T. L. & Munro, A. W. (1997). **Redox control of the catalytic cycle of flavocytochrome P-450 BM3.** *Biochemistry* **36**, 13816-13823.
136. Murataliev, M. B. & Feyereisen, R. (2000). **Interaction of NADP(H) with oxidized and reduced P450 reductase during catalysis, studies with nucleotide analogues.** *Biochemistry* **39**, 5066-5074.
137. Bosterling, B. & Trudell, J. R. (1981). **Spin trap evidence for production of superoxide radical-anions by purified NADPH-cytochrome P450 reductase.** *Biochem. Biophys. Res. Commun.* **98**, 569-575.

138. Cirino, P. C. & Arnold, F. H. (2002). **Regioselectivity and activity of cytochrome P450BM-3 and mutant F87A in reactions driven by hydrogen peroxide.** *Adv. Synth. Catal.* **344**, 932-937.
139. Cirino, P. C. & Arnold, F. H. (2003). **A self-sufficient peroxide-driven hydroxylation biocatalyst.** *Angew. Chem. Int. Edit.* **42**, 3299-3301.
140. Salazar, O., Cirino, P. C. & Arnold, F. H. (2003). **Thermostabilization of a cytochrome P450 peroxxygenase.** *Chembiochem* **4**, 891-893.

Chapter 2

Regio- and Enantioselective Alkane Hydroxylation with Engineered Cytochromes P450 BM-3

Material from this chapter appears in: Peters, M. W., Meinhold, P. & Arnold, F. H. (2003). **Regio- and enantioselective alkane hydroxylation with engineered cytochromes P450 BM-3.** *J. Am. Chem. Soc.* **125**, 13442 -13450, and is reprinted by permission of the American Chemical Society.

A. Abstract

Cytochrome P450 BM-3 from *Bacillus megaterium* was engineered using a combination of directed evolution and site-directed mutagenesis to hydroxylate linear alkanes regio- and enantioselectively using atmospheric dioxygen as an oxidant. BM-3 variant 9-10A-A328V hydroxylates octane at the 2-position to form *S*-2-octanol (40% ee). Another variant, 1-12G, also hydroxylates alkanes larger than hexane primarily at the 2-position, but forms *R*-2-alcohols (40-55% ee). These biocatalysts are highly active (rates up to 400 min⁻¹) and support thousands of product turnovers. The regio- and enantio-selectivities are retained in whole-cell biotransformations with *Escherichia coli*, in which the engineered P450s can be expressed at high levels and the cofactor is supplied endogenously.

B. Introduction

Inspired by the diversity of activities supported by the P450 scaffold in nature, we have focused on engineering P450 BM-3 to generate practical P450-based oxidation catalysts. In particular, we are interested in creating useful biocatalysts for the controlled oxidation of alkanes. Linear alkanes are difficult to hydroxylate: the alkane C-H bond is notoriously inert, due to its high (~97 kcal/mol) bond strength, making alkanes ideal solvents for use with very reactive oxidation catalysts [1]. Additionally, the activation energies for subsequent oxidations of an alcohol are similar to the energy required for the initial hydroxylation of the starting alkane, resulting in mixtures of alcohol, ketone/aldehyde, and carboxylic acid products in most alkane oxidation reactions [2]. The similarity of methylene C-H bond strengths in a linear alkane and the lack of functional groups that can serve to direct catalysis make selective hydroxylation of these compounds especially challenging. Limited selective alkane hydroxylation has been reported for bulky cycloalkanes and aryl alkanes using biomimetic transition metal complexes as catalysts and peroxides as oxidants, but these complexes do not produce hydroxylated products in useful amounts (the catalysts support very few (<20) total turnovers) [3-6].

Several biological systems are capable of dioxygen-supported alkane hydroxylation and, in some cases, even regioselective alkane hydroxylation. For example, the particulate methane monooxygenase from *Methylococcus capsulatus* (Bath) can hydroxylate butane and pentane to yield primarily *R*-2-alcohols. This enzyme does not accept larger alkanes. Soluble methane monooxygenase from the same organism hydroxylates several alkanes with little or no selectivity [7,8]. Neither enzyme is likely to serve as a practical

biocatalyst, due to their inability to be overexpressed in a suitable host organism and their rather low intrinsic activities. Alkane hydroxylase B (AlkB) from *Pseudomonas oleovorans* hydroxylates octane selectively at the terminal (or ω) position, producing 1-octanol. This enzyme can be used in engineered whole cells to generate this product in two-phase bioconversions [9]. Some P450s (several members of the Cyp4 family, Cyp52, Cyp86, Cyp153) have also been reported to catalyze the hydroxylation of terminal methyl groups of fatty acids or n-alkanes [10-13]. Nonselective cytochrome P450 alkane hydroxylation systems include the site-directed mutants of P450_{cam} of Wong and coworkers [14-16] and an engineered P450 BM-3 reported by our group [17,18]. Enantioselective (but not regioselective) hydroxylation of alkanes has been reported with whole-cell systems of soil bacteria genera such as *Bacillus* [19], *Pseudomonas* [20,21], and *Rhodococcus* [22,23], but the selectivity observed in these systems is most likely due to metabolism of specific isomers rather than the action of selective oxygenases.

The natural substrates of cytochrome P450 BM-3 are medium-chain (C12 to C18) fatty acids, which are hydroxylated at their ω -1, ω -2, and ω -3 positions using atmospheric dioxygen and NADPH) [24] (the reader is referred to Chapter 1 for details). In previous work, we used directed evolution to convert wild-type BM-3 into a fast, but non-selective, alkane hydroxylase called 139-3 [17,18]. A large increase in activity towards alkanes as small as propane was observed after five rounds of directed evolution experiments, which accumulated eleven amino acid substitutions in the heme domain.

We have begun to further engineer P450 BM-3 for the hydroxylation of very small alkanes such as ethane and methane, activities never reported in a cytochrome P450, by applying a

combination of directed evolution and site-directed mutagenesis. The mutants obtained from these experiments hydroxylate propane at faster rates and reach higher total turnover numbers than 139-3. During the course of this work, we found that two of these mutants are highly regioselective and enantioselective towards longer alkanes. One mutant forms *R*-2-alcohols from alkanes bigger than heptane, and the other forms *S*-2-octanol from octane. The engineered P450 BM-3 enzymes described here are, to our knowledge, the only systems capable of direct, regio- and enantioselective hydroxylation of linear alkanes expressed in hosts suitable for large-scale biocatalytic processes.

C. Results and Discussion

C.1. Previous Work

In previous work with this enzyme, five rounds of directed evolution starting with wild-type cytochrome P450 BM-3 yielded the alkane hydroxylase 139-3[17,18]. In each round, a library of randomly-mutated BM-3 enzymes was screened for octane hydroxylation activity on the “surrogate” substrate *p*-nitrophenyl octyl ether. Hydroxylation of this substrate at the carbon atom containing the *p*-nitrophenoxy moiety results in the formation of *p*-nitrophenolate, which was used for colorimetric identification of active mutants. Active mutants were then tested for octane hydroxylation activity, and the most active ones were used as parents for subsequent rounds of evolution. In some cases, several active mutants were isolated from a single round of screening and recombined using DNA shuffling to obtain the parent for the next round. In these and the evolution experiments

described in this chapter, random mutagenesis and recombination were applied only to the heme domain (residues 1-429, with 429 chosen for the convenience of introducing a *SacI* restriction site into the heme domain gene); the reductase domain was left untouched. The complete BM-3 enzyme (modified heme domain attached to the unmodified reductase domain) was used in all the hydroxylation reactions described here.

Of the eleven amino acid substitutions in the alkane hydroxylase 139-3 heme domain, only one (V78A) occurs at a residue that contacts the fatty acid substrate in the (wild-type) enzyme [18]. The reader is referred to Appendix B, which summarizes the mutations. The mechanisms by which the mutations contribute to the new activity are difficult to rationalize. The rather broad distribution of 139-3's hydroxylated alkane products (Table 2.1, Figure 2.2), however, suggests that its active site is rather large and that its alkane substrates are "loosely" bound. This is not surprising since the surrogate substrate used to identify these mutants is quite large relative to octane, the intended substrate. The one active site substitution, in fact, replaces valine with a smaller, alanine side chain.

P450 BM-3 mutant 139-3 shows significant activity on propane, even though small alkane substrates were not used to screen the mutant libraries in the directed evolution experiments. We postulated that by continuously decreasing the size of the screening substrate, improvements in catalytic activity will eventually lead to activity towards even smaller alkanes.

To improve the activity towards propane further, and perhaps even achieve activity towards ethane, we continued to apply iterative rounds of mutagenesis and screening, using propane

as a substrate. The BM-3-catalyzed hydroxylation reaction results in the oxidation of one equivalent of NADPH for each equivalent of hydroxylated substrate. Using a 96-well plate reader, the rate of NADPH oxidation in the presence of BM-3-containing cell lysate and substrate can be monitored spectrophotometrically at 340 nm to quickly identify mutants with high activity towards any given substrate. Alternatively, the concentration of the oxidized form of NADPH, NADP^+ , can be measured spectrophotometrically in cell lysate [25]. It is possible that the reducing equivalents of NADPH become uncoupled to substrate oxidation, leading to false positives in a mutant library, but gas chromatographic analysis of reaction mixtures can confirm when an increased NADPH oxidation rate is accompanied by more or faster product formation.

C.2. Alkane Hydroxylation Reactions

To measure these alkane hydroxylation activities, ethanol solutions of liquid alkanes were added to buffer solutions containing the enzymes such that the total ethanol in the reaction mixture was one percent. Several solvents, including ethanol, methanol, acetone, and dimethyl sulfoxide, were tested, and ethanol was shown to support the most product turnovers. Reactions with liquid alkanes that contained no co-solvent produced no detectable products. In the absence of substrate, NADPH has been reported to inactivate BM-3 by over-reducing the flavin cofactors in its reductase domain [26]. To avoid this problem, substrate was added to the enzyme first and incubated for a few seconds before NADPH was added. Dioxygen was not added to the reactions, limiting the amount of

possible product formed to the 225-250 μM of oxygen present in air-saturated buffer. The addition of excess dioxygen to the reactions by direct bubbling or rapid stirring did not increase and often decreased the total product turnover, possibly by denaturing the protein. Reaction mixtures for all BM-3 mutants containing 0.5-1.0 μM enzyme produced 225-250 μM products. We also noticed that total turnover numbers measured in systems containing less than ~ 50 nM protein were less than expected – i.e., 10 nM protein in a reaction gave much less than half the total turnovers of a 20 nM reaction. At very low concentrations of BM-3, the FMN cofactor has been reported to diffuse out of the protein and inactivate it [27]. Given this fact and the dilution effects on total turnover we witnessed, a highly active mutant could be capable of even more turnovers than we can measure using this procedure.

Reactions using propane did not contain co-solvent because of potential competition between the solvent and the small substrate. These reactions were performed in propane-saturated buffer under an atmosphere of propane and dioxygen (provided by a balloon filled with the two gases). The addition of this atmosphere ensured that both gaseous substrates were saturated in the reaction solution, since a balloon of just propane or oxygen would dilute the concentration of the other gas. Total turnovers determined with this system were not dependent on oxygen concentration in the balloon (data not shown), illustrating that only the original ~ 250 μM of dioxygen in the buffer was available to the reaction. Additionally, we discovered that NADPH could neither be purchased nor easily purified in a form that contains less than 2-3% ethanol, which interferes with analysis of the reaction products. For this reason, an NADPH-regeneration system was used for propane reactions [28].

C.3. Directed Evolution

For the first round of directed evolution, a library of P450 BM-3 variants was generated by recombining mutant 139-3 with fifteen other mutants from the same generation that also exhibited increased activity towards *p*-nitrophenyl octyl ether and octane. The shuffled gene library was transformed into *E. coli* DH5 α competent cells, in which the enzymes were over-expressed. Due to difficulties with obtaining high transformation efficiency, only 350 mutants were screened for activity. Aliquots of the cell-free extracts from individual clones were transferred to 96-well plates, where NADPH consumption was monitored in the presence of propane. Positive clones were grown up and their enzymes purified for comparative analysis using gas chromatography. Mutant J (see Appendix B for mutations) was selected, based upon its increased rate of NADPH consumption in the presence of propane relative to 139-3. This increased rate corresponded to an increase in total production of hydroxylated products with the substrates propane (800 turnovers) and octane (3,000 turnovers). In comparison, 139-3 catalyzes 500 and 1000 turnovers for propane and octane, respectively.

Error-prone PCR of the gene for P450 BM-3 mutant J, performed under conditions designed to yield 1-2 mutations on average per gene, generated the library for the second round of directed evolution. Mutant 9-10A was selected from a library of approximately 1,000 individual BM-3 variants for its increased NADPH consumption rate in the presence of propane; it was subsequently shown to support more turnovers of propane (1,100). The properties of these mutants are detailed in Tables 2.1 and 2.2 and Figure 2.2 (see Appendix B for sequences and mutations). Neither J nor 9-10A acquired active-site mutations, nor

did they show major changes in regioselectivity towards longer alkanes, compared to 139-

3. Although these mutants supported more turnovers, their coupling efficiencies (see below) were not improved.

Random mutagenesis of 9-10A generated the library for a third round of evolution. To overcome the limitations of cofactor-dependent screens, this time, a second screen was applied to assess the amount of hydroxylation products generated by each mutant. This screen uses the surrogate substrate dimethyl ether, which is similar to propane in size and C-H bond strength. Upon hydroxylation, dimethyl ether is demethylated and forms formaldehyde, which can be detected in cell lysate with Purpald dye at concentrations as low as 10 μ M [29] (Figure 2.1).

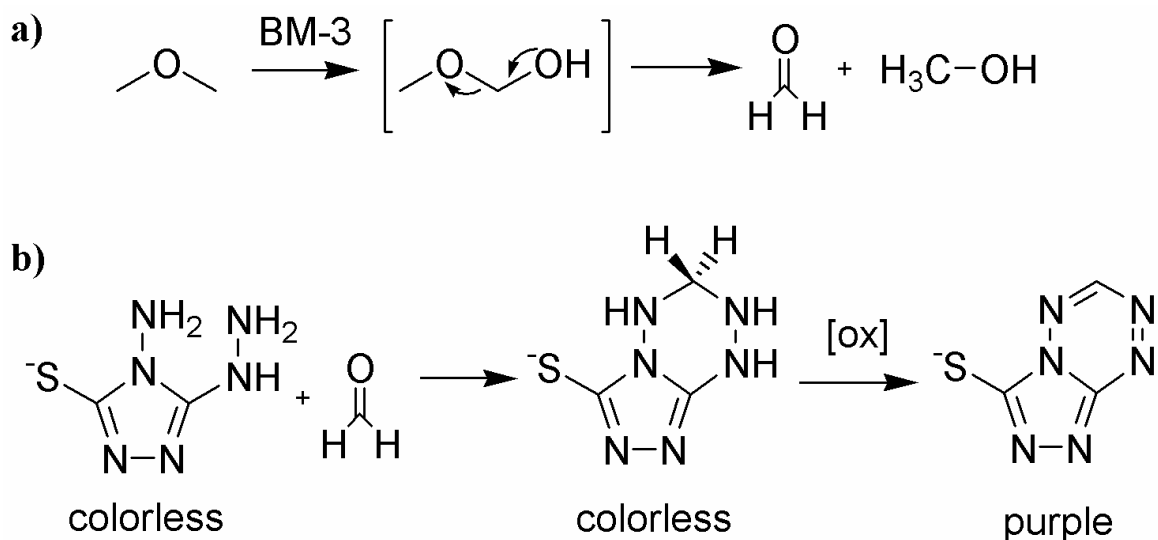


Figure 2.1. Dimethyl ether hydroxylation assay **a)** Hydroxylation of surrogate substrate dimethyl ether produces formaldehyde. **b)** Purpald reaction: Purpald reacts with formaldehyde to form a purple adduct upon air oxidation.

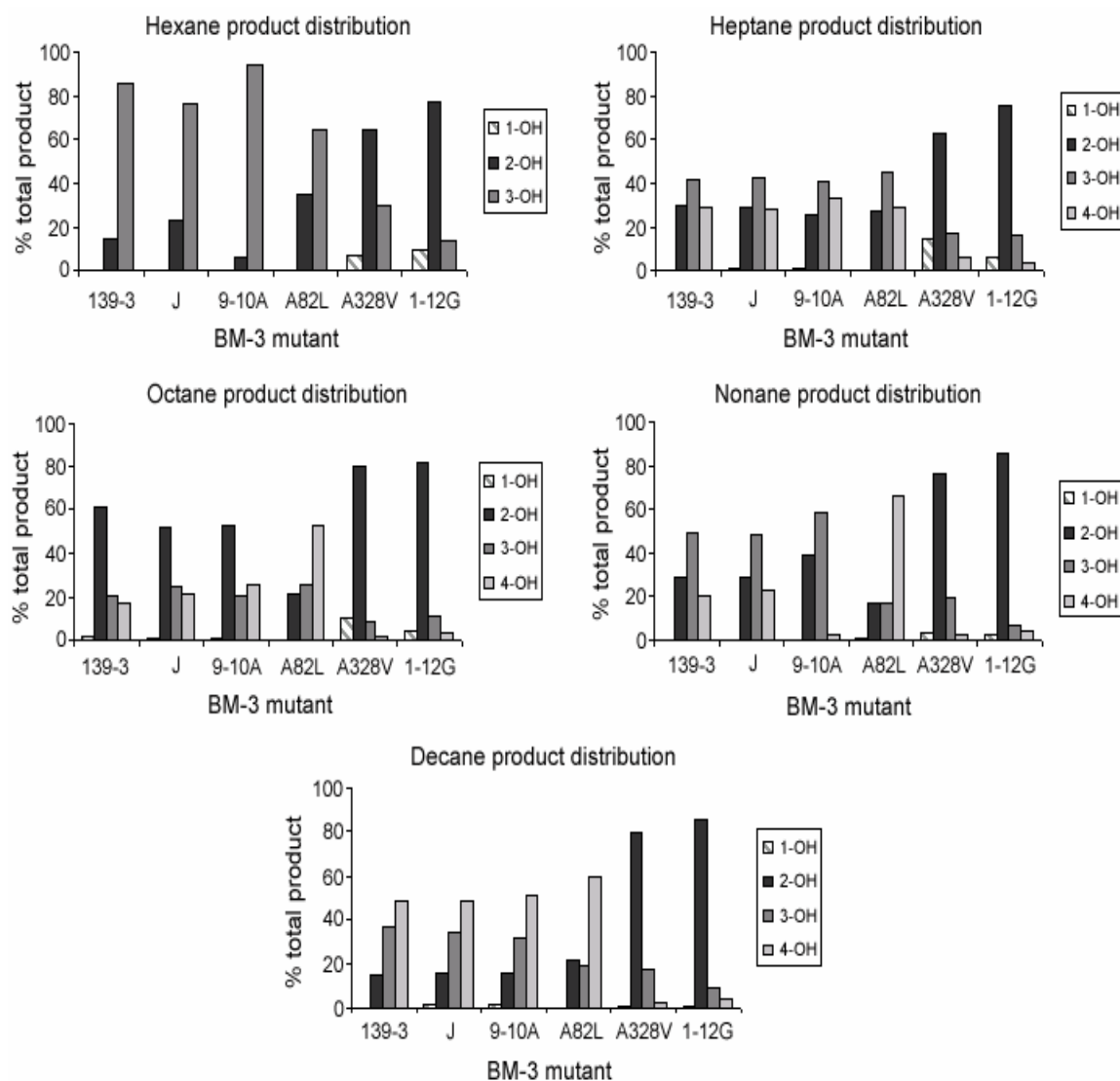


Figure 2.2. Hydroxylation product distribution of BM-3 mutants. Mutants 9-10A-A82L and 9-10A-A328V are abbreviated A82L and A328V, respectively. The reaction conditions were: 4 mM alkane substrates, 25 to 100 nM BM-3 mutant, 1% (v/v) ethanol, 500 μ M NADPH, incubation at room temperature for 4 hours. Mutants obtained by screening random mutagenesis libraries (139-3, J, 9-10A) show similar product distributions while mutants obtained by mutating active site residues (9-10A-A82L, 9-10A-A328V, 1-12G) show significant shifts in regioselectivity. Refer to Appendix B for mutations in BM-3 variants 139-3, J, 9-10A

Table 2.1. Product distributions ^[a] and % ee of selected products.

Mutant	product	propane	hexane % ee ^[c]	heptane % ee ^[c]	octane % ee ^[c]	nonane % ee ^[c]	decane % ee ^[c]
139-3	1-alcohol	3	0	0	1	0	0
	2-alcohol	97	14 14(<i>S</i>)	30 15(<i>S</i>)	61 58(<i>S</i>)	30 83(<i>S</i>)	15
	3-alcohol		86 39(<i>S</i>)	42 15(<i>S</i>)	20	50	37
	4-alcohol			29	17	21	49
	ketones ^[b]		<1	3	5	5	7
J	1-alcohol	4	0	1	1	0	2
	2-alcohol	96	23 20(<i>S</i>)	29 12(<i>S</i>)	52 57(<i>S</i>)	29 67(<i>S</i>)	16
	3-alcohol		77 46(<i>S</i>)	42 11(<i>S</i>)	25	48	35
	4-alcohol			28	22	23	48
	ketones ^[b]		<1	2	5	5	5
9-10A	1-alcohol	8	0	1	1	0	1
	2-alcohol	92	6 14(<i>S</i>)	26 7(<i>S</i>)	53 50(<i>S</i>)	39 60(<i>S</i>)	16
	3-alcohol		95 41(<i>S</i>)	41 8(<i>S</i>)	20	59	32
	4-alcohol			33	26	3	51
	ketones ^[b]		<1	3	5	5	6
9-10A-A82L	1-alcohol	5	0	0	0	1	0
	2-alcohol	95	35 39(<i>S</i>)	27 4(<i>S</i>)	22 10(<i>S</i>)	16 7(<i>S</i>)	21
	3-alcohol		65 42(<i>S</i>)	46 30(<i>S</i>)	25 17(<i>R</i>)	16	19
	4-alcohol			29	53	67	60
	ketones ^[b]		<1	2	5	5	5
9-10A-A328V	1-alcohol	10	6	14	10	3	1
	2-alcohol	90	64 21(<i>R</i>)	62 15(<i>R</i>)	80 40(<i>S</i>)	76 0	79 5(<i>S</i>)
	3-alcohol		30	17	8	19	17
	4-alcohol			6	2	3	2
	ketones ^[b]		<1	<1	<1	<1	<1
1-12G	1-alcohol	11	9	5	5	3	1
	2-alcohol	89	77 4 (<i>R</i>)	76 40(<i>R</i>)	82 39(<i>R</i>)	86 52(<i>R</i>)	86 55(<i>R</i>)
	3-alcohol		14	15	11	7	9
	4-alcohol			3	3	5	4
	ketones ^[b]		<1	<1	<1	<1	<1

Reaction conditions were: 4 mM alkane substrates, 25 to 100 nM BM-3 mutant, 1% (v/v) ethanol, 500 μ M NADPH, incubation at room temperature for 4 hours. Refer to Appendix B for mutations in BM-3 variants 139-3, J, 9-10A

^[a] Product distribution determined as ratio of a specific alcohol product to the total amount of all alcohol products (given in %). Errors are at most $\pm 1\%$.

^[b] Product distribution for ketones was similar to alcohol product distribution. The numbers reported here are the (%) total of all ketones relative to total products (alcohols + ketones).

^[c] Favored enantiomer is listed in parentheses. Errors are at most $\pm 5\%$.

Table 2.2. Catalytic properties of P450 BM-3 variants.

mutant	substrate	rate of NADPH consumption [min ⁻¹] ^[a]	background NADPH consumption [min ⁻¹] ^[a]	rate of product formation [min ⁻¹] ^[c]	coupling to NADPH [%] ^[d]	total turnovers ^[e]	fold improvement ^[f]
139-3	Octane	2400 ^[b]	170	480	20	1000	1
	Propane	190 ^[b]	50	12	6	500	1
J	Octane	3200	300	660	21	3000	3
	Propane	910	300	30	3	800	1.6
9-10A	Octane	2820	220	540	19	3000	3
	Propane	520	100	23	4	1100	2.2
9-10A-A82L	Octane	1670	270	530	32	6000	6
	Propane	390	200	54	14	2400	4.8
9-10A-A328V	Octane	1900	720	50	3	2000	2
	Propane	770	450	35	5	100	0.2
1-12G	Octane	1030	620	150	15	7500	7.5
	Propane	660	640	160	24	6000	12

^[a] Initial NADPH consumption rates were measured over 15 seconds at 340 nm as nmol NADPH/min/nmol protein. Octane reactions contained 100 nM P450, 166 μ M NADPH, and 4 mM octane in 1% ethanol and potassium phosphate buffer. Propane reactions contained 200 nM P450, 166 μ M NADPH, and propane-saturated potassium phosphate buffer. Background rates were measured under the same conditions, but without substrate. Errors are at most 10%..

^[b] The difference between these numbers and ones we reported [18] previously are due to the longer time period used to measure rates in this work (15 seconds compared to 2 seconds).

^[c] Initial rates were measured by GC over 1 minute as nmol total products/min/nmol protein. Octane reactions contained 100nM P450, 500 μ M NADPH, and 4 mM octane in 1% ethanol and potassium phosphate buffer. Propane reactions contained 1 μ M P450, 500 μ M NADPH, and propane-saturated potassium phosphate buffer. Errors are at most 10%.

^[d] Coupling determined by ratio of product formation rate to NADPH consumption rate.

^[e] Total turnover numbers determined as nmol product/nmol enzyme. Octane reactions contained 10-25 nM P450, 500 μ M NADPH, and 4 mM octane in 1% ethanol and potassium phosphate buffer. Propane reactions contained 10-25 nM protein, potassium phosphate buffer saturated with propane, and an NADPH regeneration system containing 100 μ M NADP⁺, 2 U/mL isocitrate dehydrogenase, and 10 mM isocitrate. Errors are at most 10%.

^[f] Fold improvement is based on total turnovers of hydroxylated products compared to 139-3.

This third round, in which approximately 1,500 variants were screened, failed to produce a mutant with either increased NADPH oxidation in presence of propane, or more dimethyl ether hydroxylation products. A possible explanation is that further increases in activity require amino acid substitutions not accessible by mutating only one base pair (single nucleotide changes to a codon typically access only about six of the nineteen possible amino acid substitutions). Alternatively, two or more simultaneous, or coupled, genetic mutations might be necessary for further improvements. Such events occur with very low probability and will not be found by screening only few thousand clones.

C.4. Site-Directed Mutagenesis

Wong *et al.* achieved hydroxylation activity towards butane and propane in the camphor hydroxylase cytochrome P450_{cam} by reducing the size of the enzyme's active site using structure guided site-directed mutagenesis [15]. We reasoned that decreasing the volume of the active site of 139-3 might serve to enhance its activity towards smaller substrates. Tightening up the active site might also confer regioselectivity towards longer alkanes – if the substrate is bound more tightly, fewer hydroxylation products should be possible. We therefore turned to site-directed mutagenesis of residues in the active site for further improvements.

Using a crystal structure of the heme domain of wild-type BM-3 containing a bound substrate [30], we identified two residues that should influence substrate binding (Figure 2.3).

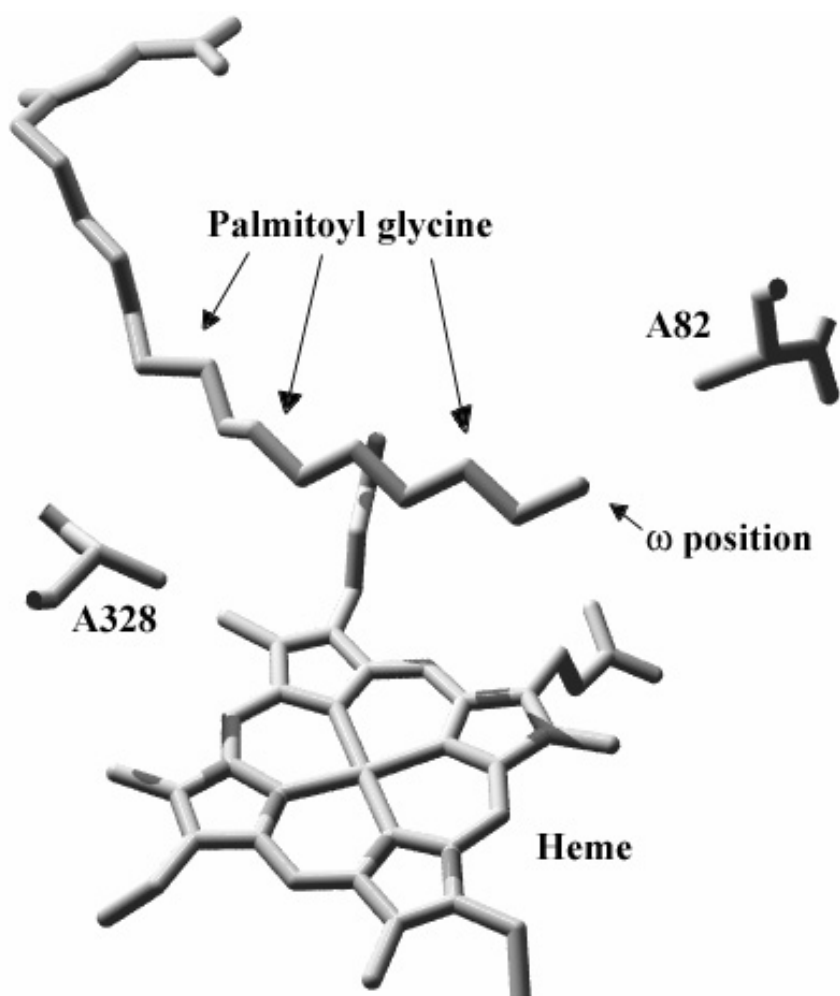


Figure 2.3. Positions of A328 and A82 in the active site of wild-type P450 BM-3. The picture was made from the coordinates of the crystal structure 1JPZ in the Protein Database. The substrate is palmitoyl glycine.

Alanine 328 sits directly above the heme cofactor and is the residue closest to the proximal side of the heme iron. Mutation of this residue to valine in the wild-type enzyme had been reported to affect substrate binding and turnover rates on fatty acids [31]. We substituted alanine 328 in 9-10A with the larger, hydrophobic valine and determined the activity of this mutant (termed 9-10A-A328V) towards several alkanes (Tables 2.1 and 2.2, Figure 2.2). Neither the propane hydroxylation activity nor the total propane turnovers improved

relative to its parent. However, we observed a dramatic shift in the regioselectivity of hydroxylation on longer alkanes (Figure 2.2). Wild-type and all mutants of BM-3 generated in this laboratory by directed evolution hydroxylate longer alkanes such as heptane, octane, and nonane with roughly equivalent distributions of the 2-, 3-, and 4-alcohols. Mutant 9-10A-A328V, on the other hand, forms primarily (>80%) 2-alcohols from these substrates. With octane, the resulting 2-alcohol is ~70% *S*-2-octanol (40% ee) (Table 2.1). Other alkanes are not hydroxylated enantioselectively. We rationalize that these changes in regioselectivity and enantioselectivity result from a reduction in possible binding geometries for these substrates in the active site.

The alkane hydroxylation product distributions for 9-10A-A328V clearly show its selectivity for the alkane 2-position. The fact that only 2-octanol is formed enantioselectively, but not 2-heptanol or 2-nonanol, suggests that a substrate-protein contact specific to the methyl group of octane furthest from the heme induces enantioselectivity towards this lone substrate. The other non-regioselective mutants, 139-3, J, and 9-10A, also exhibit similar enantioselectivity towards octane; this contact must therefore function independently of residue 328. It may be possible to engineer a mutant that is enantioselective for the *S*-2-position of other alkanes by changing other residues in the binding pocket (or outside) to mimic this contact.

The second side chain we chose to alter is located near the active site that forms after the conformational change associated with substrate binding occurs. In the crystal structure of BM-3 with bound palmitoyl glycine, alanine 82 is located within 3.5 Angstroms of the substrate ω -terminus [30]. We reasoned that changing this residue to a larger, hydrophobic

amino acid would decrease active site volume upon substrate binding. BM-3 undergoes large conformational changes upon substrate binding and catalysis [32] which makes rational design an oftentimes fruitless approach. We therefore chose to prepare a small library containing the four large, hydrophobic amino acids leucine, isoleucine, valine, and phenylalanine at position 82, and screened the library using dimethyl ether. Mutant 9-10A-A82L was identified as more active, and subsequent gas chromatographic analysis of the reaction mixtures revealed that this mutant supports more turnovers with propane (~2,400) than the 9-10A parent. The rate of propane hydroxylation and its coupling efficiency with this mutant were also improved. Hydroxylation of longer alkanes using this mutant occurred with a small shift in regioselectivity, in this case favoring the formation of primarily 3- and 4-alcohols (Table 2.1, Figure 2.2).

C.5. Recombination

To eliminate possible deleterious we had picked up in mutant 9-10A and to see whether the mutations A82L and A328V were beneficial in combination we shuffled the (heme domain) genes of J, 9-10A, 9-10A-A328V, and 9-10A-A82L using a modified DNA shuffling protocol [33]. The resulting small library (32 possible combinations) was then screened for activity on propane and dimethyl ether. Mutant 1-12G was selected from this library. Like mutant 9-10A-A328V, 1-12G hydroxylates alkanes at the 2-position (>80%). However, chiral GC analysis of the products revealed that 1-12G is as enantioselective as 9-10A-A328V, generating *R*-2-alcohols (40-55% ee) of heptane, octane, nonane, and

decane (Tables 2.1 and 2.2, Figure 2.2). Mutant 1-12G also supports thousands of turnovers on the substrates propane (6,000) and octane (7,500), resulting in approximately an order of magnitude improvement compared to 139-3. Sequencing revealed that this mutant contains all of the mutations introduced into the recombination library – it is the double mutant A328V+A82L of 9-10A. Addition of the A82L mutation to 9-10A-A328V has shifted the octane substrate in the active site such that the opposite enantiomer of its 2-alcohol is now favored (Figure 2.4).

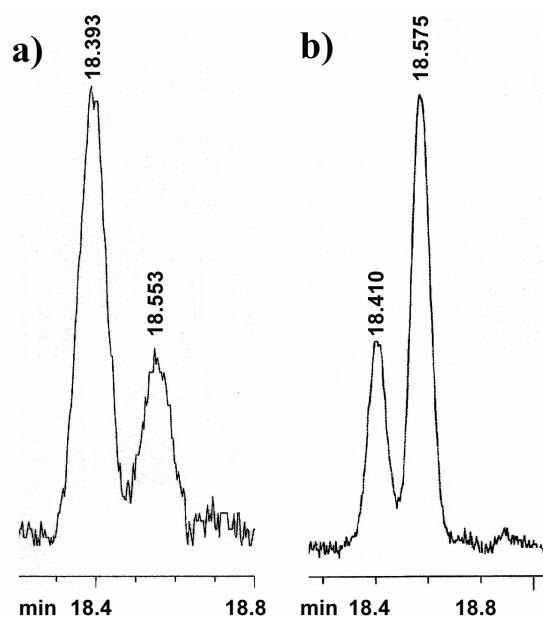


Figure 2.4. GC/FID analysis of the (-)-menthyl carbonate diastereomers of the 2-octanol produced by BM-3 catalyzed alkane oxidation. The *S*-2-octanol derivative elutes at 18.4 minutes, the *R*-2-octanol derivative elutes at 18.6 minutes. **a)** Reaction catalyzed by 9-10A-A328V (40% ee), **b)** Reaction catalyzed by 1-12G (40% ee). The reaction conditions for the hydroxylation reactions were: 4 mM octane, 25 to 100 nM BM-3 mutant, 1% (v/v) ethanol, 500 μ M NADPH, incubation at room temperature for 4 hours.

Residue 82 was chosen for its proximity to the substrate ω -terminus, but it is not clear whether the larger leucine side chain “pushes” the substrate further up the active site or

blocks the channel such that the substrate is flipped relative to its position in the A328V mutant.

In addition to its effect on selectivity, the A82L substitution, both with and without the A328V mutation, increases total turnover number and coupling to NADPH oxidation (Table 2.2). It is possible that by increasing coupling efficiency this mutation protects the heme cofactor from degradation by reduced oxygen species such as peroxide and superoxide (see below), but further analysis is required to determine the cause. The direct regio- and enantioselective hydroxylation activity towards linear alkanes exhibited by mutant 1-12G, with these rates (up to 400 min^{-1}) and total turnover numbers (6,000-7,500), is unprecedented.

C.6. Coupling of NADPH Reducing Equivalents to Product Formation

Under oxygen limiting conditions, i.e., substrate and NADPH concentrations in large excess of the 225-250 μM dioxygen present in oxygen-saturated buffer, hydroxylation reactions catalyzed by the mutants in this work form 225-250 μM of products. This upper limit to product formation suggests, as we have reported in our previous work [18], that substrate oxidation is tightly coupled to the consumption of dioxygen in these mutants. In general with P450 systems, NADPH oxidation not coupled to the formation of product is assumed to be wasted on reducing heme-bound dioxygen to active oxygen species such as peroxide and superoxide (which may subsequently inactivate the enzyme) or to water. If

oxygen reduction is the only mechanism for NADPH uncoupling, then our mutants should be fully coupled.

When we compare the NADPH consumption rates of these mutants with their product formation rates, however, we discover that a large fraction of the NADPH oxidized is not used for product formation or uncoupled oxygen reduction. Furthermore, the mutants oxidize NADPH even in absence of substrate (Table 2.2) at significantly higher rates than the wild-type enzyme, which has a relatively low background rate of about 8 min⁻¹.

Mutants generated by random mutagenesis have similar coupling efficiencies: approximately 20% for octane, and 5% for propane hydroxylation. The A82L mutation increases coupling of NADPH oxidation to octane (32%) and propane hydroxylation (14%) while the coupling efficiency of 9-10A-A328V is significantly (3 and 5% for octane and propane, respectively). Mutant 1-12G, with mutations A82L and A328V has an intermediate coupling efficiency for octane (15%), but shows the highest coupling efficiency of all mutants with propane (24%).

The background NADPH oxidation rates were measured under the same conditions but in the absence of substrate. Because no octane turnovers could be detected in the absence of ethanol, NADPH oxidation rates were measured in the presence of 1% (v/v). Ethanol does increase the background NADPH oxidation rate for most mutants, except for J and 1-12G. The background NADPH oxidation rates are similar for the mutants except for 9-10A-A328V and 1-12G. These mutants, however, exhibit very high background rates at 450 (9-10A-A328V) and 640 min⁻¹ (1-12G). The NADPH consumption rate of 1-12G with

propane was only 20 min^{-1} faster than the background rate without substrate. The higher propanol formation rate of 160 min^{-1} suggests that propane hydroxylation with this mutant outcompetes the background NADPH consumption process. Propane therefore induces electron transfer to the heme to initiate the catalytic cycle.

As described in Chapter 1, electron transfer in wild-type P450 BM-3 is highly regulated: NADPH is oxidized only in the presence of substrate and tightly coupled to substrate oxidation. The substrates we are employing differ substantially from fatty acids. They lack the carboxylate moiety and are up to three times shorter than, for example, lauric acid. In addition to uncoupling reactions in the active which can lead to the formation of superoxide, peroxide or water from the heme prior to reaction with substrate [34], several other uncoupling reactions have been described. If electron transfer from FAD to FMN is disturbed, electrons could be transferred to NADP^+ . Dioxygen can potentially accept electrons from either FAD or FMN to produce superoxide or peroxide, depending on whether one- or two-electron reduction occurs [35].

It has been proposed that the conformational changes upon substrate binding and during catalysis could be involved in the fine-tuning of the redox properties of the flavin cofactors [36]. NMR studies of the bacterial P450cam, for example, suggest that its electron donor, putidaredoxin, induces conformational changes to facilitate the oxygenation reaction [37]. It is likely that the mutations accumulated during random mutagenesis as well as the ones introduced by site-directed mutagenesis disturb the highly regulated electron transfer machinery of P450 BM-3. Having ruled out reduction of

dioxygen as the predominant uncoupling reaction, we propose an alternative, possibly reduction of NADP^+ , as the most likely.

We have noticed that when we screen for product formation using the dimethyl ether/purpald screen, the resulting mutants, 1-12G and 9-10A-A82L, are more coupled than mutants obtained by screening for NADPH consumption only and also support more total turnovers. We therefore decided to further engineer P450 BM-3 to try and reduce any uncoupling reactions by performing additional rounds of mutagenesis and strictly relying on assays that are based on product formation. This work is described in the following chapters.

C.7. Whole-Cell Biotransformations

Two major practical obstacles to implementing a biocatalytic process are the need for large amounts of purified protein and the expensive cofactors. Lysates of *E. coli* (DH5 α) containing overexpressed cytochrome P450 BM-3 mutants exhibit the same activity as purified protein (data not shown), but still require the addition of NADPH. We have used an isocitrate dehydrogenase-based NADPH regenerating system [28] to perform reactions using both cell lysate and purified protein, with results indistinguishable from using NADPH alone (consistent with the fact that these reactions are generally oxygen limited - data not shown). We were curious to see if we could use our *E. coli* system as a whole-cell catalyst, since the alkane substrates and alcohol products should be permeable to the cell membrane. To test this, we prepared cultures of *E. coli* DH5 α cells that overexpress the 9-

10A-A328V and the 1-12G mutants. Without optimizing the system, we prepared the cells and supplied them octane according to a procedure published by Witholt's group that had used *E. coli* K27 expressing wild-type BM-3 and myristic acid as a substrate [38,39]. We used isopropyl- β -D-thiogalactopyranoside (IPTG) to induce expression. Extraction of these whole-cell reaction mixtures with methylene chloride and analysis of the products revealed that both the regio- and enantioselectivity of the alkane hydroxylation products are preserved in the whole-cell system (Figure 2.5).

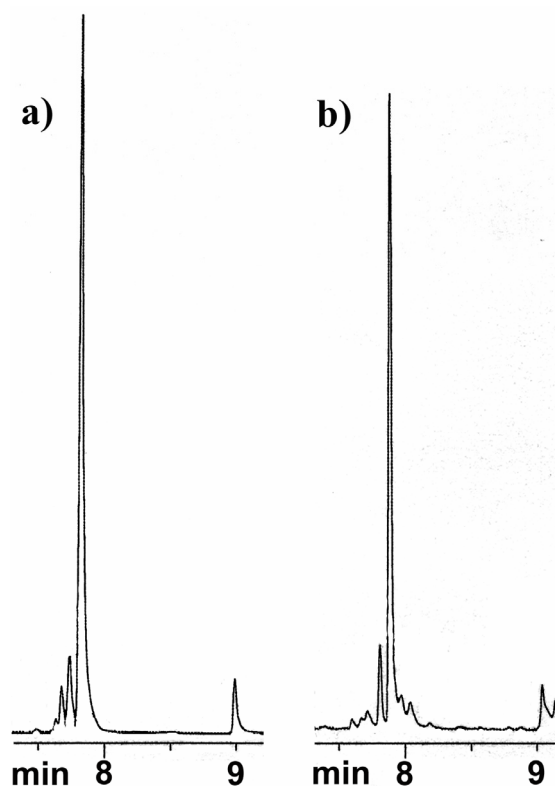


Figure 2.5. GC/FID analysis of the octane hydroxylation product using 9-10A-A328V as **a)** purified protein and **b)** a whole-cell catalyst. 3-Octanol elutes at ~7.7 minutes, 2-octanol elutes at ~7.8 minutes, 1-octanol elutes at ~9.0 minutes.

Optimization of these reaction conditions, perhaps using a system analogous to the two-phase system described by Witholt and coworkers for AlkB octane hydroxylation [9], could lead to cost-effective use of our *E. coli* cells for alkane hydroxylation.

D. Conclusions

Cytochrome P450 BM-3 is a highly “evolvable” catalyst: protein engineering by directed evolution and site-directed mutagenesis has generated variants with wide-ranging properties, including the ability to utilize different oxidants such as hydrogen peroxide for fatty acid hydroxylation [40,41], activity on nonnatural substrates [42-45] and in organic solvents [46], and greater thermostability [47]. The regio- and enantioselective alkane hydroxylation activities reported here further demonstrate the functional flexibility of the BM-3 scaffold. We might (perhaps optimistically) regard BM-3 as a “one-enzyme-fits-all” oxidation catalyst.

Regioselective alkane hydroxylation requires a catalyst that can discriminate between very similar methylene carbons. In addition, there must be a mechanism to remove the hydroxylated substrate, to prevent overoxidation. With the modifications presented in this work, the hydrophobic channel that serves as the active site of BM-3 provides the perfect environment for binding and oxidizing alkanes. It should be possible to make further improvements in the enantioselectivity of the 9-10A-A328V and 1-12G biocatalysts, using directed evolution, as has been done for several other enzyme systems [48].

E. References

1. Kerr, J. A. (1966). **Bond dissociation energies by kinetic methods.** *Chem. Rev.* **66**, 465.
2. Labinger, J. A. (2004). **Selective alkane oxidation: hot and cold approaches to a hot problem.** *J. Mol. Catal. A: Chem.* **220**, 27-35.
3. Chavez, F. A., Rowland, J. M., Olmstead, M. M. & Mascharak, P. K. (1998). **Syntheses, structures, and reactivities of cobalt(III)- alkylperoxo complexes and their role in stoichiometric and catalytic oxidation of hydrocarbons.** *J. Am. Chem. Soc.* **120**, 9015-9027.
4. Blay, G., Fernandez, I., Gimenez, T., Pedro, J. R., Ruiz, R., Pardo, E., Lloret, F. & Munoz, M. C. (2001). **Alkane oxidation by a carboxylate-bridged dimanganese(III) complex.** *Chem. Commun.*, 2102-2103.
5. Assis, M. D. & Smith, J. R. L. (1998). **Hydrocarbon oxidation with iodosylbenzene catalysed by the sterically hindered iron(III) 5-(pentafluorophenyl)-10,15,20- tris(2,6-dichlorophenyl)porphyrin in homogeneous solution and covalently bound to silica.** *J. Chem. Soc.-Perkin Trans. 2*, 2221-2226.
6. Chen, K. & Que, L. (2001). **Stereospecific alkane hydroxylation by non-heme iron catalysts: mechanistic evidence for an Fe-V = O active species.** *J. Am. Chem. Soc.* **123**, 6327-6337.
7. Wallar, B. J. & Lipscomb, J. D. (1996). **Dioxygen activation by enzymes containing binuclear non-heme iron clusters.** *Chem. Rev.* **96**, 2625-2657.
8. Elliott, S. J., Zhu, M., Tso, L., Nguyen, H. H. T., Yip, J. H. K. & Chan, S. I. (1997). **Regio- and stereoselectivity of particulate methane monooxygenase from *Methylococcus capsulatus* (Bath).** *J. Am. Chem. Soc.* **119**, 9949-9955.
9. Mathys, R. G., Schmid, A. & Witholt, B. (1999). **Integrated two-liquid phase bioconversion and product-recovery processes for the oxidation of alkanes: process design and economic evaluation.** *Biotechnol. Bioeng.* **64**, 459-477.
10. Simpson, A. E. C. M. (1997). **The cytochrome P450 4 (CYP4) family.** *Gen. Pharmacol.* **28**, 351-359.
11. Scheller, U., Zimmer, T., Becher, D., Schauer, F. & Schunck, W. H. (1998). **Oxygenation cascade in conversion of n-alkanes to alpha,omega- dioic acids catalyzed by cytochrome P450 52A3.** *J. Biol. Chem.* **273**, 32528-32534.

12. Benveniste, I., Tijet, N., Adas, F., Philipps, G., Salaun, J. P. & Durst, F. (1998). **CYP86A1 from *Arabidopsis thaliana* encodes a cytochrome P450-dependent fatty acid omega-hydroxylase.** *Biochem. Biophys. Res. Commun.* **243**, 688-693.
13. Maier, T., Forster, H. H., Asperger, O. & Hahn, U. (2001). **Molecular characterization of the 56-kDa CYP153 from *Acinetobacter* sp. EB104.** *Biochem. Biophys. Res. Commun.* **286**, 652-658.
14. Stevenson, J. A., Westlake, A. C. G., Whittock, C. & Wong, L. L. (1996). **The catalytic oxidation of linear and branched alkanes by cytochrome P450cam.** *J. Am. Chem. Soc.* **118**, 12846-12847.
15. Bell, S. G., Stevenson, J. A., Boyd, H. D., Campbell, S., Riddle, A. D., Orton, E. L. & Wong, L. L. (2002). **Butane and propane oxidation by engineered cytochrome P450(cam).** *Chem. Commun.*, 490-491.
16. Bell, S. G., Orton, E., Boyd, H., Stevenson, J. A., Riddle, A., Campbell, S. & Wong, L. L. (2003). **Engineering cytochrome P450cam into an alkane hydroxylase.** *Dalton Transactions*, 2133-2140.
17. Farinas, E. T., Schwaneberg, U., Glieder, A. & Arnold, F. H. (2001). **Directed evolution of a cytochrome P450 monooxygenase for alkane oxidation.** *Adv. Synth. Catal.* **343**, 601-606.
18. Glieder, A., Farinas, E. T. & Arnold, F. H. (2002). **Laboratory evolution of a soluble, self-sufficient, highly active alkane hydroxylase.** *Nat. Biotechnol.* **20**, 1135-1139.
19. Adam, W., Lukacs, Z., Saha-Moller, C. R., Weckerle, B. & Schreier, P. (2000). **Microbial asymmetric CH oxidations of simple hydrocarbons: a novel monooxygenase activity of the topsoil microorganism *Bacillus megaterium*.** *Eur. J. Org. Chem.*, 2923-2926.
20. Arp, D. J. (1999). **Butane metabolism by butane-grown '*Pseudomonas butanovora*'.** *Microbiology-(UK)* **145**, 1173-1180.
21. Steffan, R. J., McClay, K., Vainberg, S., Condee, C. W. & Zhang, D. L. (1997). **Biodegradation of the gasoline oxygenates methyl tert-butyl ether, ethyl tert-butyl ether, and tert-amyl methyl ether by propane-oxidizing bacteria.** *Appl. Environ. Microbiol.* **63**, 4216-4222.
22. Kulikova, A. K. & Bezborodov, A. M. (2000). **Oxidation of organic compounds by propane monooxygenase of *Rhodococcus erythropolis* 3/89.** *Appl. Biochem. Microbiol.* **36**, 227-230.

23. Kulikova, A. K. & Bezborodov, A. M. (2001). **Assimilation of propane and characterization of propane monooxygenase from *Rhodococcus erythropolis* 3/89.** *Appl. Biochem. Microbiol.* **37**, 164-167.
24. Ost, T. W. B. et al. (2001). **Structural and spectroscopic analysis of the F393H mutant of flavocytochrome P450 BM3.** *Biochemistry* **40**, 13430-13438.
25. Glieder, A. & Meinhold, P. (2003). **High-throughput screens based on NAD(P)H depletion.** In *Directed Enzyme Evolution: Screening and Selection Methods* (Arnold, F. H. & Georgiou, G., eds.), Vol. 230. Humana Press, Inc., Totowa, NJ.
26. Daff, S. N., Chapman, S. K., Turner, K. L., Holt, R. A., Govindaraj, S., Poulos, T. L. & Munro, A. W. (1997). **Redox Control of the Catalytic Cycle of Flavocytochrome P-450 BM3.** *Biochemistry* **36**, 13816-13823.
27. Strobel, H. W., Hodgson, A. V. & Shen, S. (1995). **NADPH cytochrome P450 reductase and its structural and functional domains.** In *Cytochrome P450: Structure, Mechanism, and Biochemistry* Second edit. (Ortiz de Montellano, P. R., ed.), pp. 225-244. Plenum Press, New York.
28. Schwaneberg, U., Otey, C., Cirino, P. C., Farinas, E. & Arnold, F. H. (2001). **Cost-effective whole-cell assay for laboratory evolution of hydroxylases in *Escherichia coli*.** *J. Biomol. Screen.* **6**, 111-117.
29. Hopps, H. B. (2000). **Purpald: a reagent that turns aldehydes purple.** *Aldrichimica Acta* **33**, 28-30.
30. Haines, D. C., Tomchick, D. R., Machius, M. & Peterson, J. A. (2001). **Pivotal role of water in the mechanism of P450BM-3.** *Biochemistry* **40**, 13456-13465.
31. Peterson, J. A., Hedge, A., Graham, S. & Mullin, D. (2002). *Sixth International Symposium on Cytochrome P450 Biodiversity, University of California, Los Angeles.*
32. Modi, S., Sutcliffe, M. J., Primrose, W. U., Lian, L. Y. & Roberts, G. C. K. (1996). **The catalytic mechanism of cytochrome P450 BM3 involves a 6 Angstrom movement of the bound substrate on reduction.** *Nat. Struct. Biol.* **3**, 414-417.
33. Joern, J. M. (2003). **DNA shuffling.** In *Directed Evolution Library Creation: Methods and Protocols* (Arnold, F. H. & Georgiou, G., eds.), Vol. 231. Humana Press, Inc., Totowa, NJ.
34. de Montellano, P. R. (1995). **Cytochrome P450: structure, mechanism, and biochemistry.** 2nd edit., Plenum Press, New York.

35. Bosterling, B. & Trudell, J. R. (1981). **Spin trap evidence for production of superoxide radical-anions by purified NADPH-cytochrome P450 reductase.** *Biochem. Biophys. Res. Commun.* **98**, 569-575.
36. Murataliev, M. B., Feyereisen, R. & Walker, A. (2004). **Electron transfer by diflavin reductases.** *Biochim. Biophys. Acta* **1698**, 1-26.
37. Tosha, T., Yoshioka, S., Takahashi, S., Ishimori, K., Shimada, H. & Morishima, I. (2003). **NMR study on the structural changes of cytochrome P450cam upon the complex formation with putidaredoxin: functional significance of the putidaredoxin-induced structural changes.** *J. Biol. Chem.* **278**, 39809-39821.
38. Schneider, S., Wubbolts, M. G., Oesterhelt, G., Sanglard, D. & Witholt, B. (1999). **Controlled regioselectivity of fatty acid oxidation by whole cells producing cytochrome P450(BM-3) monooxygenase under varied dissolved oxygen concentrations.** *Biotechnol. Bioeng.* **64**, 333-341.
39. Schneider, S., Wubbolts, M. G., Sanglard, D. & Witholt, B. (1999). **Production of alkanedioic acids by cytochrome P450(BM-3) monooxygenase: oxidation of 16-hydroxyhexadecanoic acid to hexadecane-1,16-dioic acid.** *Biocatal. Biotransform.* **17**, 163-178.
40. Cirino, P. C. & Arnold, F. H. (2002). **Regioselectivity and activity of cytochrome P450BM-3 and mutant F87A in reactions driven by hydrogen peroxide.** *Adv. Synth. Catal.* **344**, 932-937.
41. Cirino, P. C. & Arnold, F. H. (2003). **A self-sufficient peroxide-driven hydroxylation biocatalyst.** *Angew. Chem. Int. Edit.* **42**, 3299-3301.
42. Appel, D., Lutz-Wahl, S., Fischer, P., Schwaneberg, U. & Schmid, R. D. (2001). **A P450 BM-3 mutant hydroxylates alkanes, cycloalkanes, arenes and heteroarenes.** *J. Biotechnol.* **88**, 167-171.
43. Li, Q. S., Ogawa, J., Schmid, R. D. & Shimizu, S. (2001). **Engineering cytochrome P450 BM-3 for oxidation of polycyclic aromatic hydrocarbons.** *Appl. Environ. Microbiol.* **67**, 5735-5739.
44. Farinas, E., T., Alcalde, M. & Arnold, F. H. (2003). **Alkene epoxidation catalyzed by cytochrome P450 BM-3 139-3.** *Tetrahedron: Asymmetry* **60**, 525.
45. Otey, C., R., Silberg, J. J., Voigt, C. A., Endelmann, J. B., Bandara, G. & Arnold, F. H. (2004). **Functional evolution and structural conservation in chimeric cytochromes P450: calibrating a structure-guided approach.** *Chem. Biol.* **11**, 309-318.

46. Wong, T. S., Arnold, F. H. & Schwaneberg, U. (2004). **Laboratory evolution of cytochrome P450BM-3 monooxygenase for organic cosolvents.** *Biotechnol. Bioeng.* **85**, 351-358.
47. Salazar, O., Cirino, P. C. & Arnold, F. H. (2003). **Thermostabilization of a cytochrome P450 peroxygenase.** *Chembiochem* **4**, 891-893.
48. Jaeger, K. E., Eggert, T., Eipper, A. & Reetz, M. T. (2001). **Directed evolution and the creation of enantioselective biocatalysts.** *Appl. Microbiol. Biotechnol.* **55**, 519-530.

C h a p t e r 3

Active Site Engineering of Cytochrome P450 BM-3

A. Abstract

The roles of P450 BM-3 active site residues in determining alkane hydroxylation activity and regioselectivity were investigated. With the guidance of crystal structures of the substrate bound heme domain of wild-type BM-3, 11 active site residues in the substrate binding channel were identified that could potentially influence substrate binding. Saturation mutagenesis libraries at each of these positions were generated and activity towards octane and propane surrogate substrates was measured. Furthermore, beneficial mutations were analyzed for their effects on the regioselectivity of octane hydroxylation. These data were used to identify key single active site changes important for discriminating between different-sized alkane substrates, generating specific hydroxylation products, and/or improving general alkane hydroxylation activity. In addition, the data allowed us to select a limited number of active site mutations that were recombined to generate a reasonably sized library enriched in active variants.

B. Introduction

In this chapter, we further investigate the effects of substitutions in active site residues in P450 BM-3 on alkane hydroxylation activity. Previous work has shown that this enzyme is an excellent hydroxylation catalyst that can be engineered to accept a large array of substrates while functioning under a variety of conditions [1]. In our laboratory, BM-3 was engineered by directed evolution to hydroxylate linear alkanes at so far unmatched rates [2,3]. Chapter 2 describes further engineering by directed evolution and site directed mutagenesis to achieve a regio- and enantioselective alkane hydroxylation catalyst, named 1-12G. Here, active site variants of BM-3 are described that extend the hydroxylation regioselectivities supported by this enzyme.

P450 BM-3 consists of two distinct domains connected by a polypeptide linker: a 54 kDa heme domain in which substrate and oxygen are bound and activated and a 65 kDa reductase domain that transfers two electrons from NADPH via FAD and FMN cofactors to the heme domain. Substrate selectivity and regioselectivity of hydroxylation should depend primarily upon the size and shape of the substrate binding channel. The actual conformation of this channel is unclear, despite the availability of numerous crystal structures of substrate bound and unbound forms of the protein [4-7]. In the substrate bound structures, the substrate is located approximately 6 Å away from the heme iron, which is too far for catalysis to occur. NMR studies suggest that a conformational change occurs prior to catalysis, moving the substrate by 6 Å into the correct position and orientation [8].

In addition, these structural changes upon substrate binding initiate electron transfer from NADPH into the heme by attenuating the redox potentials of the flavin and heme cofactors, and by shifting the spin-state of the heme-iron from low- to high-spin [9,10]. This intricately regulated electron transfer process may explain why the majority of mutations we accumulated in BM-3 during our directed evolution experiments are located outside of the active site [2,3,11]. In fact, out of the 14 heme domain mutations we found in our best alkane hydroxylase mutant obtained solely by directed evolution, mutant 9-10A, only one mutation, V78A, is located in the active site.

Here, we further investigate how active site residues affect alkane hydroxylation activity and regioselectivity. Using crystal structures of the heme domain of wild-type BM-3 with bound substrates [5,6], we identified 11 residues in the substrate binding channel, located directly above the heme cofactor, that might influence substrate binding. We generated saturation mutagenesis libraries at each of these positions and screened the libraries for activity towards octane and propane surrogate substrates before examining the effects of specific mutations on alkane hydroxylation activity. These data allowed us to identify key single active site changes in 9-10A that are important for discriminating between different-sized alkane substrates, generating specific hydroxylation products, and/or improving general alkane hydroxylation activity. In addition, the data allowed us to select a limited number of active site mutations that were recombined to generate a reasonably sized library containing multiple active site substitutions.

C. Results

C.1. Screening for Alkane Hydroxylation Activity

Several problems must be solved simultaneously to identify mutants from a library with high, regioselective hydroxylation activity towards alkanes. The desired alcohol products are colorless and are formed at concentrations too low to detect by their *in situ* chemical conversion to dye-sensitive compounds such as aldehydes and ketones. Screening libraries by spectroscopically monitoring NADPH consumption rates in the presence of the alkane often selects for mutants with NADPH oxidation rates highly uncoupled to product formation. In the past, we overcame these problems with the use of surrogate substrates that mimic our desired substrates, yet yield species when hydroxylated that are easily detected either directly or with the addition of a dye. For example, the screen for the high-throughput identification of mutant BM-3 enzymes with activity towards propane was described in Chapter 2 and uses dimethyl ether (DME) as a propane surrogate substrate [11]. Upon hydroxylation, it decomposes into methanol and dye-sensitive formaldehyde. For the work described in this chapter, we additionally use hexyl methyl ether (HME) as a surrogate for octane. It shares most of the physical properties of octane, including solubility in buffer, size, shape, and strength of its C-H bonds. When HME is hydroxylated at its methoxy carbon, it also produces an equivalent of formaldehyde which is visually detected at concentrations as low as 10 μ M with the dye Purpald [12] (Figure 3.1). Hexanal, the aldehyde product formed when the α -carbon of the hexyl group is hydroxylated, is practically unreactive towards Purpald at the concentrations we encounter in our screens. Formaldehyde is approximately 42 times more sensitive to Purpald than

hexanal (Figure 3.2). This disproportionate response makes HME, in contrast to the symmetric ether DME, a regio-selective screen for terminal alkane hydroxylation.

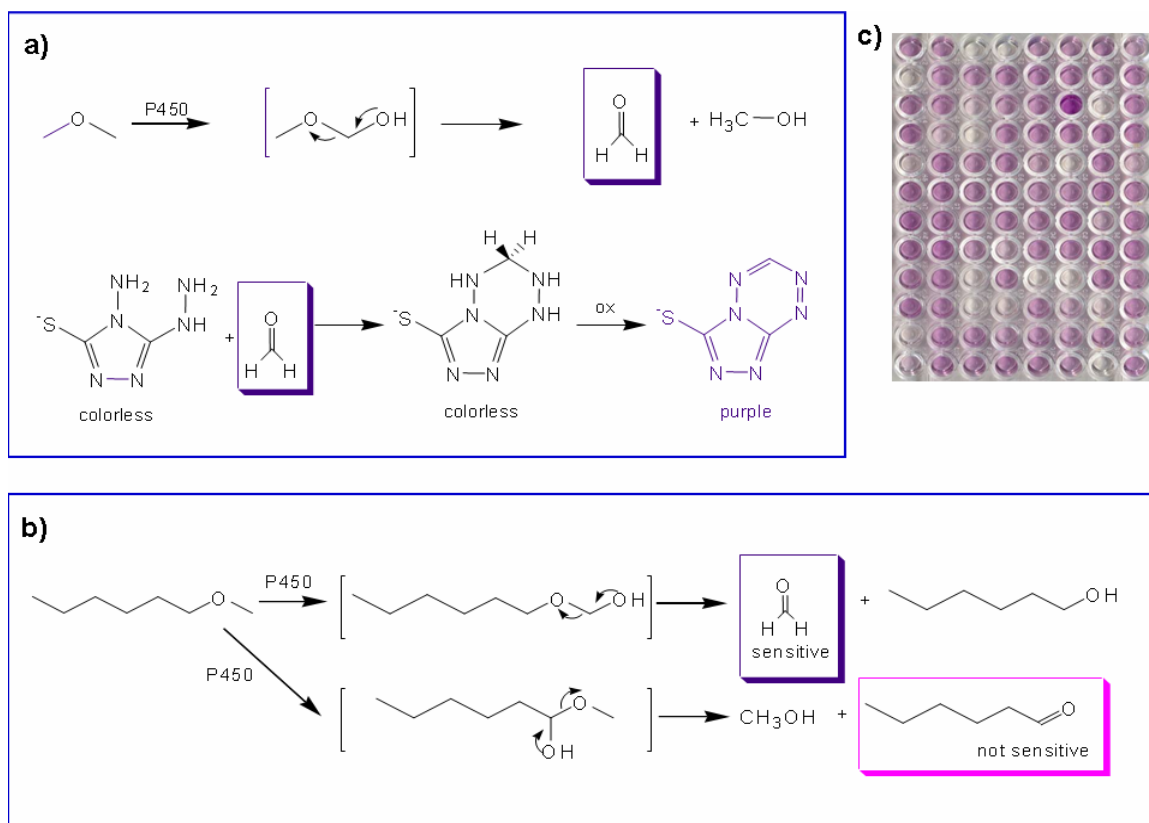


Figure 3.1. Alkylmethyl ether assays. **a)** Hydroxylation of the propane surrogate dimethyl ether produces formaldehyde which can easily be detected using the dye Purpald. **b)** Hexyl methyl ether can be used as an octane surrogate. The outcome of the screen, formation of formaldehyde and detection via Purpald, remains the same. **c)** A typical screening plate with P450-containing cell lysate, which, upon hydroxylation of the methoxy group of DME or HME and addition of Purpald, forms a purple color. Each well represents a different BM-3 variant.

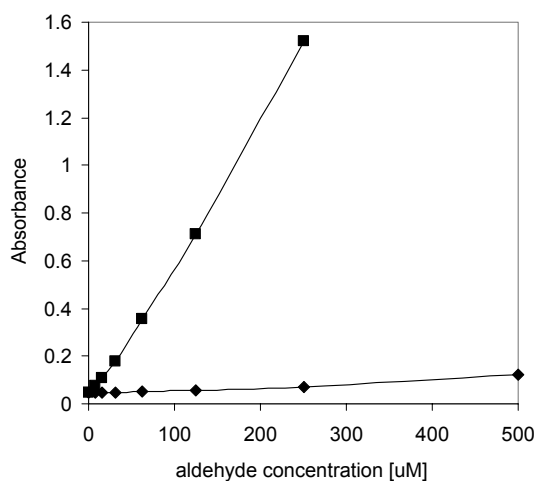


Figure 3.2. Standard curves for formaldehyde (■) and hexanal (◆) using Purpald. The assay was performed in a 96-well microtiter plate and the final volume was 250 μ L per well. The absorbance was measured using a Spectramax Plus microtiter plate reader (Molecular Devices, Sunnyvale, CA) and is therefore not normalized to a pathlength of 1cm. The sensitivity for formaldehyde is approximately 42 times greater than for hexanal.

The screen is an endpoint assay because Purpald needs to be solubilized in 2 M sodium hydroxide solution. We incubated the DME and HME reaction mixtures for 15 min before adding the Purpald solutions. Beneficial mutations therefore support more turnovers within this time and/or are more coupled to NADPH oxidation. Using both of these screens to characterize a library of mutants reveals important information about the active mutants: mutants that are selective for one substrate over the other can be immediately identified during screening.

C.2. Construction of Active Site Saturation Mutagenesis Libraries of 9-10A

We used the BM-3 heme domain crystal structures with bound substrates palmitoleic acid [5] and N-palmitoyl glycine [6], to identify 11 residues with side chains that are within 5 Å of the terminal eight carbons of the alkyl chains of the bound substrates. These were A74, L75, V78, F81, A82, F87, T88, T260, I263, A264, and A328 (Figure 3.3). Six of these positions (74, 78, 82, 87, 264, and 328) have been identified by our laboratory and other research groups as important residues for altering the activity of BM-3. For example, changes to F87 have long been known to affect the distributions of hydroxylated fatty acid products in wild-type BM-3 [13-16] and selectivity towards non-natural substrates [17]. In order to utilize peroxides in place of dioxygen and NADPH to drive hydroxylation by the peroxide shunt pathway, F87 must be altered to a small hydrophobic residue such as alanine or leucine [16,18]. Residues 74, 87, and 264 have been altered in combination with other mutations to increase the activity of wild-type BM-3 towards a variety of substrates including octane and polycyclic aromatic compounds [19-23]. Mutation of A328 to valine in the wild-type enzyme has been reported to affect substrate binding and turnover rates on fatty acids [24]. The only active site mutation acquired during our directed evolution experiments to engineer BM-3 for alkane hydroxylation was V78A. Mutant 1-12G, which has the two additional mutations, A82L and A328V, exhibits an increase in alkane hydroxylation activity and regio- and enantiopurity of products (see Chapter 2).

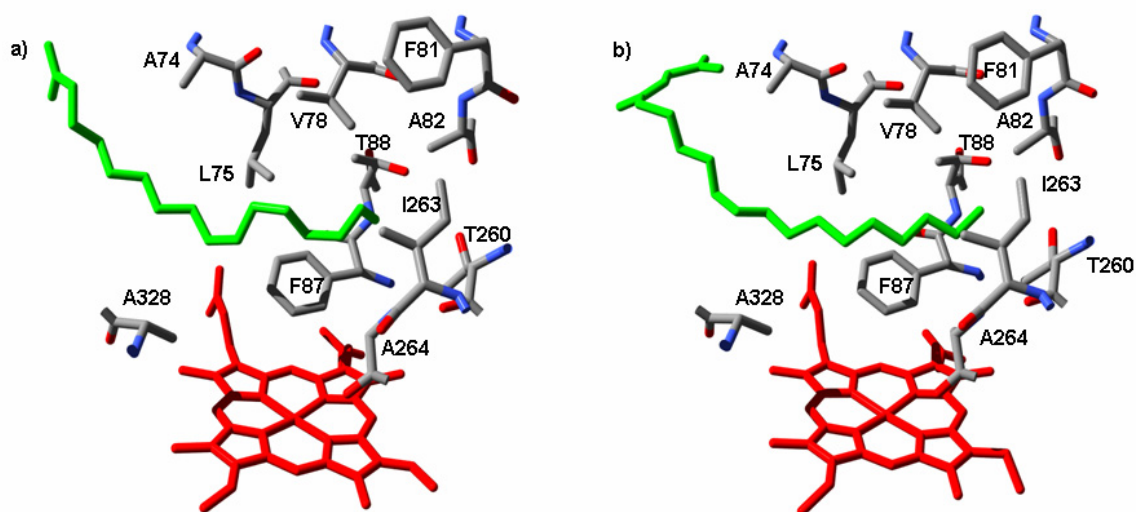


Figure 3.3. The active site of cytochrome P450 BM-3 showing the 11 active site residues in contact with the last eight carbon atoms of the bound fatty acid substrates from **a)** the crystal structure 1FAG (from the Protein Data Bank) containing the substrate palmitoleic acid [5] and **b)** the crystal structure 1JPZ containing N-palmitoyl glycine [6].

We used mutant 9-10A as the parent for generating the active site libraries because it was the most active laboratory evolved BM-3 alkane hydroxylase in which no active site residues had been intentionally altered. Additionally, as shown in Chapter 2, we already knew that active site changes to 9-10A can lead to dramatic improvements in alkane hydroxylation activity. We generated saturation mutagenesis libraries at each of these 11 active site positions in 9-10A and screened 174 mutants of each library for increased activity towards DME and HME. We also performed high throughput protein folding assays on each of these libraries to determine how active site mutations affect the integrity of the protein. Mutants that were correctly folded and retained at least some activity were isolated and eight individual colonies of each mutant were rescreened.

C.3. Active Site Saturation Mutagenesis Library Folding Data

Carbon monoxide difference spectroscopy was used to monitor incorporation of the heme cofactor. This technique can be performed in 96-well plates, enabling us to estimate the fraction of folded variants in a saturation mutagenesis library [25] (refer to Chapter 8 for experimental details). The reduced ferrous heme-CO complex with a Soret band near 450 nm is indicative of heme incorporation and thus a correctly-folded P450 [26]. P450 active site variants with a significant peak at 450 nm ($> 5\%$ of the control protein) were considered correctly folded, while variants showing no peaks in their CO difference spectra and were deemed unfolded. Depending on the residue mutated, the fraction of folded proteins ranged from 52% to 100% (Figure 3.4). This value takes into account stop codons, which account for 4.7% of all possible codons.

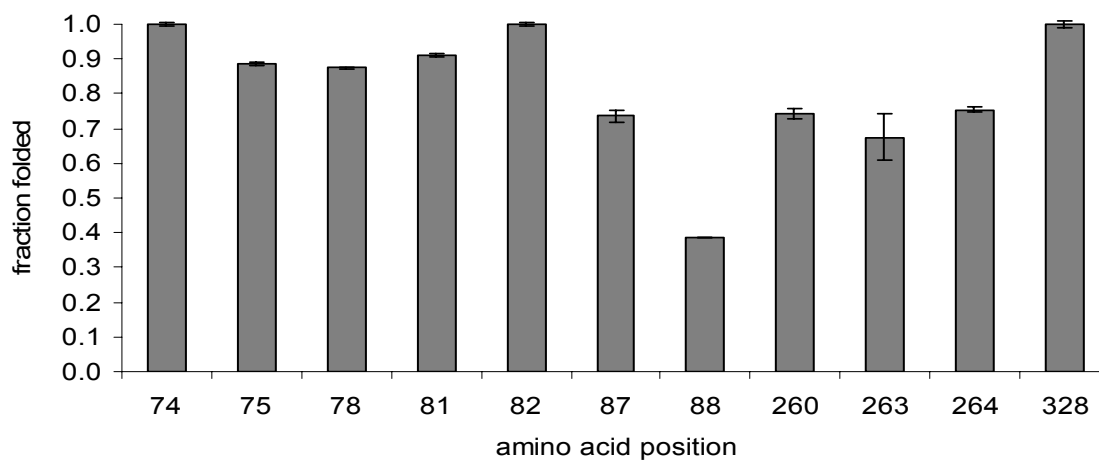


Figure 3.4. Fraction f of folded proteins in the 11 saturation mutagenesis libraries. Stop codons are encoded by 3/64 (4.7%) possible codons, leading to truncated proteins. Therefore, the fraction of folded proteins was adjusted by the adding to f the fraction $f^* = 0.049$ (F/N) of proteins that would be folded if they were not encoded by a stop codon. N is the total number of proteins screened; F is the number of folded proteins. Error bars are the standard error of two separate 96-well plates.

Several positions can accept almost any amino acid in place of the one present in the wild-type protein. Only a few residues, such as T88, are not mutable to this extent. The average fraction of folded protein is 0.81, which seems high given that the active site of P450 BM-3 is located in the core of the protein. It has been observed that mutations within the core of a protein are more disruptive on average than mutations of solvent exposed residues [27]. Core residues are coupled to a higher degree to other residues than are solvent exposed residues, thereby decreasing their site entropy and tolerance for mutation [28]. It can also be argued, however, that active site residues are often optimized for function, and not for stability. This “stability-function” hypothesis predicts that mutations in the active site are not destabilizing but generally decrease the catalytic activity [29]. This possibility was addressed by analyzing the libraries for function.

C.4. Active Site Saturation Mutagenesis Library Screening Data

The saturation libraries were screened with DME and HME, and the activity of each mutant towards these substrates was compared to that of 9-10A. Only mutants with improved activity towards either substrate were selected for further analysis and incorporation into an active site recombination library. However, taken as a whole, the screening results from each library revealed the importance of the corresponding active site position with respect to alkane hydroxylation activity. Figure 3.5 shows the screening results of a typical library. Refer to Appendix C for activity profiles of all other libraries.

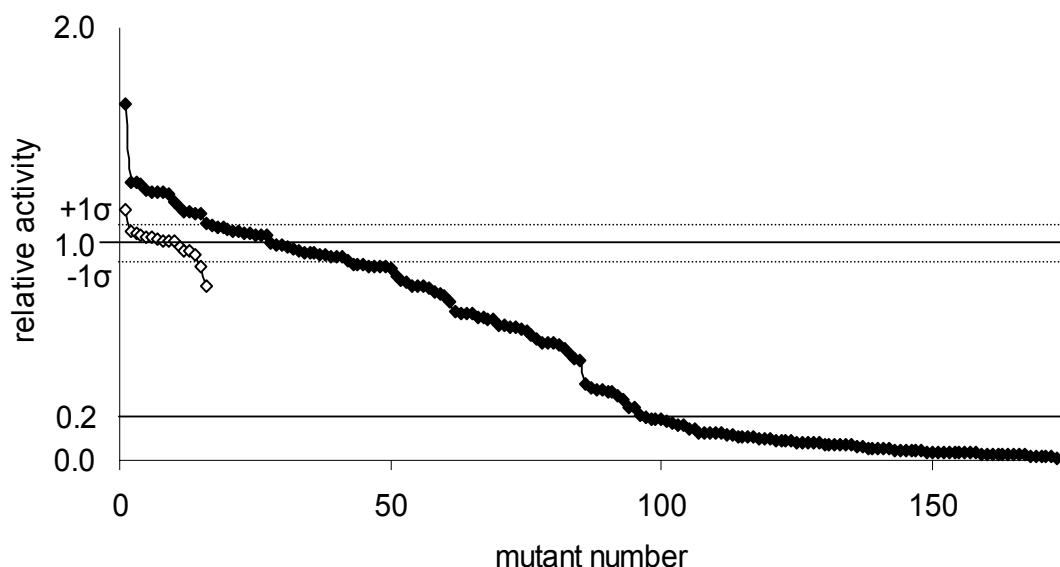


Figure 3.5. DME activity profile for the V78 saturation mutagenesis library. The activity of each of the 174 library members was normalized to the average 9-10A activity and is plotted in descending order (◆). The activities of 16 parental clones cultured in the same 96-well plate under the same conditions are shown (◇) to illustrate the variability of the assay. The coefficient of variance (CV) for this particular plate was 8%. Overall, the CV of the screen was 13%. Enzymes with more than 20 % of 9-10A's activity were deemed active for further analysis. Please refer to Chapter 8 for experimental details, and to Appendix C for activity profiles of the other saturation mutagenesis libraries.

The libraries were analyzed based on the fraction of active members of all folded members using a conservative cutoff level of 20% of 9-10A's activity. These data illustrate, which of the amino acids can be mutated without losing activity towards the screening substrate (Figure 3.6).

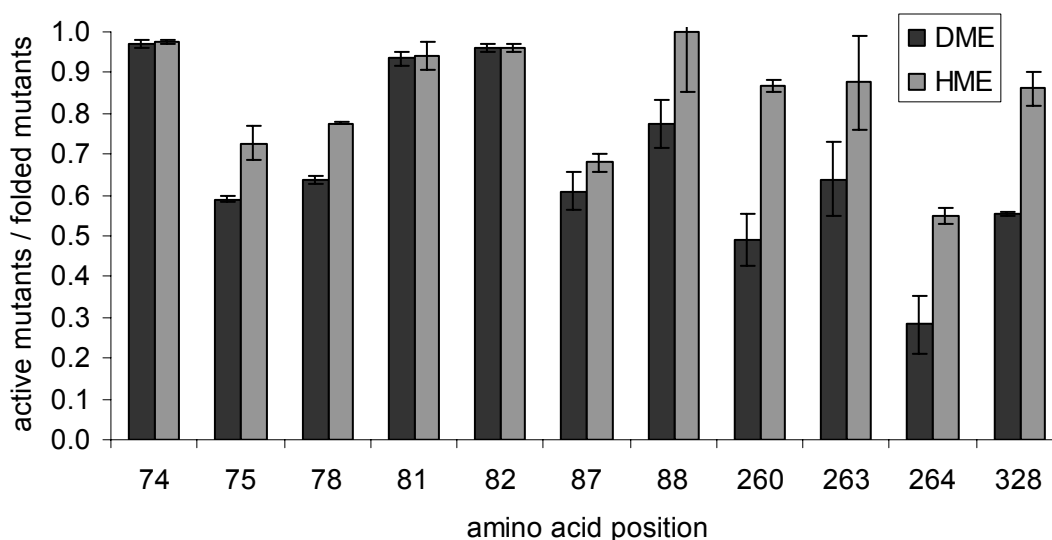


Figure 3.6. Fraction of folded mutants that remain active towards DME and HME in the saturation mutagenesis libraries at each of the 11 positions. Error bars are based on the standard deviation of two separate 96-well plates.

The positions A74, F81, T260 and A82 accept any amino acid substitution compatible with correct folding without losing hydroxylation activity. At positions 75, 78, 87, 88, 260, 263 and 328, 60 to 90% of the folded mutants remain active. Only at position 264, the fraction of active mutants drops to 20%. This position is somewhat sensitive to mutation in terms of activity on HME and DME.

The fraction of functional proteins for a given position can be estimated using the neutrality of a random mutation (ν) [30]. ν has been calculated previously for other proteins and ranged from 0.38 to 0.56 [31]. However, some proteins, such as lac repressor, 3-methyladenine DNA glycosylase, and T4 lysozyme, seem to be more tolerant towards random mutations, with ν values of 0.65, 0.66, and 0.84, respectively [32-34]. Variations in neutrality of different proteins are likely to depend on the size, expression

level, or level of conservation of the protein, making a meaningful comparison of ν between proteins difficult. Random mutagenesis studies that target the catalytic centers of proteins have been performed on a limited number of enzymes. These studies indicate that tolerance for mutations is generally limited, with ν ranging from 0.19 and 0.56 [33], thus supporting the “stability-function” hypothesis described above.

For the eleven BM-3 residues studied here, the average ν is 0.70. The degree of substitutability of the BM-3 active site is high compared to other proteins. One explanation could be that the active site residues targeted for mutagenesis are important for binding and orienting substrate, but do not participate in the catalytic mechanism, which is primarily governed by the cysteine-ligated heme. In any case, the observed tolerance to mutation within the active site makes BM-3 highly evolvable. In addition to its other favorable properties, such as high activity, solubility and expressibility, this trait makes BM-3 a good target for engineering approaches.

C.5. Improved Mutants Selected from Saturation Mutagenesis Libraries

Based on the beneficial mutations we picked from each library (Table 3.1), we grouped the amino acid positions into four categories: a) amino acid positions at which no mutant showed a change in DME and HME activity, b) positions at which improvements in activity towards the smaller substrate DME were found, c) positions at which improvements in activity towards the larger substrate HME were found, and d) positions at which no improved mutants could be identified but having many with decreased activity

towards DME and HME. In Chapter 2, we had observed that mutating active site residues putatively in contact with bound substrates induce changes to the distributions of hydroxylated products. We therefore performed octane hydroxylation reactions with *E. coli* cell lysate of each mutant in a library with increased activity towards DME or HME, and grouped the mutants within each library according to their distributions of formed octanols (Table 3.2). In all cases, each group of mutants with similar product distributions proved to be the same after sequencing.

Only one of the 11 saturation mutagenesis libraries, the library for position 74, showed no change among its full length (i.e., corrected for stop codons introduced during the library construction) members in either DME or HME activity relative to 9-10A. Ten mutants were randomly selected from the library and their product distributions with octane determined. All 10 mutants exhibited a product distribution similar to unmodified 9-10A. In the crystal structures of BM-3 with a bound fatty acid substrate, the alanine 74 side chain is at least 6.3 Å from the last eight carbon atoms of the substrate which are most likely in the same position as a bound octane molecule in the active site, but this residue should contact carbon atoms of a longer alkane. In decane reactions with the 10 selected mutants, however, no difference in their product distribution was found. Three of these mutants were randomly chosen for sequencing and found to be A74T, A74H, and A74P. Their similar activities on DME and HME and their similar regioselectivities suggest that the octane hydroxylation rates are not affected either.

Table 3.1. Activities of single active site mutants towards the screening substrates DME and HME.

mutation	DME ^[b]	HME ^[b]	DME/HME
9-10A	1.00	1.00	1.00
L75I ^[c]	0.74	1.00	0.7
L75W	0.49	1.43	0.3
A78T	1.37	0.95	1.4
A78F	1.64	0.40	4.1
A78S ^[c]	0.87	0.95	0.9
A82T	1.32	0.88	1.5
A82S	1.07	1.06	1.0
A82F	2.27	0.53	4.3
A82I	1.70	0.56	3.0
A82C	1.08	0.38	2.8
A82G	1.23	0.81	1.5
F87I	0.94	2.42	0.4
F87V	0.98	1.43	0.7
F87L	0.96	1.58	0.6
T88C	0.31	1.16	0.3
T260L	1.20	0.73	1.6
T260S	0.48	1.57	0.3
T260N	1.11	0.48	2.3
A328F	1.50	1.71	0.9
A328M	1.30	1.65	0.8
A328L	1.42	1.62	0.9

^[a] Mutations are in variant 9-10A (with amino acid mutations R47C, V78A, K94I, P142S, T175I, A184V, F205C, S226R, H236Q, E252G, R255S, A290V, L353V).

^[b] Terminal hydroxylation activity of dimethyl ether and hexyl methyl ether are reported relative to 9-10A.

^[c] Mutations L75I and A78S exhibited increased HME activity compared to 9-10A in the initial screen but were found to be only as active as 9-10A in the rescreen.

Table 3.2. Regioselectivities, rate of product formation and total turnover numbers of octane hydroxylation reactions catalyzed by variants of BM-3 containing single active site mutations^[a].

Mutation ^[b]	1-ol [%]	2-ol [%]	3-ol [%]	4-ol [%]	Others ^[c]	rate ^[d]	ttn ^[e]
9-10A	0	51	21	27	1	540	3000
L75I	3	42	18	17	20	210	4500
L75W	3	46	18	24	9	200	4000
A78T	4	22	27	45	2	500	4000
A78F	4	37	17	31	11	380	3000
A78S	5	48	18	20	9	260	2500
A82T	5	23	25	44	3	340	2700
A82S	6	40	19	26	9	300	2600
A82F	4	26	20	48	2	140	3000
A82I	4	11	21	59	5	600	3500
A82C	5	26	26	42	1	200	3000
A82G	7	52	17	23	1	360	2000
F87I	8	70	6	3	13	60	2600
F87V	5	52	13	4	26	240	3600
F87L	7	55	22	12	4	60	2300
T88C	4	51	21	22	2	460	4000
T260L	7	67	11	10	5	260	2500
T260S	6	39	26	29	0	160	3000
T260N	6	29	23	42	0	300	2500
A328F	6	88	4	0	2	40	2800
A328M	24	71	0	0	5	10	700
A328L	13	87	0	0	0	20	1000

^[a] Reactions were carried out using cell lysate instead of purified protein.

^[b] Mutations are in variant 9-10A (with amino acid mutations R47C, V78A, K94I, P142S, T175I, A184V, F205C, S226R, H236Q, E252G, R255S, A290V, L353V).

^[c] These are overoxidation products (ketones and aldehydes) with similar product distribution as the alcohols.

^[d] Measured as nmol octanol/nmol P450/minute.

^[e] Measured as nmol octanol/nmol P450 produced in 4 hour reaction.

Three of the 11 saturation mutagenesis libraries contained mutants with improved activity towards DME, determined by the ratio of each mutant's DME and HME activities relative to the comparable activities in 9-10A. In the crystal structures we used to identify active

site residues, the wild-type amino acids at these positions, 78, 82, and 260, contact the three terminal carbon atoms of the fatty acid substrate which are located directly above the heme cofactor where propane must bind for activation. The mutant 910A-A78F has a relative DME activity 4 times greater than its relative HME activity, suggesting it has an increased preference for the small alkane propane over octane. As expected from our previous work, changes at position 82, especially the mutations A82C, A82T, A82I, and A82F, increased the preference of 9-10A for the smaller substrate. At position 260, the mutations T260N and T260L increased the DME activity of 9-10A over the corresponding HME activity. The octanol product distributions of all of these mutants tend to favor the formation of 4-octanol, suggesting that the “back” end of DME is hydroxylated by these mutants (Figure 3.7)

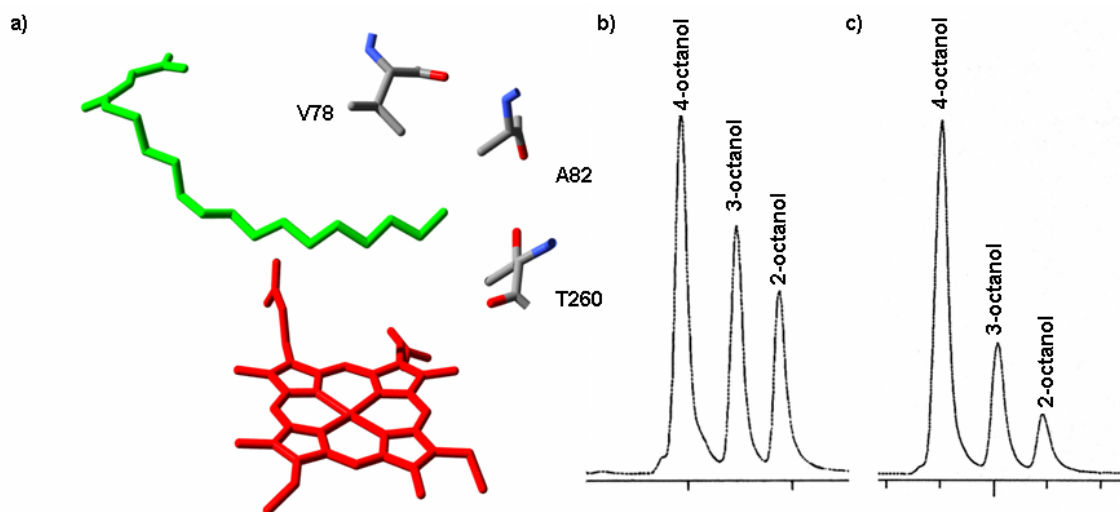


Figure 3.7. a) Active site positions 78, 82 and 260, at which mutations with increased activity towards DME relative to HME were identified. Select gas chromatograph traces of octane hydroxylation products catalyzed by mutants b) A78T, c) A82I.

Five of the 11 saturation mutagenesis libraries contained mutants with improved activity towards HME without a comparable change in DME activity. In the crystal structure, these five residues, L75, F87, T88, T260, and A328, contact the eight carbons of the bound substrate where octane probably binds during catalysis. The beneficial mutations at these positions, L75W, L75I, F87L, F87I, F87V, T88C, T260S, A328L, A328F, and A328M, primarily consist of large neutral side chains that alter the shape of the binding pocket above the heme and in the channel where the non-hydroxylated end of octane lies. The octanol product distributions of these mutants are primarily shifted towards the terminal position since they were selected based on their activity in an HME screen that favors this type of hydroxylation (Figure 3.8)

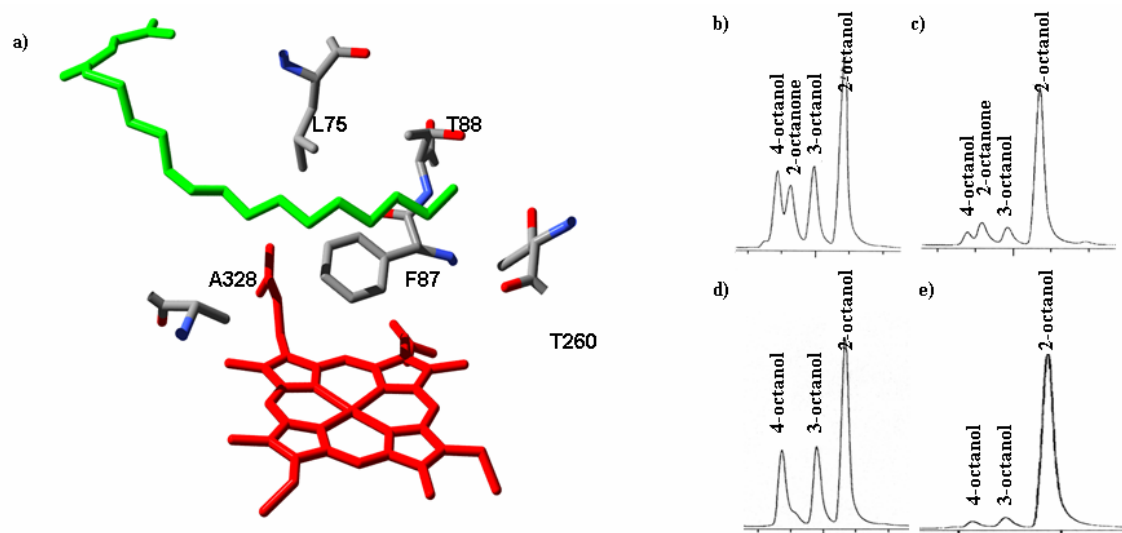


Figure 3.8. a) Active site residues with increased activity towards HME relative to DME. Select gas chromatograph traces of octane hydroxylation products catalyzed by mutants b) L75I, c) F87I, d) T88C, e) A328F.

Finally, three of the 11 libraries, for positions 81, 263, and 264, contained no 9-10A mutants with improved DME or HME activity. But not all of the mutants were active, as seen with position 74. These results suggest that the wild-type residue at these positions is optimal for alkane hydroxylation and that the position is sensitive to mutation.

C.6. Recombination of Active Site Mutations

Active site mutations that increased the activity towards at least one of the screening substrates, as well as the wild-type residues were recombined to form a large library containing all possible combinations of these mutations. The mutation L75I which was not found to increase activity was selected for its change in regioselectivity and added to the library to increase its diversity. The mutations A82L and A328V were added to the library because of their beneficial effects described in Chapter 2. Mutation A82V was added due to constraints in designing the degenerate primer used to construct the library.

Many of the mutations are too close to each other to be recombined using methods such as DNA shuffling [35]. Therefore, the library was constructed in stages using designed oligonucleotide primers containing the mutations (see Chapter 8 for details). The libraries were screened using 1-12G as a control because we were interested in finding mutants with improved activities relative to our best alkane hydroxylase mutant to date. Mutants from the partial and the final recombination libraries exhibiting improved DME or HME activity relative to 1-12G were selected for further characterization.

The first recombination library screened contained all possible combinations of the mutations A78, T78, F78, S78, A82, T82, S82, F82, I82, C82, G82, L82, V82, T260, N260, and L260. Approximately 350 members of this small (81 possible combinations) library were screened with DME, and random members were sequenced to verify that it had been constructed properly. The next library combined the mutations F87, I87, V87, L87, T88, C88, A328, L328, F328, V328, and M328 with the mutations in the first library. Approximately 9,000 members of this library (3,240 possible combinations) were screened with DME and HME, and 13 mutants were isolated based on their improved activity towards either substrate relative to the 1-12G control. The mutations L75, I75, and W75 were then introduced into these 13 mutants to form a small library of 39 possible combinations, of which 174 members were also screened with DME and HME to produce 3 new mutants.

C.7. Characterization of Active Site Mutants

The octane hydroxylation activities were determined for the 24 single active site mutants selected from the 11 saturation mutagenesis libraries (Table 3.1). Octane and propane hydroxylation activities were determined for the 16 recombined mutants. These data are presented in the following Chapters.

In some cases, increased DME response in the screen was associated with increased total turnovers on octane when the regioselectivity of the mutant favored the formation of 3- and 4-octanols. Alternatively, mutants with high activity towards HME in the screen generally

produced more total turnovers on octane than the positive 9-10A controls, especially when the product distributions of the mutants favored the formation of 1- and 2-octanols.

All of the selected single active site mutants of 9-10A exhibit similar levels of product formation relative to 9-10A, but none of the mutants have levels higher than our best mutant to date, 1-12G. The rates of product formation with octane are, for the most part, similar in magnitude to the rates of 9-10A and 1-12G on these substrates. The major differences among these mutants reside in their varying distributions of octanol regioisomers, reflecting the role of their active site changes in perturbing the conformation of the bound substrate during catalysis.

D. Discussion

Our work is focused on obtaining mutants of cytochrome P450 BM-3 that can convert target alkanes into alcohols at high rates and total turnover numbers (ttn). The BM-3 catalytic mechanism is complex. Substrate binding, efficient electron transfer through the protein in response to the new substrate, coupling of the transferred electrons to the heme cofactor during catalysis, and product release must be accomplished if multiple turnovers on new substrates are to occur. A mutant performing well at these tasks should support more catalytic turnovers than a mutant deficient in one or more of these areas. For this reason, we use ttn in our screens as our primary indicator of improved activity towards a new substrate. Our DME and HME screens identify mutants that hydroxylate ever larger amount of these substrates within a reasonable amount of time (i.e., 15 minutes), and an

improved mutant in this work is defined by its relative increase in ttn on the screening and desired substrates.

We have used directed evolution to obtain variants of BM-3 with improved alkane hydroxylation activity. Starting with wild-type BM-3, we randomly mutated the heme domain of the enzyme, and then screened libraries of these mutants for increased activity towards alkanes [2,3,11]. After 7 rounds of evolution we accumulated 13 mutations in the BM-3 heme domain to generate mutant 9-10A. Only one of these mutations, V78A, was located in the active site. The removal of the V78A mutation from 9-10A retains the high rates and total turnover numbers of 9-10A towards alkanes but returns its altered product regioselectivity to wild-type's product distribution. When additional active site changes were made to 9-10A with the intention of improving binding of small substrates, the enzyme became a much more effective catalyst [11]. Comparable active site changes in wild-type BM-3 do not lead to the large increases in alkane hydroxylase activity we see in our evolved mutants (data not shown).

Although we have determined that the non-active site mutations in 9-10A are responsible for its high activity towards alkanes, the active site mutation V78A does alter the distribution of product regioisomers (9-10A produces 51% 2-, 21% 3- and 27% 4-octanol from octane while 9-10A-V78A produces 27% 2-, 34% 3- and 39% 4-octanol), suggesting that this residue interacts with the substrates during catalysis. We have also shown that the right combination of additional active site mutations to 9-10A can result in higher activities towards alkanes and also impart new regio- and enantioselective activities [11]. For example, BM-3 mutant 9-10A-A328V converts octane into 80% *R*-2-octanol, and mutant

9-10A-A82L-A328V (also named 1-12G), hydroxylates alkanes with two-fold higher ttn than any of our previous mutants *and* converts octane into 82% *S*-2-octanol.

Ideally, we would like to look at the effects of all possible combinations of active site mutations on 9-10A, but the 20^{11} possible mutants cannot be screened. Therefore, to create a more practically sized active site library with a high probability of containing active mutants, we first screened saturation mutagenesis libraries at each of 11 active site positions. Using crystal structures of BM-3 to identify active site residues to test is not without difficulties, however. First, the active site is formed with a large conformational change during substrate binding. Structures of BM-3 without bound substrate show these same active site residues in different positions relative to the heme [4,7]. The conformation with bound small alkane substrates is unknown. Secondly, in the BM-3 structures with bound substrate, the ferric heme cofactor is too far from the substrate to represent the actual conformation of the active site during catalysis. It is not clear whether or not the substrate shifts relative to the active site residues they contact or the heme shifts to meet the substrate in their crystallographic conformations upon reduction of the heme before its activation by dioxygen [8]. The fact that no amino acid substitution at position 74 affects the regioselectivity of octane hydroxylation suggests that octane is bound to 9-10A in a similar position as the comparable portion of bound fatty acid substrates in the crystal structures.

We obtained 24 mutants with single active site mutations in 9-10A that increase the productivity of 9-10A on either DME or HME and then used these mutations to construct a multiple active site library. In addition to its role as a filter for finding active site mutations for the recombination library, screening these 11 saturation mutagenesis libraries provides

information on how particular active site residues influence a specific catalytic activity. For example, we examined a library of all possible mutations at position 74, which is within 5 Å of the ω -9 position of the fatty acid substrate but much farther from the terminal eight carbon atoms. This residue could be changed to *any* other amino acid in 9-10A without altering the enzyme's activity towards the screening substrates or regioselectivity towards octane. This suggests that the residue, even when replaced with a larger side chain, does not contact octane during catalysis and confirms our assumptions that octane is bound in the active site similarly to the alkyl tail of the fatty acid substrates. Screening data from the other saturation mutagenesis libraries further confirm our assumptions about alkane binding in the active site. The residues that can be changed to increase DME activity, A78, A82, and T260, all contact the terminal three carbon atoms of the bound fatty acid substrate in the crystal structures. Mutant 9-10A-V78F, which has one of the highest ratios of DME activity relative to HME activity, appears to attenuate the binding of larger substrates like HME and octane while promoting the binding and hydroxylation of small substrates by partially blocking the active site with a large aromatic side chain. At the other 8 positions, few or no residues are found that increase DME activity, suggesting that these other positions do not form part of the DME binding site in BM-3. Alternatively, 6 of the 11 chosen active site residues, L75, A82, F87, T88, T260, and A328, could be modified to increase HME activity relative to DME activity. In the crystal structures these five residues contact most of the terminal eight carbon atoms of the fatty acid substrates. The remaining positions, F81, I263, and A264, are most effective with the wild-type amino acid in 9-10A.

The single active site mutants used to construct the recombination library were chosen for their response to the DME and HME screens. Their activities towards octane were determined separately. None of the 24 single active site mutations in 9-10A supported more total turnovers on any of our target substrates than 1-12G, although the mutants oftentimes out-performed 9-10A. The major effect of these active site mutations in 9-10A is on octanol product distribution. Because screening on HME identifies mutants selective for the terminal position of the substrate, mutants with an overall increase in 1- and 2-octanol production were generally selected with this screen over mutants that favor 3- and 4-octanol production. Alternatively, mutants selected based on DME activity tended to favor the formation of 3- and 4-octanol.

Octane is challenging to hydroxylate selectively because it contains no functional groups to facilitate binding of the substrate in a single conformation while it reacts with the active heme iron-oxo species. Each of these mutants, however, possesses a modified active site that binds octane differently to produce the varied regioselectivities reported here. These binding differences can be expected to be even more pronounced with complex substrates with functional groups and three dimensional structures that favor single binding conformation and can result in the very clean formation of a single hydroxylation product with these substrates. Data supporting this hypothesis are provided in Chapter 5.

As we have demonstrated with mutant 1-12G, multiple active site changes to 9-10A can increase the ttn of alkane hydroxylation. To find new 9-10A mutants with beneficial multiple active site mutations, we created a library containing all possible combinations of the 24 single active site mutants described above and screened the library with DME and

HME to find mutants more active than 1-12G on either substrate. As described in the next chapter, out of 9,700 possible recombination mutants, 16 were isolated and their activities towards propane and octane were determined.

The combination of random mutagenesis and active site residue mutagenesis is a powerful approach for engineering new activities for P450 BM-3. The iterative process of generating libraries of variants containing mutations throughout the protein and screening them for improved variants generally accumulates non-active site mutations because most of the residues in an enzyme are not in the active site, statistically biasing the experiment to find mutations at these positions. In our work with cytochrome P450 BM-3, we have shown that active site engineering primarily affects substrate binding, resulting in changes in hydroxylation regioselectivity and substrate specificity that would be difficult to obtain by random mutagenesis. Both approaches were necessary to obtain the improved mutants described throughout this thesis. Libraries consisting of mostly non-active site mutations were initially created to increase the activity towards alkanes in general, and active site libraries to tighten the substrate specificity and regioselectivity

Selective alkane hydroxylation is difficult due to the lack of functional groups in alkanes to direct catalysis and the fact that their overoxidation to ketones and acids is as energetically favored as their hydroxylation. Many chemical catalysts have been used to hydroxylate various types of alkanes under relatively mild conditions using both hydrogen peroxide and dioxygen [36], but the regioselective hydroxylation of medium chain linear alkanes at positions other than the terminal one has not been reported with any of these systems. In contrast to most chemical catalysts, P450 BM-3 has been evolved in our laboratory to

convert alkanes to alcohols at higher rates and ttn under mild conditions. Additionally, as we have demonstrated in this work, we can modify the active site of these evolved enzymes to obtain mutants that support the conversion of linear alkanes with distinct regioselectivities.

E. References

1. Miles, C. S., Ost, T. W. B., Noble, M. A., Munro, A. W. & Chapman, S. K. (2000). **Protein engineering of cytochromes P-450**. *Biochim. Biophys. Acta* **1543**, 383-407.
2. Farinas, E. T., Schwaneberg, U., Glieder, A. & Arnold, F. H. (2001). **Directed evolution of a cytochrome P450 monooxygenase for alkane oxidation**. *Adv. Synth. Catal.* **343**, 601-606.
3. Glieder, A., Farinas, E. T. & Arnold, F. H. (2002). **Laboratory evolution of a soluble, self-sufficient, highly active alkane hydroxylase**. *Nat. Biotechnol.* **20**, 1135-1139.
4. Ravichandran, K. G., Bodupalli, S. S., Hasemann, C. A., Peterson, J. A. & Deisenhofer, J. (1993). **Crystal structure of hemoprotein domain of P450BM-3, a prototype for microsomal P450's**. *Science* **261**, 731-736.
5. Li, H. & Poulos, T. L. (1997). **The structure of the cytochrome P450BM-3 haem domain complexed with the fatty acid substrate, palmitoleic acid**. *Nat. Struct. Biol.* **4**, 140-146.
6. Haines, D. C., Tomchick, D. R., Machius, M. & Peterson, J. A. (2001). **Pivotal role of water in the mechanism of P450BM-3**. *Biochemistry* **40**, 13456-13465.
7. Sevioukova, I. F., Li, H., Zhang, H., Peterson, J. A. & Poulos, T. L. (1999). **Structure of a cytochrome P450-redox partner electron-transfer complex**. *Proc. Natl. Acad. Sci.* **96**, 1863-1868.
8. Modi, S., Sutcliffe, M. J., Primrose, W. U., Lian, L. Y. & Roberts, G. C. K. (1996). **The catalytic mechanism of cytochrome P450 BM3 involves a 6 Angstrom movement of the bound substrate on reduction**. *Nat. Struct. Biol.* **3**, 414-417.
9. Daff, S. N., Chapman, S. K., Turner, K. L., Holt, R. A., Govindaraj, S., Poulos, T. L. & Munro, A. W. (1997). **Redox control of the catalytic cycle of flavocytochrome P-450 BM3**. *Biochemistry* **36**, 13816-13823.
10. Ost, T. W. B., Clark, J., Mowat, C. G., Miles, C. S., Walkinshaw, M. D., Reid, G. A., Chapman, S. K. & Daff, S. (2003). **Oxygen activation and electron transfer in flavocytochrome P450BM3**. *J. Am. Chem. Soc.* **125**, 15010-15020.
11. Peters, M. W., Meinhold, P. & Arnold, F. H. (2003). **Regio- and enantioselective alkane hydroxylation with engineered cytochromes P450 BM-3**. *J. Am. Chem. Soc.* **125**, 13442 -13450.

12. Hopps, H. B. (2000). **Purpald: a reagent that turns aldehydes purple.** *Aldrichimica Acta* **33**, 28-30.
13. Graham-Lorence, S., Truan, G. L., Peterson, J. A., Falck, J. R., Wei, S., Helvig, C. & Capdevila, J. H. (1997). **An active site substitution, F87V, converts cytochrome P450 BM-3 into a regio- and stereoselective (14S, 15R)-arachidonic acid epoxxygenase.** *J. Biol. Chem.* **272**, 1127-1135.
14. Oliver, C. F., Modi, S., Sutcliffe, M. J., Primrose, W. U. & Roberts, G. C. K. (1997). **A single mutation in cytochrome P450 BM3 changes substrate orientation in a catalytic intermediate and the regiospecificity of hydroxylation.** *Biochemistry* **36**, 1567-1572.
15. Li, H. Y. & Poulos, T. L. (1999). **Fatty acid metabolism, conformational change, and electron transfer in cytochrome P-450(BM-3).** *Biochim. Biophys. Acta* **1441**, 141-149.
16. Cirino, P. C. & Arnold, F. H. (2002). **Regioselectivity and activity of cytochrome P450BM-3 and mutant F87A in reactions driven by hydrogen peroxide.** *Adv. Synth. Catal.* **344**, 932-937.
17. Li, Q. S., Ogawa, J., Schmid, R. D. & Shimizu, S. (2001). **Residues size at position 87 of cytochrome P450 BM-3 determines its stereoselectivity in propylbenzene and 3-chlorostyrene oxidation.** *FEBS Lett.* **508**.
18. Li, Q. S., Ogawa, J. & Shimizu, S. (2001). **Critical role of the residue size at position 87 in H₂O₂-dependent substrate hydroxylation activity and H₂O₂ inactivation of cytochrome P450BM-3.** *Biochem. Biophys. Res. Commun.* **280**, 1258-1261.
19. Li, Q. S., Schwaneberg, U., Fischer, M., Schmitt, J., Pleiss, J., Lutz-Wahl, S. & Schmid, R. D. (2001). **Rational evolution of a medium chain-specific cytochrome P-450 BM-3 variant.** *Biochim. Biophys. Acta* **1545**.
20. Li, Q. S., Ogawa, J., Schmid, R. D. & Shimizu, S. (2001). **Engineering cytochrome P450 BM-3 for oxidation of polycyclic aromatic hydrocarbons.** *Appl. Environ. Microbiol.* **67**, 5735-5739.
21. Cowart, L. A., Falck, J. R. & Capdevila, J. H. (2001). **Structural determinants of active site binding affinity and metabolism by cytochrome P450BM-3.** *Arch. Biochem. Biophys.* **387**, 117-124.
22. Li, Q. S., Schwaneberg, U., Fischer, P. & Schmid, R. D. (2000). **Directed evolution of the fatty-acid hydroxylase P-450 BM3 into an indole-hydroxylating catalyst.** *Chem. Eur. J.* **6**, 1531-1536.

23. Appel, D., Lutz-Wahl, S., Fischer, P., Schwaneberg, U. & Schmid, R. D. (2001). **A P450 BM-3 mutant hydroxylates alkanes, cycloalkanes, arenes and heteroarenes.** *J. Biotechnol.* **88**, 167-171.
24. Peterson, J. A., Hedge, A., Graham, S. & Mullin, D. (2002). *Sixth International Symposium on Cytochrome P450 Biodiversity, University of California, Los Angeles.*
25. Otey, C. (2003). **High-throughput carbon monoxide binding assay for cytochrome P450.** In *Screening and Selection for Directed Enzyme Evolution* (Arnold, F. H. & Georgiou, G., eds.), Vol. 230. Humana Press, Inc., Totowa, NJ.
26. Omura, T. & Sato, R. (1964). **The carbon monoxide-binding pigment of liver microsomes. I. Evidence for its hemoprotein nature.** *J. Biol. Chem.* **239**, 2370-2378.
27. Reidhaar-Olson, J. F. & Sauer, R. T. (1988). **Combinatorial cassette mutagenesis as a probe of the informational content of protein sequences.** *Science* **241**, 53-57.
28. Voigt, C. A., Mayo, S. L., Arnold, F. H. & Wang, Z. G. (2001). **Computational method to reduce the search space for directed protein evolution.** *Proc. Natl. Acad. Sci.* **98**, 3778-3783.
29. Shoichet, B. K., Baase, W. A., Kuroki, R. & Matthews, B. W. (1995). **A relationship between protein stability and protein function.** *Proc. Natl. Acad. Sci.* **92**, 452-456.
30. Bloom, J. D., Silberg, J. J., Wilke, C. O., Drummond, D. A., Adami, C. & Arnold, F. H. (2005). **Thermodynamic prediction of protein neutrality.** *Proc. Natl. Acad. Sci.* **102**, 606-611.
31. Bloom, J. D., Meyer, M. M., Meinhold, P., Otey, C. R., Macmillan, D. & Arnold, F. H. (2005). **Evolving strategies for enzyme engineering.** *Curr. Opin. Struct. Biol.* **accepted**.
32. Markiewicz, P., Kleina, L. G., Cruz, C., Ehret, S. & Miller, J. H. (1994). **Genetic studies of the lac repressor. XIV. Analysis of 4000 altered *Escherichia coli* lac repressors reveals essential and non-essential residues, as well as "spacers" which do not require a specific sequence.** *J. Mol. Biol.* **240**, 421-433.
33. Guo, H. H., CHoe, J. & Loeb, L. A. (2004). **Protein tolerance to random amino acid change.** *Proc. Natl. Acad. Sci.* **101**, 9205-9210.

34. Rennell, D., Bouvier, S. E., Hardy, L. W. & Poteete, A. R. (1991). **Systematic mutation of bacteriophage T4 lysozyme.** *J. Mol. Biol.* **222**, 67-88.
35. Stemmer, W. P. C. (1994). **DNA shuffling by random fragmentation and reassembly: *in vitro* recombination for molecular evolution.** *Proc. Natl. Acad. Sci. USA* **91**, 10747-10751.
36. Arakawa, H. et al. (2001). **Catalysis research of relevance to carbon management: progress, challenges, and opportunities.** *Chem. Rev.* **101**, 953-996.

C h a p t e r 4

Engineered Cytochrome P450 BM-3 Variants with Terminal Hydroxylation Activity

A. Abstract

Saturation mutagenesis of selected active site residues followed by recombination of beneficial mutations generated a library of approximately 9,000 BM-3 variants that catalyze the hydroxylation of linear alkanes with varying regioselectivity. By applying a high-throughput screening assays that detects terminal hydroxylation activity, we were able to identify a variant that hydroxylates octane at its terminal position with 50% selectivity.

B. Introduction

Biocatalysis provides a useful alternative to classic chemical synthesis due to the inherent specificity of enzymes [1] and directed evolution has proven a powerful methodology to tailor biocatalysts for specific applications [2,3]. Oftentimes, the substrate specificity of an enzyme needs to be altered to enable conversion of a new substrate. A more difficult task is to engineer regio- and enantioselectivity. Enantioselective catalysts that accept only a single enantiomer or regioisomer of a substrate have been created using directed evolution [2]. Engineered enzymes that regio- and enantioselectively functionalize achiral compounds, however, are rarely reported. In particular, the regio- and enantioselective hydroxylation of saturated hydrocarbons remains a problem in chemical synthesis [4] and would lead to improved utilization of petrochemicals and natural gas and provide valuable synthons for the pharmaceutical industry.

Progress has been made with synthetic catalysts, but remains hindered by the problems of overoxidation, and lack of regioselectivity and enantioselectivity [5]. Indeed, without restricted access of the substrate molecule to the catalytic center, the regioselectivity of hydroxylation is typically governed by the relative bond dissociation energies; i.e., tertiary and secondary carbon atoms are favored over primary carbon atoms. Cytochromes P450 catalyze the hydroxylation of non-activated carbon atoms on a wide variety of substrates using a single reactive iron-oxo species chelated by a porphyrin. Model studies with metalloporphyrins show that the regioselectivity of n-alkane hydroxylation is determined by the relative bond dissociation energies. Therefore, hydroxylation of the internal methylene groups is highly favored [6] and significant

terminal hydroxylation activity is only observed upon sterically restricting substrate access [7].

P450 BM-3 hydroxylates fatty acid substrates at subterminal (ω -1, ω -2, and ω -3) positions at approximately equal amounts (the exact regioselectivity varies with the chain length of the substrate). Various groups have engineered this enzyme to alter the substrate specificity [8-12] as well as regioselectivity [13-15]. However, a BM-3 variant with terminal hydroxylation activity has not been engineered (Variant F87A has been reported to support ω -hydroxylation of lauric acid [16]. Contradicting results obtained in our and other laboratories, however, show that this mutation actually broadens the regioselectivity and shifts hydroxylation away from the terminal position [17,18]).

In Chapter 2 of this thesis we describe how the regioselectivity of BM-3-catalyzed alkane hydroxylation could be altered by targeting important active site residues for mutation. Saturation mutagenesis of eleven active site residues that are in close contact to the substrate is described in Chapter 3. Mutations that increased activity towards dimethyl ether (DME) or hexyl methyl ether (HME) Beneficial mutations were recombined, generating a library of approximately 9,000 BM-3 variants. Each of these mutants contains a characteristic active site and catalyzes the hydroxylation of linear alkanes with varying regioselectivity. This chapter discusses the regioselectivity of octane hydroxylation of improved mutants, one of which hydroxylates octane at its terminal position with 50% selectivity.

C. Results and Discussion

C.1. Properties of Improved Mutants and Correlation with the Screening Data

As described in Chapter 3, we identified 11 active site residues that are in close proximity to bound fatty acid substrates in crystal structures of BM-3 [19,20]. To create a practically-sized library of variants with combinations of active site mutations, we first screened saturation mutagenesis libraries at each of 11 active site positions to identify a small pool of single active site mutants. Beneficial mutations were then recombined into a multiple active site library. After screening the saturation mutagenesis libraries, we obtained 24 mutants with single active site mutations in 9-10A that increase the productivity of 9-10A on either DME or HME (see Table 3.1 in Chapter 3) and then recombined these mutations to construct a multiple active site library.

Because we were interested in finding mutants with improved activity relative to our best alkane hydroxylase mutant to date, mutant 1-12G [15] was used as a control in the screening procedure that used HME and DME as surrogate substrates. The library contains approximately 9,000 P450 BM-3 variants, each of which contains a characteristic active site. Most mutants (> 64 %) in this library were active towards HME while only 39% were active towards DME. A total of 16 mutants with improved activity towards DME or HME relative to 1-12G (Table 4.1) were selected for purification and further characterization.

Octane was used as a model substrate for alkane hydroxylation, and rates of product formation, total turnover numbers, and regioselectivities were determined (Table 4.2).

Table 4.1. Mutations^[a] in active site variants and activity towards the screening substrates DME and HME.

	A75	A78	A82	F87	A328	DME ^[b]	HME ^[b]
9-10A						0.5	0.6
1-12G			L		V	1.0	1.0
77-9H		T	G		L	0.9	1.5
1-7D	I	F	G		L	1.3	1.5
68-8F		F	G		L	1.9	1.2
49-9B			G	V	L	0.4	2.1
35-7F		F	S		L	1.8	1.5
1-5G	I	F	S		L	1.4	1.4
13-7C		T			L	1.4	1.1
49-1A		T	G	V	L	0.3	2.0
2-4B	I	T			L	1.2	1.7
12-10C			G	V	V	0.7	1.9
11-8E				V	L	0.6	2.0
41-5B		F	G		V	1.6	0.9
29-3E		F	G		F	1.5	0.5
7-11D			F		V	1.5	0.8
29-10E			F		F	1.6	0.7
53-5H		F	S		F	1.4	0.7

^[a] mutations are relative to 9-10A which contains amino acid substitutions R47C, V78A, K94I, P142S, T175I, A184V, F205C, S226R, H236Q, E252G, R255S, A290V, and L353V.

^[b] terminal hydroxylation activity of dimethyl ether and hexyl methyl ether are reported relative to 1-12G, the previously most active mutant towards octane.

Table 4.2. Product distribution^[a], rates and total turnover numbers of octane hydroxylation reactions catalyzed by variants of BM-3 containing active site mutations.

	4-ol [%]	3-ol [%]	2-ol [%]	1-ol [%]	ttn ^[b]	rate ^[c] [min ⁻¹]
9-10A	27	21	51	0	3000	540
A82L	53	25	18	0	6000	540
A328V	0	8	91	0	2000	50
1-12G	4	11	79	3	7500	150
77-9H	0	3	45	52	1300	160
1-7D	1	6	55	38	1300	220
68-8F	2	8	58	31	1400	180
49-9B	0	2	76	20	3800	310
35-7F	1	6	74	18	2000	200
1-5G	1	7	74	17	2200	380
13-7C	1	8	74	17	2600	310
49-1A	0	2	81	15	3700	350
2-4B	1	8	76	14	3900	320
12-10C	1	6	77	12	3100	240
11-8E	0	2	87	8	5700	550
41-5B	5	15	68	7	1800	370
29-3E	3	10	79	6	3200	160
7-11D	2	13	78	6	2200	150
29-10E	1	8	84	5	3200	140
53-5H	1	5	87	3	7400	660

^[a] Product distribution determined as ratio of a specific alcohol product to the total amount of alcohol products (given in %). Errors are at most 3%. The formation of ketones was also observed but is less than 10% of the total amount of product.

^[b] Initial rates of product formation were measured by GC over 60 s as nmol total products/min/nmol protein. The reactions contained P450 (100 nM), NADPH (500 μ M), and octane (4 mM) in ethanol (1%) and potassium phosphate buffer (0.1 M, pH 8.0). Errors are at most 10%.

^[c] Total turnover numbers determined as nmol product/nmol protein. The reactions contained P450 (25 nM), NADPH (500 μ M), and octane (4 mM) in ethanol (1%) and potassium phosphate buffer (0.1 M, pH 8.0). Errors are at most 10%.

In general, mutants with high total turnover of HME in the screen generally produced more 1-octanol than compared to 1-12G. The regioselectivity alone does not necessarily correlate with HME activity. However, the total amount of 1-octanol formed (percent of 1-octanol multiplied by ttn) correlates with the amount of HME converted (Figure 4.1). For example, mutant 77-9H is not improved relative to 1-12G when considering rates and total turnovers on octane, but this mutant converts octane to 52% 1-octanol, and is highly active towards HME in the screen. The deviation from the linear trendline in Figure 4.1 could be due partly to the fact that during the screening no account is taken for varying protein concentration in the lysate. The proportion of 1-octanol in the product mixture varies from three to 51%.

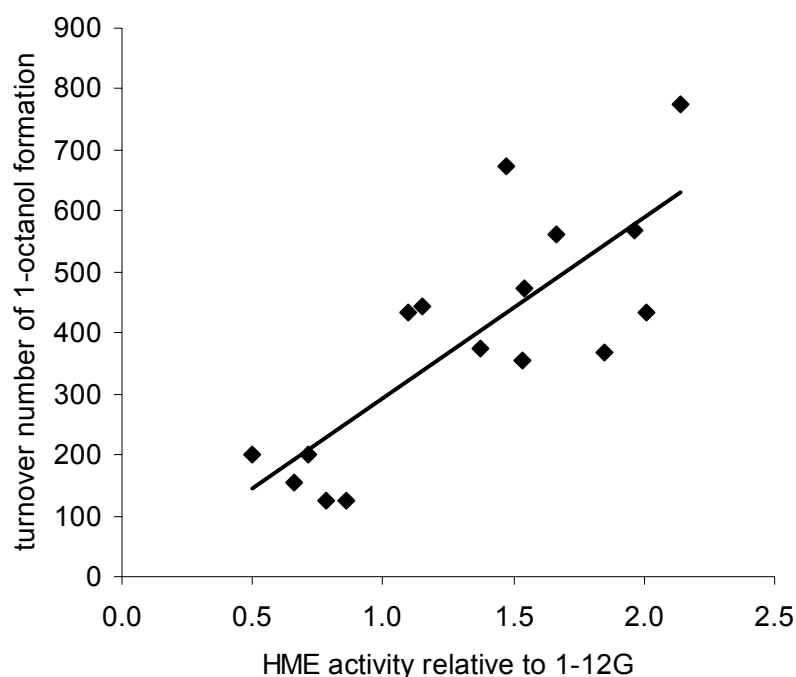


Figure 4.1. The amount of 1-octanol formed during an octane hydroxylation reaction correlates well with the screening data (HME activity).

C.2. Regioselectivity of Mutant 77-9H on *n*-Alkanes and Fatty Acids

Mutant 77-9H, the variant with the highest proportion of terminal hydroxylation activity, was characterized in greater detail. Alkanes of varying chain length (C₆ to C₁₀) were used as substrates and the products were analyzed using gas chromatography with authentic standards. Unexpectedly, only octane is hydroxylated primarily at its terminal position. Alkanes shorter or longer than octane are primarily hydroxylated at the 2-position (Table 4.3 / Figure 4.2).

Table 4.3. Product distributions^[a] of 77-9H-catalyzed alkane hydroxylation reactions.

Substrate	1-ol [%]	2-ol [%]	3-ol [%]	4-ol [%]	5-ol [%]
hexane	11.4	83.8	4.9		
heptane	21.3	74.3	4.2	0.2	
octane	51.8	45.1	2.8	0.3	
nonane	9.7	88.1	1.5	0.7	0.0
decane	5.5	91.8	2.0	0.7	0.0

^[a] Product distribution determined as ratio of a specific alcohol product to the total amount of alcohol products (given in %). Errors are at most 3%. The formation of ketones was also observed but is less than 10% of the total amount of product.

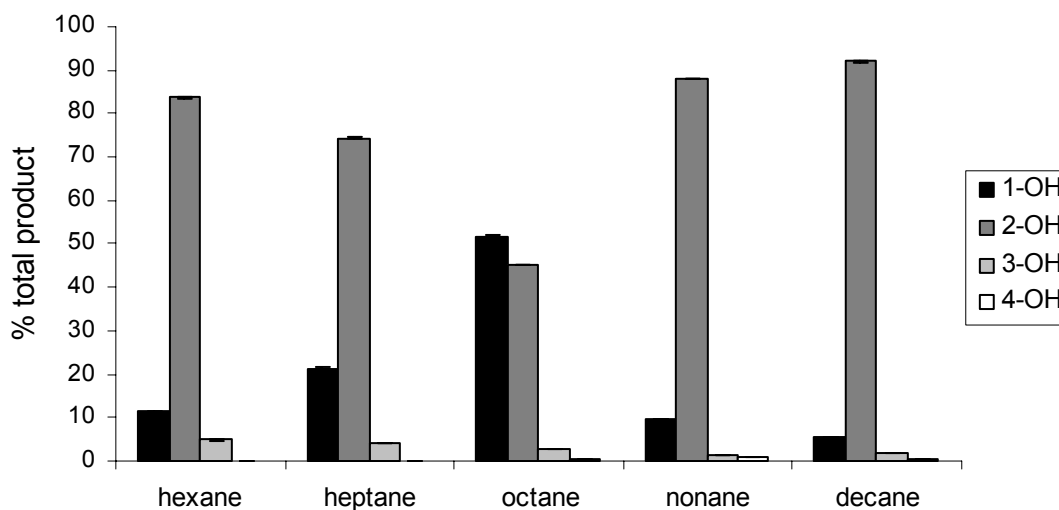


Figure 4.2. Regioselectivity of 77-9H-catalyzed alkane hydroxylation.

The active site of 77-9H is therefore not highly restricted in proximity of the activated oxygen to prevent subterminal hydroxylation. The specificity for the terminal methyl group of octane probably arises due to specific interactions of active site residues with certain octane methylene groups and/or the opposite methyl group. The surrogate substrate hexyl methyl ether, which was used for screening of terminal hydroxylation activity, has the same chain length as octane. The mutations that enable terminal hydroxylation of this substrate likely act in a similar fashion when octane is the substrate but not when the length of the substrate is altered.

The wild-type enzyme hydroxylates lauric and palmitic acid primarily at subterminal positions. Lauric acid is primarily (48 %) hydroxylated at the ω -1 position, and palmitic acid is primarily (48 %) hydroxylated at the ω -2 position [21]. Mutant 77-9H follows the same trend (Table 4.4).

Table 4.4. Product distributions^[a] of 77-9H-catalyzed fatty acid hydroxylation reactions.

Substrate	ω [%]	ω -1 [%]	ω -2 [%]	ω -3 [%]
lauric acid	7.5	52.1	2.8	37.5
palmitic acid	8.9	5.2	83.0	3.0

^[a] Product distribution determined as ratio of a specific hydroxylation product to the total amount of hydroxylation products (given in %). Errors are at most 3%.

We have only altered residues that contact the terminal eight carbons of the substrate based on the crystal structure with bound palmitoylglycine [20]. Interactions of amino acid residues outside of this region with the fatty acid substrates have not been altered.

We therefore might expect changes in regioselectivity to be less drastic than with alkane substrates.

P450 BM-3 Mutant F87A has been reported to support ω -hydroxylation of lauric acid [16]. Contradicting results obtained in our laboratory [17] and by others [18] show that this mutation actually broadens the regioselectivity and shifts hydroxylation away from the terminal position. To address this controversy, we engineered the F87A substitution into wild-type and 9-10A and analyzed the alkane and fatty acid hydroxylation product regioisomers. The data for lauric acid hydroxylation with the wt F87A mutant are in agreement with our previous report [17]. Neither variant supports terminal hydroxylation activity on alkanes (Table 4.5) or on fatty acids (Table 4.6).

Table 4.5. Product distributions^[a] of wt F87A- and 9-10A F87A-catalyzed alkane hydroxylation reactions.

Mutant	Substrate	1-ol [%]	2-ol [%]	3-ol [%]	4-ol [%]	5-ol [%]
wt F87A	hexane	0	54	46		
	heptane	0	36	61	3	
	octane	0	14	43	44	
	nonane	0	7	20	2	72
	decane	0	10	9	0	81
9-10A F87A	hexane	0	42	57		
	heptane	2	62	34	3	
	octane	1	55	37	7	
	nonane	0	24	46	5	25
	decane	0	14	23	1	62

^[a] Product distribution determined as ratio of a specific alcohol product to the total amount of alcohol products (given in %). Errors are at most 3%. The formation of ketones was also observed but is less than 10 % of the total amount of product.

Table 4.6. Product distributions^[a] of wt F87A- and 9-10A F87A-catalyzed fatty acid hydroxylation.

Mutant	Substrate	ω [%]	ω -1 [%]	ω -2 [%]	ω -3 [%]	ω -4 [%]	ω -5 [%]	ω -6 [%]	ω -7 [%]
Wt F87A	lauric acid	0	5	9	39	20	27	0	0
	palmitic acid	0	11	36	18	22	13	0	0
9-10A F87A	lauric acid	0	5	6	28	14	47	0	0
	palmitic acid	0	0	1	1	2	8	20	68

^[a] Product distribution determined as ratio of a specific alcohol product to the total amount of alcohol products (given in %). Errors are at most 3% for WT F87A and 6% for 9-10A F87A.

The highly desirable terminal hydroxylation of linear alkanes has been achieved using synthetic catalysts with varying degrees of success. To our best knowledge, the highest selectivity for terminal hydroxylation of linear alkanes using chemical catalysts was achieved using molecular-sieve catalysts. With these, n-alkanes, such as octane, can be oxidized primarily (65% of all products) at the terminal methyl group, yielding octanoic acid, octanal and n-octanol [22]. In comparison, the enzymes used by several microorganisms for the utilization of linear alkanes as a source of carbon and energy [23] hydroxylate n-alkanes exclusively at their terminal position [24]. Some P450s (several members of the Cyp4 family, Cyp52, Cyp86, Cyp153) catalyze the hydroxylation of terminal methyl groups of fatty acids or n-alkanes [25-28]. These enzymes must therefore override the inherent specificity of the catalytic species for the methylene groups by restricting substrate access to the heme iron so that only the terminal methyl

carbon is positioned correctly above the heme-iron. However, the known P450s with terminal hydroxylation activity are membrane bound and have a multi-component nature, making them difficult to manipulate or produce in large quantities. Additionally, none of these proteins has its crystal structure solved. The work presented in this chapter opens up the prospect of converting the fast and easily expressible P450 BM-3 into a terminal alkane hydroxylase.

C.3. Total Turnover Numbers, Rates and Coupling Efficiency

Total turnover numbers (ttn) and rates of product formation were measured for the different alkanes (Table 4.7). To determine ttn, the enzymes were diluted to a concentration at which the P450 is neither oxygen-limited nor inactivated due to dialysis of the flavins, a likely inactivation mechanism at low P450 concentrations [29]. The total turnover number was found to be substrate dependent and generally increases with the alkane chain length. The observed decrease in ttn for decane hydroxylation might be an artefact of the limited solubility of decane in the reaction buffer (calculated as ~ 0.4 mM in water with 2% ethanol [30]) and not an inherent property of the enzyme itself. Rates of substrate hydroxylation appear to follow the same trend.

Table 4.7. Total turnover, product formation rates, NADPH oxidation rates, and coupling efficiency of 77-9H-catalyzed alkane hydroxylations.

Substrate	ttn ^[a]	rate of product formation [min ⁻¹] ^[b]	rate of NADPH oxidation [min ⁻¹] ^[c]	coupling efficiency [%] ^[d]
hexane	1800 ± 130	251 ± 29	1560 ± 60	16.1 ± 2.0
heptane	1730 ± 110	112 ± 9	1630 ± 20	6.9 ± 0.6
octane	3040 ± 150	236 ± 24	1630 ± 30	14.5 ± 1.7
nonane	4240 ± 680	742 ± 30	1150 ± 100	65.6 ± 9.3
decane	2831 ± 225	318 ± 47	940 ± 50	33.4 ± 7.2

^[a] Total turnover numbers determined as nmol product/nmol protein. The reactions contained P450 (25 nM), an NADPH regeneration system (166 μ M NADP⁺, 6.6 U/mL isocitrate dehydrogenase, 41.6 mM isocitrate) and octane (4 mM) in ethanol (2 %) and potassium phosphate buffer (0.1 M, pH 8.0).

^[b] Rates of product formation were measured by GC over 20 s as nmol total products/min/nmol protein. The reactions contained P450 (200 nM), NADPH (500 μ M) and octane (2 mM) in ethanol (2%) and potassium phosphate buffer (0.1 M, pH 8.0).

^[c] Rates of NADPH oxidation were measured over 20 s at 340 nm as nmol NADPH/min/nmol protein. The reactions contained P450 (200 nM), NADPH (160 μ M), and octane (2 mM) in ethanol (2 %) and potassium phosphate buffer (0.1 M, pH 8.0). The background NADPH oxidation rate (without substrate) rate was 220/min.

^[d] Coupling efficiency is the ratio of product formation rate to NADPH oxidation rate.

Wildtype P450 BM-3 tightly regulates electron transfer from the cofactor (NADPH) to the heme when fatty acids are the substrates. In absence of substrate, a weakly-bound water molecule acts as the sixth, axial ligand. Substrate replaces this water molecule, resulting in a shift in spin-state of the heme iron to the high-spin form and an increase (~140 mV) in heme iron reduction potential, inducing reduction of the ferric [31,32]. However, with mutant BM-3 enzymes and nonnatural substrates, NADPH consumption is not necessarily coupled to the formation of product, but instead reduces heme-bound dioxygen to water or the reactive oxygen species peroxide and superoxide [29]. To

determine the coupling efficiency of mutant 77-9H, rates of NADPH oxidation upon addition of the alkane substrates were measured and compared to product formation rates (Table 4.6). It was found that rates of product formation correlate well with coupling efficiency; i.e., the more the reaction is coupled to NADPH oxidation, the higher the rate of product formation (Figure 4.3).

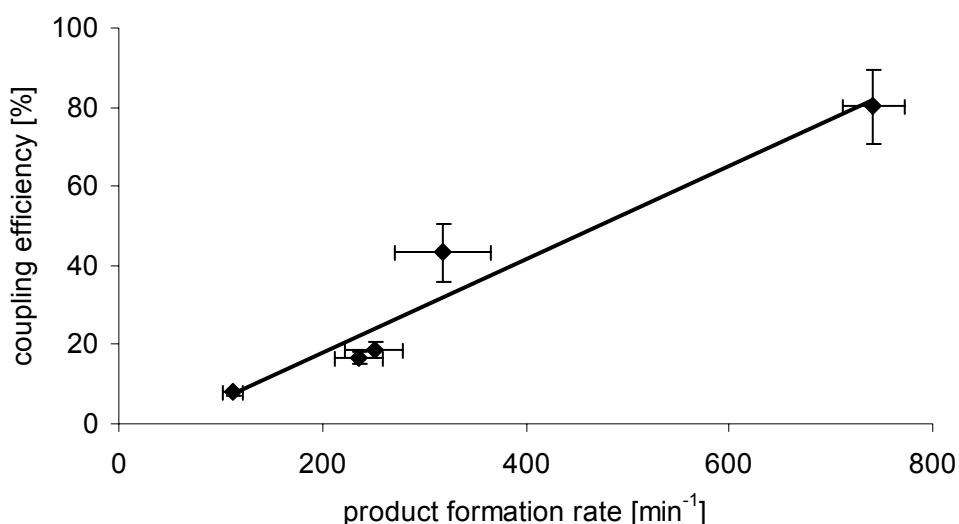


Figure 4.3. The coupling efficiency ((product formation rate) / (NADPH oxidation rate)) correlates with the product formation rate.

We had anticipated that the oxidation of the disfavored terminal methyl group of octane might lead to a decrease in the rate of product formation. However, here we show that the rate of product formation is correlated to coupling efficiency. Interestingly, the highest coupling efficiency (65.6%) was observed for nonane, and not octane.

D. Conclusions

We have created a library of approximately 9,000 different P450 active site mutants. Members of this library were screened for terminal alkane hydroxylation activity. And to our best knowledge, this is the first report of an engineered P450 BM-3 exhibiting this activity. Wild-type P450 BM-3 hydroxylates its preferred substrates, medium-chain fatty acids (C12 to C18), at subterminal positions. The terminal carbon is not hydroxylated [33]. Similarly, reports of engineered, bacterial alkane hydroxylating P450s do not describe terminal hydroxylation activity [8,34]. The first law of directed evolution - “you get what you screen for” [35] - was once again proven true. Mutant 77-9H preferentially hydroxylates the terminal carbon of octane which has approximately the same chain length as the screening substrate hexyl methyl ether. Alkanes larger or smaller are hydroxylated at this position to a much lesser degree. We anticipate that by screening with methyl ether derivatives of alkanes of various chain lengths it will be possible to generate a terminal hydroxylase mutant with an even higher proportion of terminal hydroxylation. Additionally, the screen can be adapted for the regioselective hydroxylation of more complex substrates by using methyl ether derivatives of them as surrogate substrates. In such an approach, the same library of active site mutants should yield promising results. We also anticipate that a variety of substrates can be hydroxylated regioselectively by at least one of the variants. Indeed, as described in Chapter 5, mutations in the active site can yield variants that hydroxylate complex substrates such as 2-cyclopentylbenzoxazole with high regio- and enantioselectivity, yielding potentially valuable intermediates for chemical synthesis [36].

E. References

1. Panke, S., Held, M. & Wubbolts, M. (2004). **Trends and innovations in industrial biocatalysis for the production of fine chemicals.** *Curr. Opin. Biotech.* **15**, 272-279.
2. Jaeger, K. E. & Eggert, T. (2004). **Enantioselective biocatalysis optimized by directed evolution.** *Curr. Opin. Biotech.* **15**, 305-313.
3. Valetti, F. & Gilardi, G. (2004). **Directed evolution of enzymes for product chemistry.** *Nat. Prod. Rep.* **21**, 490-511.
4. Li, Z. & Chang, D. L. (2004). **Recent advances in regio- and stereoselective biohydroxylation of non-activated carbon atoms.** *Curr. Org. Chem.* **8**, 1647-1658.
5. Arakawa, H. et al. (2001). **Catalysis research of relevance to carbon management: progress, challenges, and opportunities.** *Chem. Rev.* **101**, 953-996.
6. Bartoli, J. F., Brigaud, O., Battioni, P. & Mansuy, D. (1991). **Hydroxylation of linear alkanes catalyzed by iron porphyrins - particular efficacy and regioselectivity of perhalogenated porphyrins.** *J. Chem. Soc.-Chem. Commun.*, 440-442.
7. Cook, B. R., Reinert, T. J. & Suslick, K. S. (1986). **Shape selective alkane hydroxylation by metalloporphyrin catalysts.** *J. Am. Chem. Soc.* **108**, 7281-7286.
8. Appel, D., Lutz-Wahl, S., Fischer, P., Schwaneberg, U. & Schmid, R. D. (2001). **A P450 BM-3 mutant hydroxylates alkanes, cycloalkanes, arenes and heteroarenes.** *J. Biotechnol.* **88**, 167-171.
9. Carmichael, A. B. & Wong, L. L. (2001). **Protein engineering of *Bacillus megaterium* CYP102 - The oxidation of polycyclic aromatic hydrocarbons.** *Eur. J. Biochem.* **268**, 3117-3125.
10. Li, Q. S., Ogawa, J., Schmid, R. D. & Shimizu, S. (2001). **Engineering cytochrome P450 BM-3 for oxidation of polycyclic aromatic hydrocarbons.** *Appl. Environ. Microbiol.* **67**, 5735-5739.
11. Li, Q. S., Schwaneberg, U., Fischer, P. & Schmid, R. D. (2000). **Directed evolution of the fatty-acid hydroxylase P-450 BM3 into an indole-hydroxylating catalyst.** *Chem. Eur. J.* **6**, 1531-1536.

12. Oliver, C. F., Modi, S., Primrose, W. U., Lian, L. Y. & Roberts, G. C. K. (1997). **Engineering the substrate specificity of *Bacillus megaterium* cytochrome P-450 BM3: hydroxylation of alkyl trimethylammonium compounds.** *Biochem. J.* **327**, 537-544.
13. Li, Q. S., Ogawa, J., Schmid, R. D. & Shimizu, S. (2001). **Residues size at position 87 of cytochrome P450 BM-3 determines its stereoselectivity in propylbenzene and 3-chlorostyrene oxidation.** *FEBS Lett.* **508**.
14. Graham-Lorence, S., Truan, G. L., Peterson, J. A., Falck, J. R., Wei, S., Helvig, C. & Capdevila, J. H. (1997). **An active site substitution, F87V, converts cytochrome P450 BM-3 into a regio- and stereoselective (14S, 15R)-arachidonic acid epoxigenase.** *J. Biol. Chem.* **272**, 1127-1135.
15. Peters, M. W., Meinhold, P. & Arnold, F. H. (2003). **Regio- and enantioselective alkane hydroxylation with engineered cytochromes P450 BM-3.** *J. Am. Chem. Soc.* **125**, 13442 -13450.
16. Oliver, C. F., Modi, S., Sutcliffe, M. J., Primrose, W. U. & Roberts, G. C. K. (1997). **A single mutation in cytochrome P450 BM3 changes substrate orientation in a catalytic intermediate and the regiospecificity of hydroxylation.** *Biochemistry* **36**, 1567-1572.
17. Cirino, P. C. & Arnold, F. H. (2002). **Regioselectivity and activity of cytochrome P450BM-3 and mutant F87A in reactions driven by hydrogen peroxide.** *Adv. Synth. Catal.* **344**, 932-937.
18. Lentz, O., Urlacher, V. & Schmid, R. D. (2004). **Substrate specificity of native and mutated cytochrome P450 (CYP102A3) from *Bacillus subtilis*.** *J. Biotechnol.* **108**, 41-49.
19. Li, H. & Poulos, T. L. (1997). **The structure of the cytochrome P450BM-3 haem domain complexed with the fatty acid substrate, palmitoleic acid.** *Nat. Struct. Biol.* **4**, 140-146.
20. Haines, D. C., Tomchick, D. R., Machius, M. & Peterson, J. A. (2001). **Pivotal role of water in the mechanism of P450BM-3.** *Biochemistry* **40**, 13456-13465.
21. Boddupalli, S. S., Pramanik, B. C., Slaughter, C. A., Estabrook, R. W. & Peterson, J. A. (1992). **Fatty-acid monooxygenation by P450BM-3 - product identification and proposed mechanisms for the sequential hydroxylation reactions.** *Arch. Biochem. Biophys.* **292**, 20-28.

22. Thomas, J. M., Raja, R., Sankar, G. & Bell, R. G. (1999). **Molecular-sieve catalysts for the selective oxidation of linear alkanes by molecular oxygen.** *Nature* **398**, 227-230.
23. van Beilen, J. B., Li, Z., Duetz, W. A., Smits, T. H. M. & Witholt, B. (2003). **Diversity of alkane hydroxylase systems in the environment.** *Oil Gas Sci. Technol.* **58**, 427-440.
24. van Beilen, J. B., Kingma, J. & Witholt, B. (1994). **Substrate-specificity of the alkane hydroxylase system of *Pseudomonas oleovorans* Gpo1.** *Enz. Microb. Technol.* **16**, 904-911.
25. Simpson, A. E. C. M. (1997). **The cytochrome P450 4 (CYP4) family.** *Gen. Pharmacol.* **28**, 351-359.
26. Scheller, U., Zimmer, T., Becher, D., Schauer, F. & Schunck, W. H. (1998). **Oxygenation cascade in conversion of n-alkanes to alpha,omega- dioic acids catalyzed by cytochrome P450 52A3.** *J. Biol. Chem.* **273**, 32528-32534.
27. Benveniste, I., Tijet, N., Adas, F., Philipps, G., Salaun, J. P. & Durst, F. (1998). **CYP86A1 from *Arabidopsis thaliana* encodes a cytochrome P450-dependent fatty acid omega-hydroxylase.** *Biochem. Biophys. Res. Commun.* **243**, 688-693.
28. Maier, T., Forster, H. H., Asperger, O. & Hahn, U. (2001). **Molecular characterization of the 56-kDa CYP153 from *Acinetobacter* sp. EB104.** *Biochem. Biophys. Res. Commun.* **286**, 652-658.
29. de Montellano, P. R. (1995). **Cytochrome P450: structure, mechanism, and biochemistry.** 2nd edit., Plenum Press, New York.
30. Skrecz, A., Shaw, D. & Maczynski, A. (1999). *Journal of Physical and Chemical Reference Data* **28**, 983.
31. Daff, S. N., Chapman, S. K., Turner, K. L., Holt, R. A., Govindaraj, S., Poulos, T. L. & Munro, A. W. (1997). **Redox control of the catalytic cycle of flavocytochrome P-450 BM3.** *Biochemistry* **36**, 13816-13823.
32. Ost, T. W. B., Clark, J., Mowat, C. G., Miles, C. S., Walkinshaw, M. D., Reid, G. A., Chapman, S. K. & Daff, S. (2003). **Oxygen activation and electron transfer in flavocytochrome P450BM3.** *J. Am. Chem. Soc.* **125**, 15010-15020.
33. Miura, Y. & Fulco, A. J. (1975). **Omega-1, omega-2 and omega-3 hydroxylation of long-chain fatty acids, amides and alcohols by a soluble enzyme system from *Bacillus Megaterium*.** *Biochim. Biophys. Acta* **388**, 305-317.

34. Farinas, E. T., Schwaneberg, U., Glieder, A. & Arnold, F. H. (2001). **Directed evolution of a cytochrome P450 monooxygenase for alkane oxidation.** *Adv. Synth. Catal.* **343**, 601-606.
35. Zhao, H. M. & Arnold, F. H. (1997). **Combinatorial protein design: strategies for screening protein libraries.** *Curr. Opin. Struct. Biol.* **7**, 480-485.
36. Munzer, D. F., Meinhold, P., Peters, M. W., Feichtenhofer, S., Griengl, H., Arnold, F. H., Glieder, A. & de Raadt, A. (2005). **Stereoselective hydroxylation of an achiral cyclopentanecarboxylic acid derivative using engineered P450s BM-3.** *Chem. Commun.* DOI: 10.1039/b501527h.

Chapter 5

Regio- and Enantioselective Hydroxylation of an Achiral Cyclopentanecarboxylic Acid Derivative Using Engineered Cytochromes P450 BM-3

Material from this chapter appears in: Munzer, D. F., Meinhold, P., Peters, M. W., Feichtenhofer, S., Griengl, H., Arnold, F. H., Glieder, A. & de Raadt, A. (2005). **Stereoselective hydroxylation of an achiral cyclopentanecarboxylic acid derivative using engineered P450s BM-3.** *Chem. Commun.* **20**, 2597-2599, and is reprinted by permission of the Royal Society of Chemistry.

A. Abstract

Two discrete strategies for improving the preparative outcome of enzymatic hydroxylation reactions are protein and substrate engineering. The carboxylic acid moiety of cyclopentanecarboxylic acid, which is not converted by P450 BM-3 or variants thereof, was protected with benzoxazole. This modified substrate, 2-cyclopentanebenzoxazole was regio- and enantioselectively, using cytochrome P450 BM-3 mutants engineered for regio- and enantioselective hydroxylation of linear alkanes. The reaction proceeds at rates of up to 230 min^{-1} , with high ttn of up to 9,200 and an *ee* of as high as 88 %.

B. Introduction

As described in Chapter 1, cytochrome P450 BM-3 has been engineered to accept nonnatural substrates with enhanced regioselectivity, enantioselectivity, catalytic rates and total turnover. Mutations in the active site, for example, enable the enzyme to hydroxylate alicyclic, heterocyclic, aromatic and even polyaromatic compounds [1-4]. As described in Chapter 2, linear alkanes can be hydroxylated by mutants engineered for this purpose. And as shown in Chapter 3, engineering of the active site enabled us to adjust the regioselectivity of linear alkane hydroxylation. This poses the possibility that other compounds might also be hydroxylated regio- and enantioselectively, if they were to be accepted as substrates.

If a given compound is not accepted as a substrate, it can still be engineered to improve its reactivity in a biotransformation, as in the docking/protecting (d/p) group concept for biotransformations [5,6]. Similar to the common practice of using protective groups in organic chemistry, a (d/p) group is introduced into an enzyme substrate before the biotransformation is performed, and finally the d/p group is removed. The aims of this concept are to improve the predictability of the hydroxylation position, prevent undesired side reactions, and aid substrate detection, and product recovery. This approach has been successfully applied to carboxylic acids, ketones, aldehydes, and alcohols [6]. Overall, this approach improves the applicability of bioconversions in chemical synthesis, especially for preparing chiral molecules. In this chapter, we show that protein engineering in combination with substrate engineering improves the synthetic outcome of a biohydroxylation.

A method for direct biohydroxylation of cyclic carboxylic acids to produce preparatively valuable starting materials, such as carboxylic acid **1** to compound **4** (Figure 5.1), would be a valuable addition to an organic chemist's synthetic "tool box."

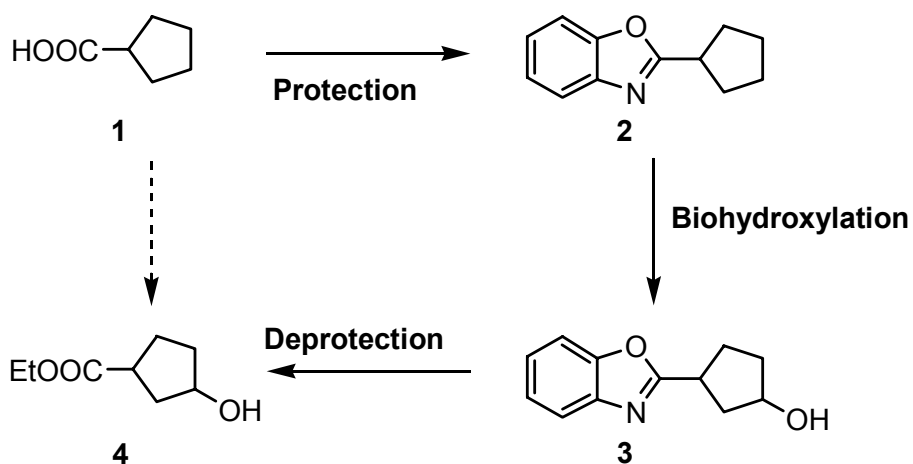


Figure 5.1. The conversion of carboxylic acid **1** to product **4** employing the docking/protecting group concept.

Carbovir (Figure 5.2), for example, is a carboxylic nucleoside potentially active against human HIV [7]. (*R,R*)-**4** would be a potentially useful precursor to this much needed medication. Unfortunately, finding microorganisms containing monooxygenase systems capable of hydroxylating substances such as **1** has proven difficult, especially when a specific product stereoselectivity is required. In addition, these simple carboxylic acids are troublesome to purify from complex fermentation/biotransformation mixtures due to their polarity and lack of UV absorbance [6].

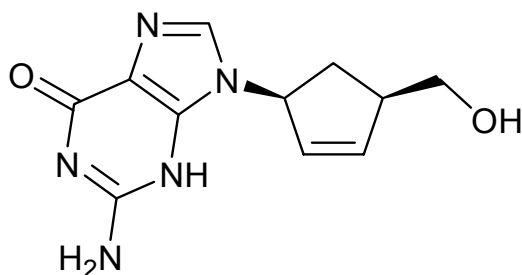


Figure 5.2. Structure of carbovir

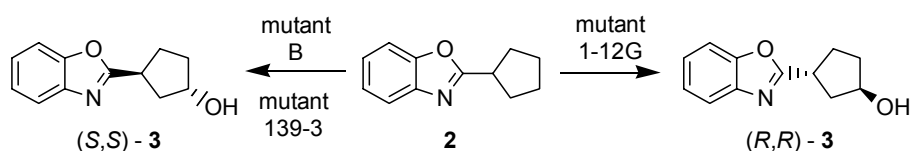
The d/p group concept was found to circumvent these problems, at least in part. Carboxylic acid **1** has been chemically modified to give model compound 2-cyclopentylbenzoxazole **2** (Figure 5.1). The resulting substrate is easy to manipulate as well as amenable to biohydroxylation with whole cell systems such as *Cunninghamella blakesleeana* DSM 1906 [8-10]. Protecting group removal provides end product **4**. Regardless of the microorganisms and fermentation conditions used, however, only a single diastereoisomer, (*S,S*)-**4**, could be obtained with synthetically useful diastereoselectivities [8-10]. Side products were also formed during this transformation because the microorganisms used catalyzed further, undesired transformations, such as oxidation. Consequently, we tested P450 BM-3 mutants engineered for regio- and enantioselective alkane hydroxylation for their ability to hydroxylate model compound **2**.

C. Results and Discussion

C.1. Whole-Cell Biotransformations

Our collaborators in Austria performed initial whole-cell biotransformations using *E. coli* DH5 α cells transformed with plasmids carrying the genes of 13 different P450 mutants (see Appendix D for experimental details). The mutants included in this set of experiments were created in previous studies [11,12] as well as in the experiments described in Chapter 2. Results for the wild-type and three of these mutants are listed in Table 5.1 (mutations are listed in Appendix B). All of the mutants tested in this set of experiments contain the same active site, with the exception of 9-10A-A328V and 1-12G. The enantioselectivities obtained using the remaining ten mutants were therefore unexpectedly similar to 139-3.

Table 5.1. Biohydroxylation of **2** with whole cell P450 BM-3 systems.



BM-3 variant	Main Isomer 3	<i>ee</i>	<i>de</i>
wild-type	S, S	1.5%	87%
139-3	S, S	79%	87%
B	S, S	82%	87%
1-12G	R, R	89%	87%

Refer to Appendix D for experimental details

Biohydroxylation using the wild-type enzyme in *E. coli* gave very low enantioselectivity (1.5%, *S,S*) and high diastereoselectivity (87%). Mutant 139-3 also afforded (*S,S*)-**3**, but in high *ee* (79%) and *de* (96%). Mutant B gave comparable selectivities to 139-3. In dramatic contrast, mutant 1-12G was found to produce the highly sought (*R,R*)-**3** in high selectivities (89% *ee*, 94% *de*). The yields of **3** were modest, ranging from 0.4% to 15%. Total turnover numbers of the enzymes are reported in below (Table 5.3) and are sufficient to expect higher yields. For example, a reasonable estimate of the BM-3 concentration in a culture is 50 mg/L (0.42 μ M). Thus, 10,000 turnovers would produce 4.2 mM of product. Here, only 0.012 to 0.45 mM of product are produced from 3 mM substrate. To improve the yields of these whole cell biotransformations it is therefore necessary to optimize the reaction conditions and/or the host organism. Sufficient aeration of the growth medium, for example, is necessary to support the central metabolism of the host organism so that it can supply enough cofactors for the desired monooxygenation reaction. Metabolic engineering aimed at increasing the intracellular NADPH concentration of non-growing *E. coli* cells has successfully been applied in a whole-cell monooxygenase reaction to significantly enhance the product yield [13].

C.2. Characterization of Purified Enzymes

Upon obtaining these promising results, we decided to purify the enzymes from the four strains listed in Table 5.1 for *in vitro* enzymatic bioconversions. Results are summarized in Table 5.2.

Table 5.2. Biohydroxylation of **2** with purified enzymes.

BM-3 variant	% 3 ^[a]	Main Isomer	<i>ee</i>	<i>de</i>
wild-type	20.0	<i>R, R</i>	25.3	n.d. ^[b]
139-3	85.9	<i>S, S</i>	84.5	93.6
B	89.6	<i>S, S</i>	87.9	96.4
1-12G	97.6	<i>R, R</i>	87.7	95.3

Refer to Chapter 8 for experimental details.

^[a] Proportion of **3** with respect to total products as determined with HPLC.

^[b] wt protein did not yield sufficient product to accurately determine *de* of **3**.

Within experimental error, employing the purified enzymes produced results comparable to those in whole cell reactions. However, pure wild-type BM-3 produced two new results: **3** slightly favored in the (*R,R*) configuration and an unknown compound, tentatively identified as a product hydroxylated in the 2 position of the cyclopentane ring, as the major product (~80%).

Total turnover numbers (ttn) and rates of formation of **3** were measured (Table 5.3). To determine ttn, the enzymes were diluted to a concentration at which the P450 is neither oxygen-limited nor inactivated due to dialysis of the flavins, a likely inactivation mechanism at low P450 concentrations [14]. The three mutant enzymes catalyze the reaction at approximately the same rate, which is two orders of magnitude greater than that of wild-type. The total turnover number varies, however. Mutant B catalyzes about an order of magnitude more turnovers than wild-type.

Table 5.3. Rates and total turnover numbers (ttn) of P450 BM-3 catalyzed hydroxylation reactions.

BM-3 variant	ttn ^[a]	Rate ^[b]
Wt	1260 ± 130	2.6 ± 0.3
139-3	3970 ± 1080	231 ± 19
B	9200 ± 2040	215 ± 4
1-12G	6840 ± 1970	213 ± 14

Refer to Chapter 8 for experimental details.

^[a] ttn is reported as nmol **3** per nmol protein. The protein is inactivated after 12 hours of incubation.

^[b] Rates (nmol **3** per nmol protein per min) were determined by measuring formation of **3** over one minute.

The P450 BM-3 mutants examined in this work have at least 9 amino acid substitutions, including at least one active site mutation (A78V) (see Appendix B for details). With linear alkanes such as octane, these mutations increase the regioselectivity of subterminal hydroxylation [12,15]. Mutant 1-12G has the highest regioselectivity with linear alkanes [15] and also exhibits the highest regioselectivity with substrate **2** (97.6%). Although the mutants were engineered for the hydroxylation of short, linear alkanes, and not for substrates such as compound **2**, *ee*'s and *de*'s of almost 90% were obtained. The fact that 1-12G produces the (*R,R*) diastereomer of **3** is notable. This enzyme had previously been shown to catalyze the hydroxylation of octane primarily to *R*-2-octanol (39% *ee*), while all the other mutants produce mainly *S*-2-octanol (up to 58% *ee*) [15]. In addition to the active site mutation V78A, 1-12G contains mutations A82L and A328V. Only in this particular combination do these mutations generate *R*-2-octanol from octane and *R,R*-**3** from **2**. Consequently, this mutant favors a different binding conformation of the prochiral

molecule **2** in which the pentyl ring is flipped by 180° relative to the conformation in all the other mutants.

Wild-type P450 BM-3 and the most promising mutants thereof (139-3, B and L) were found to be inactive towards cyclopentanecarboxylic acid **1**. Employing substrate engineered, achiral **2**, however, enabled the biohydroxylation, and two out of the four possible isomers of **3** were prepared in high stereoselectivities. This result endorses the use of substrate engineering to broaden the range of compounds accepted by P450 enzymes. It also further demonstrates the functional flexibility of P450 BM-3 and supports the notion that the P450 BM-3 can be regarded as a “one-enzyme-fits-all” oxidation catalyst [15].

We proposed that total turnover numbers, and stereoselectivities can be further improved by directly screening BM-3 mutant libraries with substrate **2**. This, however, would require a high-throughput screening system for the detection of regio- and enantioselective hydroxylation of this compound. Currently, only high-throughput gas chromatography would be suitable for this task, as colorimetric hydroxylation assays can typically not distinguish between different regioisomers and diastereomers.

The success in applying enzymes engineered for the selective hydroxylation of linear alkanes for compound **2**, prompted us to investigate the use of the 16 active site variants from the recombination library described in Chapter 4. Preliminary data are presented in Table 5.4.

Table 5.4. Biohydroxylation of **2** with purified enzymes with multiple active site substitutions.

BM-3 variant	ttn ^[a]	% 3 ^[b]	Main Isomer	<i>ee</i>	<i>de</i>
wild-type	1260	20.0	<i>R, R</i>	25.3	n.d. ^[c]
139-3	4000	85.9	<i>S, S</i>	84.5	93.6
1-12G	7000	97.6	<i>R, R</i>	87.7	95.3
77-9H	11,000	99.7	<i>R, R</i>	1.4	97.9
1-7D	6,000	99.7	<i>S, S</i>	71.4	98.3
68-8F	12,000	99.8	<i>S, S</i>	81.9	99.5
49-9B	4,000	92.9	<i>S, S</i>	44.0	61.1
35-7F	7,500	99.7	<i>S, S</i>	68.8	97.5
1-5G	7,500	99.8	<i>S, S</i>	68.6	98.4
13-7C	10,000	99.7	<i>R, R</i>	63.3	96.3
49-1A	4,000	91.0	<i>R, R</i>	0.2	49.2
2-4B	9,000	99.7	<i>R, R</i>	70.0	91.8
12-10C	4,000	53.4	<i>S, S</i>	82.3	65.9
11-8E	5,500	88.5	<i>S, S</i>	29.4	42.9
41-5B	4,000	99.6	<i>S, S</i>	87.3	95.3
29-3E	6,000	99.7	<i>S, S</i>	60.3	99.2
7-11D	7,500	99.7	<i>S, S</i>	60.8	98.9
29-10E	9,500	99.5	<i>S, S</i>	32.8	98.6
53-5H	5,000	99.1	<i>S, S</i>	55.8	97.6

Refer to Chapter 8 for experimental details.

^[a] ttn is reported as nmol **3** per nmol protein. The error is 20% at most. The protein is inactivated after 12 hours of incubation.

^[b] Proportion of **3** with respect to total products as determined with HPLC.

^[c] wt protein did not yield sufficient product to accurately determine *de* of **3**.

All mutants presented in this table have a propensity to hydroxylate the terminal or subterminal carbon of octane. They also tend to hydroxylate **2** at the 3-position of the cyclopentane ring. The regioselectivity on octane can therefore be used as a starting point for identifying mutants that might be useful for the hydroxylation of **2** to form **3**. The

enantiomeric and diastereomeric excess (*ee* and *de*, respectively), however, varies dramatically from mutant to mutant and is not predictable. While other variants could be identified that produce *R,R*-**3**, 1-12G remains the most enantioselective mutant. Variants with low *de* produce significant amounts of *R,S*-**3** or *S,R*-**3**; products which had not been observed previously at these high concentrations.

All of these variants presented in Table 5.4 support thousands of catalytic turnovers. Therefore, with a screen for enantioselectivity in hand, they can be used as starting points for the generation of enantioselective hydroxylation catalysts, which could enable new applications of biohydroxylation in organic synthesis.

D. References

1. Appel, D., Lutz-Wahl, S., Fischer, P., Schwaneberg, U. & Schmid, R. D. (2001). **A P450 BM-3 mutant hydroxylates alkanes, cycloalkanes, arenes and heteroarenes.** *J. Biotechnol.* **88**, 167-171.
2. Li, Q. S., Ogawa, J., Schmid, R. D. & Shimizu, S. (2001). **Engineering cytochrome P450 BM-3 for oxidation of polycyclic aromatic hydrocarbons.** *Appl. Environ. Microbiol.* **67**, 5735-5739.
3. Li, Q. S., Schwaneberg, U., Fischer, P. & Schmid, R. D. (2000). **Directed evolution of the fatty-acid hydroxylase P-450 BM3 into an indole-hydroxylating catalyst.** *Chem. Eur. J.* **6**, 1531-1536.
4. Carmichael, A. B. & Wong, L. L. (2001). **Protein engineering of *Bacillus megaterium* CYP102 - The oxidation of polycyclic aromatic hydrocarbons.** *Eur. J. Biochem.* **268**, 3117-3125.
5. Braunegg, G., de Raadt, A., Feichtenhofer, S., Griengl, H., Kopper, I., Lehmann, A. & Weber, H. J. (1999). **The concept of docking/protecting groups in biohydroxylation.** *Angew. Chem. Int. Edit.* **38**, 2763-2766.
6. de Raadt, A., Griengl, H. & Weber, H. (2001). **The concept of docking and protecting groups in biohydroxylation.** *Chem. Eur. J.* **7**, 27-31.
7. Parker, W., White, E., Shaddix, S., Ross, L., Buckheit, R., Jr, Germany, J., Secrist, J., 3d, Vince, R. & Shannon, W. (1991). **Mechanism of inhibition of human immunodeficiency virus type 1 reverse transcriptase and human DNA polymerases alpha, beta, and gamma by the 5'-triphosphates of carbovir, 3'-azido-3'-deoxythymidine, 2',3'- dideoxyguanosine and 3'-deoxythymidine. A novel RNA template for the evaluation of antiretroviral drugs.** *J. Biol. Chem.* **266**, 1754-1762.
8. de Raadt, A. et al. (1996). **Microbial hydroxylation of 2-cycloalkylbenzoxazoles .3. Determination of product enantiomeric excess and cleavage of benzoxazoles.** *Tetrahedron: Asymmetry* **7**, 491-496.
9. de Raadt, A. et al. (1996). **Microbial hydroxylation of 2-cycloalkylbenzoxazoles .1. Product spectrum obtained from *Cunninghamella blakesleeana* DSM 1906 and *Bacillus megaterium* DSM 32.** *Tetrahedron: Asymmetry* **7**, 467-472.
10. de Raadt, A. et al. (1996). **Microbial hydroxylation of 2-cycloalkylbenzoxazoles .2. Determination of product structures and enhancement of enantiomeric excess.** *Tetrahedron: Asymmetry* **7**, 473-490.

11. Farinas, E. T., Schwaneberg, U., Glieder, A. & Arnold, F. H. (2001). **Directed evolution of a cytochrome P450 monooxygenase for alkane oxidation.** *Adv. Synth. Catal.* **343**, 601-606.
12. Glieder, A., Farinas, E. T. & Arnold, F. H. (2002). **Laboratory evolution of a soluble, self-sufficient, highly active alkane hydroxylase.** *Nat. Biotechnol.* **20**, 1135-1139.
13. Walton, A. Z. & Stewart, J. D. (2004). **Understanding and improving NADPH-dependent reactions by nongrowing *Escherichia coli* cells.** *Biotechnol. Prog.* **20**, 403-411.
14. de Montellano, P. R. (1995). **Cytochrome P450: structure, mechanism, and biochemistry.** 2nd edit., Plenum Press, New York.
15. Peters, M. W., Meinhold, P. & Arnold, F. H. (2003). **Regio- and enantioselective alkane hydroxylation with engineered cytochromes P450 BM-3.** *J. Am. Chem. Soc.* **125**, 13442 -13450.

C h a p t e r 6

Direct Conversion of Ethane to Ethanol by Engineered Cytochrome P450 BM-3

A. Abstract

During the work described in Chapter 2, it became clear that mutations in the active site of P450 BM-3 are key to engineering the P450 to bind and position new substrates. In Chapter 3, extensive analysis of 11 active site residues is presented. While the results of this work provided information about the amenability of the active site to mutations and the effects of these mutations on regioselectivity of substrate hydroxylation, the ultimate goal of this work was to engineer an active site capable of binding and oxidizing the smallest alkanes, ethane and methane. No P450 or porphyrin-based catalyst has been shown to oxidize ethane and methane, which are known substrates only for methane monooxygenases [1] and, in the case of ethane, some of their homologs from alkane-assimilating microorganisms [2]. This chapter describes the direct oxidation of ethane to ethanol using dioxygen, catalyzed by one of the active site variants. Mutant 53-5H was found to be the most active propane hydroxylase, and additionally catalyzes the selective conversion of ethane to ethanol without overoxidation to acetaldehyde or acetic acid. Upon performing one further round of random mutagenesis, this time targeting the reductase domain of the enzyme, a mutant with improved productivity was identified. Achieving P450-catalyzed oxidation of ethane is a key step in the pathway to P450-catalyzed methane oxidation, and opens new opportunities for bioconversion of natural gas to fuels and chemicals.

B. Introduction

Most natural gas sources remain untapped as energy and chemical feedstocks, due to the difficulty of transporting the gas to facilities that can either use it as a fuel or convert the methane and ethane components into useful compounds. A catalyst for the selective oxidation of gaseous alkanes under mild conditions into easily transported alcohols could allow economical exploitation of both local, small natural gas resources and vast, remote reserves. Although catalytic alkane hydroxylation has been reported by many groups [3], selective conversion of ethane and methane mainly to their corresponding alcohols has yet to be demonstrated [4]. For example, limited (i.e., < 500 total turnovers) catalytic ethane oxidation is supported by a variety of transition metal catalysts, but these systems produce mixtures containing significant amounts of acetaldehyde and acetic acid in addition to ethanol [5-11]. Harsh oxidants such as hydrogen peroxide or sulfuric acid are usually required, although catalytic systems using dioxygen have also been reported [9-11]. The ideal catalyst should convert ethane to ethanol with high selectivity and productivity, be easily prepared from relatively common, nontoxic materials, function at ambient temperature and pressure, use dioxygen from the air as the oxidant, and produce little or no hazardous waste.

Biological systems have evolved efficient and productive metalloenzymes that convert alkanes into alcohols using dioxygen from the air. Methane monooxygenases (MMO) catalyze the conversion of methane to methanol, thereby enabling methanotrophic bacteria to use methane as a source of carbon and energy [1]. Microorganisms that grow on larger gaseous alkanes (ethane, propane, butane) have also been reported [2] and putatively use

similar enzymes for the first, alkane oxidation step [12,13]. The relatively well-studied MMOs have long been a source of inspiration for designers of chemical catalysts [14]. Unfortunately, these structurally complex enzymes have never been functionally expressed in a heterologous organism suitable for bioconversion and process optimization, and therefore have proven to be of little practical use themselves for production of alcohols.

We previously used laboratory evolution techniques to convert P450 BM-3 into a hydroxylation catalyst for small alkanes [15-17]. One of the reasons this P450 was chosen is that all of the machinery required for catalysis--the hydroxylase domain and reductase domain--is included on a single polypeptide chain [18], unlike MMOs and most other P450 enzymes. Although they support analogous oxygen insertion reactions on a wide variety of larger substrates, none of the thousand-plus members of the P450 enzyme superfamily are known to catalyze the oxidation of ethane or methane.

Communication between the heme and reductase domains of BM-3 is substrate-dependent and fine-tuned to transfer a pair of electrons from an NADPH cofactor through two reductase-bound flavins, and subsequently shuttle the electrons, one at a time, into the hydroxylase domain during catalysis [19]. Engineering the protein for activity on a new substrate, such as ethane, must conserve this regulated communication, and thus poses significant technical challenges. The engineered enzyme must bind ethane, a substrate considerably smaller than a fatty acid, directly above the heme in the active site of the hydroxylase domain. This substrate binding event must initiate electron transfer from the reductase domain to the heme domain during catalysis. Once electron transfer occurs, the active iron-oxo species must be capable of breaking the high energy C-H bond in ethane

(101.1 kcal mol⁻¹ vs. 95-99 kcal mol⁻¹ for the secondary C-H bonds of the fatty acid substrates [20] of wild-type BM-3). Finally, the singly-hydroxylated product must be released from the active site before further oxidation can occur.

Crystal structures of BM-3 heme domain with and without substrate are available [21-23]; a structure of the reductase domain, however, is not. Furthermore, large conformational changes in both domains during catalysis [24] make it difficult to identify amino acid substitutions which can address all these issues. Therefore, an ‘evolutionary’ strategy in which mutations are accumulated in multiple generations of random mutagenesis and screening [25] is likely the most efficient way to engineer an ethane hydroxylase. The approach has been to use directed evolution methods to adapt the enzyme to exhibit higher turnover on smaller and smaller alkanes (Figure 6.1), since high productivity is indicative of good solutions to the multiple engineering problems described above.

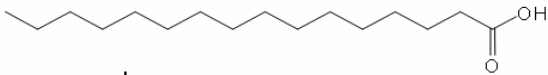
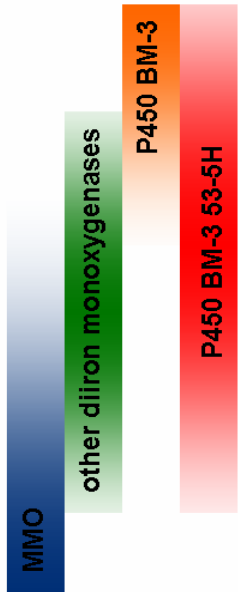
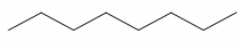
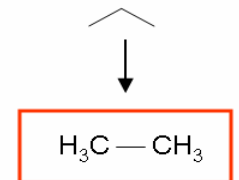
Substrate	C-H bond dissociation energy (kcal mol ⁻¹)		Alkane hydroxylating enzyme systems
	1°	2°	
			
↓	98-101	95-99	
			
↓	100.4	98.6	
	101.1		
CH ₄	104.9		

Figure 6.1. Reduction of substrate size and increase in C-H bond dissociation energy achieved by directed evolution. Directed evolution was used to convert wild-type P450 BM-3 stepwise from a fatty acid hydroxylase into an enzyme capable of activating the higher-energy C-H bond of ethane. The figure shows the substrate range of wild-type P450 BM-3 and its mutant 53-5H and, for comparison, the range of substrates of other alkane monooxygenases.

C. Results and Discussion

In the first generations, we increased the activity of BM-3 towards octane using iterations of random mutagenesis of the heme domain (residues 1-429) and screening based on the hydroxylation of the (octane surrogate) substrate *p*-nitrophenyl octyl ether. The resulting mutant, 139-3, contained 11 amino acid substitutions distributed throughout the

hydroxylase domain and exhibited good activity on octane [16]. It had also acquired a small but appreciable activity on propane, producing 2-propanol and a very small (less than 3%) amount of 1-propanol. As described in Chapter 2, the propane-hydroxylating activity of this mutant was subsequently increased by introducing random mutations in the heme domain. The resulting libraries were screened for activity towards the substrate dimethyl ether, a propane surrogate. Mutant 9-10A obtained in this way was much more active towards propane than 139-3 and produced significantly more 1-propanol (8 %) [17]. The increase in 1-propanol was particularly interesting because the propane terminal C-H bond energy (100.4 kcal/mol) is similar to the C-H bond energy of ethane (101.1 kcal/mol) [20].

Propane hydroxylation activity was further increased by introducing two active site mutations (A82L, A328V) into 9-10A, resulting in mutant 1-12G (described in Chapter 2). Upon saturating buffer containing this mutant with ethane, the ferric heme iron of this enzyme shows a characteristic, substrate-dependent shift from the low-spin to the high-spin state by UV/Vis spectroscopy, indicating ethane binding (Figure 6.2).

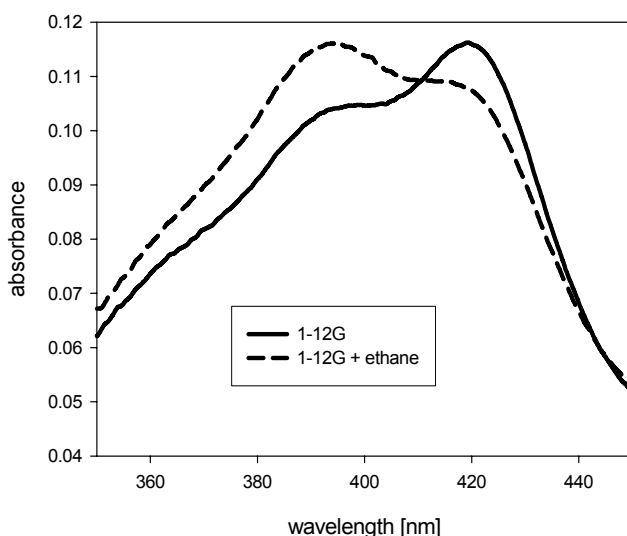


Figure 6.2. UV/VIS Spectra of P450 BM-3 mutant 1-12G (3 μ M in 0.1 M potassium phosphate buffer, pH 8.0) in its unbound, low-spin configuration (solid line), and in its high-spin configuration in ethane-saturated buffer (approximately 2 mM ethane) (dashed line).

However, despite numerous reactions under various conditions, no ethanol concentrations significantly above background were achieved with this mutant. To obtain an ethane-hydroxylating P450, we continued to engineer mutant 9-10A. This variant was chosen over the more active variant 1-12G as the basis for targeting mutations to the active site because none of its active site residues had previously been modified. To create a practically-sized library of variants with combinations of active site mutations, we first screened saturation mutagenesis libraries at each of 11 active site positions to identify a small pool of single active site mutants (see Chapter 3). Beneficial mutations, most of which were not accessible by the previously applied random mutagenesis due to the conservative nature of the genetic code, were then recombined into a multiple active site

library. This library contained approximately 9,000 P450 BM-3 variants, each of which contains a characteristic active site. A total of 16 mutants with improved activity towards DME or HME relative to 1-12G (Table 4.1) were selected for purification and further characterization.

In Chapter 4, we discussed these mutants in regards to their regioselectivity of octane hydroxylation. For the work described in this chapter, we picked the mutant with the highest propane hydroxylation activity among the mutants: mutant 53-5H catalyzes thousands of turnovers of propane to propanol at a rate of 370 min^{-1} (Table 6.1).

Table 6.1. Propane hydroxylation activities of wild-type and mutant cytochromes P450 BM-3.

BM-3 variant	ttn ^[a]	rate ^[b]
9-10A	1100	23
77-9H 1	1500	37
68-8F 1	2000	59
13-7C 1	3300	48
49-9B 1	890	37
35-7F 1	960	31
49-1A 1	500	15
23-11B 1	500	15
12-10C 1	1600	53
41-5B 1	850	66
11-8E 1	1900	120
7-11D 1	4200	120
29-3E 1	3200	160
29-10E 1	3000	180
53-5H 1	5000	370

^[a] Total turnover number (ttn) was measured using GC after completion of the reaction and is reported as (nmol product)/(nmol protein). Errors are at most 10%. Reactions conditions were: purified protein (25 nM) in potassium phosphate buffer (0.1 M, pH 8.0, saturated with propane and dioxygen), NADPH regeneration system (0.1mM NADP⁺, 10 U/mL isocitrate dehydrogenase, 25 mM isocitrate). The vial was pressurized with 20 psi of propane and stirred at 25°C for 4 hours

^[b] Initial rates of propanol and octanol formation were measured over 1 min by GC and are reported as (nmol product)/(min/nmol protein). Errors are at most 15%. Reactions conditions were: purified protein (100 nM) in potassium phosphate buffer (0.1 M, pH 8.0, saturated with propane and dioxygen), NADPH (0.5 mM). The reactions were performed at 25°C.

Notably, mutant 53-5H also hydroxylates ethane to generate ethanol. 53-5H contains three active-site mutations, A78F, A82S, and A328F, all of which replace alanine with a larger side chain, thus presumably reducing the volume of the active site and positioning small alkane substrates above the heme during catalysis. In addition to its activity towards ethane,

53-5H exhibits the highest regioselectivity (89% 2-octanol) and enantioselectivity (65% S-2-octanol) towards octane encountered in any BM-3 variant (Table 6.2), further evidence of tighter substrate binding in the engineered active site.

Table 6.2. Alkane hydroxylation activities of wild-type and mutant cytochromes P450 BM-3.

BM-3 variant	number of amino acid substitutions	active site amino acid substitutions	ethane		propane		octane ^[a]			
			rate ^[b]	ttn ^[c]	rate ^[d]	ttn ^[c]	rate ^[d]	ttn ^[c]	% 2-octanol	% ee ^[e]
Wild-type BM-3	—	—	—	—	—	—	30	150	17	n.d. ^[f]
9-10A	13	V78A	—	—	23	1100	540	3000	82	50 (S)
53-5H	15	V78F, A82S, A328F	0.4	50	370	5000	660	8000	89	65 (S)
35-E11	17	V78F, A82S, A328F	0.4	250	210	6000	420	8000	89	65 (S)

^[a] Octane reactions were performed in presence of 1% ethanol.

^[b] Rates of ethanol formation were measured over 30 min using gas chromatography (GC) coupled to an electron capture detector (ECD), and are reported as (nmol ethanol)/(min/nmol enzyme). Errors are at most 10%.

^[c] Total turnover number (ttn) was measured using GC after completion of the reaction and is reported as (nmol product)/(nmol protein). Errors are at most 10%.

^[d] Initial rates of propanol and octanol formation were measured over 1 min by GC and are reported as (nmol product)/(min/nmol protein). Errors are at most 15%.

^[e] ee of 2-octanol (main product) was measured by GC; the favored enantiomer is listed in parenthesis. ^[f] Wild-type P450 BM-3 primarily produces 3- and 4-octanol. The yields of 2-octanol were not sufficient for the determination of ee for wt BM-3.

Ethane hydroxylation by 53-5H was measured after 12-hour incubations of the enzyme in ethane-saturated buffer containing an ethanol-free NADPH regeneration system (commercial NADPH contains 2-3% ethanol). At less than 1 min^{-1} , the rate of ethanol formation is low. The reaction is also highly uncoupled to NADPH oxidation in the presence of ethane, which proceeds at a rate of 660 min^{-1} (Table 6.3).

Table 6.3. Rates of NADPH oxidation by ethane hydroxylation catalysts 53-5H and 35-E11.

53-5H			35-E11	
	NADPH oxidation rate [min^{-1}] ^[a]	Coupling efficiency [%] ^[b]	NADPH oxidation rate [min^{-1}] ^[a]	Coupling efficiency [%] ^[b]
no substrate	540		390	
Ethane	660	0.06 ^[c]	520	0.08 ^[c]
Propane	930	40	800	26
Octane	820	80	660	64

^[a] Errors are at most 5%. ^[b] Coupling efficiency is estimated from product formation rate / NADPH oxidation rate in presence of substrate. ^[c] NADPH oxidation rates cannot be measured on the same time scale as ethanol formation rates.

Nonetheless, 53-5H consistently produces at least 50 equivalents of ethanol, independent of the starting concentration of enzyme (Figures 6.2 and 6.3).

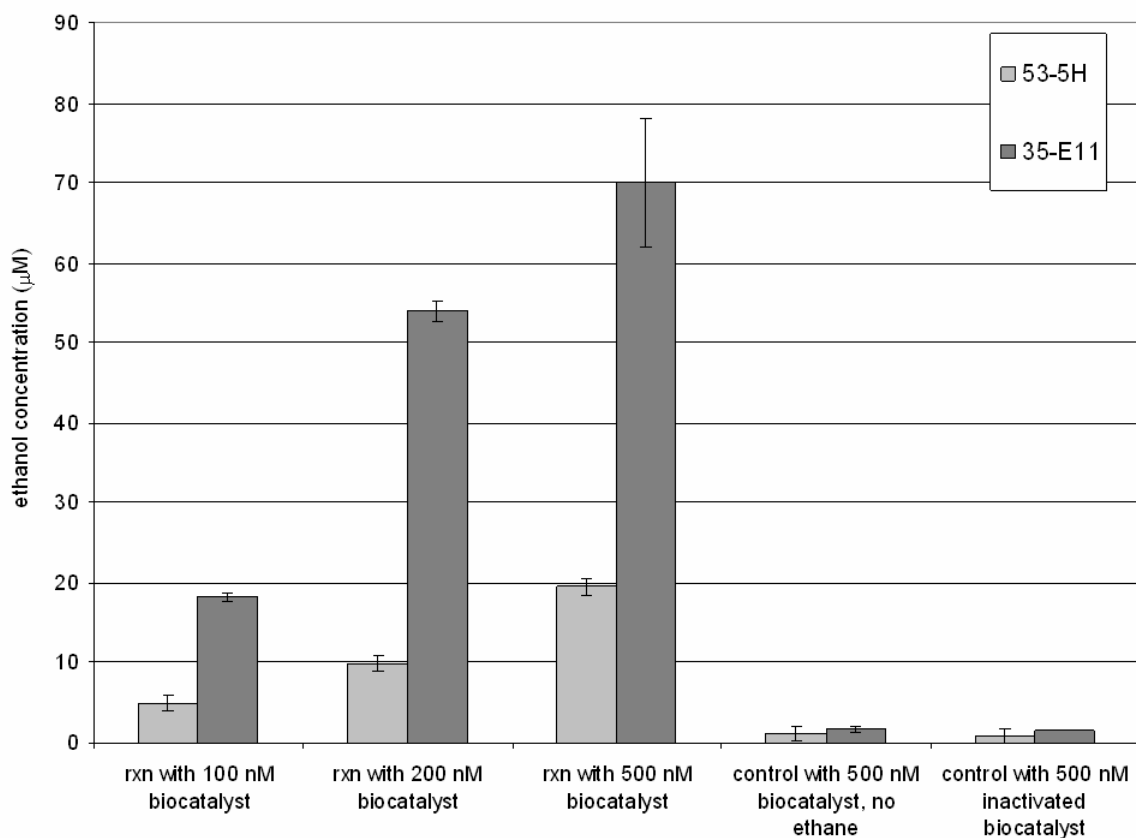


Figure 6.3. Final ethanol concentrations in 53-5H and 35-E11 catalyzed reactions. The reactions (5 mL) were carried out under the following conditions: To 100- 500 nM purified protein in 0.1 M potassium phosphate buffer (pH 8.0) saturated with ethane and dioxygen, 300 μ L NADPH regeneration system (1.66 mM NADP^+ , 167 U/mL isocitrate dehydrogenase, 416 mM isocitrate) was added to initiate the reaction. The vial was pressurized with 20 psi of ethane and stirred at 25°C for 12 hours. Conversion of ethane to ethanol using 200 nM protein corresponds to 50 and 250 turnovers per enzyme active site of 53-5H and 35-E11, respectively. Halving or doubling the enzyme concentration yielded approximately correspondingly lower or higher product concentrations, respectively. Control reactions, either without ethane or with inactivated protein, did not contain ethanol concentrations above the background level of 1 μ M ($1.2 \pm 0.1 \mu\text{M}$ for the control reaction without ethane, or $0.8 \pm 0.1 \mu\text{M}$ for the control reaction with inactivated P450 in which sulfuric acid is added before initiation of the reaction. See Chapter 8 for details). Error bars are the standard deviation of three experiments.

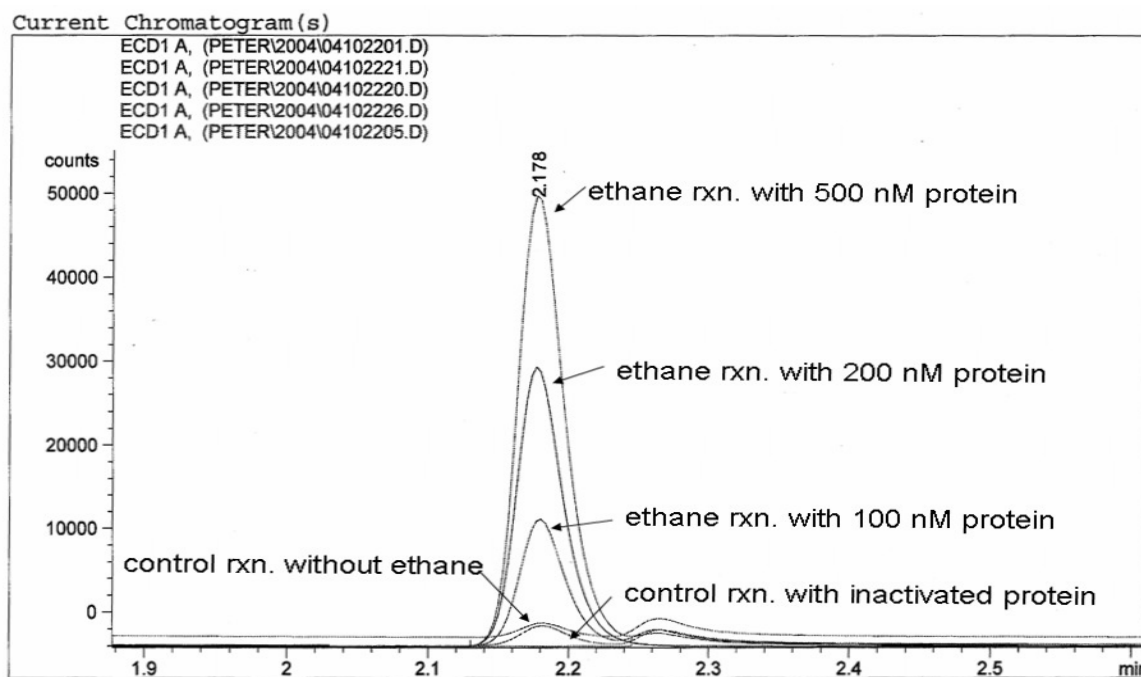


Figure 6.4. Gas chromatograms of ethanol reaction mixtures using variant 53-5H as the catalyst. Prior to analysis, ethanol was derivatized to form ethyl nitrite for detection via an electron capture detector (ECD).

We tested for overoxidation of ethanol by supplying ethanol as a substrate and monitoring ethanol depletion by gas chromatography, and monitoring the production of acetaldehyde and acetic acid by ^{13}C NMR using ^{13}C -labeled ethanol. No (i.e., less than 10%, the detection limit of these experiments) overoxidation products were detected in these experiments (Figure 6.5).

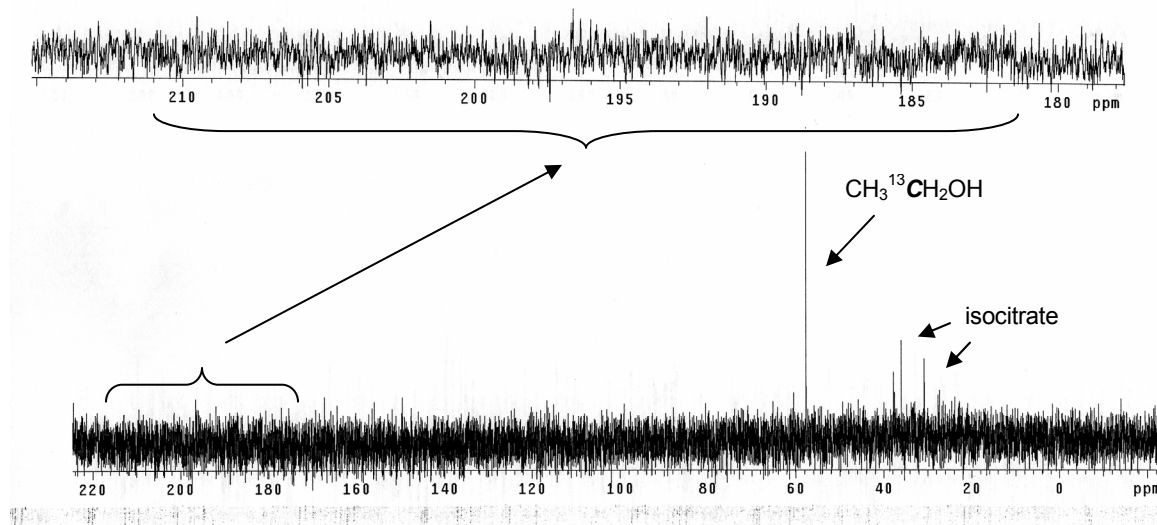


Figure 6.5. ^{13}C NMR spectrum (Varian Mercury 300 MHz) of singly ^{13}C -labeled ethanol incubated with 53-5H and NADPH regeneration system in 0.1M potassium phosphate buffer, pH 8.0, with 10% deuterium oxide added. No ^{13}C -labeled carbonyl peaks due to overoxidation of ethanol are detected.

In general, the hydrophobic active sites in P450s assist in the release of singly-hydroxylated products, and we have witnessed very little (typically less than 5%) overoxidation of longer and more hydrophobic alcohols in any BM-3 mutants. In addition, as shown in Chapter 2 (Table 2.1), there exists a trend that alkane-hydroxylating mutants overoxidize longer-chain alkanes, such as decane, to a higher extent ($\leq 7\%$) than shorter ones such as hexane ($\leq 1\%$) [17]. Mutant 53-5H also catalyzes the rapid (660 min^{-1}) and efficient (80% coupled) conversion of octane primarily to 2-octanol in the presence of 1% ethanol, demonstrating that ethanol does not inhibit the catalyst (Tables 6.2 and 6.3). These results demonstrate that the 101.1 kcal/mol C-H bond dissociation energy of ethane does not pose a fundamental barrier to a cytochrome P450, as a P450-based biocatalyst can cleanly convert ethane into ethanol without undesired side reactions.

We performed a further round of directed evolution to increase the ethane activity of 53-5H, this time targeting mutations to the reductase domain, including the polypeptide linker that connects it to the heme domain. In previous, unpublished work in our laboratory, the amino acid substitution E464G in the linker region had been implicated in increasing total turnover in selected BM-3 mutants, presumably by facilitating communication between the highly mutated hydroxylase domain and the as-yet unmodified reductase domain. Alone, this mutation does not enhance the production of ethanol by 53-5H, but further improvement was found upon screening a library of 53-5H containing this mutation and random mutations in the reductase domain for high activity towards dimethyl ether accompanied by reduced NADPH consumption rates in the absence of substrate. The resulting mutant 35-E11 contains all 15 of the hydroxylase domain substitutions found in 53-5H, the linker mutation E464G, and a new mutation, leading to the substitution I710T, located in the reductase domain. Compared to 53-5H, mutant 35-E11 exhibits a fivefold increase in total turnover of ethane to ethanol (total turnover number (tn) = 250, Table 6.2). In a typical reaction with ethane, 200 nM of mutant 35-E11 produces over 50 μ M of ethanol (Figure 6.2). The rate of product formation by 35-E11 equals that of 53-5H, while the NADPH consumption rate in the presence of ethane has decreased to $\sim 520 \text{ min}^{-1}$ (Table 6.3). The increased productivity likely reflects a prolonged catalyst lifetime, achieved by reducing non-productive cofactor oxidation, which inactivates the protein by forming various reactive species. Amino acid residue I710 is located, by comparison to the crystal structure of the homologous rat P450 reductase [26], near the FAD cofactor. Increased coupling efficiency has also been demonstrated in the past: For propane, NADPH oxidation in

mutant 139-3, a predecessor of 1-12G is only 9 % coupled to product formation. In contrast, the coupling efficiency of 53-5H catalyzed propane hydroxylation is 40 %.

Wild-type P450 BM-3 tightly regulates electron transfer from the NADPH binding reductase domain (containing FAD and FMN) to the heme in the attached heme domain. Substrate binding to the heme iron results in displacement of a weakly-bound water molecule that acts as the sixth axial ligand of the substrate-free heme iron. This results in an increase (~ 140 mV) in heme iron reduction potential and a shift in spin-state equilibrium to the high-spin form, inducing reduction of the ferric heme iron by the reductase domain [19,27]. In addition, when substrate is not bound, the reductase domain of P450 BM-3 is slowly inactivated by the accumulation of three reducing equivalents in the flavins of the reductase. In the presence of NADPH, substrate binding is therefore necessary to maintain enzyme activity. Mutants 53-5H and 35-E11 in their substrate-free form are low-spin (Figure 6.5). Ethane, however, does not induce the characteristic spin-shift, as it does for mutant 1-12G (Figure 6.2).

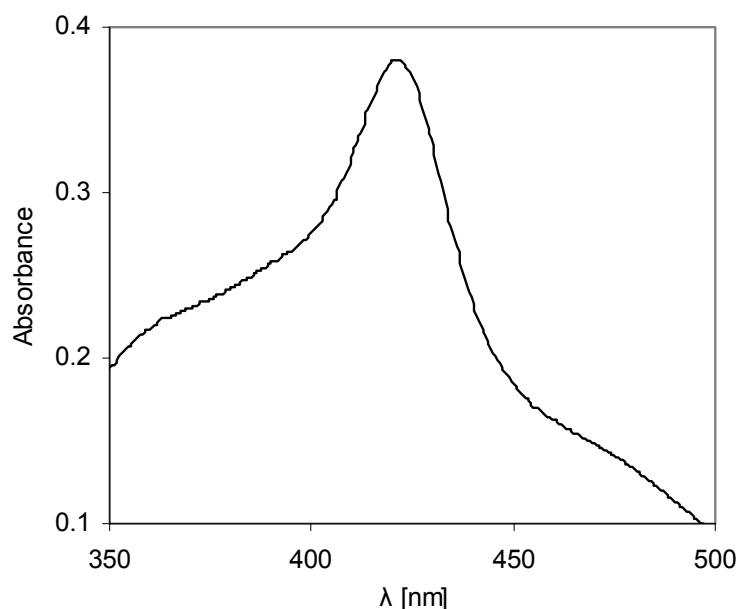


Figure 6.6. Absorption spectrum of 53-5H (3 μ M in 0.1 M potassium phosphate buffer, pH 8.0). The ferric heme iron is in low-spin form. A shift low- (A_{max} at 418 nm) to high-spin (A_{max} at 390 nm) ferric iron upon addition of ethane could not be detected. Addition of octane did not induce an increase at 390 nm. The spectrum of 35-E11 is identical. Earlier mutants, e.g., 9-10A exhibit a significant spin shift upon incubation with good substrates, such as octane.

Interestingly, even propane and octane, which can be hydroxylated at high rates and total turnover numbers, do not induce the spin-shift observed for 1-12G with the same substrates. The presence of ethane in the reaction buffer, however, induces NADPH oxidation (Table 6.3). The difference in background rate without substrate and with ethane is ca. 220 and 140 min^{-1} for 53-5H and 35-E11, respectively, indicating that ethane is bound in the active site of the enzyme. In comparison, propane induces a NADPH oxidation rate of around 400 min^{-1} for both enzymes (Table 6.3).

The strategy of adapting P450 BM-3 to ever smaller substrates appears to have been successful. The wild-type enzyme is inactive on propane. Evolving it to become an

octane hydroxylase, however, generated a small amount of activity towards propane. Similarly, increasing the newly acquired propane activity produced measurable activity towards ethane. Although the activity is still low for practical purposes, we have shown that continual improvements can be achieved, and we anticipate that further directed evolution will generate a biocatalyst with similar productivity to what we have obtained with propane (6,000 turnovers). It is also possible that high activity towards ethane will be accompanied by the emergent ability to convert methane to methanol. Thus this enzyme may provide the foundation for a novel biocatalytic route to methanol production from methane.

D. References

1. Hanson, R. S. & Hanson, T. E. (1996). **Methanotrophic bacteria.** *Microbiol. Rev.* **60**, 439-471.
2. Kulikova, A. K. (1995). **Microorganisms assimilating gaseous hydrocarbons (C₂ - C₄).** *Appl. Biochem. Microbiol.* **31**, 136-146.
3. Shilov, A. E. & Shul'pin, G. B. (1997). **Activation of C-H bonds by metal complexes.** *Chem. Rev.* **97**, 2879-2932.
4. Arakawa, H. et al. (2001). **Catalysis research of relevance to carbon management: progress, challenges, and opportunities.** *Chem. Rev.* **101**, 953-996.
5. Basicakes, N., Hogan, T. E. & Sen, A. (1996). **Radical-initiated functionalization of methane and ethane in fuming sulfuric acid.** *J. Am. Chem. Soc.* **118**, 13111-13112.
6. Shul'pin, G. B., Suss-Fink, G. & Shul'pina, L. S. (2001). **Oxidations by the system "hydrogen peroxide-manganese(IV) complex-carboxylic acid" Part 3. Oxygenation of ethane, higher alkanes, alcohols, olefins and sulfides.** *J. Mol. Catal. A: Chem.* **170**, 17-34.
7. Shul'pin, G. B., Suss-Fink, G. & Shul'pina, L. S. (2000). **Oxidative functionalisation of ethane with hydrogen peroxide catalysed by chromic acid.** *J. Chem. Res.*, 576-577.
8. Nizova, G. V., Krebs, B., Suss-Fink, G., Schindler, S., Westerheide, L., Gonzalez Cuervo, L. & Shul'pin, G. B. (2002). **Hydroperoxidation of methane and other alkanes with H₂O₂ catalyzed by a dinuclear iron complex and an amino acid.** *Tetrahedron* **58**, 9231-9237.
9. Lin, M. & Sen, A. (1994). **Direct catalytic conversion of methane to acetic-acid in an aqueous medium.** *Nature* **368**, 613-615.
10. Lin, M. R., Hogan, T. & Sen, A. (1997). **A highly catalytic bimetallic system for the low-temperature selective oxidation of methane and lower alkanes with dioxygen as the oxidant.** *J. Am. Chem. Soc.* **119**, 6048-6053.
11. Lin, M. R., Shen, C. Y., Garcia-Zayas, E. A. & Sen, A. (2001). **Catalytic Shilov chemistry: platinum chloride-catalyzed oxidation of terminal methyl groups by dioxygen.** *J. Am. Chem. Soc.* **123**, 1000-1001.

12. Sluis, M. K., Sayavedra-Soto, L. A. & Arp, D. J. (2002). **Molecular analysis of the soluble butane monooxygenase from 'Pseudomonas butanovora'.** *Microbiology* **148**, 3617-3629.
13. Kotani, T., Yamamoto, T., Yurimoto, H., Sakai, Y. & Kato, N. (2003). **Propane monooxygenase and NAD⁺-dependent secondary alcohol dehydrogenase in propane metabolism by *Gordonia* sp. strain TY-5.** *J. Bacteriol.* **185**, 7120-7128.
14. Tshuva, E. Y. & Lippard, S. J. (2004). **Synthetic models for non-heme carboxylate-bridged diiron metalloproteins: strategies and tactics.** *Chem. Rev.* **104**, 987-1011.
15. Farinas, E. T., Schwaneberg, U., Glieder, A. & Arnold, F. H. (2001). **Directed evolution of a cytochrome P450 monooxygenase for alkane oxidation.** *Adv. Synth. Catal.* **343**, 601-606.
16. Glieder, A., Farinas, E. T. & Arnold, F. H. (2002). **Laboratory evolution of a soluble, self-sufficient, highly active alkane hydroxylase.** *Nat. Biotechnol.* **20**, 1135-1139.
17. Peters, M. W., Meinhold, P. & Arnold, F. H. (2003). **Regio- and enantioselective alkane hydroxylation with engineered cytochromes P450 BM-3.** *J. Am. Chem. Soc.* **125**, 13442 -13450.
18. Narhi, L. O., Fulco, A.J. (1986). **Characterization of a catalytically self-sufficient 119,000- dalton cytochrome P450 monooxygenase induced by barbiturates in *Bacillus megaterium*.** *J. Biol. Chem.* **261**, 7160-7169.
19. Ost, T. W. B., Clark, J., Mowat, C. G., Miles, C. S., Walkinshaw, M. D., Reid, G. A., Chapman, S. K. & Daff, S. (2003). **Oxygen activation and electron transfer in flavocytochrome P450BM3.** *J. Am. Chem. Soc.* **125**, 15010-15020.
20. Lide, D. R. (1999). In *Handbook of chemistry and physics*, pp. 9-64. CRC Press, Boca Raton.
21. Ravichandran, K. G., Bodupalli, S. S., Hasemann, C. A., Peterson, J. A. & Deisenhofer, J. (1993). **Crystal structure of hemoprotein domain of P450BM-3, a prototype for microsomal P450's.** *Science* **261**, 731-736.
22. Li, H. & Poulos, T. L. (1997). **The structure of the cytochrome P450BM-3 haem domain complexed with the fatty acid substrate, palmitoleic acid.** *Nat. Struct. Biol.* **4**, 140-146.
23. Haines, D. C., Tomchick, D. R., Machius, M. & Peterson, J. A. (2001). **Pivotal role of water in the mechanism of P450BM-3.** *Biochemistry* **40**, 13456-13465.

24. Modi, S., Sutcliffe, M. J., Primrose, W. U., Lian, L. Y. & Roberts, G. C. K. (1996). **The catalytic mechanism of cytochrome P450 BM3 involves a 6 Angstrom movement of the bound substrate on reduction.** *Nat. Struct. Biol.* **3**, 414-417.
25. Valetti, F. & Gilardi, G. (2004). **Directed evolution of enzymes for product chemistry.** *Nat. Prod. Rep.* **21**, 490-511.
26. Hubbard, P. A., Shen, A. L., Paschke, R., Kasper, C. B. & Kim, J. J. P. (2001). **NADPH-cytochrome P450 oxidoreductase - Structural basis for hydride and electron transfer.** *J. Biol. Chem.* **276**, 29163-29170.
27. Daff, S. N., Chapman, S. K., Turner, K. L., Holt, R. A., Govindaraj, S., Poulos, T. L. & Munro, A. W. (1997). **Redox control of the catalytic cycle of flavocytochrome P-450 BM3.** *Biochemistry* **36**, 13816-13823.

Chapter 7

Discussion of the Engineering Strategy

A. Random vs. Targeted Mutagenesis

Directed evolution involving random mutagenesis of the full gene has proven to be a useful tool for engineering proteins. When improving characteristics such as rate, thermostability, or pH-dependence, directed evolution may be superior to rational design since the mechanisms for such changes are frequently not well enough understood for rational engineering to be successful. Changing the substrate specificity or regioselectivity of an enzyme, however, might require mutations within the active site and it became apparent during this work that this was true for P450 BM-3. Mutations within the active site of BM-3 are only rarely to be found by random mutagenesis of the full protein since only a few residues are mutated and chances are greater for these residues to be on the surface rather than in the core of the protein where the active site typically is located. Additionally, single nucleotide changes to a codon typically access only about six of the nineteen possible amino acid substitutions. We therefore chose to take advantage of structural and mutational data available for P450 BM-3 to target mutagenesis to specific active site residues.

B. Single vs. Multiple, Simultaneous Substitutions

The number of amino acid residues that can be randomized simultaneously depends on the strategy for finding improved mutants – screening or selection. If, for example, four amino acid residues are mutated simultaneously, the complete library consists of 160,000 possible variants. This is usually beyond the upper limit for high-throughput screening

systems. With limited resources, and an assay that requires single colonies to be grown in each well of a 96-well plate, screening of 10,000 variants already becomes a very demanding and time-intensive process. We identified 11 active site residues that are in close proximity to bound fatty acid substrates in crystal structures of BM-3 [1,2]. Ideally, we would like to look at the effects of all possible combinations of mutations at these sites, but screening 20^{11} possible mutants is impossible. To create a more manageable active site library with a high probability of containing active mutants, we first screened saturation mutagenesis libraries at each of 11 active site positions to identify a small pool of single active site mutants and then recombined beneficial mutations into a multiple active site library containing approximately 9,000 variants.

The reason for recombining only beneficial mutations was to create a reasonably sized library highly enriched in active variants. In doing so, we made two assumptions: a) mutations that are beneficial separately will also be beneficial in combination with others, and b) improved mutants are more likely to be identified by recombining beneficial mutations than neutral or deleterious ones.

Both assumptions are problematic, because they leave out the possibility for synergistic effects. Recent engineering studies of various enzymes have targeted several active site residues for mutagenesis simultaneously. In combination with powerful screening or selection systems, this approach was successful in identifying improved variants (reviewed in [3]). The best mutants discovered by targeted mutagenesis almost always contain multiple mutations. These mutations are often beneficial as single mutations, but evidence is accumulating that at least some of them are beneficial only in combination [4]. A

possible reason for these synergistic effects is that multiple active site mutations can cause significant structural changes in the active site, as has been noted for tRNA synthetases [5]. In this case, targeted mutagenesis strategies that simultaneously mutate multiple residues offer an approach to uncover coupled mutations that cannot be found with random mutagenesis or saturation mutagenesis of single residues. Given the limits of our screening system, however, we felt this strategy was reasonable and the most manageable.

C. Alternative Strategies

The number of active site residues of P450 BM-3 that putatively interact with the substrate is large. To take advantage of beneficial effects of combinations of this large number of mutations in the future, a selection system will become necessary. In absence of such a system, other alternatives can be sought to access coupled mutations that are not necessarily beneficial on their own.

One approach that has been successfully implemented is to perform saturation mutagenesis of a first amino acid, then isolate the best mutant, then perform saturation mutagenesis of a second mutant and so on. This way, in contrast to our approach, mutations can be uncovered that are coupled to the previously randomized amino acid. However, there is no rationale for choosing the sequence of amino acids to be mutated, and the number of possible pathways quickly becomes as intractable just as when several mutations are randomized simultaneously. A similar approach is to target a limited number of amino acids for randomization, say three, of which all possible combinations, in this case 8000,

can be screened for improved activity. The selected, best mutant can then be subjected to the same procedure again.

A third approach is to use random oligonucleotide mutagenesis to generate diversity by incorporating random mutations, encoded on a synthetic oligonucleotide, into the active site region of the gene. The number of mutations in individual enzymes within the population can be controlled by varying the length of the target sequence and the degree of randomization during synthesis of the oligonucleotides. The advantages of this more defined approach are that all possible amino acid mutations and also coupled mutations can be found. We tried this approach during the engineering of P450 BM-3 for alkane hydroxylation. The oligonucleotide primer was randomized at the nucleotide codons encoding seven active site residues to yield an average mutation rate of approximately two per gene. At this mutation rate the library size is approximately 7,800 and is still manageable. The library was screened as described in the foregoing chapters but no improved mutants could be identified. The problem, however, was not the method itself (which has proven to be successful in many studies [6-8]), but unwanted errors on the oligonucleotide.

D. Selection Systems for Identifying P450 Alkane Hydroxylases

By using a selection system capable of identifying the most active variant out of a large pool (e.g., millions) of mutants, the number of mutants containing simultaneous mutations can be enhanced. We have accumulated and established in this laboratory several

engineered bacterial strains that grow on *n*-alcohols. Clark and coworkers engineered *E. coli* strains that can grow on small-chain alcohols [9,10]. Although it has not been demonstrated that these strains could grow on gaseous alkanes, it is likely that expression of an active P450 monooxygenase will enable them to use gaseous alkanes as the sole carbon source. Witholt and co-workers have developed *E. coli* and *Pseudomonas putida* strains that grow on medium-chain primary alcohols. These strains have been used by the Witholt laboratory to identify homologs of the multicomponent alkane monooxygenase *alkB* [11]. By incorporating a P450 monooxygenase that can efficiently convert *n*-alkanes into primary alcohols in these bacterial strains, we will enable them to grow on a variety of *n*-alkanes.

E. References

1. Li, H. & Poulos, T. L. (1997). **The structure of the cytochrome P450BM-3 haem domain complexed with the fatty acid substrate, palmitoleic acid.** *Nat. Struct. Biol.* **4**, 140-146.
2. Haines, D. C., Tomchick, D. R., Machius, M. & Peterson, J. A. (2001). **Pivotal role of water in the mechanism of P450BM-3.** *Biochemistry* **40**, 13456-13465.
3. Bloom, J. D., Meyer, M. M., Meinhold, P., Otey, C. R., Macmillan, D. & Arnold, F. H. (2005). **Evolving strategies for enzyme engineering.** *Curr. Opin. Struct. Biol.* **accepted**.
4. Hill, C. M., Li, W. S., Thoden, J. B., Holden, H. M. & Raushel, F. M. (2003). **Enhanced degradation of chemical warfare agents through molecular engineering of the phosphotriesterase active site.** *J. Am. Chem. Soc.* **125**, 8990-8991.
5. Wang, L. & Schultz, P. G. (2005). **Expanding the genetic code.** *Angew. Chem. Int. Edit.* **44**, 34-66.
6. Shinkai, A., Patel, P. H. & Loeb, L. A. (2001). **The conserved active site motif of *Escherichia coli* DNA polymerase I is highly mutable.** *J. Biol. Chem.* **276**, 18836-18842.
7. Landis, D. M., Gerlach, J. L., Adman, E. T. & Loeb, L. A. (1999). **Tolerance of 5-fluorodeoxyuridine resistant human thymidylate synthases to alterations in active site residues.** *Nucl. Acids Res.* **27**, 3702-3711.
8. Black, M. E., Newcomb, T. G., Wilson, H. M. P. & Loeb, L. A. (1996). **Creation of drug-specific herpes simplex virus type 1 thymidine kinase mutants for gene therapy.** *Proc. Natl. Acad. Sci.* **93**, 3525-3529.
9. Clark, D. & Cronan, J. E. (1980). ***Escherichia coli* mutants with altered control of alcohol dehydrogenase and nitrate reductase.** *J. Bacteriol.* **141**, 177-183.
10. Clark, D. P. & Rod, M. L. (1987). **Regulatory mutations that allow the growth of *Escherichia coli* on butanol as carbon source.** *J. Mol. Evol.* **25**, 151-158.
11. Smits, T. H. M., Balada, S. B., Witholt, B. & van Beilen, J. B. (2002). **Functional analysis of alkane hydroxylases from Gram-negative and Gram-positive bacteria.** *J. Bacteriol.* **184**, 1733-1742.

Chapter 8

Materials and Experimental Procedures

A. Reagents

All chemicals, including liquid alkanes and product standards were purchased from Sigma-Aldrich (St. Louis, MO). Solvents (hexanes, chloroform, methylene chloride) were purchased from EMD (Gibbstown, NJ) or Mallinckrodt (Paris, KY). Ethanol was purchased from AAPER (Shelbyville, KY). Ethane (99.95% or 99.99%), propane (99.5%), and dimethyl ether (99.8%)) were purchased from Special Gas Services (Warren, NJ). Methane (99.0%) and ethane of higher purity (99.99%) was purchased from Sigma-Aldrich but as this did not change the outcome of the experiments it was not routinely used. Hexyl methyl ether was purchased from TCI America (Portland, OR). NADP⁺ for experiments described in Chapter 2 was purchased from Sigma-Aldrich. For experiments described in all other chapters, NADP⁺ was purchased from BioCatalytics, Inc. (Pasadena, CA), as was NADPH. Restriction enzymes (BamHI, SacI, EcoRI) were purchased from Roche (Indianapolis, IN) or New England Biolabs (Beverly, MA), Taq DNA polymerase from Roche (Indianapolis, IN), Pfu turbo DNA polymerase from Stratagene (La Jolla, CA), and T4 DNA ligase from Invitrogen (Carlsbad, CA). isopropyl β -D-1-thiogalactopyranoside (IPTG) was from MP Biomedicals, Inc. (Aurora, OH). Protease inhibitors phenyl methyl sulfonyl fluoride (PMSF), pepstatin, and leupeptin were purchased from Gibco BRL (Gaithersburg, MD), Roche (Indianapolis, IN), and USB (Cleveland, OH) respectively.

B. Expression of P450 BM-3 (Chapters 2-6)

The P450 BM-3 gene or mutants thereof, which include a silent mutation to introduce a *SacI* site 130 bp upstream of the end of the heme domain, were cloned behind the double *tac* promoter of the expression vector pCWori (pBM3_WT18-6, see Appendix B for details). *E. coli* DH5 α , transformed with these plasmids, was used for expression of P450 BM-3 on a 500 mL scale, as well as for expression in 96-well plates. For protein production, supplemented terrific broth (TB) medium (500 mL, 100 μ g/mL ampicillin, 50 μ g/mL thiamine) was inoculated with an overnight culture (1 mL) and incubated at 30°C and 250 rpm shaking. After 12 hours of incubation, the rotation speed was lowered to 200 rpm, δ -aminolevulinic acid hydrochloride (δ -ALA; 0.5 mM) was added, and expression was induced by addition of isopropyl β -D-1-thiogalactopyranoside (IPTG; 1 mM). Cells were harvested by centrifugation 20 to 24 hours after induction. Yields varied from day to day and depending on the mutant being expressed from about 10 to 100 mg/L.

C. Purification of P450 BM-3

C.1. Single-Step Purification of P450 BM-3 (Chapters 2-6)

All purification steps were performed on ice or at 4°C. The cell pellet was resuspended with Tris-HCl buffer (20 mL, 25 mM, pH 7.9, 100 μ M PMSF) and lysed by sonication (2 x 1 min, output control 7, duty cycle 60%; Sonicator, Heat Systems – Ultrasonic, Inc.). The lysate was then centrifuged at 75,000 x g for 45 min and further cleared by filtration using a

Steriflip 22 μm filter (Millipore, Billerica, MA). The enzyme was purified essentially as described [1] by ion exchange chromatography using an Äkta Explorer FPLC System (Pharmacia Biotech) and Toyopearl[®] SuperQ-650M column packing. The P450 containing fractions were collected and concentrated using a Centriprep YM-30 centrifugal filtration device. The protein solution was then buffer-exchanged with potassium phosphate buffer (100 mM, pH 8.0) using a PD-10 Desalting column (Amersham Pharmacia Biotech). P450 enzyme concentrations were quantified by CO-binding difference spectra of the reduced heme as described [2], using an extinction coefficient of $91 \text{ mM}^{-1} \text{ cm}^{-1}$ for the 450 nm minus 490 nm peak. P450 total expression yields were estimated from CO-binding difference spectra of the clarified lysates. Protein solutions were stored at -80°C .

C.2. Four-Step Purification of P450 BM-3

To obtain highly pure protein preparations for ethane reactions described in Chapter 6, the protein was purified in four steps according to published procedures [3,4]. No difference in background ethanol concentration, or productivity and rate of alkane hydroxylation was observed using these preparations. Therefore, for all practical purposes, the purification system described above was employed.

All purification steps were performed on ice or at 4°C . The cell pellet was thawed and resuspended in 20 mL of buffer A (50 mM KPi, pH 7.4, 2 mM DTT, 0.1 mM EDTA, 0.1 mM PMSF). Protease inhibitors, pepstatin and leupeptin at $1 \mu\text{g/mL}$ each were added to the lysis buffer. The cells were lysed by sonication (2 min, output control 7, duty cycle 60%,

Sonicator, Heat Systems – Ultrasonic, Inc.). The lysate was centrifuged at 75,000 x g for 45 minutes at 4°C and the red-colored supernatant was further cleared through a 0.22 µm filter (Millipore, Billerica, MA)

A HiPrep 16/10 Q FF anion exchange column (Amersham, Piscataway, NJ) was equilibrated with at least one column volume of buffer A. After the cell extract was loaded, the column was washed with 3 volumes of 0.2 M KCl in buffer A at a flow rate of 4 mL/min. A gradient of 0.2 – 0.5M KCl in buffer A was used to elute the protein.

Next, a 2'5'-ADP-Sepharose affinity column (1.5 x 10 cm) (Amersham, Piscataway, NJ) was equilibrated with approximately 40 mL of buffer B (0.1 M KPi, pH 7.4, 0.5 mM DTT). The pooled red fractions from the previous step were applied directly, without prior concentration, and the column was washed with an additional 60 to 80 mL of buffer B and 50 mL buffer C (0.5 M KPi, pH 7.4, 0.5 mM DTT). The protein was eluted with 15 mM NADP⁺ in buffer C. The red eluent was collected and concentrated to approximately 0.7 mL using a Centriprep YM-30 concentrator (Millipore, Billerica, MA).

A HiPrep 16/60 Sephacryl S-200 HR column (Amersham, Piscataway, NJ) was equilibrated with 2 column volumes of buffer D (0.1 M KPi, pH 7.4, 1 mM DTT, 0.1 mM EDTA, 0.1 mM PMSF) before loading the concentrated protein. The protein was eluted at a flow rate of 0.2 mL/min; pure fractions were collected and once again concentrated to approximately 1 mL using a Centriprep YM-30 concentrator.

To remove NADP⁺ and trace amounts of ethanol, the protein was dialyzed against 3.5 L of 0.1 M KPi, pH 8.0 using 12-14 kDa MWCO dialysis tubing. The protein was determined to

be homogeneous on a protein gel, and the protein concentration was determined in triplicate by CO-difference spectroscopy [2]. Protein solutions were stored at -80°C.

D. Library Generation of P450 BM-3 Mutants and Site Directed Mutagenesis

D.1. Recombination of P450 BM-3 Variants (Chapter 2)

The first generation of mutants was created by StEP recombination of mutant 139-3 [5] with fifteen other mutants from the same generation, according to published procedures [6]. Mutant J was isolated from a library of ~350 mutants, based on its increased NADPH depletion rate using propane as a substrate (see section E.2 for details).

D.2. Random Mutagenesis of P450 BM-3 (Chapter 2)

Libraries for the second (~1,000 mutants) and third (~1,500 mutants) generations were created by error-prone PCR using the Genemorph kit (Stratagene, La Jolla, CA) according to the manufacturer's protocol, using approximately 50 ng of plasmid DNA as template and primers BamHI-forw (5'-GGAAACAGGATCCATCGATGC-3') and SacI-rev (5'-GTGAAGGAATACCGCCAAGC-3'). Mutant 9-10A was isolated from this library based on its increased NADPH depletion rate in the presence of propane (see section E.2 for details).

D.3. Site-Directed/Saturation Mutagenesis (Chapter 2)

Base mutations were introduced into mutant 9-10A by PCR overlap extension mutagenesis [7]. Position A82 was mutated to L, I, V and F using mutagenic primers

A82forw (5'-GGAGACGGGTTATTTACAAGC-3') and

A82rev (5'-GCTTGTAATAACCCGTCTCCAANAAAATCACG-3').

Position A328 was mutated to V using mutagenic primers

A328Vforw (5'-GCTTATGGCCAACTGTTCTGC-3') and

A328Vrev (5'-GCAGGAACAGTTGGCCATAAGC-3').

For each mutation, two separate PCRs were performed, each using a perfectly complementary primer (BamHI-forw (5'-GGAAACAGGATCCATCGATGC-3') and SacI-rev (5'-GTGAAGGAATACCGCCAAGC-3')) at the end of the sequence and a mutagenic primer. The resulting two overlapping fragments that contain the base substitution were then annealed in a second PCR, and the complete mutated gene amplified.

D.4. Recombination of P450 BM-3 Variants (Chapter 2)

The fifth generation of mutants was created by recombination of mutants 139-3, J, 9-10A, 9-10A-A82L and 9-10A-A328V (see Appendix B for mutations) using a modification of Stemmer's DNA shuffling protocol [8]. Mutant 1-12G was identified as the most active enzyme towards the surrogate screening substrate dimethyl ether (see section E.3 for details).

D.5. Random Mutagenesis of Variant 1-12G (Chapter 3)

The random library of 1-12G was created by error-prone PCR using four different concentrations of MnCl_2 (0, 50, 100, and 150 μM) to induce mutations, Taq DNA polymerase (Roche), approximately 50 ng of plasmid DNA as template, and primers BamHI-forw (5'-GGAAACAGGATCCATCGATGC-3') and SacI-rev (5'-GTGAAGGAATACCGCCAAGC-3').

The amplified gene (with mutations) was then cut with BamHI and SacI restriction enzymes and ligated with T4 DNA ligase into pBM3_WT18-6, previously cut with BamHI and SacI to remove the wild-type gene. The ligation mixtures were then transformed into *E. coli* DH5 α cells that had previously been made electro-competent. The transformed cells were plated onto Luria-Bertani (LB) agar plates to form single colonies for picking. For each Mn^{2+} concentration, a small library of 88 mutants in a 96-well plate (8 wells containing parent 1-12G) was picked and screened for activity towards dimethyl ether and hexyl methyl ether as described below (section E.3). The library prepared with a Mn^{2+} concentration of 100 μM yielded ~40-50% of the mutants with no activity in the screen. Subsequently, 1500 members of this library were screened for activity towards dimethyl ether and hexyl methyl ether.

D.6. Construction of Saturation Mutagenesis Libraries (Chapter 3)

Mutations were introduced into mutant 9-10A by PCR overlap extension mutagenesis using Pfu turbo DNA polymerase [7]. The following amino acids were chosen for

saturation mutagenesis: A74, L75, A78, F81, A82, F87, T88, T260, L263, I264 and A328. The primers for each saturation library contained all possible combinations of bases, NNN (N = A, T, G, or C), at the codon for a particular residue (in bold). The primers in the forward direction for each library were:

74NNNfor (5'-GTCA**ANN**NCTTAAATTTGCACG-3')

75NNNfor (5'-GTCAAGCG**NNN**AAATTTGCACG-3')

78NNNfor (5'-GCTTAAATTT**NNN**CGTGATTTTGCAGG-3')

81NNNfor (5'-CGTGAT**NNN**GCAGGAGAC-3')

82NNNfor (5'-CGTGATTTT**NNN**GGAGAC-3')

87NNNfor (5'-GAGACGGGTT**ANN**NACAAGCTGGAC-3')

88NNNfor (5'-GGAGACGGGTTATTT**NNN**AGCTGGACG-3')

260NNNfor (5'-CAAATTATT**NNN**TTCTTAATTGCGGGAC-3')

263NNNfor (5'-ACATTCTT**ANN**NGCGGGACACGAAAC-3')

264NNNfor (5'-ACATTCTTAATT**NNN**GGACACGAAAC-3')

328NNNfor (5'-CCA**ACTNNN**CCTGCGTTTTCC-3')

The reverse primers for each of these libraries complement their corresponding forward primers. For each mutation, two separate PCRs were performed, each using a perfectly complementary primer, BamHI-forw (5'-GGAAACAGGATCCATCGATGC-3') and SacI-rev (5'-GTGAAGGAATACCGCCAAGC-3'), at the end of the sequence and a mutagenic primer. The resulting two overlapping fragments that contain the mutations were then annealed during a second PCR to amplify the complete mutated gene. The full gene was then cut with BamHI and SacI restriction enzymes and ligated with T4 ligase

(Invitrogen) into pBM3_WT18-6, previously cut with BamHI and SacI to remove the wild-type gene. The ligation mixtures were subsequently transformed into *E. coli* DH5 α cells that had previously been made electro-competent. The cells were then plated onto Luria-Bertani (LB) agar plates to form single colonies for picking.

D.7. Construction of Recombination Libraries (Chapters 3 and 4)

Beneficial mutations that were found by screening the saturation mutagenesis libraries (L75 (W), A78 (T, F), A82 (T, S, F, I, C, G), F87 (I, V, L), T88 (C), T260 (N, L), A328 (L, F, M)) were recombined in a combinatorial fashion. Saturation libraries of amino acid positions A74, F81, L263 and I264 did not yield improved mutants, thus only beneficial mutations at the remaining seven sites were recombined. The mutation L75I which was not found to increase activity was selected for its change in regioselectivity and added to the library to increase its diversity. The mutations A82L and A328V were added to the library because of their beneficial effects described in Chapter 2. Mutation A82V was added due to constraints in designing the degenerate primer used to construct the library.

Mutations were added sequentially using overlap extension PCR with degenerate primers (see above) or a mixture of primers (mutation sites in the primers are in bold letters; the reverse primers for each of these libraries complement their corresponding forward primers).

Mutations at amino acid position 78 and 82 were introduced into 9-10A using primers:

78A/T 82A/T/S/F/I/C/G/L/V for* (5'-

GCTTAAATT**CRC**CGTGATTTT**DBC**GGAGACG-3'),

78F 82A/T/S/F/I/C/G/L/V for (5'-GCTTAAATT**CTT**TCGTGATTTT**DBC**GGAGACG-3').

Next, mutations at position 260 were introduced using primers:

260Tfor* (5'-CAAATTATTACATTCTTAATTGCGGGAC-3'),

260Nfor (5'-CAAATTATTA**A**CTTCTTAATTGCGGGAC-3'),

260Lfor (5'-CAAATTATT**CTTT**TCTTAATTGCGGGAC-3').

Next, mutations at position 87 and 88 were introduced using primers:

87F/I/V/L 88Tfor* (5'-GAGACGGGTTANT**Y**ACAAGCTGGAC-3'),

87F/I/V/L 88Cfor (5'-GAGACGGGTTANT**YTG**TAGCTGGAC-3').

Next, mutations at position 328 were introduced using primers:

328Afor* (5'-CCAAC**TG**CTCCTGCGTTTTCC-3'),

328L/F/Vfor (5'-CCAAC**TB**TCCTGCGTTTTCC-3'),

328Mfor (5'-CCAAC**AT**GCCTGCGTTTTCC -3').

Finally, mutations at position 75 were introduced using primers:

75L/Ifor* (5'-CTTAAGTCAAGCG**MT**TAAATTC-3'),

75Wfor (5'-CTTAAGTCAAGCG**TG**GAAATTC-3').

Mutants selected for improved activity towards HME were found only at amino acid positions 75, 78, 82, 87 and 328. We are confident, however, that the all mutations were recombined. While building the library, we screened and sequenced ten improved members of a partial library containing mutations at positions 78, 82 and 260 to verify that the library had been constructed properly. All possible amino acids at position 75 and 260, and four out of eight amino acids at position 78 were found.

D.8. Construction of the Reductase Library (Chapter 6)

The mutation E464G was found by directed evolution of another BM-3 variant not reported in this work (Katsu Takahashi, unpublished). A random mutant library of the reductase portion of the BM-3 gene containing this mutation (1285 to 3147 bp) was PCR-amplified using primers *SacI*-for (5'-GACTTTGAAGATCATACAAACTACGAGCTCG-3') and *EcoRI*-rev (5'-AGATCTGCTCATGTTTGACAGCTTATCATCGATGAATTC-3') in the presence of 100 μ M $MnCl_2$. The amplified DNA was restriction digested using *SacI* and *EcoRI* and then ligated with T4 DNA ligase into the pCWori plasmid containing the gene for 53-5H with its reductase portion removed with *SacI* and *EcoRI*. A library containing 2,610 members was picked and screened as described [9].

D.9. Construction of F87A Variants of Wild-Type P450 BM-3 and Variant 9-10A (Chapter 5)

The F87A mutations was introduced into wild-type P450 BM-3 and mutant 9-10A[9] by PCR overlap extension mutagenesis as described above. The mutagenic primers were F87Afor (5'-GAGACGGGTTAGCAACAAGCTGGAC-3') and F87Arev (5'-GTCCAGCTTGTTGCTAACCCGTCTC-3')

E. High-Throughput Screening of P450 BM-3 Mutant Libraries

E.1. Preparation of Cell Lysates for High-Throughput Screening (Chapters 2-4, 6)

Single colonies were picked and inoculated by hand or using a Qpix colony picking robot (Genetix, Beaverton, OR) into 1-mL deep-well plates containing Luria-Bertani (LB) medium (350 μ L, supplemented with 100 mg/mL ampicillin), except for a row of eight wells in which single colonies of the best parent from the previous library were picked for reference and a single control well with no cells added. The plates were incubated at 30°C, 250 rpm, and 80% relative humidity in a Kühner ISF-1-W incubator shaker (Kühner, Birsfelden, Switzerland). After 24 hours, clones from this preculture were inoculated using a 96-pin replicator (V&P Scientific, San Diego, CA) into 2-mL deep-well plates containing TB medium (400 μ L, supplemented with 100mg/mL ampicillin, 10 μ M IPTG and 0.5 mM δ -ALA). The cultures were grown at 30°C, 250 rpm, and 80% relative humidity for another 24 hours. Cells were then pelleted and stored frozen at -20°C until they were

resuspended in phosphate buffer (500 μ L, 0.1 M, pH 8.0, containing 0.5 mg/mL lysozyme, 2 Units/mL DNaseI, and 10 mM MgCl_2). After 60 min at 37°C, the lysates were centrifuged in Allegra 25R Centrifuge (Beckman Coulter, Fullerton, CA) and the supernatant was diluted for activity measurements in 96-well microtiter plates.

E.2. High-Throughput Protein Folding Assay (Chapter 3)

Carbon monoxide difference spectroscopy yields a spectral peak at approximately 450 nm when comparing bound and unbound forms [2]. This difference demonstrates the presence of a correctly-folded cytochrome P450. Binding of carbon monoxide in the presence of a biologically inactive form of a cytochrome P450 yields a spectral peak at 420 nm [10]. Thus CO binding effectively assays for the presence of a correctly-folded cytochrome P450, an incorrectly-folded P420, or a lack of either. The assay has been modified for high-throughput in microtiter plates [11].

Into each well of a 96-well microtiter plate, 40 μ L of a sodium hydrosulfite solution (300 mM) and then 160 μ L of P450-containing cell lysate were added. A baseline spectrum was taken before placing the plate into a chamber. The chamber was evacuated and subsequently filled with carbon monoxide. The plate was incubated for approximately 10 minutes before removing it to record the difference spectrum from 400-500 nm using a Spectramax Plus microtiter plate reader (Molecular Devices, Sunnyvale, CA).

E.3. High-Throughput NADPH Consumption Assay (Chapters 2 and 6)

The recombination library (see D.1.) and first mutant library (see D.2.) were screened in 96-well plates for NADPH depletion in presence of propane. To 30 μL of *E. coli* supernatant, 170 μL of phosphate buffer (0.1 M, pH 8.0) saturated with propane was added. The reaction was initiated by addition of 50 μL NADPH (0.8 mM), and NADPH oxidation was monitored at 340 nm for five minutes using a Spectramax Plus microtiter plate reader (Molecular Devices, Sunnyvale, CA). The next library (see D.2.), in which no improved mutants found were found, was additionally screened for NADP^+ formation in presence of propane as the substrate, as described [12,13]. In brief, residual NADPH was destroyed with acid after an appropriate amount of time, followed by conversion of NADP^+ to a highly fluorescent alkali product at high pH, which was then measured fluorometrically. Mutants were selected from these libraries based upon increased NADPH consumption. The medium from LB plates for each selected mutant was then streaked onto LB-agar plates and allowed to grow overnight at 37°C. Single colonies of each mutant were picked into rows of eight, one row per mutant, into 1-mL 96-well plates containing LB and a row of parent. These plates were processed and screened as described above. The activity of each mutant was determined by the ratio of the average NADPH oxidation rate of each row of mutants to the average NADPH oxidation rate of the parent row.

E.4. High-Throughput Product-Formation Assays (Chapters 2-4 ,6)

For direct measurement of product formation, screens based on the demethylation of dimethyl ether (DME) and/or hexyl methyl ether (HME) were used for the later generation libraries (D.3. to D.9.).

For the DME screen, 120 μ L of phosphate buffer (0.1 M, pH 8.0) saturated with DME was added to 30 μ L of *E. coli* supernatant. For the HME screen, 120 μ L of phosphate buffer (0.1 M, pH 8.0), followed by 2 μ L of 400mM HME in ethanol were added to 30 μ L of *E. coli* supernatant. After 1 min of incubation at room temperature, NADPH (50 μ L, 0.8 mM) was added to the diluted lysate and substrate. 50 μ L of purpald solution (168 mM in 2 M NaOH) was added 15 min after initiating the reaction to form a purple product with the formaldehyde that was generated upon demethylation of the substrate. The purple color was read approximately 15 min later at 550 nm using a Spectramax Plus microtiter plate reader (Molecular Devices, Sunnyvale, CA). Mutants were selected from these libraries based upon an increase in their absorbance at 550 nM relative to the average of the absorbance of the eight parent wells. The medium from LB plates for each selected mutant was then streaked onto LB-agar plates and allowed to grow overnight at 37°C. Single colonies of each mutant were picked into rows of eight, one row per mutant, into 1-mL 96-well plates containing LB and a row of parent. These plates were processed and screened as described above. The activity of each mutant was determined by the ratio of the average absorbance at 550 nm of each row of mutants to the average absorbance at 550 nm of the parent row.

F. Determination of NADPH Consumption Rates (Chapters 2-4, 6)

The enzymes were purified and quantified as described above. Initial rates of NADPH consumption were measured at 25°C in 1 cm pathlength cuvettes using a BioSpec-1601 UV/VIS spectrophotometer (Shimadzu, Columbia, MD) or a Cary 100 UV/VIS spectrophotometer (Varian, Walnut Creek, CA). For the liquid alkanes, substrate stock solutions in ethanol (10 μ L) were added to the protein solution (100 to 200 nM final concentration) in potassium phosphate buffer (0.1 M, pH 8.0) and incubated for 2 min. The reaction was initiated by addition of 200 μ L NADPH (0.8 mM), and the decrease in absorption at 340 nm was monitored. Rates using gaseous alkane substrates (methane, ethane, and propane) were measured using 200 nM protein, substrate saturated potassium phosphate buffer (0.1 M, pH 8.0), and the same amount of NADPH. In addition, NADPH depletion rates in absence of substrate were measured for each enzyme. Rates were determined at least in triplicate.

G. Alkane Hydroxylation Reactions

G.1. Linear Alkanes (C5 to C10) (Chapters 2-4, 6)

To measure alkane hydroxylation activities, ethanol solutions of liquid alkanes (hexane to decane) were added to buffer solutions containing the enzymes such that the total ethanol in the reaction mixture was one percent (v/v). Several solvents, including ethanol, methanol, acetone, and dimethyl sulfoxide, were tested, and ethanol was shown to support the most

product turnovers. Reactions with liquid alkanes that contained no co-solvent produced no detectable products. In the absence of substrate, NADPH has been reported to inactivate BM-3 by over-reducing the flavin cofactors in its reductase domain [14]. To avoid this problem, substrate was added to the enzyme first and incubated for a few seconds before NADPH was added. Dioxygen was not added to the reactions, limiting the amount of possible product formed to the 225-250 μM of oxygen present in air-saturated buffer. The addition of excess dioxygen to the reactions by direct bubbling or rapid stirring did not increase and often decreased the total product turnover, possibly by denaturing the protein. Reaction mixtures for all BM-3 mutants containing 0.5-1.0 μM enzyme produced 225-250 μM products. We also noticed that total turnover numbers measured in systems containing less than ~ 25 nM protein were less than expected – i.e., 10 nM protein in a reaction gave much less than half the total turnovers of a 20 nM reaction. At very low concentrations of BM-3, the FMN cofactor has been reported to diffuse out of the protein and inactivate it [15]. Given this fact and the dilution effects on total turnover we witnessed, later mutants that efficiently hydroxylate linear alkanes might be capable of even more turnovers than reported.

To determine total turnover numbers and regioselectivity (i.e., the product regioisomers a given enzyme produces) product distributions, reactions with the liquid alkanes hexane, heptane, octane, nonane, and decane were performed in closed 20 mL scintillation vials and stirred at low speed using magnetic stirring bars. In a typical 3.0 mL reaction, purified protein was added to potassium phosphate buffer (0.1 M, pH 8.0) such that the total enzyme concentration equaled 25 to 100 nM. 30 μL of substrate solution (400 mM in

ethanol) was added to this solution to give 4 mM total substrate and 1% ethanol. For the experiments described in Chapter 4, 60 μL of substrate solution (200 mM in ethanol) was added to this solution to give 4 mM total substrate and 2% ethanol. After a few seconds, 300 μL of NADPH (5 mM in 0.1 M potassium phosphate buffer, pH 8.0) or 300 μL of a NADPH-regeneration system (300 μL , 1.66 mM NADP⁺, 66 U/mL isocitrate dehydrogenase, 416 mM isocitrate) was added to the reaction and the vial was capped. After 4 or 12 hours of stirring (the enzymes are inactive after 4 hours) at room temperature, a 1.5 mL aliquot of the reaction was removed from the vial and quenched with 300 μL of chloroform in a 2 mL microcentrifuge tube. An internal standard containing 15 μL of 10 mM 1-hexanol was added to the tube. The tube was vortexed and then centrifuged at 10,000 g for 2 minutes in a microcentrifuge. The chloroform layer was removed with a pipet and analyzed by gas chromatography. Control reactions without substrate revealed no detectable background levels of these specific products. All reactions were performed in triplicate.

To analyze the formation of overoxidation products as described in Chapter 6, the reactions were performed under similar conditions as described above. The reactions were carried out in potassium phosphate buffer (0.1 M, pH 8.0, 3 mL), containing purified protein (200 nM), substrate (octane, nonane, or decane, 50 μM) or the 1-alcohol (1-octanol, 1-nonanol 1-decanol (4 mM)). After 1 min, NADPH (500 μM) was added to the reaction before the vial was capped and pressurized with dioxygen (20 psi). At the end of the reaction, an aliquot (1500 μL) was removed from the vial. All reactions were carried out in triplicate.

For the determination of product formation rates (measured at 21°C), the reactions (5 mL) were performed similarly, except for the use of more enzyme (200 nM) and NADPH (500 μ M) instead of a regeneration system. Additionally, the vials were not pressurized with dioxygen. Aliquots of the reaction (1400 μ L) were removed at 20, 40 and 60 s. In all cases, the aliquots were quenched with CHCl_3 (300 μ L) and HCl (6 M, 100 μ L) in a 2 mL microcentrifuge tube. An internal standard containing 1-hexanol (14 μ L, 10 mM) for octane, nonane and decane reactions or 1-octanol (14 μ L, 10 mM) for hexane and heptane reactions was added to the tube. The tube was vortexed and then centrifuged at 10,000 g for 2 minutes in a microcentrifuge. The chloroform layer was removed with a pipet and analyzed by gas chromatography to determine product concentrations. Control reactions performed by repeating these steps without the addition of substrate revealed no detectable background levels of these specific products. All reactions were carried out in triplicate.

G.2. Chiral Analysis of Alkane Reactions (Chapters 2 and 6)

Chiral analysis of liquid alkane hydroxylation products was performed with a slight modification of an existing method [16], starting with extracting 9 mL alkane reactions (using the reaction conditions above) with 2 mL CH_2Cl_2 in a 15 mL centrifuge tube. After centrifugation at 2800 g for 15 minutes, the organic layer was removed with a pipet and dried over a small amount of anhydrous MgSO_4 . The MgSO_4 was removed by filtration, and 1 μ L of pyridine and 2.5 μ L (-)-menthyl chloroformate was added. After an hour, 1

mL of deionized water was added to the reaction. After vortexing and letting the layers separate, the organic phase was removed with a pipet and dried with anhydrous MgSO_4 . The drying agent was again removed with a pipet filter and the remaining solution analyzed by gas chromatography. Control reactions were performed by repeating these steps without the addition of substrate and revealed no background levels of these specific products. All reactions were performed in triplicate.

G.3. Propane Hydroxylation Reactions (Chapters 2-4, 6)

Reactions using propane did not contain co-solvent because of potential competition between the solvent and the small substrate. These reactions were performed in propane-saturated buffer under an atmosphere of propane and dioxygen (provided by a balloon filled with the two gases). The addition of this atmosphere ensured that both gaseous substrates were saturated in the reaction solution, since a balloon of just propane or oxygen would dilute the concentration of the other gas. Total turnovers determined with this system were not dependent on oxygen concentration in the balloon (data not shown), illustrating that only the original $\sim 250 \mu\text{M}$ of dioxygen in the buffer was available to the reaction. Additionally, we discovered that NADPH could neither be purchased nor easily purified in a form that contains less than 2-3% ethanol, which interferes with analysis of the reaction products. For this reason, an NADPH-regeneration system was used for propane reactions [17].

Propane hydroxylation reactions were performed in 20 mL scintillation vials. In a typical reaction, enzyme (either purified or in cell lysate) was added to 4.7 mL of propane-saturated 0.1 M potassium phosphate buffer pH 8.0 to a final concentration of 50-100 nM. To this mixture, 300 μ L of NADPH-regeneration system (1.66 mM NADP⁺, 167 U/mL isocitrate dehydrogenase, 416 mM isocitrate) was quickly added. The flask was topped with a balloon filled with equal amounts of propane and dioxygen. After stirring for two hours at room temperature, the propane hydroxylation products were derivatized to alkyl nitrites using a published method [18]. To the reaction mixture, 0.3 g of sodium nitrite and 2 mL 10 μ M chloroform in hexane was added and the mixture cooled on ice. While on ice, 0.2 mL concentrated sulfuric acid was added. The flask was stoppered with a rubber stopper and stirred on ice for 15 minutes. The reaction was rinsed into a separatory funnel with 20 mL of deionized water. The organic phase was washed twice with 20 mL of water and analyzed by gas chromatography. Control reactions were performed by repeating these steps without the substrate, to correct for background levels of propanol. All reactions were carried out in triplicate.

Propanol formation rates were measured in two different ways. For the data presented in Chapter 2, rates were measured in 4 mL reactions containing 1 μ M P450 and propane saturated 0.1M potassium phosphate buffer, pH 8 which were initiated with 500 μ M NADPH. Aliquots of this mixture (933 μ L) were removed at 20 s intervals and quenched with 67 μ L of 6 N HCl containing 3 mM 1-pentanol internal standard (200 μ M final concentration). The samples were analyzed by GC-FID (see below). For the data presented in all other chapters, propane hydroxylation reactions were carried out in 5 mL

reactions were carried out in 20 mL glass vials as described above similarly to those described for propane. For rate determination, the reaction was stopped after 1 min by adding 200 μ L of sulfuric acid. 50 μ L of 5 mM 1-butanol was added to the reaction mixture as an internal standard. Propanol and 1-butanol were subsequently derivatized to their corresponding alkyl nitrites as described above. Control reactions were performed without substrate did not contain detectable amounts of propanols. All reactions were performed in triplicate.

G.4. Ethane Reactions (Chapter 6)

Ethane reactions were carried out in 20 mL glass vials similarly to those described for propane. An NADPH regeneration system was used because commercially-available NADPH contains 2-3% ethanol. A 5.0 mL reaction mixture contained 100 to 500 nM purified protein in 0.1 M potassium phosphate buffer (pH 8.0) saturated with ethane and dioxygen. 300 μ L of the regeneration system (1.66 mM NADP⁺, 167 U/mL isocitrate dehydrogenase, 416 mM isocitrate) was added. The vial was immediately topped with a septum, pressurized with 20 psi of ethane and stirred at 25°C. For determination of total turnover, the reaction was allowed to proceed for 12 hours. For rate determination, the reaction was stopped at 0, 15 and 30 min. 50 μ L of 5 mM 1-butanol was added to the reaction mixture as an internal standard. Ethanol and 1-butanol were subsequently derivatized to their corresponding alkyl nitrites according to a published procedure [18]. Control reactions were performed without substrate and with inactivated protein (the

protein was inactivated by adding 200 μ L sulfuric acid before initiation of the reaction). Reaction buffer saturated with ethane and oxygen did not contain an ethanol concentration above this background of ~ 1.0 μ M. All reactions were carried out in triplicate.

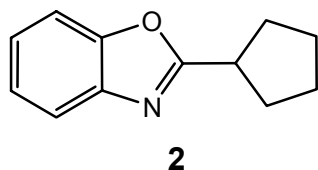
H. Fatty Acid Hydroxylation Reactions (Chapter 4)

For the determination of total turnover numbers and regioselectivity, reactions (1 mL) with lauric acid and palmitic acid were performed for 3 hours at 25°C in 2 mL microcentrifuge tubes. The reactions were carried out in Tris-HCl buffer (0.1 M, pH 8.2, 0.650 mL), containing purified protein (25 nM). Substrate (sodium salt of the fatty acids (20 mM), dissolved in sodium carbonate (50 mM) at 80°C, 0.1 mL) was added to the reaction to give 2 mM total substrate. To initiate the reaction, NADPH (0.25 mL, 2 mM) was added and mixed. The reaction was terminated and acidified by adding HCl (14 μ L, 6N). An internal standard of 10-hydroxycapric acid in dimethylsulfoxide (10 μ L, 10 mM) was added to each reaction. The products were extracted by adding ethyl acetate (0.5 mL). The tube was vortexed and then centrifuged at 10,000 g for 2 minutes in a microcentrifuge. The ethyl acetate layer was removed with a pipet and dried using a Savant Speed Vac at medium heat for 30 minutes. The residue was derivitized by adding 0.1 mL of a 50:50 pyrimidine:(bis-trimethylsilyltrifluoroacetamide with 1% TMSCl) and reacting at 80°C for 20 minutes. The derivatization solution was injected directly into the GC for product analysis. All reactions were carried out in triplicate.

Authentic standards for hydroxylated fatty acids were available only for 12-hydroxylauric acid and 16-hydroxypalmitic acid, which were used to quantify all hydroxyl-fatty acids of the same chain length. The ω -1, ω -2 and ω -3 hydroxy-fatty acids were identified relative to the product retention times from reactions with wild-type P450 BM-3 for which the relative amounts of product regioisomers is well established [19,20].

I. Hydroxylation Reactions of 2-Cyclopentanelbenzoxazole (Chapter 5)

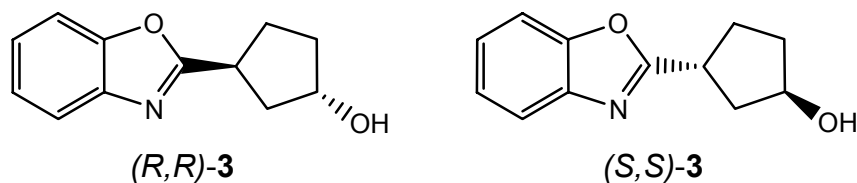
Hydroxylation reactions of 2-cyclopentanelbenzoxazole **2** for the determination of enantioselectivity and total turnover number of were carried out similarly to those described for octane.



Hydroxylation reactions were performed in 20 mL glass vials and stirred at low speed using magnetic stirring bars. The 5 mL reaction mixture containing purified protein (25 nM of mutant protein or 100 nM of wt), 1 mM substrate **2**, and 1% ethanol in potassium phosphate buffer (0.1 M, pH 8.0) was initiated by the addition of 500 μ L NADPH (10 mM). After 12 hours of stirring at room temperature, a 1.5 mL aliquot of the reaction was removed from the vial and quenched with 300 μ L of chloroform in a 2 mL microcentrifuge tube. An internal standard containing 15 μ L coumarin (20 mM in ethanol) was added to the

tube. The tube was vortexed and then centrifuged at 10,000 g for 2 minutes in a microcentrifuge. The chloroform layer was removed with a pipette and analyzed by gas chromatography to determine total turnover numbers and product distributions. Control reactions performed by repeating these steps without the addition of substrate revealed no detectable background levels of these specific products. All reactions were carried out in at least triplicate

To determine formation rates of **3** (measured at 21°C), 5 mL reactions containing 100 nM (139-3, B, 1-12G) or 200 nM (wt) protein were set up as described above.



Aliquots (1.4 mL) were removed from the reaction at 20 second intervals for one minute and quenched in 2 mL microcentrifuge tubes containing 300 μ L chloroform, 100 μ L 6 N HCl, and 14 μ L 20 mM coumarin in ethanol. The tubes were vortexed and centrifuged at \sim 10,000 g for 2 minutes to separate the layers. The chloroform layer was removed and analyzed by gas chromatography. Rates were determined in triplicate.

J. Gas Chromatography

Identification and quantification of analytes were performed using purchased standards and 5-point calibration curves with internal standards. All samples were injected at a volume of 1.0 μL and analyses were performed at least in triplicate.

J.1. Linear Alkane Oxidation Products (C5 to C10) (Chapters 2-4, 6)

Analyses of hydroxylation products of linear alkanes were performed on a Hewlett Packard 5890 Series II Plus gas chromatograph with a flame ionization detector (FID) and fitted with a HP-7673 autosampler system. Direct analysis of hexane, heptane, octane, nonane, and decane hydroxylation products was performed on an HP-5 capillary column (crosslinked 5% phenyl methyl siloxane, 30 m length, 0.32 mm ID, 0.25 μm film thickness) connected to the FID detector. A typical temperature program for separating the alcohol products is 250°C injector, 300°C detector, 50°C oven for 3 minutes, then 10°C/minute gradient to 200°C, 25°C/minute gradient to 250°C, then 250°C for 3 minutes.

Overoxidation products of alkanes were analyzed on a Hewlett Packard 6890 Series gas chromatography System coupled to a Hewlett Packard 5973 Mass Selective Detector. The alcohol, aldehyde, acid and diol products were separated using an INNOWax capillary column (Agilent Technologies, 30 m length, 0.25 mm ID, 0.25 μm film thickness) with the temperature program of 250°C injector, 60°C oven for 1 minutes, then 10°C/minute gradient to 250°C, then 250°C for 2 minutes.

J.2. Chiral Analysis of Alkane Reactions (Chapter 2 and 6)

The (-)-menthyl chloroformate-derivatized chiral products were separated as diastereomers on a CycloSil-B chiral capillary column (Agilent Technologies, 30 m length, 0.32 mm ID, 0.25 μ m film thickness) connected to the FID detector [21]. Each pair of diastereomers required a different temperature program for full resolution, but a typical program is as follows: chiral octanol analysis - 250°C injector, 300°C detector, 100°C oven for 1 minute, then 10°C/minute gradient to 190°C, hold at 190°C for 10 minutes, 10°C/minute gradient to 250°C, then 250°C for 3 minutes.

J.3. Gaseous Alkane (C1 to C4) Oxidation Products (Chapters 2,3 and 6)

Analysis of the alkyl nitrite derivatives of methanol, ethanol and propanol was performed on a Hewlett-Packard 5890 Series II Plus gas chromatograph (Hewlett-Packard, San Fernando, CA, U.S.A) with an electron capture detector (ECD) using an HP-1 column (Agilent Technologies; 30m length, 0.53 mm ID, 2.65 μ M film thickness) or an HP-1 capillary column (Agilent Technologies; crosslinked 1% phenyl methyl siloxane, 30 m length, 0.32 mm ID, 0.25 μ m film thickness) [18]. The temperature program was: 60°C injector, 150°C detector, 35° oven for 3 min, 10°C/min gradient to 60°C, 25°C/min gradient to 200°C, and then 200°C for 5 min.

For propane oxidation rates described in Chapter 2, A GC/FID fitted with an HP FFAP (cross-linked FFAP, 30 m length, 0.25 mm ID, 0.25 μ m film thickness) using the

temperature program: 250°C injector, 300°C detector, 50°C oven for 3 minutes, then 10°C/minute gradient to 200°C, 25°C/minute gradient to 220°C, then 220°C for 3 minutes.

J.4. Fatty Acid Hydroxylation Products (Chapter 4)

Trimethylsilyl-derivatized fatty acids and their hydroxylated products were analyzed by injecting 1 μ l onto an HP-5 capillary column (crosslinked 5% phenyl methyl siloxane, 30 m length, 0.32 mm ID, 0.25 μ m film thickness) connected to the FID detector. A typical temperature program for separating the derivatized products is 250°C injector, 300°C detector, 150°C oven for 1 minutes, then 10°C/minute gradient to 250°C, then 250°C for 5 minutes. Authentic standards for 12-hydroxylauric acid and 16-hydroxypalmitic acid were used to identify the ω -hydroxy-fatty acids, while the ω -1, ω -2 and ω -3 hydroxy-fatty acids were identified based on reactions with wild-type P450 BM-3 for which the hydroxylation pattern is known [19,20]. Products were verified according to the retention time and fragmentation pattern of the known ω , ω -1, ω -2, and ω -3 controls by GC-MS using a Varian Star 3400cx gas chromatograph with an HP-5 capillary column (crosslinked 5% phenyl methyl siloxane, 30 m length, 0.25 mm ID, 0.25 μ m film thickness) connected to a Varian Saturn 2000 GC/MS detector using the following temperature program: 250°C injector, 150°C oven for 2 minutes, then 10°C/minute gradient to 250°C, then 250°C for 5 minutes.

J.5. Hydroxylation Reactions of 2-Cyclopentylbenzoxazole (Chapter 5)

Analysis of the hydroxylation products of 2-cyclopentanebenzoxazole **2** was performed using authentic standards and a 5-point calibration curve with coumarin as an internal standard. The injection volume was 1 μL . Analysis was performed on a Hewlett-Packard 5890 Series II Plus gas chromatograph connected to a FID detector using a CycloSil-B column (J&W Scientific, 30 m length, 0.320 mm ID, 0.25 μm film thickness) for chiral analysis or a HP-5MS column (Agilent Technologies, 30 m length, 0.25 mm ID, 0.25 μm film thickness) for the determination of rates and total turnover numbers. The temperature program for the CycloSil-B column was: 100°C injector, 250°C detector, 100° oven for 3 min, 10°C/min gradient to 170°C, 170°C for 10 min, 25°C/min gradient to 200°C, and then 200°C for 8 min. The temperature program for the HP-5MS column was: 100°C injector, 250°C detector, 100° oven for 3 min, 10°C/min gradient to 210°C, 25°C/min gradient to 250°C, and then 250°C for 3 min.

K. Overoxidation of Ethanol by BM-3 Variant 53-5H (Chapter 6)

Ethanol (20 μM) was used as the substrate under the reaction conditions described above (section G.4). No decrease in ethanol concentration was observed within experimental error ($\pm 3 \mu\text{M}$) over the course of the reaction. NMR (Varian Mercury 300 MHz) spectroscopy was used to monitor reactions of 53-5H with singly ^{13}C -labeled ethanol (HO- $^{13}\text{CH}_2\text{CH}_3$, 57 ppm). Concentrations of ^{13}C -labeled ethanol as low as 50 μM in the presence of 10 μM P450 (in 0.1M potassium phosphate buffer, pH 8, with 10% deuterium

oxide added) could be detected using the ^{13}C channel of the NMR. The longer relaxation rates of the carbonyl carbon atoms in acetaldehyde (206 ppm) and acetic acid (176 ppm) decrease their carbon NMR signal heights by 25-40% in our experiments, making their detection limit approximately 100 μM . Reactions using 10 μM 53-5H, 1 mM ^{13}C -ethanol, 100 μM NADP^+ , 50 mM isocitrate, and 10 U/mL isocitrate dehydrogenase were stirred 12 hours at room temperature. Deuterium oxide (10% final concentration) was then added to each reaction, and NMR spectra (averaging $\sim 20,000$ scans each) were recorded. Control reactions using 50 nM of 53-5H from the same batch, 4 mM of octane, 100 μM NADP^+ , 50 mM isocitrate, and 10 U/mL isocitrate dehydrogenase were also performed and the products characterized to verify that the P450 was fully active. No overoxidation products were detected in these experiments, indicating that, in the presence of 1 mM ethanol, 53-5H catalyzes less than 10 total turnovers of ethanol.

L. Absorption Spectra of BM-3 Variants 1-12G, 53-5H and 35-E11 (Chapter 6)

The absorption spectra were taken using a 3 μM solution of purified P450 in potassium phosphate buffer (0.1 M, pH 8.0) in a quartz cuvette. Ethane was added either by bubbling ethane for 2 to 10 min at approximately one bubble sec^{-1} , or by pressurizing the cuvette with ethane (20 psi). The shift in equilibrium from low- (A_{max} at 418 nm) to high-spin (A_{max} at 390 nm) configuration of the ferric heme iron was measured.

M. Whole-Cell Reactions (Chapter 2)

The procedure for whole-cell reactions of *E. coli* (DH5 α) overexpressing mutants 9-10A-A328V and 1-12G was only slightly modified from Witholt's published method [22]. An overnight culture of cells (in 3 mL LB with 100 μ g/mL ampicillin) was used to inoculate 75 mL of M9 minimal medium containing 0.5% w/v glucose, 0.2 mM calcium chloride, 5 mM MgSO₄, and 100 μ g/mL ampicillin. The culture was then shaken for 24 hours at 37°C and 250 rpm. The cells were collected by centrifugation at 2200 g for 10 minutes and resuspended in 20 mL of 0.2 M potassium phosphate buffer pH 7.4 containing 0.5% glucose, 100 μ g/mL ampicillin, 1 mM IPTG, and 0.5 mM δ -aminolevulinic acid, 5 mM alkane (from a 500 mM stock of alkane in dimethyl sulfoxide). This mixture was shaken for 8 hours at 37°C and 250 rpm. Product distributions were measured by gas chromatography after extracting this culture with 1 mL of chloroform. Chiral analysis of the reaction products was performed after extracting the culture with 2 mL of CH₂Cl₂ and derivatizing the organic layer with (-)-menthyl chloroformate.

N. References

1. Schwaneberg, U., Sprauer, A., Schmidt-Dannert, C. & Schmid, R. D. (1999). **P450 monooxygenase in biotechnology I: single-step, large-scale purification method for cytochrome P450 BM-3 by anion-exchange chromatography.** *J. Chromatogr. A.* **848**, 149-159.
2. Omura, T. & Sato, R. (1964). **The carbon monoxide-binding pigment of liver microsomes. I. Evidence for its hemoprotein nature.** *J. Biol. Chem.* **239**, 2370-2378.
3. Li, H. Y., Darwish, K. & Poulos, T. L. (1991). **Characterization of recombinant *Bacillus megaterium* cytochrome P450 BM-3 and its 2 functional domains.** *J. Biol. Chem.* **266**, 11909-11914.
4. Farinas, E. T., Schwaneberg, U., Glieder, A. & Arnold, F. H. (2001). **Directed evolution of a cytochrome P450 monooxygenase for alkane oxidation.** *Adv. Synth. Catal.* **343**, 601-606.
5. Glieder, A., Farinas, E. T. & Arnold, F. H. (2002). **Laboratory evolution of a soluble, self-sufficient, highly active alkane hydroxylase.** *Nature Biotech.* **20**, 1135-1139.
6. Zhao, H., Giver, L., Shao, Z., Affholter, A. & Arnold, F. H. (1998). **Molecular evolution by staggered extension process (StEP) in vitro recombination.** *Nature Biotechnology* **16**, 258-261.
7. Higuchi, R., Krummel, B. & Saiki, R. K. (1988). **A general method of in vitro preparation and specific mutagenesis of DNA fragments: study of protein and DNA interactions.** *Nucl. Acids Res.* **16**, 7351-7367.
8. Joern, J. M. (2003). **DNA shuffling.** In *Directed Evolution Library Creation: Methods and Protocols* (Arnold, F. H. & Georgiou, G., eds.), Vol. 231, pp. 85-89. Humana Press, Inc., Totowa, NJ.
9. Peters, M. W., Meinhold, P. & Arnold, F. H. (2003). **Regio- and enantioselective alkane hydroxylation with engineered cytochromes P450 BM-3.** *J. Am. Chem. Soc.* **125**, 13442 -13450.
10. Yu, C. A. & Gunsalus, I. C. (1974). **Cytochrome P-450cam. 2. Interconversion with P-420.** *J. Biol. Chem.* **249**, 102-106.
11. Otey, C. (2003). **High-throughput carbon monoxide binding assay for cytochrome P450.** In *Screening and Selection for Directed Enzyme Evolution* (Arnold, F. H. & Georgiou, G., eds.), Vol. 230. Humana Press, Inc., Totowa, NJ.

12. Tsotsou, G. E., Cass, A. E. G. & Gilardi, G. (2002). **High throughput assay for cytochrome P450BM3 for screening libraries of substrates and combinatorial mutants.** *Biosensors & Bioelectronics* **17**, 119-131.
13. Glieder, A. & Meinhold, P. (2003). **High-throughput screens based on NAD(P)H depletion.** In *Directed Enzyme Evolution: Screening and Selection Methods* (Arnold, F. H. & Georgiou, G., eds.), Vol. 230. Humana Press, Inc., Totowa, NJ.
14. Daff, S. N., Chapman, S. K., Turner, K. L., Holt, R. A., Govindaraj, S., Poulos, T. L. & Munro, A. W. (1997). **Redox control of the catalytic cycle of flavocytochrome P-450 BM3.** *Biochemistry* **36**, 13816-13823.
15. Strobel, H. W., Hodgson, A. V. & Shen, S. (1995). **NADPH cytochrome P450 reductase and its structural and functional domains.** In *Cytochrome P450: Structure, Mechanism, and Biochemistry* Second edit. (Ortiz de Montellano, P. R., ed.), pp. 225-244. Plenum Press, New York.
16. Westley, J. W. & Halpern, B. (1968). **Use of (-)-menthyl chloroformate in the optical analysis of asymmetric amino and hydroxyl compounds by gas chromatography.** *J. Org. Chem.* **33**, 3978-3980.
17. Schwaneberg, U., Otey, C., Cirino, P. C., Farinas, E. & Arnold, F. H. (2001). **Cost-effective whole-cell assay for laboratory evolution of hydroxylases in *Escherichia coli*.** *J. Biomol. Screen.* **6**, 111-117.
18. Nguyen, H. T. H., Takenaka, N., Bandow, H. & Maeda, Y. (2001). **Trace level determination of low-molecular-weight alcohols in aqueous samples based on alkyl nitrite formation and gas chromatography.** *Anal. Sci.* **17**, 639-643.
19. Boddupalli, S. S., Pramanik, B. C., Slaughter, C. A., Estabrook, R. W. & Peterson, J. A. (1992). **Fatty-acid monooxygenation by P450BM-3 - product identification and proposed mechanisms for the sequential hydroxylation reactions.** *Arch. Biochem. Biophys.* **292**, 20-28.
20. Cirino, P. C. & Arnold, F. H. (2002). **Regioselectivity and activity of cytochrome P450BM-3 and mutant F87A in reactions driven by hydrogen peroxide.** *Adv. Synth. Catal.* **344**, 932-937.
21. Westley, J. W. & Halpern, B. (1968). **Use of (-)-menthyl chloroformate in optical analysis of asymmetric amino and hydroxyl compounds by gas chromatography.** *J. Org. Chem.* **33**, 3978-&.
22. Schneider, S., Wubbolts, M. G., Sanglard, D. & Witholt, B. (1998). **Production of chiral hydroxy long chain fatty acids by whole cell biocatalysis of pentadecanoic acid with and *E. coli* recombinant containing cytochrome P450 BM-3 monooxygenase.** *Tetrahedron: Asymmetry* **9**, 2833-2844.

A p p e n d i x A

Stability of Cytochrome P450 BM-3 Alkane Hydroxylase Mutants

A. Introduction

Enzymes used for biocatalysis applications need to be sufficiently stable in order to resist thermal denaturation under process conditions. We engineered P450 BM-3 for improved alkane hydroxylation activity by introducing mutations and screening for improved activity, but mutations generally decrease the stability of a protein. To avoid identifying highly unstable mutants, lysis of *E. coli* cells containing BM-3 variants was performed for one hour at 37°C. The stability of improved mutants, however, was not determined. Here we briefly examine the stabilities of the wild-type enzyme and selected variants.

B. Results

To characterize the thermostability of wild-type P450 BM-3 and the variants identified by screening mutant libraries, we performed three separate assays. The fraction of folded heme domain remaining after heat-treatment was determined from the fraction of the ferrous heme-CO complex that retained the absorbance peak at 450 nm, which characterizes a properly-folded P450. We also determined the fraction of remaining NADPH-driven activity after heat treatment by measuring the fraction of the protein that retained measurable NADPH oxidation rates in presence of hexyl methyl ether. This measurement provides information instability caused by altered heme-reductase interactions.

Temperature-dependent inactivation of P450 BM-3 has been shown to be caused by the reductase domain, and more specifically on the dissociation of the FAD cofactor [1]. Except for variant 35-E11, which contains two mutations in the reductase domain, the

reductase domain was not altered during the course of work described in this thesis. It is likely, however, that conformational changes in the heme domain due to its accumulated mutations have a destabilizing effect on the reductase domain. To assess whether the reductase domain was destabilized, the fraction of active reductase domain after heat treatment was determined from the fraction of reductase domain that retained cytochrome c reductase activity. The reductase portion of P450 BM-3 is able to perform this reaction independently from the heme domain.

The data were fit to a two-state model, and the resulting calculated temperatures corresponding to half denaturation for the 15-min heat incubations are listed in Table A.1. The values are in good agreement to the midpoints of the melting curves. According to this measure of stability, the variants obtained by random mutagenesis have lost significant stability. The heme domain of mutant 9-10A, the last variant obtained from random mutagenesis experiments described in this thesis, is approximately 10 °C less stable than wild-type. Mutations within the active site of 53-5H did not further decrease the stability. Mutations in the reductase domain of mutant 35-E11 also have no further destabilizing effects. Although the variants (except for 35-E11) do not contain mutations in the reductase domain, this domain seems to have lost stability. This is evident from the decreased NADPH oxidation and cytochrome c reduction activity. Conformational changes in the reductase domain induced by the mutated heme domain could account for this effect.

It has been proposed that the stability of a protein is important for its robustness to amino acid substitutions [2]. The important implication for directed evolution experiments is

that applying random mutagenesis to an unstable protein will yield libraries with mostly unfolded proteins. The threshold of stability at which this becomes important for P450 BM-3 has not been determined. It may, however, become necessary to increase the stability before applying further rounds of mutagenesis to identify mutants with improved activity. Directed evolution has proven to be effective method for increasing enzyme thermostability [3].

Table A.1. Thermostability parameters for wild-type P450 BM-3 and variants selected for improved alkane hydroxylation activity.

BM-3 variant	T ₅₀ for 15 min incubations [°C] ^[a]		
	T ₅₀ heme ^[b]	T ₅₀ NADPH oxidation ^[c]	T ₅₀ cyt c reduction ^[d]
wt	54.8 ± 0.6	46.9 ± 0.3	43.7 ± 0.5
139-3	54.7 ± 0.8	46.5 ± 0.1	n.a. ^[e]
J	49.6 ± 0.6	46.4 ± 0.1	n.a. ^[e]
9-10A	45.0 ± 0.7	44.4 ± 0.2	n.a. ^[e]
53-5H	44 ± 0.2	43.9 ± 0.2	34.9 ± 0.7
35-E11	44.8 ± 0.2	43.6 ± 0.2	34.9 ± 0.3

^[a] Calculated by fitting the data to a two-state denaturation equation. See Experimental section below for details.

^[b] T₅₀ heme is calculated from the percentage of 450 nm CO-binding peak of cytochrome P450 BM-3 variants remaining after 15-min incubations at varying temperatures

^[c] T₅₀ NADPH oxidation is calculated from the percentage of NADPH oxidation activity of cytochrome P450 BM-3 variants in presence of hexyl methyl ether remaining after 15-min incubations at varying temperatures

^[d] T₅₀ cyt c reduction is calculated from the percentage of cytochrome c reduction activity of cytochrome P450 BM-3 variants in presence of hexyl methyl ether remaining after 15-min incubations at varying temperatures.

^[e] T₅₀ cyt c reduction values for 139-3, J, and 9-10A could not be calculated because their activities did not drop to zero at elevated temperature and a two-state denaturation model could not be applied.

C. Experimental

Purified protein (40 μ L, 1 μ M for NADPH oxidation assay, 25 nM for cytochrome c assay, 25 μ M for CO-binding assay) in potassium phosphate buffer (0.1 M, pH 8.0) was incubated for 15 min at 20 different temperatures ranging from 30 to 65°C in a 96-well PCR plate in a PCR machine (PTC 200 DNE Engine, MJ Research, Watertown, MA). Samples were cooled to 4 °C for 5 min and then incubated at 25 °C prior to performing assays. Each assay was performed in triplicate at each temperature.

For the CO-binding assay, 30 μ L of protein were added to 170 μ L of 100 mM sodium hydrosulfite in potassium phosphate buffer (0.3 mM, pH 8.0). A baseline spectrum was taken before placing the plate into a chamber. The chamber was evacuated and subsequently filled with carbon monoxide. The plate was incubated for approximately 10 minutes before removing it to record the difference spectrum from 400-500 nm using a Spectramax Plus microtiter plate reader (Molecular Devices, Sunnyvale, CA).

For the NADPH depletion assay, 30 μ L of protein were added to 170 μ L potassium phosphate buffer (0.1 M, pH 8.0). Substrate (2 μ L, 400 mM in ethanol) was added and the mixture was incubated for 2 min at room temperature before NADPH (50 μ L, 0.8 mM) was added to initiate the reaction. NADPH oxidation was monitored at 340 nm in a Spectramax Plus microtiter plate reader (Molecular Devices, Sunnyvale, CA).

For the cytochrome c reduction assay, 30 μ L of protein was added to 170 μ L potassium phosphate buffer (0.1 M, pH 8.0) containing 150 μ M cytochrome c. The reaction was initiated by addition of NADPH (50 μ L, 0.5 mM) and cytochrome c reduction was

monitored at 550 nM using a Spectramax Plus microtiter plate reader (Molecular Devices, Sunnyvale, CA).

D. References

1. Munro, A. W., Lindsay, J. G., Coggins, J. R., Kelly, S. M. & Price, N. C. (1996). **Analysis of the structural stability of the multidomain enzyme flavocytochrome P-450 BM3.** *Biochim. Biophys. Acta* **1296**, 127-137.
2. Bloom, J. D., Silberg, J. J., Wilke, C. O., Drummond, D. A., Adami, C. & Arnold, F. H. (2005). **Thermodynamic prediction of protein neutrality.** *Proc. Natl. Acad. Sci.* **102**, 606-611.
3. Wintrode, P. L. & Arnold, F. H. (2001). **Temperature adaption of enzymes: lessons from laboratory evolution.** In *Evolutionary Protein Design* (Arnold, F. H., ed.), pp. 161-225. Academic Press, New York.

A p p e n d i x B

Sequences of Wild-type and Mutant Cytochromes P450 BM-3 and pCWori Vector

General Information

Cytochrome P450 BM-3 (GenBank number J04832) is composed of 1048 amino acids (3144 bp). The heme domain of cytochrome P450 BM-3 contains 471 amino acids (1413 bp) while the reductase domain is comprised of 577 amino acids (1731 bp). The P450 BM-3 gene and the genes of P450 BM-3 mutants derived from this gene include a silent mutation to introduce a *SacI* site 130 bp upstream of the end of the heme domain. The genes were cloned behind the double *tac* promoter of the expression vector pCWori (pBM3_WT18-6). This plasmid was used for all cloning procedures as well as for protein expression.

In random mutagenesis experiments targeting the heme domain, error prone PCR was applied to the region stretching from the *Bam*HI site to the *SacI* site, thereby omitting the last 32 amino acids (96 bp) of the heme domain. In random mutagenesis experiments targeting the reductase domain, error prone PCR was applied to the region stretching from the *SacI* to the *Eco*RI site.

Figure B.1 lists the nucleotide sequence of full-length, wild-type cytochrome P450 BM-3.

Figure B.2 lists the amino acid sequence of full-length, wild-type cytochrome P450 BM-3.

Figure B.3 lists the nucleotide sequence of the pCWori vector containing wild-type P450 BM-3 (pBM3_WT18-6). The two *Ptac* promoters in this vector begin at nucleotide positions 167 and 262 (refer to plasmid map in Figure B.4).

Figure B.4 shows the plasmid map of the pCWori vector containing wild-type P450 BM-3 (pBM3_WT18-6).

Table B.1 lists the mutations of P450 BM-3 mutants generated by random mutagenesis and recombination prior to my involvement in the project.

Table B.2 lists P450 BM-3 mutants described in Chapter 2.

Table B.3 lists single active site mutants of P450 BM-3 described in Chapter 3.

Table B.4 lists amino acid substitutions of multiple active site mutants of P450 BM-3 described in Chapter 3.

Table B.5 lists amino acid substitutions of reductase mutants described in Chapter 5.

Figure B.1. Nucleotide sequence of full-length, wild-type cytochrome P450 BM-3.

1	ATGACAATTA	AAGAAATGCC	TCAGCCAAAA	ACGTTTGGAG	AGCTTAAAAA
51	TTTACCGTTA	TTAAACACAG	ATAAACCGGT	TCAAGCTTTG	ATGAAAATTG
101	CGGATGAATT	AGGAGAAATC	TTTAAATTCG	AGGCGCCTGG	TCGTGTAACG
151	CGCTACTTAT	CAAGTCAGCG	TCTAATTAAA	GAAGCATGCG	ATGAATCACG
201	CTTTGATAAA	AACTTAAGTC	AAGCGCTTAA	ATTTGTACGT	GATTTTGCAG
251	GAGACGGGTT	ATTTACAAGC	TGGACGCATG	AAAAAAATTG	GAAAAAAGCG
301	CATAATATCT	TACTTCCAAG	CTTCAGTCAG	CAGGCAATGA	AAGGCTATCA
351	TGCGATGATG	GTCGATATCG	CCGTGCAGCT	TGTTCAAAAG	TGGGAGCGTC
401	TAAATGCAGA	TGAGCATATT	GAAGTACCGG	AAGACATGAC	ACGTTTAAACG
451	CTTGATACAA	TTGGTCTTTG	CGGCTTTAAC	TATCGCTTTA	ACAGCTTTTA
501	CCGAGATCAG	CCTCATCCAT	TTATTACAAG	TATGGTCCGT	GCACTGGATG
551	AAGCAATGAA	CAAGCTGCAG	CGAGCAAATC	CAGACGACCC	AGCTTATGAT
601	GAAAACAAGC	GCCAGTTTCA	AGAAGATATC	AAGGTGATGA	ACGACCTAGT
651	AGATAAAATT	ATTGCAGATC	GCAAAGCAAG	CGGTGAACAA	AGCGATGATT
701	TATTAACGCA	TATGCTAAAC	GGAAAAGATC	CAGAAACGGG	TGAGCCGCTT
751	GATGACGAGA	ACATTCGCTA	TCAAATTATT	ACATTCTTAA	TTGCGGGACA
801	CGAAACAACA	AGTGGTCTTT	TATCATTTGC	GCTGTATTTT	TTAGTGAAAA
851	ATCCACATGT	ATTACAAAAA	GCAGCAGAAG	AAGCAGCACG	AGTTCTAGTA
901	GATCCTGTTC	CAAGCTACAA	ACAAGTCAAA	CAGCTTAAAT	ATGTCGGCAT
951	GGTCTTAAAC	GAAGCGCTGC	GCTTATGGCC	AACTGCTCCT	GCGTTTTCCC
1001	TATATGCAAA	AGAAGATACG	GTGCTTGGAG	GAGAATATCC	TTTAGAAAAA
1051	GGCGACGAAC	TAATGGTTCT	GATTCTCAG	CTTCACCGTG	ATAAAACAAT
1101	TTGGGGAGAC	GATGTGGAAG	AGTTCCGTCC	AGAGCGTTTT	GAAAATCCAA
1151	GTGCGATTCC	GCAGCATGCG	TTTAAACCGT	TTGGAAACGG	TCAGCGTGCG
1201	TGTATCGGTC	AGCAGTTCGC	TCTTCATGAA	GCAACGCTGG	TACTTGGTAT
1251	GATGCTAAAA	CACTTTGACT	TTGAAGATCA	TACAAACTAC	GAGCTCGATA
1301	TTAAAGAAAC	TTTAACGTTA	AAACCTGAAG	GCTTTGTGGT	AAAAGCAAAA
1351	TCGAAAAAAA	TTCCGCTTGG	CGGTATTCCCT	TCACCTAGCA	CTGAACAGTC
1401	TGCTAAAAAA	GTACGCAAAA	AGGCAGAAAA	CGCTCATAAT	ACGCCGCTGC
1451	TTGTGCTATA	CGGTTCAAAT	ATGGGAACAG	CTGAAGGAAC	GGCGCGTGAT
1501	TTAGCAGATA	TTGCAATGAG	CAAAGGATTT	GCACCGCAGG	TCGCAACGCT
1551	TGATTACACAC	GCCGGAAATC	TTCCGCGCGA	AGGAGCTGTA	TTAATTGTAA
1601	CGGCGTCTTA	TAACGGTCAT	CCGCCTGATA	ACGCAAAGCA	ATTTGTTCGAC
1651	TGGTTAGACC	AAGCGTCTGC	TGATGAAGTA	AAAGGCGTTC	GCTACTCCGT
1701	ATTTGGATGC	GGCGATAAAA	ACTGGGCTAC	TACGTATCAA	AAAGTGCCTG
1751	CTTTTATCGA	TGAAACGCTT	GCCGCTAAAG	GGGCAGAAAA	CATCGCTGAC
1801	CGCGGTGAAG	CAGATGCAAG	CGACGACTTT	GAAGGCACAT	ATGAAGAATG
1851	GCGTGAACAT	ATGTGGAGTG	ACGTAGCAGC	CTACTTTAAC	CTCGACATTG
1901	AAAACAGTGA	AGATAATAAA	TCTACTCTTT	CACTTCAATT	TGTCGACAGC
1951	GCCGCGGATA	TGCCGCTTGC	GAAAATGCAC	GGTGCCTTTT	CAACGAACGT
2001	CGTAGCAAGC	AAAGAACTTC	AACAGCCAGG	CAGTGCACGA	AGCACGCGAC
2051	ATCTTGAAAT	TGAACTTCCA	AAAGAAGCTT	CTTATCAAGA	AGGAGATCAT
2101	TTAGGTGTTA	TTCTTCGCAA	CTATGAAGGA	ATAGTAAACC	GTGTAACAGC
2151	AAGGTTTCGGC	CTAGATGCAT	CACAGCAAAT	CCGTCTGGAA	GCAGAAGAAG
2201	AAAAATTAGC	TCATTTGCCA	CTCGCTAAAA	CAGTATCCGT	AGAAGAGCTT
2251	CTGCAATACG	TGGAGCTTCA	AGATCCTGTT	ACGCGCACGC	AGCTTCGCGC

```

2301 AATGGCTGCT AAAACGGTCT GCCCGCCGCA TAAAGTAGAG CTTGAAGCCT
2351 TGCTTGAAAA GCAAGCCTAC AAAGAACAAG TGCTGGCAAA ACGTTTAACA
2401 ATGCTTGAAC TGCTTGAAAA ATACCCGGCG TGTGAAATGA AATTCAGCGA
2451 ATTTATCGCC CTTCTGCCAA GCATACGCCC GCGCTATTAC TCGATTTCTT
2501 CATCACCTCG TGTCGATGAA AAACAAGCAA GCATCACGGT CAGCGTTGTC
2551 TCAGGAGAAG CGTGGAGCGG ATATGGAGAA TATAAAGGAA TTGCGTCGAA
2601 CTATCTTGCC GAGCTGCAAG AAGGAGATAC GATTACGTGC TTTATTTCCA
2651 CACCGCAGTC AGAATTTACG CTGCCAAAAG ACCCTGAAAC GCCGCTTATC
2701 ATGGTCGGAC CGGGAACAGG CGTCGCGCCG TTTAGAGGCT TTGTGCAGGC
2751 GCGCAAACAG CTAAAAGAAC AAGGACAGTC ACTTGAGAGAA GCACATTTAT
2801 ACTTCGGCTG CCGTTCACCT CATGAAGACT ATCTGTATCA AGAAGAGCTT
2851 GAAAACGCCC AAAGCGAAGG CATCATTACG CTTCATACCG CTTTTTCTCG
2901 CATGCCAAAT CAGCCGAAAA CATACGTTCA GCACGTAATG GAACAAGACG
2951 GCAAGAAATT GATTGAACTT CTTGATCAAG GAGCGCACTT CTATATTTGC
3001 GGAGACGGAA GCCAAATGGC ACCTGCCGTT GAAGCAACGC TTATGAAAAG
3051 CTATGCTGAC GTTCACCAAG TGAGTGAAGC AGACGCTCGC TTATGGCTGC
3101 AGCAGCTAGA AGAAAAAGGC CGATACGCAA AAGACGTGTG GGCTGGG

```


Figure B.2. Amino acid sequence of full-length, wild-type cytochrome P450 BM-3.

1	MTIKEMPQPK	TFGELKNLPL	LNTDKPVQAL	MKIADELGEI	FKFEAPGRVT
51	RYLSSQRLIK	EACDESRFDK	NLSQALKFVR	DFAGDGLFTS	WTHEKNWKKA
101	HNILLPSFSQ	QAMKGYHAMM	VDIAVQLVQK	WERLNADDEHI	EVPEDMTRLT
151	LDTIGLCGFN	YRFNSFYRDQ	PHPFITSMVR	ALDEAMNKLQ	RANPDDPAYD
201	ENKRQFQEDI	KVMNDLVDKI	IADRKASGEQ	SDDLTHMLN	GKDPETGEPL
251	DDENIRYQII	TFLIAGHETT	SGLLSFALYF	LVKNPHVLQK	AAEEAARVLV
301	DPVPSYKQVK	QLKYVGMVLN	EALRLWPTAP	AFSLYAKEDT	VLGGEYPLEK
351	GDELMVLIPQ	LHRDKTIWGD	DVEEFRPERF	ENPSAIPQHA	FKPFGNGQRA
401	CIGQQFALHE	ATLVLGMMLK	HFDFEDHTNY	ELDIKETLTL	KPEGFVVKAK
451	SKKIPLGGIP	SPSTEQSAKK	VRKKAENAHN	TPLLVLVYGSN	MGTAEGTARD
501	LADIAMSKGF	APQVATLDSH	AGNLPREGAV	LIVTASYNGH	PPDNAKQFVD
551	WLDQASADEV	KGVRYSVFGC	GDKNWATTYQ	KVPAFIDETL	AAKGAENIAD
601	RGEADASDDF	EGTYEEWREH	MWSDVAAYFN	LDIENSEDNK	STLSLQFVDS
651	AADMPLAKMH	GAFSTNVVAS	KELQQPGSAR	STRHLEIELP	KEASYQEGDH
701	LGVIPRNYEG	IVNRVTARFG	LDASQQIRLE	AEEEKLAHLP	LAKTVSVEEL
751	LQYVELQDPV	TRTQLRAMAA	KTVCPPHKVE	LEALLEKQAY	KEQVLAKRLT
801	MLELLEKYP	CEMKFSEFIA	LLPSIRPRYY	SISSSPRVDE	KQASITVSVV
851	SGEAWSGYGE	YKGIASNYLA	ELQEGDTITC	FISTPQSEFT	LPKDPETPLI
901	MVGPGTGAV	FRGFVQARKQ	LKEQGQSLGE	AHLYFGCRSP	HEDYLYQEEL
951	ENAQSEGIIT	LHTAFSRMPN	QPKTYVQHVM	EQDGKKLIEL	LDQGAHFYIC
1001	GDGSQMAPAV	EATLMKSYAD	VHQVSEADAR	LWLQQLEEK	RYAKDVWAG

Figure B.3. Nucleotide sequence of the pCWori vector containing wild-type cytochrome P450 BM-3 (pBM3_WT18-6).

```

1   ATGACAATTA AAGAAATGCC TCAGCCAAAA ACGTTTGGAG AGCTTAAAAA
51  TTTACCGTTA TTAAACACAG ATAAACCGGT TCAAGCTTTG ATGAAAATTG
101 CGGATGAATT AGGAGAAATC TTTAAATTCG AGGCGCCTGG TCGTGTAACG
151 CGCTACTTAT CAAGTCAGCG TCTAATTAAA GAAGCATGCG ATGAATCACG
201 CTTTGATAAA AACTTAAGTC AAGCGCTTAA ATTTGTACGT GATTTTGCAG
251 GAGACGGGTT ATTTACAAGC TGGACGCATG AAAAAAATTG GAAAAAGCG
301 CATAATATCT TACTTCCAAG CTTCAGTCAG CAGGCAATGA AAGGCTATCA
351 TGCGATGATG GTCGATATCG CCGTGCAGCT TGTTCAAAAG TGGGAGCGTC
401 TAAATGCAGA TGAGCATATT GAAGTACCGG AAGACATGAC ACGTTTAACG
451 CTTGATACAA TTGGTCTTTG CGGCTTTAAC TATCGCTTTA ACAGCTTTTA
501 CCGAGATCAG CCTCATCCAT TTATTACAAG TATGGTCCGT GCACTGGATG
551 AAGCAATGAA CAAGCTGCAG CGAGCAAATC CAGACGACCC AGCTTATGAT
601 GAAAACAAGC GCCAGTTTCA AGAAGATATC AAGGTGATGA ACGACCTAGT
651 AGATAAAATT ATTGCAGATC GCAAAGCAAG CGGTGAACAA AGCGATGATT
701 TATTAACGCA TATGCTAAAC GGAAAAGATC CAGAAACGGG TGAGCCGCTT
751 GATGACGAGA ACATTCGCTA TCAAATTATT ACATTCCTTA TTGCGGGACA
801 CGAAACAACA AGTGGTCTTT TATCATTTGC GCTGTATTTT TTAGTGAAAA
851 ATCCACATGT ATTACAAAAA GCAGCAGAAG AAGCAGCACG AGTTCTAGTA
901 GATCCTGTTC CAAGCTACAA ACAAGTCAAA CAGCTTAAAT ATGTCGGCAT
951 GGTCTTAAAC GAAGCGCTGC GCTTATGGCC AACTGCTCCT GCGTTTTCCC
1001 TATATGCAAA AGAAGATACG GTGCTTGGAG GAGAATATCC TTTAGAAAAA
1051 GGCGACGAAC TAATGGTTCT GATTCCCTCAG CTTACCCGTG ATAAAACAAT
1101 TTGGGGAGAC GATGTGGAAG AGTTCCTGTC AGAGCGTTTT GAAAATCCAA
1151 GTGCGATTCC GCAGCATGCG TTTAAACCGT TTGGAAACGG TCAGCGTGCG
1201 TGTATCGGTC AGCAGTTCGC TCTTCATGAA GCAACGCTGG TACTTGGTAT
1251 GATGCTAAAA CACTTTGACT TTGAAGATCA TACAAACTAC GAGCTCGATA
1301 TTAAAGAAAC TTTAACGTTA AAACCTGAAG GCTTTGTGGT AAAAGCAAAA
1351 TCGAAAAAAA TTCCGCTTGG CGGTATTCCT TCACCTAGCA CTGAACAGTC
1401 TGCTAAAAAA GTACGCAAAA AGGCAGAAAA CGCTCATAAT ACGCCGCTGC
1451 TTGTGCTATA CGGTTCAAAT ATGGGAACAG CTGAAGGAAC GGCGCGTGAT
1501 TTAGCAGATA TTGCAATGAG CAAAGGATTT GCACCGCAGG TCGCAACGCT
1551 TGATTACAC GCCGGAAATC TTCCGCGCGA AGGAGCTGTA TTAATTGTAA
1601 CGGCGTCTTA TAACGGTCAT CCGCCTGATA ACGCAAAGCA ATTTGTCGAC
1651 TGGTTAGACC AAGCGTCTGC TGATGAAGTA AAAGGCGTTC GCTACTCCGT
1701 ATTTGGATGC GGCGATAAAA ACTGGGCTAC TACGTATCAA AAAGTGCCTG
1751 CTTTTATCGA TGAAACGCTT GCCGCTAAAG GGGCAGAAAA CATCGCTGAC
1801 CGCGGTGAAG CAGATGCAAG CGACGACTTT GAAGGCACAT ATGAAGAATG
1851 GCGTGAACAT ATGTGGAGTG ACGTAGCAGC CTACTTTAAC CTCGACATTG
1901 AAAACAGTGA AGATAATAAA TCTACTCTTT CACTTCAATT TGTCGACAGC
1951 GCCGCGGATA TGCCGCTTGC GAAAATGCAC GGTGCGTTTT CAACGAACGT
2001 CGTAGCAAGC AAAGAACTTC AACAGCCAGG CAGTGCACGA AGCACGCGAC
2051 ATCTTGAAAT TGAACCTCCA AAAGAAGCTT CTTATCAAGA AGGAGATCAT
2101 TTAGGTGTTA TTCCTCGCAA CTATGAAGGA ATAGTAAACC GTGTAACAGC
2151 AAGGTTCCGC CTAGATGCAT CACAGCAAAAT CCGTCTGGAA GCAGAAGAAG
2201 AAAAATTAGC TCATTTGCCA CTCGCTAAAA CAGTATCCGT AGAAGAGCTT

```

2251	CTGCAATACG	TGGAGCTTCA	AGATCCTGTT	ACGCGCACGC	AGCTTCGCGC
2301	AATGGCTGCT	AAAACGGTCT	GCCCCCGCA	TAAAGTAGAG	CTTGAAGCCT
2351	TGCTTGAAAA	GCAAGCCTAC	AAAGAACAAG	TGCTGGCAAA	ACGTTTAACA
2401	ATGCTTGAAC	TGCTTGAAAA	ATACCCGGCG	TGTGAAATGA	AATTCAGCGA
2451	ATTTATCGCC	CTTCTGCCAA	GCATACGCCC	GCGCTATTAC	TCGATTTCTT
2501	CATCACCTCG	TGTCGATGAA	AAACAAGCAA	GCATCACGGT	CAGCGTTGTC
2551	TCAGGAGAAG	CGTGGAGCGG	ATATGGAGAA	TATAAAGGAA	TTGCGTCGAA
2601	CTATCTTGCC	GAGCTGCAAG	AAGGAGATAC	GATTACGTGC	TTTATTTCCA
2651	CACCGCAGTC	AGAATTTACG	CTGCCAAAAG	ACCTTGAAAC	GCCGCTTATC
2701	ATGGTCGGAC	CGGGAACAGG	CGTCGCGCCG	TTTAGAGGCT	TTGTGCAGGC
2751	GCGCAAACAG	CTAAAAGAAC	AAGGACAGTC	ACTTGGAGAA	GCACATTTAT
2801	ACTTCGGCTG	CCGTTACACT	CATGAAGACT	ATCTGTATCA	AGAAGAGCTT
2851	GAAAACGCCC	AAAGCGAAGG	CATCATTACG	CTTCATACCG	CTTTTTCTCG
2901	CATGCCAAAT	CAGCCGAAAA	CATACGTTCA	GCACGTAATG	GAACAAGACG
2951	GCAAGAAATT	GATTGAACTT	CTTGATCAAG	GAGCGCACTT	CTATATTTGC
3001	GGAGACGGAA	GCCAAATGGC	ACCTGCCGTT	GAAGCAACGC	TTATGAAAAG
3051	CTATGCTGAC	GTTACCAAG	TGAGTGAAGC	AGACGCTCGC	TTATGGCTGC
3101	AGCAGCTAGA	AGAAAAAGGC	CGATACGCAA	AAGACGTGTG	GGCTGGGTAA
3151	GAATTCATCG	ATGATAAGCT	GTCAAACATG	AGCAGATCTG	AGCCCGCCTA
3201	ATGAGCGGGC	TTTTTTTTTCA	GATCTGCTTG	AAGACGAAAG	GGCCTCGTGA
3251	TACGCCTATT	TTTATAGGTT	AATGTCATGA	TAATAATGGT	TTCTTAGCGT
3301	CAAAGCAACC	ATAGTACGCG	CCCTGTAGCG	GCGCATTAAAG	CGCGGCGGGT
3351	GTGGTGGTTA	CGCGCAGCGT	GACCGCTACA	CTTGCCAGCG	CCCTAGCGCC
3401	CGCTCCTTTC	GCTTTCCTTC	CTTCCTTCT	CGCCACGTTT	GCCGGCTTTC
3451	CCCGTCAAGC	TCTAAATCGG	GGGCTCCCTT	TAGGGTTCCG	ATTTAGTGCT
3501	TTACGGCACC	TCGACCCCAA	AAAACCTTGAT	TTGGGTGATG	GTTACAGTAG
3551	TGGGCCATCG	CCCTGATAGA	CGTTTTTTTCG	CCCTTTGACG	TTGGAGTCCA
3601	CGTTCTTTAA	TAGTGGACTC	TTGTTCCAAA	CTGGAACAAC	ACTCAACCCT
3651	ATCTCGGGCT	ATTCTTTTGA	TTTATAAGGG	ATTTTGCCGA	TTTCGGCCTA
3701	TTGGTTAAAA	AATGAGCTGA	TTTAACAAAA	ATTTAACGCG	AATTTTAACA
3751	AAATATTAAC	GTTTACAATT	TCAGGTGGCA	CTTTTCGGGG	AAATGTGCGC
3801	GGAACCCCTA	TTTGTTTATT	TTTCTAAATA	CATTCAAATA	TGTATCCGCT
3851	CATGAGACAA	TAACCCTGAT	AAATGCTTCA	ATAATATTGA	AAAAGGAAGA
3901	GTATGAGTAT	TCAACATTTT	CGTGTGCCCC	TTATTCCTT	TTTTGCGGCA
3951	TTTTGCCTTC	CTGTTTTTGC	TCACCCAGAA	ACGCTGGTGA	AAGTAAAAGA
4001	TGCTGAAGAT	CAGTTGGGTG	CACGAGTGGG	TTACATCGAA	CTGGATCTCA
4051	ACAGCGGTAA	GATCCTTGAG	AGTTTTTCGCC	CCGAAGAACG	TTTTCCAATG
4101	ATGAGCACTT	TTAAAGTTCT	GCTATGTGGC	GCGGTATTAT	CCCGTGTTGA
4151	CGCCGGGCAA	GAGCAACTCG	GTCGCCGCAT	ACACTATTCT	CAGAATGACT
4201	TGGTTGAGTA	CTCACCAGTC	ACAGAAAAGC	ATCTTACGGA	TGGCATGACA
4251	GTAAGAGAAT	TATGCAGTGC	TGCCATAACC	ATGAGTGATA	ACACTGCGGC
4301	CAACTTACTT	CTGACAACGA	TCGGAGGACC	GAAGGAGCTA	ACCGCTTTTT
4351	TGCACAACAT	GGGGGATCAT	GTAACTCGCC	TTGATCGTTG	GGAACCGGAG
4401	CTGAATGAAG	CCATACCAAA	CGACGAGCGT	GACACCACGA	TGCCTGCAGC
4451	AATGGCAACA	ACGTTGCGCA	AACATTTAAC	TGGCGAACTA	CTTACTCTAG
4501	CTTCCCGGCA	ACAATTAATA	GACTGGATGG	AGGCGGATAA	AGTTGCAGGA
4551	CCACTTCTGC	GCTCGGCCCT	TCCGGCTGGC	TGGTTTATTG	CTGATAAATC
4601	TGGAGCCGGT	GAGCGTGGGT	CTCGCGGTAT	CATTGCAGCA	CTGGGGCCAG

4651	ATGGTAAGCC	CTCCCGTATC	GTAGTTATCT	ACACGACGGG	GAGTCAGGCA
4701	ACTATGGATG	AACGAAATAG	ACAGATCGCT	GAGATAGGTG	CCTCACTGAT
4751	TAAGCATTGG	TAAGTGTCTG	ACCAAGTTTA	CTCATATATA	CTTTAGATTG
4801	ATTTAAAACT	TCATTTTTTA	TTTAAAAGGA	TCTAGGTGAA	GATCCTTTTT
4851	GATAATCTCA	TGACCAAAT	CCCTTAACGT	GAGTTTTTCGT	TCCACTGAGC
4901	GTCAGACCCC	GTAGAAAAGA	TCAAAGGATC	TTCTTGAGAT	CCTTTTTTTC
4951	TGCGCGTAAT	CTGCTGCTTG	CAAACAAAAA	AACCACCGCT	ACCAGCGGTG
5001	GTTTGTTCG	CGGATCAAGA	GCTACCAACT	CTTTTTCCGA	AGGTAACTGG
5051	CTTCAGCAGA	GCGCAGATAC	CAAATACTGT	CCTTCTAGTG	TAGCCGTAGT
5101	TAGGCCACCA	CTTCAAGAAC	TCTGTAGCAC	CGCCTACATA	CCTCGCTCTG
5151	CTAATCCTGT	TACCAGTGGC	TGCTGCCAGT	GGCGATAAGT	CGTGTCTTAC
5201	CGGGTTGGAC	TCAAGACGAT	AGTTACCGGA	TAAGGCGCAG	CGGTCGGGCT
5251	GAACGGGGGG	TTCGTGCACA	CAGCCCAGCT	TGGAGCGAAC	GACCTACACC
5301	GAAGTGAAT	ACCTACAGCG	TGAGCTATGA	GAAAGCGCCA	CGCTTCCCGA
5351	AGGGAGAAAG	GCGGACAGGT	ATCCGGTAAG	CGGCAGGGTC	GGAACAGGAG
5401	AGCGCACGAG	GGAGCTTCCA	GGGGGAAACG	CCTGGTATCT	TTATAGTCCT
5451	GTCGGGTTTC	GCCACCTCTG	ACTTGAGCGT	CGATTTTTGT	GATGCTCGTC
5501	AGGGGGGCGG	AGCCTATGGA	AAAACGCCAG	CAACGCGGCC	TTTTTACGGT
5551	TCCTGGCCTT	TTGCTGGCCT	TTTGCTCACA	TGTTCTTTCC	TGCGTTATCC
5601	CCTGATTCTG	TGGATAACCG	TATTACCGCC	TTTGAGTGAG	CTGATACCGC
5651	TCGCCGCAGC	CGAACGACCG	AGCGCAGCGA	GTCAGTGAGC	GAGGAAGCGG
5701	AAGAGCGCCT	GATGCGGTAT	TTTCTCCTTA	CGCATCTGTG	CGGTATTTCA
5751	CACCGCATAT	ATGGTGCAT	CTCAGTACAA	TCTGCTCTGA	TGCCGCATAG
5801	TTAAGCCAGT	ATACACTCCG	CTATCGCTAC	GTGACTGGGT	CATGGCTGCG
5851	CCCCGACACC	CGCCAACACC	CGCTGACGCG	CCCTGACGGG	CTTGTCTGCT
5901	CCCGGCATCC	GCTTACAGAC	AAGCTGTGAC	CGTCTCCGGG	AGCTGCATGT
5951	GTCAGAGGTT	TTCACCGTCA	TCACCGAAAC	GCGCGAGGCA	GAACGCCATC
6001	AAAAATAATT	CGCGTCTGGC	CTTCCTGTAG	CCAGCTTTCA	TCAACATTAA
6051	ATGTGAGCGA	GTAACAACCC	GTCGGATTCT	CCGTGGGAAC	AAACGGCGGA
6101	TTGACCGTAA	TGGGATAGGT	TACGTTGGTG	TAGATGGGCG	CATCGTAACC
6151	GTGCATCTGC	CAGTTTGAGG	GGACGACGAC	AGTATCGGCC	TCAGGAAGAT
6201	CGCACTCCAG	CCAGCTTTCC	GGCACCGCTT	CTGGTGCCGG	AAACCAGGCA
6251	AAGCGCCATT	CGCCATTACG	GCTGCGCAAC	TGTTGGGAAG	GGCGATCGGT
6301	GCGGGCCTCT	TCGCTATTAC	GCCAGCTGGC	GAAAGGGGGA	TGTGCTGCAA
6351	GGCGATTAA	TTGGGTAAAC	CCAGGGTTTT	CCCAGTCACG	ACGTTGTAAA
6401	ACGACGGCCA	GTGAATCCGT	AATCATGGTC	ATAGCTGTTT	CCTGTGTGAA
6451	ATTGTTATCC	GCTCACAATT	CCACACAACA	TACGAGCCGG	AAGCATAAAG
6501	TGTAAAGCCT	GGGGTGCCTA	ATGAGTGAGC	TAATCACAAT	TAATTGCGTT
6551	GCGCTCACTG	CCCCTTTTCC	AGTCGGGAAA	CCTGTCGTGC	CAGCTGCATT
6601	AATGAATCGG	CCAACGCGCG	GGGAGAGGCG	GTTTGCGTAT	TGGGCGCCAG
6651	GGTGGTTTTT	CTTTTACCA	GTGAGACGGG	CAACAGCTGA	TTGCCCTTCA
6701	CCGCCTGGCC	CTGAGAGAGT	TGCAGCAAGC	GGTCCACGCT	GGTTTGGCCC
6751	AGCAGGCGAA	AATCCTGTTT	GATGGTGGTT	AACGGCGGGA	TATAACATGA
6801	GCTGTCTTCG	GTATCGTCGT	ATCCCACTAC	CGAGATATCC	GCACCAACGC
6851	GCAGCCCGGA	CTCGGTAATG	GCGCGCATTG	CGCCCAGCGC	CATCTGATCG
6901	TTGGCAACCA	GCATCGCAGT	GGGAACGATG	CCCTCATTCA	GCATTTGCAT
6951	GGTTTGTTGA	AAACCGGACA	TGGCACTCCA	GTCGCCTTCC	CGTTCCGCTA
7001	TCGGCTGAAT	TTGATTGCGA	GTGAGATATT	TATGCCAGCC	AGCCAGACGC

```

7051 AGACGCGCCG AGACAGAACT TAATGGGCCC GCTAACAGCG CGATTTGCTG
7101 GTGACCCAAT GCGACCAGAT GCTCCACGCC CAGTCGCGTA CCGTCTTCAT
7151 GGGAGAAAAT AATACTGTGTG ATGGGTGTCT GGTTCAGAGAC ATCAAGAAAT
7201 AACGCCGGAA CATTAGTGCA GGCAGCTTCC ACAGCAATGG CATCCTGGTC
7251 ATCCAGCGGA TAGTTAATGA TCAGCCCACT GACGCGTTGC GCGAGAAGAT
7301 TGTGCACCGC CGCTTTACAG GCTTCGACGC CGCTTCGTTT TACCATCGAC
7351 ACCACCACGC TGGCACCCAG TTGATCGGCG CGAGATTTAA TCGCCGCGAC
7401 AATTTGCGAC GCGCGGTGCA GGGCCAGACT GGAGGTGGCA ACGCCAATCA
7451 GCAACGACTG TTTGCCCCGCC AGTTGTTGTG CCACGCGGTT GGGAATGTAA
7501 TTCAGCTCCG CCATCGCCGC TTCCACTTTT TCCCGCGTTT TCGCAGAAAC
7551 GTGGCTGGCC TGGTTCACCA CGCGGGAAAC GGTCTGATAA GAGACACCGG
7601 CATACTCTGC GACATCGTAT AACGTTACTG GTTTCACATT CACCACCCTG
7651 AATTGACTCT CTTCCGGGCG CTATCATGCC ATACCGCGAA AGGTTTTGCG
7701 CCATTCGATG GTGTCCTGGC ACGACAGGTT TCCCGACTGG AAAGCGGGCA
7751 GTGAGCGCAA CGCAATTAAT GTGAGTTAGC TCACTCATTA GGCACCCCAG
7801 GCTTTACACT TTATGCTTCC GGCTCGTATA ATGTGTGGAA TTGTGAGCGG
7851 ATAACAATTT CACACAGGAA ACAGGATCGA TCCATCGATG AGCTTACTCC
7901 CCATCCCCCT GTTGACAATT AATCATCGGC TCGTATAATG TGTGGAATTG
7951 TGAGCGGATA ACAATTTTAC ACAGGAAACA GGATCAGCTT ACTCCCCATC
8001 CCCCTGTTGA CAATTAATCA TCGGCTCGTA TAATGTGTGG AATTGTGAGC
8051 GGATAACAAT TTCACACAGG AAACAGGATC CATCGATGCT TAGGAGGTCA
8101 T

```

Figure B.4. Plasmid map of pCWori vector containing wild-type P450 BM-3 (pBM3_WT18-6).

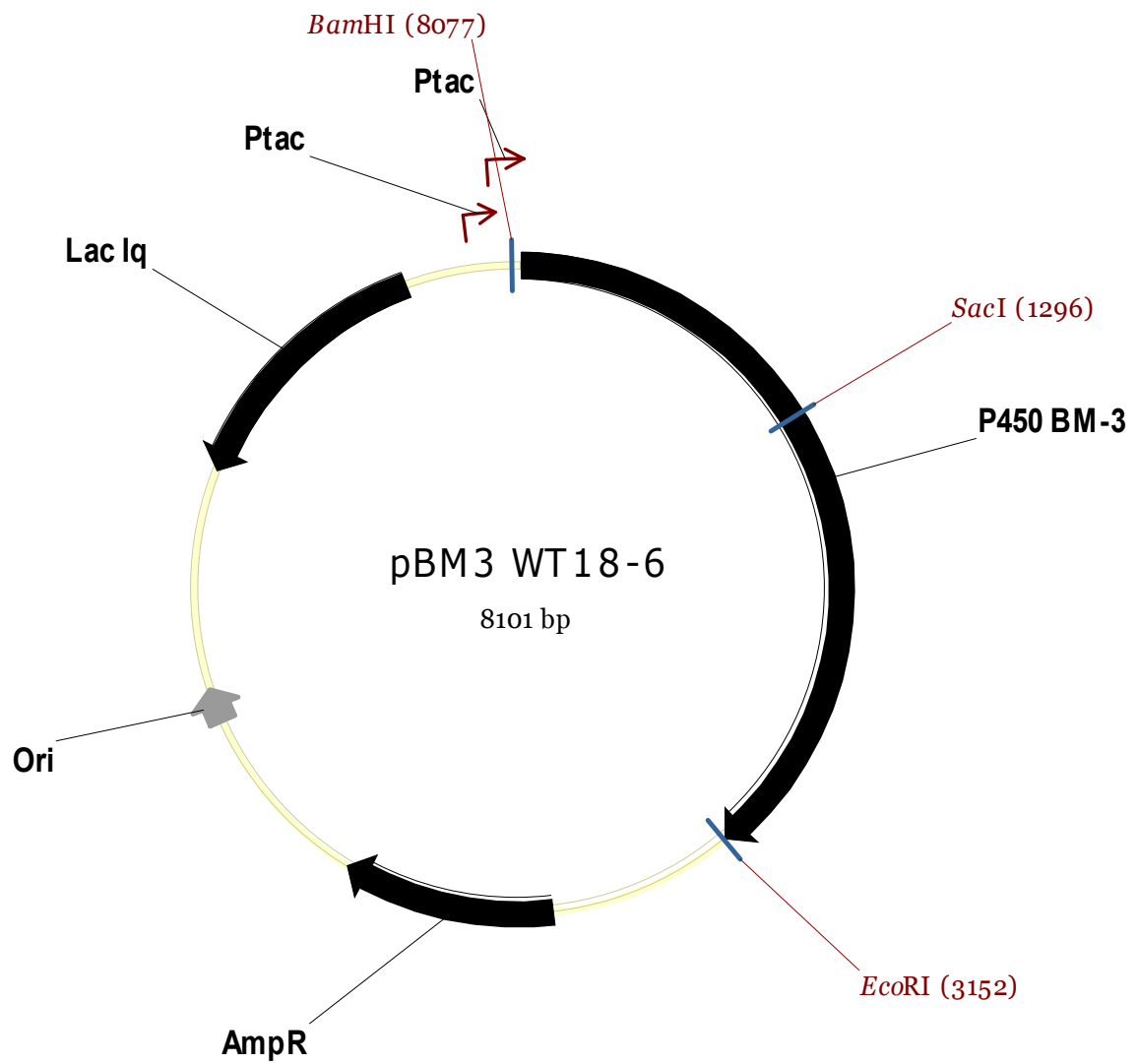


Table B.1. P450 BM-3 variants generated by random mutagenesis and recombination prior to my involvement in the project.

Amino acid position (wt)	DNA substitution	Amino acid substitution of mutants						
Variant		35-4	139-3	139-37	A	B	L	J
Reference		[1,2]	[2,3]	[2]	[2]	[2]	[2]	[2,4]
E5	A15G					E ^[a]		
V78	T236C	A	A	A	A	A	A	A
K99	A297G					K ^[a]		
F107	C324T		F ^[a]	F ^[a]	F ^[a]	F ^[a]	F ^[a]	F ^[a]
A112	A336G						A ^[a]	
H138	C415T		Y					
G157	G472T				C			
N159	C480T			N ^[a]				
F162	T487C						L	
D168	G505A						N	
T175	C527T		I	I	I	I	I	I
V178	G535A		I					
A184	553-555 ^[b]				I	I		
A184	C554T		V	V			V	V
N186	A559G			D				
R203	C612T			R ^[a]				
F205	T617G							C
D217	A653T			V				
D223	T669A				E	E		
S226	C681G							R
G227	G682A				S	S		
H236	709-711 ^[c]				R			
H236	T711G	Q	Q	Q		Q	Q	Q
E252	A758G	G	G	G	G	G	G	G
R255	C766A		S					S
V281	T845C				A			
A290	C872T		V	V	V	V	V	V
A295	G886A		T					
P303	A912C			P ^[a]				
Q308	A924G					Q ^[a]		
A328	C986T							
L353	C1060G		V	V	V	V	V	V
G396	G1189A			M				
E372	A1119G							E ^[a]
Q397	G1194A		Q ^[a]					
T411A	A1234G						A	
P525P	G1575C					P ^[a]		

^[a] Synonymous mutation^[b] A184I DNA mutation was GCA to ATA^[c] H236R DNA mutation was CAT to CGG

Table B.2. P450 BM-3 variants described in Chapter 2.

Amino acid Position (wt)	DNA substitution	Amino acid substitution of mutants				
		J	9-10A	9-10A- A82L	9-10A- A328V	1-12G
Reference		[2,4]	[2,4]	[2,4]	[2,4]	[2,4]
R47	C142T		C	C	C	C
V78	T236C	A	A	A	A	A
A82	247-249 ^[2]			L		L
K94	A284T		I	I	I	I
F107	C324T	F ^[a]	F ^[a]	F ^[a]	F ^[a]	F ^[a]
P142	C427T		S	S	S	S
T175	C527T	I	I	I	I	I
A184	C554T	V	V	V	V	V
F205	T617G	C	C	C	C	C
S226	C681G	R	R	R	R	R
H236	T711G	Q	Q	Q	Q	Q
E252	A758G	G	G	G	G	G
R255	C766A	S	S	S	S	S
A290	C872T	V	V	V	V	V
A328	C986T				V	V
L353	C1060G	V	V	V	V	V
E372	A1119G	E ^[a]	E ^[a]	E ^[a]	E ^[a]	E ^[a]

^[a] Synonymous mutation^[b] A82L DNA mutation was GCA to CTT

Table B.3. Variants of P450 BM-3 containing single active site mutations as described in Chapter 3.

Name	DNA position	DNA substitutions ^[a]	Amino acid substitution ^[a]
9-10A-L75I	226-228	CTT→ATT	L75I
9-10A-L75W	226-228	CTT→TGG	L75W
9-10A-A78T	235-237	GCA→ACA	A78T
9-10A-A78F	235-237	GCA→TTC	A78F
9-10A-A78S	235-237	GCA→TCC	A78S
9-10A-A82T	247-249	GCA→ACA	A82T
9-10A-A82S	247-249	GCA→TCA	A82S
9-10A-A82F	247-249	GCA→TTC	A82F
9-10A-A82I	247-249	GCA→ATC	A82I
9-10A-A82C	247-249	GCA→TGC	A82C
9-10A-A82G	247-249	GCA→GGG	A82G
9-10A-F87I	262-264	TTT→ATC	F87I
9-10A-F87V	262-264	TTT→GTG	F87V
9-10A-F87L	262-264	TTT→TTG	F87L
9-10A-T88C	265-267	ACA→TGT	T88C
9-10A-T260L	781-783	ACA→CTC	T260L
9-10A-T260S	781-783	ACA→TCA	T260S
9-10A-T260N	781-783	ACA→AAC	T260N
9-10A-A328F	985-987	GCT→TTC	A328F
9-10A-A328M	985-987	GCT→ATG	A328M
9-10A-A328L	985-987	GCT→CTC	A328L

^[a] Mutations are relative to 9-10A (see Table B.2 for details). Wild-type P450 BM-3 has a valine at position 78.

Table B.4. Variants of P450 BM-3 containing multiple active site mutations as described in Chapters 3, 4, and 5.

Mutant	Reference	A75 ^[a]	A78 ^[a]	A82 ^[a]	F87 ^[a]	A328 ^[a]
77-9H			T	G		L
1-7D		I	F	G		L
68-8F			F	G		L
49-9B				G	V	L
35-7F			F	S		L
1-5G		I	F	S		L
13-7C			T			L
49-1A			T	G	V	L
2-4B		I	T			L
12-10C				G	V	V
11-8E					V	L
41-5B			F	G		V
29-3E			F	G		F
7-11D				F		V
29-10E				F		F
53-5H	[5]		F	S		F

^[a] Mutations are relative to 9-10A (see Table B.2 for details). Wild-type P450 BM-3 has a valine at position 78.

Table B.5. Amino acid substitutions in reductase mutants described in Chapter 5.

Amino acid position (wt)	DNA substitution	Amino acid substitution of mutants	
Variant		53-5H-E464G ^[a]	35-E11 ^[a]
Reference		[5]	[5]
E464	A1394G	G	G
I710	T2132C		T
L771	A2313G		L ^[b]

^[a] only mutations in the reductase domain are listed. Heme domain mutations are those listed for 53-5H in Table B.4.

^[b] Synonymous mutation

References

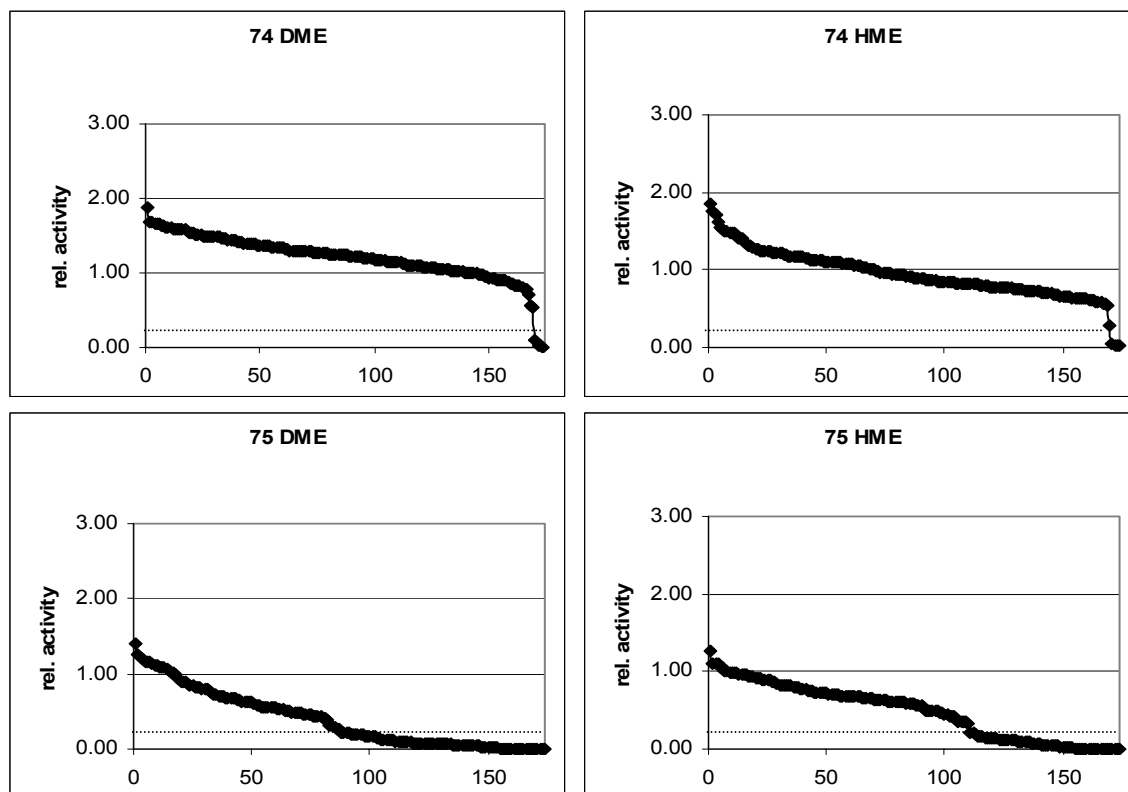
1. Farinas, E. T., Schwaneberg, U., Glieder, A. & Arnold, F. H. (2001). **Directed evolution of a cytochrome P450 monooxygenase for alkane oxidation.** *Adv. Synth. Catal.* **343**, 601-606.
2. Munzer, D. F., Meinhold, P., Peters, M. W., Feichtenhofer, S., Griengl, H., Arnold, F. H., Glieder, A. & de Raadt, A. (2005). **Stereoselective hydroxylation of an achiral cyclopentanecarboxylic acid derivative using engineered P450s BM-3.** *Chem. Commun.* DOI: 10.1039/b501527h.
3. Glieder, A., Farinas, E. T. & Arnold, F. H. (2002). **Laboratory evolution of a soluble, self-sufficient, highly active alkane hydroxylase.** *Nat. Biotechnol.* **20**, 1135-1139.
4. Peters, M. W., Meinhold, P. & Arnold, F. H. (2003). **Regio- and enantioselective alkane hydroxylation with engineered cytochromes P450 BM-3.** *J. Am. Chem. Soc.* **125**, 13442 -13450.
5. Meinhold, P., Peters, M. W. & Arnold, F. H. (2005). **Direct conversion of ethane to ethanol by engineered cytochrome P450 BM3.** *Science* submitted.

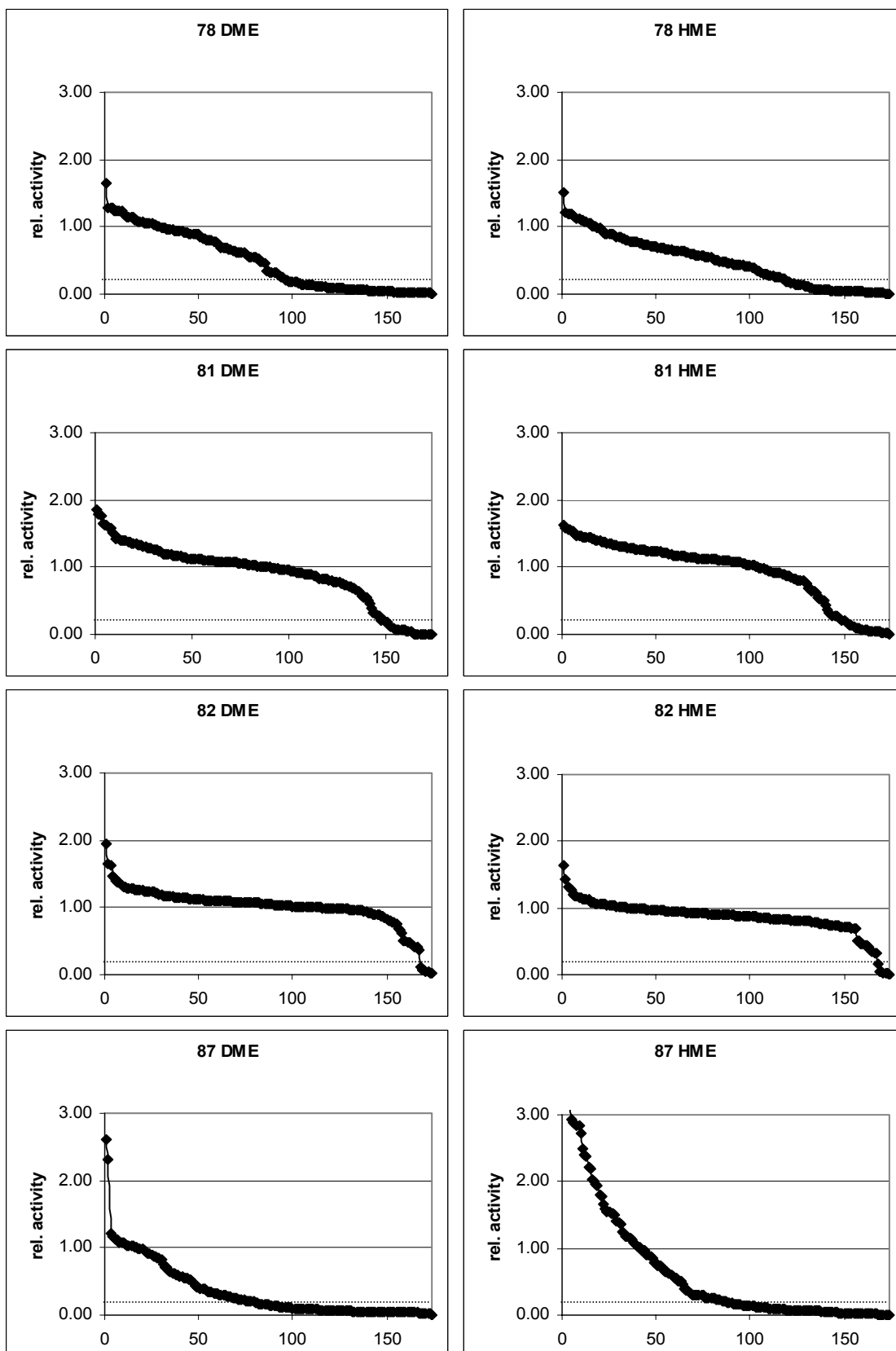
A p p e n d i x C

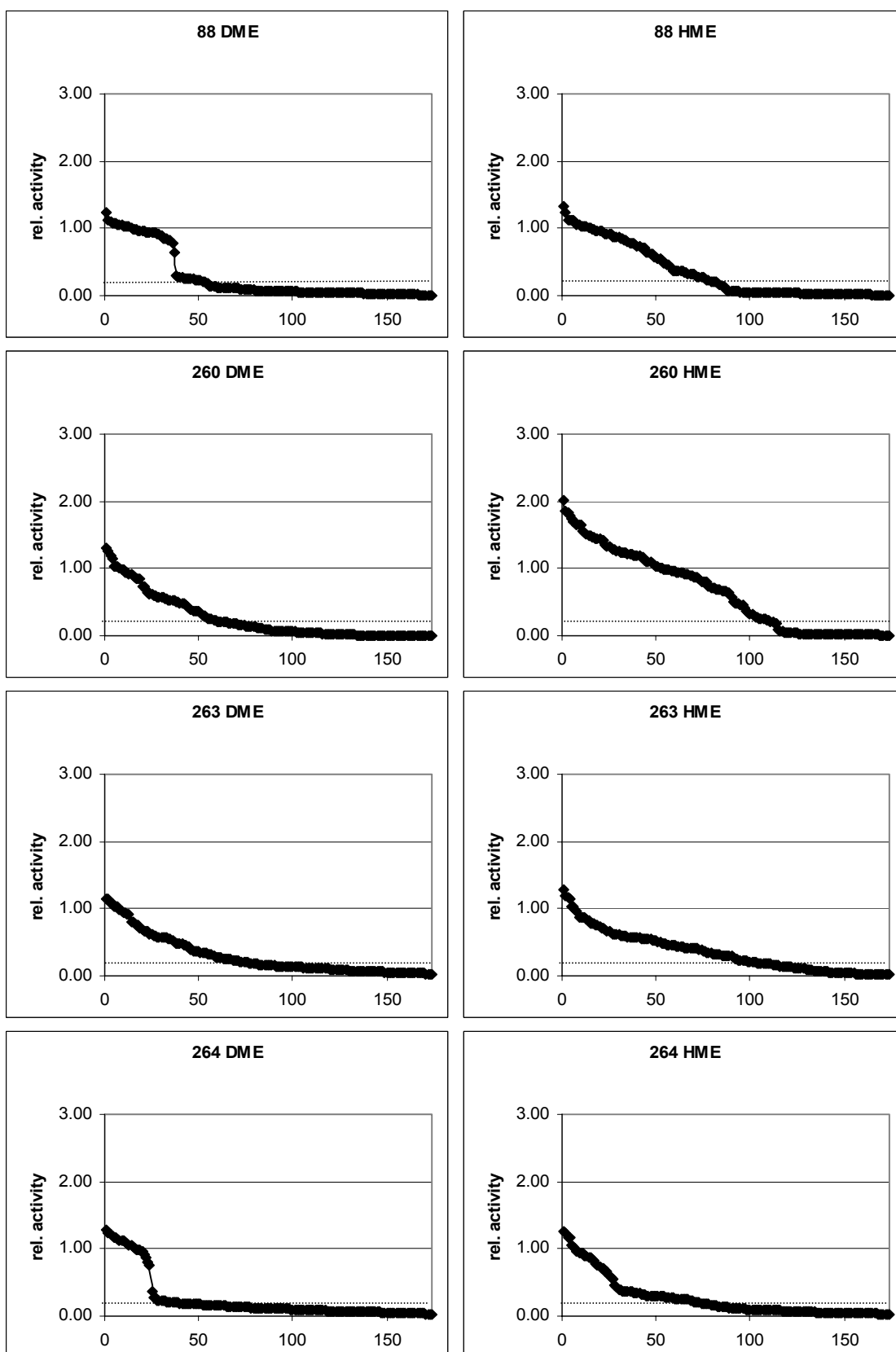
Activity Profiles of Active Site Saturation Libraries

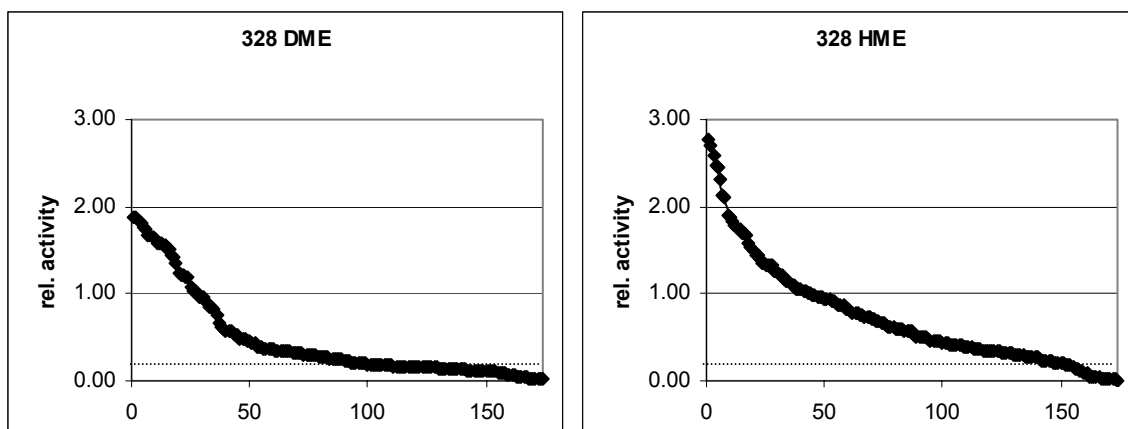
The activity profiles of the saturation mutagenesis libraries are plotted in figure C.1. For each profile, the activity of each of the 174 library members was normalized to the average 9-10A activity and is plotted in descending order. Mutants with greater than 20% of 9-10A's activity (dashed line) were considered active. The coefficient of variance of the screen was determined to be 13% based on activities of 16 parental clones cultured in the same 96-well plates under identical conditions. The screen was performed in 96-well plate format in which each well of the microtiter plates containing *E. coli* cell lysate grown from a single colony was screened for activity. Eight wells in each plate were filled with mutant 9-10A for comparison and one well was left empty as a negative control. Please refer to Chapter 8 for experimental details.

Figure C.1. Activity profiles of saturation mutagenesis libraries.









A p p e n d i x D

Materials and Methods Used by Collaborators at the TU Graz

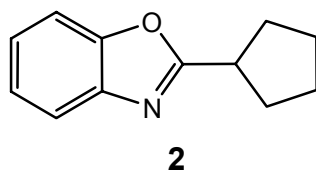
The following section lists the experimental procedures for the synthesis of substrates and product standards as well as for whole cell biotransformations described in Chapter 5. This work was performed by Dieter F. Münzer, Sabine Feichtenhofer, Anna de Raadt and Anton Glieder at the Technical University of Graz, Austria.

A. Instrumentation

All chemicals were purchased from Sigma-Aldrich, Fluka or Merck. If required, chemicals and solvents were purified according to Perrin and Armarego [1]. Optical rotations were measured on a Perkin Elmer Polarimeter 341. ^1H and ^{13}C NMR were recorded on a Gemini 200 (Varian) or UNITY / INOVA 500 (Varian). HETCOR, DEPT and COSY experiments were carried out as required. CDCl_3 was used as solvent and as internal standard. Before use, the CDCl_3 was filtered through a short plug of basic alumina to remove traces of acid. The minor isomer is given in italics. Chiral HPLC was determined with an Agilent 1100 Series HPLC system containing column unity, degasser, quaternary pump, autosampler, UV and RI detector. A Lichrosorb SJ 60, 10 μm normal phase precolumn was used. LC was performed on Silica gel 60 (Merck, 70 - 230 mesh) using mixtures of ethyl acetate and petroleum ether unless otherwise stated. GC analysis was carried out on an Agilent 6890 N network GC system with a 7683 series autosampler, FID and a Agilent 19091J-413 HP 5 column (30 m). TLC was performed on Silica gel 60 F254 aluminium plates (Merck) and compounds detected with UV (254 nm) and dipping into either reagent A (1 g vanillin, 140 mL ethanol or methanol, 20 mL concentrated H_2SO_4) or

reagent B (10% H_2SO_4 , 10% $(\text{NH}_4)_6\text{Mo}_7\text{O}_{24} \times 4 \text{H}_2\text{O}$ and 0.8% $\text{Ce}(\text{SO}_4)_2 \times 4 \text{H}_2\text{O}$ in water). The TLC plates were then developed by heating with a heat gun. Mixtures of petroleum ether/ethyl acetate were used as eluent. Centrifugation was carried out with a Beckman Coulter Avanti J-20 XP centrifuge with a JA-10 rotor. For the biotransformations a Memmert BE 600 incubator was used.

B. Synthesis of substrate 2-cyclopentylbenzoxazole 2

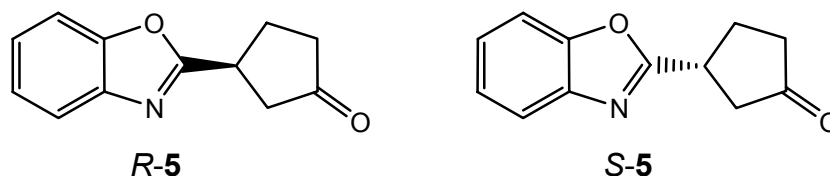


The biotransformation substrate **2** was synthesized using published methods [2-4].

C. Synthesis of Product Standards

For the identification of the peaks in HPLC and GC, for example for the determination of the *ee/de* of the hydroxylated products **3**, reference compounds were chemically synthesized.

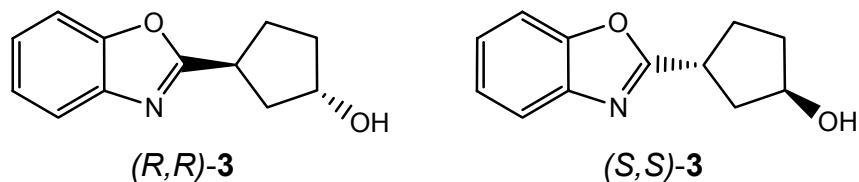
D. Synthesis of Racemic Ketone **5**



The title compound was obtained in 34% yield from reacting racemic 3-oxocyclopentanecarboxylic acid (1.07 g, 8.35 mmol) with 2-aminophenol (0.91 g, 8.35 mmol) as described (Method B) in the published synthesis for benzoxazoles [2-4]. The desired ketone **5** was purified by column chromatography (pet. ether : ethyl acetate = 5:1 to 3:1). Physical data are identical to literature [2-4].

E. Synthesis of Product **3** Standards

For the determination of *ee/de* values of product **3** obtained from the biohydroxylation, three different reference mixtures were used.



(S,S)-3 (79% *ee*, 95% *de*, **reference 1**) was obtained from biohydroxylation of **2** with *Sphingomonas* sp. HXN-200 [5,6]. The absolute configuration of this sample was

determined by comparing optical rotation ($[\alpha]_{\text{D}}^{20} = +20.1^\circ$, $c = 2.1$ in CH_2Cl_2) to the published value [2-4].

A mixture of all four diastereoisomers of **3**, [(*S,R*)-**3** and (*R,S*)-**3**] : [(*S,S*)-**3** and (*R,R*)-**3**] = 5:1 (NMR, **reference 2**), was also required for reference purposes. The mixture was obtained by reducing racemic ketone **5** with NaBH_4 in methanol. Accordingly, 1.5 eq of NaBH_4 were suspended in 2 mL of methanol. After 30 seconds, a solution of 80 mg (0.40 mmol) of ketone **5** in 1 mL of methanol was added to the stirred suspension. After five minutes the reaction was complete (TLC). To the reaction mixture, 5 mL of CH_2Cl_2 were added, the solution was washed with equal amounts of 5% aqueous HCl , saturated aqueous NaHCO_3 and water, dried over Na_2SO_4 , filtered and concentrated down under reduced pressure. Column chromatography (pet. ether : ethyl acetate = 2:1) gave 65 mg of **3** (80% yield) as a colourless syrup.

^1H -NMR (CDCl_3): $\delta = 1.71\text{--}2.46$ (m, 7H), 3.49, 3.72 (m, *p*, 1H), 4.46, 4.58 (2 \times bm, 1H), 7.28, 7.45, 7.63 (3 \times m, 2H, 1H, 1H). ^{13}C -NMR (CDCl_3): $\delta = 29.0, 30.1, 35.1, 35.8, 36.7, 37.3, 40.4, 40.9, 73.4, 73.5, 110.4, 110.5, 119.6, 124.2, 124.4, 124.6, 124.7, 141.2, 150.9, 170.3, 171.3$.

A mixture of (*S,S*)-**3** and (*S,R*)-**3** (**reference 3**) was also prepared. The mixture was obtained by the oxidation of **reference 1** with pyridinium chlorochromate (PCC) in CH_2Cl_2 and subsequent reduction of the isolated ketone **5** to alcohol **3** with NaBH_4 in methanol. For the oxidation, 1.5 eq of PCC were suspended in 1 mL of CH_2Cl_2 and a solution of 45 mg (0.22 mmol) of **3** (79% *ee*, 95% *de*) in 1 mL of CH_2Cl_2 was added.

The colour of the reaction mixture changed from brown to dark grey. After 1 h the reaction was complete (TLC); the reaction mixture was immediately put onto silica gel and, after column chromatography (pet. ether : ethyl acetate = 1:1), 36 mg (81% yield) of ketone **5** were obtained as white crystals. Physical data were identical to literature [2-4]. Subsequently, 25 mg of **5** were reduced as described for **reference 2**. 20 mg (80% yield) of the desired mixture were obtained. In this case, chromatography was not necessary.

F. Cultivation of BM-3 mutants for whole cell biotransformations

The following mutants were tested: 35-4, 139-3, 139-29, 139-37, A, B, J, L, 9-10A, 9-10A-A328V, 9-10A-A-82L, 1-12G as well as the wild-type (see Appendix B for mutations). *E. coli* DH5 α , transformed with these plasmids, was used for the biotransformations. All experiments were conducted in parallel. All mutants were cultivated and stored on LBamp agar plates. For the stage 1 cultures 10 mL Greiner tubes were used. 2 mL LB medium (10 g tryptone, 5 g yeast extract and 5 g NaCl. These were dissolved in distilled H₂O and made up to 1L) together with 100mg/L ampicillin were inoculated with the respective *E. coli* cells which had been previously grown on agar. These stage 1 cultures were then incubated over night (18.5 h) at 100 rpm and 30°C. For stage 2 cultures 1L Erlenmeyer flasks were used. 150 mL TB medium (solution 1: 12 g tryptone, 24 g yeast extract and 4 mL glycerine. These were dissolved in distilled H₂O and made up to 900 mL of solution 2: 100 mL buffer consisting of 0.17 M KH₂PO₄ and 0.72 M K₂HPO₄. Each solution was

sterilised separately and then mixed. The pH value should lie between 6 and 8.) together with 100 mg/L ampicillin and, in one run, 1.5 mL/L trace element solution (0.5 g $\text{CaCl}_2 \times 2\text{H}_2\text{O}$, 0.18 g $\text{ZnSO}_4 \times 7\text{H}_2\text{O}$, 0.1 g $\text{MnSO}_4 \times \text{H}_2\text{O}$, 20.1 g $\text{Na}_2\text{-EDTA}$, 16.7 g $\text{FeCl}_3 \times 6\text{H}_2\text{O}$, 0.16 g $\text{CuSO}_4 \times 5\text{H}_2\text{O}$, 0.18 g $\text{CoCl}_2 \times 6\text{H}_2\text{O}$ in 1L distilled H_2O) were inoculated with 1 mL stage 1 culture. They were then incubated at 100 rpm and 30°C for 8h.

G. Substrate addition

After the previously mentioned 8h, substrate **2** (3 mM) was dissolved in EtOH (84 mg **2** in 1 mL abs. EtOH) and this added to the stage 2 culture. In addition, 50 mg/L ampicillin was also added. After incubation for a further 15h, additional ampicillin (50 mg/L) was added. Each experiment was stopped (see the following section) after a final 21h of incubation.

H. Sample processing and purification

Each experiment was stopped by the following procedure: the respective culture was centrifuged (4400 g) and the supernatant liquid extracted three times with ethyl acetate. The organic phases were collected, dried with Na_2SO_4 , filtered and concentrated down under reduced pressure. The crude extracts were purified with column chromatography (pet. ether : ethyl acetate; 10:1 followed by 2:1). During chromatography, priority was placed on not influencing the *de* of **3**.

I. Analytics

The determination of the *ee/de* of the products **3** from the whole cell biotransformation was achieved with reference compounds/mixtures (all 4 diastereoisomers of **3**) and chiral HPLC (Daicel Chiralpak AD-H, 1mL/min, *n*-heptane:ethanol = 95.5:4.5, 230 nm; retention times: 23.3 min (*S,S*)-**3**, 25.9 min (*R,R*)-**3**, 27.9 min (*S,R*)-**3**, 29.8 min (*R,S*)-**3**).

J. References

1. Perrin, D. D. & Armarego, W. L. F. (1988). **Purification of laboratory chemicals**. 3rd edit., Pergamon press, Oxford.
2. de Raadt, A. et al. (1996). **Microbial hydroxylation of 2-cycloalkylbenzoxazoles .3. Determination of product enantiomeric excess and cleavage of benzoxazoles**. *Tetrahedron: Asymmetry* **7**, 491-496.
3. de Raadt, A. et al. (1996). **Microbial hydroxylation of 2-cycloalkylbenzoxazoles .1. Product spectrum obtained from *Cunninghamella blakesleeana* DSM 1906 and *Bacillus megaterium* DSM 32**. *Tetrahedron: Asymmetry* **7**, 467-472.
4. de Raadt, A. et al. (1996). **Microbial hydroxylation of 2-cycloalkylbenzoxazoles .2. Determination of product structures and enhancement of enantiomeric excess**. *Tetrahedron: Asymmetry* **7**, 473-490.
5. Chang, D. L., Feiten, H. J., Witholt, B. & Li, Z. (2002). **Regio- and stereoselective hydroxylation of N-substituted piperidin-2-ones with *Sphingomonas* sp. HXN-200**. *Tetrahedron: Asymmetry* **13**, 2141-2147.
6. Chang, D. L., Feiten, H. J., Engesser, K. H., van Beilen, J. B., Witholt, B. & Li, Z. (2002). **Practical syntheses of N-substituted 3-hydroxyazetidines and 4-hydroxypiperidines by hydroxylation with *Sphingomonas* sp. HXN-200**. *Organic Letters* **4**, 1859-1862.